Regulation of Rho-activating proteins by heterotrimeric G proteins:

Sensitivity of Gα RhoGEF interaction is determined by dissociation kinetics

Dissertation zur Erlangung des

Doktorgrades der Naturwissenschaften

(Dr. rer. nat.)

dem Fachbereich der Pharmazie

der Philipps-Universität Marburg

vorgelegt von

Eva-Lisa Bodmann

aus Mainz

Marburg/Lahn 2014

Erstgutachter: Prof. Dr. Moritz Bünemann

Zweitgutachter: Prof. Dr. Carsten Culmsee

Eingereicht am 02.10.2014

Tag der mündlichen Prüfung am 14.11.2014

Hochschulkennziffer: 1180

Meinen Großvätern

Alois Bodmann und

Hans Joachim von Haenlein

Table of contents

1 Publications

1.1 Published abstracts

Bodmann, E-L., Müller, A-L., and Bünemann, M. (2014). Prolonged interactions between $G\alpha_{13}$ and Leukemia-associated RhoGEF are associated with high sensitivity of receptor-induced LARG activation. Proceedings of the British Pharmacological Society*12*: abst027P

Müller, A-L., Bodmann, E-L., and Bünemann, M. (2014). Real time imaging of $G\alpha_{13}$ signaling reveal hypersensitive LARG activation. Naunyn Schmiedebergs Arch Pharmacol *387*: S15

Bodmann, E-L., Rinne, A., Lutz, S., Wieland, T., and Bünemann, M. (2013). RGS2 fine tunes dynamics of $G\alpha_q$-p63RhoGEF interaction without attenuating Rho signaling. Naunyn Schmiedebergs Arch Pharmacol *386*: S11

Bodmann, E-L., Rinne, A., Lutz, S., Wieland, T., and Bünemann, M. (2012). Dynamics of G-protein-p63RhoGEF-interactions. Naunyn Schmiedebergs Arch Pharmacol *385*: S12

1.2 Article

Bodmann, E.-L., Rinne, A., Brandt, D., Lutz, S., Wieland, T., Grosse, R., et al. (2014). Dynamics of $G\alpha_q$-protein-p63RhoGEF interaction and its regulation by RGS2. Biochem. J. *458*: 131–40.

2 Abbreviations

a.u.	Arbitrary unit
ACh	Acetylcholine
AGS	Activator of G protein signaling
Ang II	Angiotensin II
APS	Ammonium persulfate
AT 1-R	Angiotensin 1 receptor
AUC	Area under the curve
BRET	Bioluminescence resonance energy transfer
BSA	Bovine serum albumin
CaMKII	Ca^{2+}/calmodulin-dependent kinase II
CCD	Charge coupled device
CR	Conserved region
CRE	cAMP responsive element
DAG	Diacylglycerol
Dbl	Diffuse B cell lymphoma
DH	Dbl homology
ERK5	Extracellular signal regulated kinase 5
ET-1	Endothelin 1
FAK	Focal adhesion kinase
FCS	Fetal calf serum
FRAP	Fluorescence recovery after photobleaching
FRET	Fluorescence resonance energy transfer
GAP	GTPase activating protein
GDI	Guanine nucleotide dissociation inhibitor
GDP	Guanosine diphosphate
GEF	Guanine nucleotide exchange factor
GFP	Green fluorescent protein
GPCR	G protein coupled receptor
GRK	G protein coupled receptor kinase
GST	Glutathione-S-transferase

GTP	Guanosine-5´-triphosphate
HEK	Human embryonic kidney
His	Histamine
HRP	Horse radish peroxidase
IP_3	Inositol 1,4,5 triphosphate
IPTG	Isopropyl-β-D-1-thiogalactopyranoside
JNK	c-Jun N-terminal kinase
Kir	Inward rectifier K^+ channel
LARG	Leukemia-associated RhoGEF or ARHGEF12 or KIAA0382
M_3-R	Muscarinic M3 receptor
mDia	Mammalian Dia protein or mammalian homolog of Drosophila Diaphanous
MEF	Mouse embryonic fibroblast
MLC	Myosin light chain
MLCK	MLC kinase
MLCP	MLC phosphatase
MLK3	Mitogen-activated kinase
MLL	Mixed lineage leukemia
mTur2	mTurquoise2
NA	Noradrenaline
NFκB	Nuclear factor κB
NLS	Nuclear localization sequence
NMR	Nuclear magnetic resonance spectroscopy
NO	Nitric oxide
p115RhoGEF	Lymphoid blast crisis like 2 (LSC) or Lip or LBCL2 or ARHGEF1 or SUB1.5
p63RhoGEF	GEFT or ARHGEF25
PAGE	Polyacrylamide gel electrophoresis
PCR	Polymerase chain reaction
PDE	Phosphodiesterase
PDZ	Post synaptic density protein, Drosophila disc large tumor suppressor, zonula occludens-1 protein
PDZ-RhoGEF	ARHGEF11 or GTRAP48 or KIAA0380

PEI	Polyethylenimine
PH	Pleckstrin homology
PIP	Phosphatidylinositol phosphate
PKC	Protein kinase C
PKN	Protein Kinase N
PLCβ	Phospholipase C β
PVDF	Polyvinylidene fluoride
RBD	Rho binding domain
RFP	Red fluorescent protein
RGS	Regulator of G protein signaling
RH	RGS homology
Rho	Ras homologous
RhoGDI	Rho guanine nucleotide dissociation inhibitor
RNAse A	Ribonuclease A
ROCK	Rho-associated coiled-coil kinase
ROI	Region of interest
S_1P	Sphingosine 1 phosphate
SDS	Sodium dodecyl sulfate
SFK	Src family kinase
SNP	Single nucleotide polymorphism
SRE	Serum response element
SRF	Serum response factor
$t_{1/2}$	Half time
Txa_2	Thromboxane A2
Txa_2-R	Thromboxane A2 receptor
V-p63	Venus-p63RhoGEF
VSMC	Vascular smooth muscle cell
YFP	Yellow fluorescent protein
α_1-AR	α_1 adrenergic receptor
α_{2A}-AR	α_{2A} adrenergic receptor
β_2-AR	β_2 adrenergic receptor

3 Summary

Activation of RhoGTPases downstream of G protein coupled receptors is important for many physiological functions, such as blood pressure regulation. The subfamilies Rho, Rac and Cdc42 are the best understood RhoGTPases and the present study focused on signaling towards the Rho subfamily member RhoA. In its active state RhoA regulates the cytoskeleton by its influence on actin dynamics, activates important signal transducers such as Rho-associated coiled-coil kinase, which phosphorylates and thereby inactivates myosin light chain phosphatase and induces gene transcription via serum response factor.

Most RhoGTPases cycle between a GDP-bound inactive and a GTP-bound active state. The exchange of GTP for GDP and therefore activation is mediated through Rho guanine nucleotide exchange factors (RhoGEFs). In the case of RhoA the largest family of RhoGEFs is functionally and structurally characterized by a DH domain adjunct to a PH domain. The DH domain holds GEF activity and the PH domain has mainly regulatory functions. Some of these RhoGEFs can be activated by $G\alpha_{q/11}$ and/or $G\alpha_{12/13}$ and the present work focused on their regulation: Downstream of $G\alpha_{13}$ RH-RhoGEFs are activated. This group of RhoGEFs shares a regulator of G protein signaling homology domain (RH) in addition to the DH-PH domain, which is also present in the $G\alpha_q$-activated p63RhoGEF. Knock-out of the RH-RhoGEF leukemia-associated RhoGEF (LARG) protects against salt-induced hypertension in mice and the acute response of vascular smooth muscle cells to angiotensin II treatment is mediated mainly by p63RhoGEF. For both proteins several other physiological functions have been described. Nevertheless, little had been known about why RhoGEFs are activated downstream of two Gα subfamilies and the temporal as well as spatial dynamics of their receptor-mediated activation. Therefore we developed FRET-based assays monitoring RhoGEF activation in living cells for the first time.

The Förster resonance energy transfer (FRET) occurs between two fluorophores - in the present study fused to the proteins of interest - with a distance of less than 10nm. Thus an increase in FRET upon stimulation with the agonist reflects convergence of the proteins of interest. Changes in FRET were recorded in single, living cells with a high-speed CCD-camera.

The interaction between LARG and $G\alpha_{13}$ was monitored in cells transfected with $G\alpha_{13}$-mTur2 and YFP-LARG. The stimulation of thromboxane A2 receptor induced a robust increase in FRET. Surprisingly, as shown by the slow decrease in FRET between LARG and $G\alpha_{13}$, the interaction of LARG and $G\alpha_{13}$ dissociated very slowly (estimated $t_{1/2}$>5min) compared to the $G\alpha_{13}$ inactivation ($t_{1/2}$=17.50s). This observation was also reflected in the kinetics of LARG translocation to the plasma membrane. Thus LARG and $G\alpha_{13}$ interact rapidly upon activation of $G\alpha_{13}$, but either LARG inhibits $G\alpha_{13}$ inactivation or stays in a complex with $G\alpha_{13}$ after inactivation of the same. In our opinion the prolonged interaction is most likely the reason for the almost 100-fold higher

sensitivity towards stimulation with a thromboxane agonist of the $G\alpha_{13}$ LARG interaction compared with the $G\alpha_{13}$ activation.

The p63RhoGEF activation was studied by monitoring the interaction of $G\alpha_q$-CFP and Venus-p63RhoGEF. A robust increase in FRET was observed upon stimulation of $G\alpha_q$ coupled receptors. In contrast to the LARG $G\alpha_{13}$ interaction, the p63RhoGEF $G\alpha_q$ interaction mirrored closely the $G\alpha_q$ activation as well as inactivation. In addition also the sensitivity of p63RhoGEF $G\alpha_q$ interaction and $G\alpha_q$ activation was in the same range (EC_{50} of 500nM histamine). Both observations were also true in a trimeric complex of p63RhoGEF and $G\alpha_q$ with the regulator of G protein signaling RGS2. RGS2 was previously shown to accelerate $G\alpha_q$ inactivation *in vitro* and consequently we observed an accelerated dissociation of p63RhoGEF and $G\alpha_q$ in the presence of RGS2. Additionally, we could monitor an increase in FRET between p63RhoGEF and RGS2, which is the first evidence for such a trimeric complex in living cells. Thus our data strongly support the concept of a functional activation-dependent p63RhoGEF $G\alpha_q$ RGS2 complex. In this complex RGS2 inhibits downstream signaling. This could be an explanation for severe hypertension, which has been observed in RGS2 knock-out mice (Tang et al., 2003).

In summary, LARG as well as p63RhoGEF are both activated upon stimulation of G protein coupled receptors. Nevertheless LARG´s sensitivity towards receptor activation and duration of signaling seems to be remarkably higher and longer than p63RhoGEF´s. The inactivation of p63RhoGEF is further accelerated by RGS2, which also decreases downstream signaling.

Keywords: Förster resonance energy transfer (FRET), $G\alpha_q$, $G\alpha_{13}$, G protein coupled receptor (GPCR), histaminergic receptor, thromboxane A2 receptor, p63RhoGEF, leukemia-associated RhoGEF (LARG), regulator of G protein signaling 2 (RGS2)

Zusammenfassung

Die Aktivierung der RhoGTPasen durch G-Protein gekoppelte Rezeptoren ist wichtig für viele physiologische Funktionen wie zum Beispiel die Blutdruckregulation. Am besten sind die Unterfamilien Rho, Rac und Cdc42 der RhoGTPasen verstanden. In der vorliegenden Arbeit liegt der Fokus auf Signaltransduktions-Mechanismen, welche RhoA - ein Mitglied der Rho Unterfamlie - aktivieren. Aktives RhoA reguliert zum Beispiel das Zytoskelett durch seinen Einfluss auf die Aktin-Dynamik und reguliert die Rho-Kinase ROCK, welche die Myosin-Leichtketten-Phosphatase durch Phosphorylierung inaktiviert. RhoA induziert weiterhin mittels des Serum responsiven Faktors Gentranskription.

Die meisten RhoGTPasen wechseln zwischen einem GDP-gebunden inaktiven und einem GTP-gebunden aktiven Zustand hin und her. Der Austausch von GDP durch GTP und somit die Aktivierung wird durch Rho Guanin Austausch Faktoren (RhoGEFs) vermittelt. Die größte Familie der RhoA-aktivierenden RhoGEFs ist funktionell und strukturell durch eine DH Domäne und eine direkt anschließenden PH Domäne charakterisiert. Die DH Domäne stellt die GEF Aktivität bereit, die PH Domäne hat vor allem regulatorische Funktionen. Manche dieser RhoGEFs werden durch $G\alpha_{q/11}$ und/oder $G\alpha_{12/13}$ aktiviert. Die vorliegende Arbeit beschäftigt sich mit der Regulation dieser RhoGEFs. Unterhalb von $G\alpha_{13}$ werden RH-RhoGEFs aktiviert. Alle RH-RhoGEFs besitzen eine *Regulator of G protein signaling* homologe (RH) Domäne zusätzlich zur DH-PH Domäne, welche auch das $G\alpha_q$-aktivierte p63RhoGEF besitzt. Nach genetischer Depletion des RH-RhoGEFs LARG sind Mäuse gegen Salz-induzierten Bluthochdruck geschützt und die akute Reaktion auf Behandlung mit Angiotensin II fehlt den p63RhoGEF defizienten Mäusen. Für beide Proteine sind weitere physiologische Funktionen beschrieben. Trotzdem war bisher unklar, warum RhoGEFs durch zwei Gα-Unterfamilien aktiviert werden. Auch über die zeitliche und räumliche Dynamik der Rezeptor-vermittelten Aktivierung war wenig bekannt. Deshalb entwickelten wir FRET-basierte Messmethoden, welche es ermöglichen, die RhoGEF Aktivierung zum ersten Mal in lebenden Zellen zu beobachten. Förster Resonanz Energie Transfer (FRET) findet zwischen zwei Fluorophoren statt - in dieser Studie sind die Fluorophore an interessierende Proteine fusioniert –, welche einen Abstand von höchsten 10nm besitzen. Daher reflektiert ein Anstieg im FRET nach Stimulation mit dem Agonisten die Annäherung der interessierenden Proteine. In einzelnen, lebenden Zellen wurden Änderungen in FRET mit einer Hochgeschwindigkeitskamera detektiert.

Die Interaktion zwischen LARG und $G\alpha_{13}$ wurde in Zellen beobachtet, welche mit $G\alpha_{13}$-mTur2 und YFP-LARG transfiziert waren. Die Stimulation des Thromboxan A2 Rezeptors führte zu einem robusten Anstieg des FRET Signals. Wie sich in der langsamen Abnahme des FRET Signals zwischen LARG und $G\alpha_{13}$ zeigte, dissoziierten LARG und $G\alpha_{13}$ überraschenderweise deutlich langsamer ($t_{1/2}$>5min) als $G\alpha_{13}$ inaktivierte ($t_{1/2}$=17,50s). Dies konnte auch in der Kinetik der LARG Translokation zur Plasmamembrane beobachtet werden. Somit verursacht die Aktivierung des $G\alpha_{13}$, dessen schnelle Interaktion mit LARG. Bemerkenswerterweise inhibiert LARG entweder die $G\alpha_{13}$´s

Inaktivierung oder es bindet an $G\alpha_{13}$ auch nach dessen Inaktivierung. Wir gehen davon aus, dass die verlängerte Interaktion die Ursache für die fast 100fach erhöhte Sensitivität der LARG-$G\alpha_{13}$-Interaktion für die Stimulation mit einem Thromboxan Agonisten im Vergleich zur $G\alpha_{13}$-Aktivierung ist.

Die Aktivierung von p63RhoGEF wurde durch Beobachtung der Interaktion von $G\alpha_q$-CFP und Venus-p63RhoGEF untersucht. Ein robuster Anstieg im FRET wurde nach Stimulation von $G\alpha_q$-gekoppelten Rezeptoren detektiert. Im Gegensatz zur LARG-$G\alpha_{13}$-Interaktion reflektiert die p63RhoGEF-$G\alpha_q$-Interaktion zeitlich sehr genau sowohl die $G\alpha_q$-Aktivierung als auch seine Inaktivierung. Außerdem zeigen die p63RhoGEF-$G\alpha_q$-Interaktion und die $G\alpha_q$-Aktivierung eine ähnliche Sensitivität (EC_{50} von 500nM Histamin). Beide Beobachtungen wurden auch in einem trimären Komplex aus p63RhoGEF, $G\alpha_q$ und dem *Regulator of G protein signaling* RGS2 bestätigt. In der Vergangenheit wurde eine beschleunigte $G\alpha_q$-Inaktivierung durch RGS2 *in vitro* beschrieben und folgerichtig beobachteten wir eine beschleunigte Dissoziation von p63RhoGEF und $G\alpha_q$ in Anwesenheit von RGS2. Zusätzlich konnten wir einen Anstieg im FRET zwischen p63RhoGEF und RGS2 beobachten. Diese Beobachtung war der erste Beweis für diesen trimären Komplex in lebenden Zellen und unterstützt das Konzept eines funktionalen, aktivierungsabhängigen p63RhoGEF-$G\alpha_q$-RGS2-Komplexes. In diesem Komplex inhibiert RGS2 die nachgeordnete Signalweiterleitung. Dies könnte den deutlichen Bluthochdruck erklären, welcher für Mäuse ohne RGS2 beschrieben wurde (Tang et al., 2003).

Zusammenfassend werden sowohl LARG als auch p63RhoGEF durch die Stimulation der G-Protein gekoppelter Rezeptoren aktiviert. Trotzdem ist LARGs Sensitivität für die Rezeptoraktivierung deutlich höher und die Dauer der Signalweiterleitung länger als es für p63RhoGEF gezeigt wurde. Die Inaktivierung von p63RhoGEF wird zudem durch RGS2 weiter beschleunigt. Dies hat eine Abnahme der nachgeordneten Signalweiterleitung zur Folge.

Schlüsselworte: Förster Resonanz Energie Transfer (FRET), $G\alpha_q$, $G\alpha_{13}$, G-Protein gekoppelter Rezeptor (GPCR), Histamin Rezeptor, Thromboxan A2 Rezeptor, p63RhoGEF, Leukämie assoziiertes RhoGEF (LARG), *Regulator of G protein signaling 2* (RGS2)

4 Introduction

4.1 The GPCR Gα RhoGEF RhoGTPase signaling axis mediates signal transduction into and within cells

The human body consists of roughly $3.72*10^{13}$ cells (Bianconi et al., 2013). Inter- and intracellular signaling is essential for all physiological functions of the human body and is tightly regulated. Control of the signaling is achieved through changes in and detection of e.g. hormone levels within the body as well as by proteins, which function as cellular switches by cycling between an active and an inactive state.

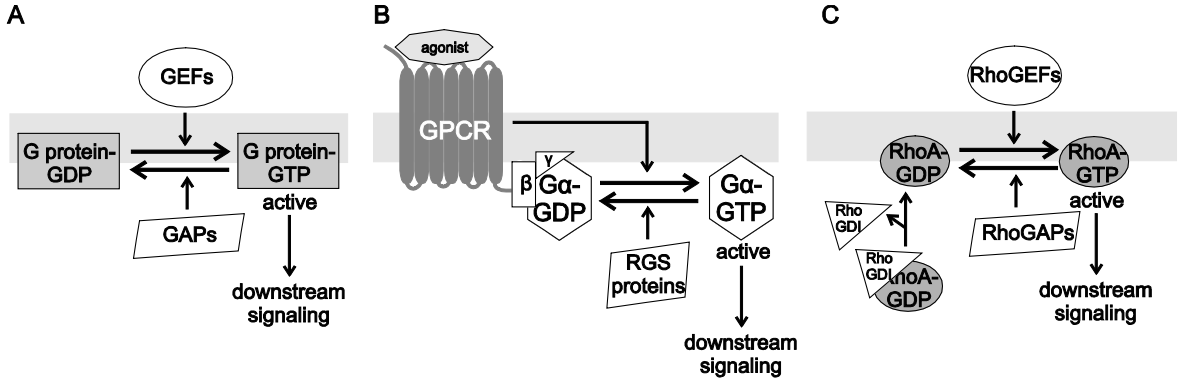

Fig. 1 The activation and inactivation of G proteins by GEFs, GAPs and GDIs
A G proteins exist in an active GTP-bound and in an inactive GDP-bound state. The proteins can cycle between the two states by hydrolysis of GTP and exchange of GDP for GTP. GTP exchange factors (GEFs) facilitate the latter, whereas GTPase activating proteins (GAPs) accelerate the intrinsic GTPase activity of the G protein. The GTP dissociation inhibitors (GDI) negatively regulate GTP binding. In ***B*** the G protein cycle is shown for trimeric G proteins and further Gβγ signaling was neglected for simplicity. In ***C*** the G protein cycle is shown for the small GTPase RhoA.

An omnipresent class of cellular switches are guanine nucleotide binding proteins (G proteins) and their regulation were in the focus of the present study (McCudden et al., 2005). These proteins exist in a guanosine-5´-triphosphate (GTP)-bound active conformation and a guanosine diphosphate (GDP)-bound inactive conformation (fig. 1A and (McCudden et al., 2005)). G proteins get inactivated by their intrinsic ability to hydrolyze GTP to GDP and inorganic phosphate (Gilman, 1987; Kaziro et al., 1991). The hydrolysis rate and the exchange of GDP for GTP are regulated processes (fig. 1A, (Kaziro et al., 1991)). GTPase activating proteins (GAPs) increase the hydrolysis rate and thus accelerate G protein inactivation (Siderovski and Willard, 2005). The binding of GDP to G proteins is regulated by guanine nucleotide exchange factors (GEFs) and guanine nucleotide dissociation inhibitors (GDIs). GDIs keep the G protein inactive by keeping GDP whereas GEFs activate the G protein by promoting GDP release and GTP binding (Goss et al., 1984). The G protein´s affinity is in the same range for GDP and GTP. Nevertheless GTP binds, because it is present in a 10 GTP:1 GDP stoichiometry in the cytosol (Bos et al., 2007).

The family of G proteins is subdivided into trimeric and small G proteins (fig. 1B, C and for further information see 4.3 and 4.4, respectively). Chapter 4.3 focuses on the trimeric G protein, the Gα subunit first and then on Gα´s GDI Gβγ. The trimeric G proteins are activated by their GEFs G protein coupled receptors (GPCRs, see also 4.2). These proteins build the largest receptor class and mediate a good portion of communication from the cell environment into the cell (Rosenbaum et al., 2009). The inactivation of trimeric G proteins is accelerated by GAPs, like the regulator of G protein signaling (RGS) protein family. They are discussed later (see 4.6) and one member of the family, RGS2, was studied in respect to regulation of $G\alpha_q$ in the present work. A multitude of effectors are activated by trimeric G proteins including GEFs for small G proteins. The RhoGEFs are discussed in more detail later on (see 4.5). The aim of this study was to gain further insights into the interaction of the RhoGEFs LARG and p63RhoGEF with their activators $G\alpha_q$ and $G\alpha_{13}$, respectively. Finally the RhoGEFs activate the small GTPase RhoA and this leads to further downstream signaling (see 4.4). The effect of the two mentioned RhoGEFs on the downstream signaling was also investigated in the present thesis. In summary, the present thesis investigated the temporal as well as spatial regulation of the GPCR Gα RhoGEF RhoGTPase signaling axis (see red arrows in fig. 2), with p63RhoGEF and LARG as model RhoGEFs. By this we aimed to supply missing information on the temporal as well as spatial regulation of this axis in living cells. Since this signaling axis is implicated in many physiological processes, as for example regulation of vascular tone (see 4.7).

4.2 GPCRs transduce extracellular signals into intracellular signaling cascades

Approximately 800 GPCRs are encoded in the human genome and roughly 36% of the established drugs as listed in *drug bank* target GPCRs (Ma and Zemmel, 2002; Fredriksson et al., 2003; Rask-Andersen et al., 2011). GPCRs generally transmit environmental signals into the cell, but some can also signal from intracellular membranes (Calebiro et al., 2010; Irannejad et al., 2013). They link the extra and intracellular space by seven membrane-spanning α-helices, a ligand binding site, which is accessible from the extracellular lumen and the binding site for downstream signaling partners at the intracellular face of the GPCR (Pogozheva et al., 1997).

An agonist binds to the ligand binding site and induces a conformational change of the agonist binding site within a few microseconds as assessed by simulation and nuclear magnetic resonance spectroscopy (NMR, (Dror et al., 2011a, 2011b; Nygaard et al., 2013)). This leads to changes in the transmembrane domains, mainly transmembrane helices III and VI. These changes are proceeded into the intracellular parts of the receptor, which recruits downstream signaling partners (Rosenbaum et al., 2009; Kahsai et al., 2011; Kobilka, 2013). The exact changes in conformation differ between receptors and may even differ at the same receptor according to various agonists (Kobilka and Deupi, 2007; Bhattacharya and Vaidehi, 2010). In general these major conformational changes were observed with rate constants of 30 to 50 ms for various GPCRs by means of

intramolecular fluorescence resonance energy transfer (FRET, (Vilardaga et al., 2003; Hoffmann et al., 2005, 2012; Hein et al., 2006; Maier-Peuschel et al., 2010; Ziegler et al., 2011)).
Mainly three protein families execute further downstream signaling: trimeric G proteins, G protein coupled receptor kinases (GRKs) and β-arrestins (Reiter et al., 2012). The active receptor serves as GEF for the recruited trimeric G protein and induces further signaling of the G protein subunits (see 4.3, (Tuteja, 2009)). GPCRs are entitled as G protein coupled receptors due to this mechanism. In contrast, GRKs and β–arrestin mediate a signaling pathway independent of G proteins.
β-arrestin is recruited by the active GPCR conformation and the GRK-dependent phosphorylation of the same. The interaction of β-arrestin with the GPCR competes with G proteins for binding to the GPCR, and thus antagonizes G protein dependent GPCR signaling (Lefkowitz, 1998). Furthermore β-arrestin binding triggers internalization of the receptor via clathrin-coated pits and thereby desensitizes the cellular response towards the agonist (Lefkowitz, 1998). Moreover, it became evident that GRK β-arrestin recruitment does not only induce desensitization, but in fact gives rise to a number of spatially and temporally G protein-independent signaling pathways, mainly by β-arrestin's function as scaffold protein (Reiter et al., 2012). Noteworthy, the signaling within the GPCRs can be modified by lipids, ions, allosteric modulators and voltage changes in close proximity to the receptor as well as homo- and heterooligomerization of receptors (Ponimaskin et al., 2002; Papoucheva et al., 2004; Terrillon and Bouvier, 2004; Ben-Chaim et al., 2006; Rinne et al., 2013; Katritch et al., 2014; Langmead and Christopoulos, 2014).

4.3 Trimeric G proteins are activated by GPCRs and regulate intracellular effectors

Heterotrimers are built by GDP-bound Gα and the obligate heterodimer Gβγ and are localized at the plasma membrane (McCudden et al., 2005). The trimeric G protein is recruited to a GPCR upon its activation (see 4.2). This leads to release of GDP from the Gα subunit, followed by GTP binding and subsequent severe conformational changes of Gα and Gβγ (see 4.3.1.1.) After activation, the G protein subunits transfer the signal to a distinct set of effector proteins (see fig 2, (Oldham and Hamm, 2008)). This is also the case if the G protein is already bound to an inactive GPCR, which is known as precoupling and may have some impact on activation-kinetics (Galés et al., 2006; Qin et al., 2008, 2011). The activation cycle is completed by hydrolysis of GTP to GDP (Oldham and Hamm, 2008).

4.3.1 The Gα subunit is the switch within the trimeric G protein

In mammals, 16 genes encoding Gα subunits have been identified (McCudden et al., 2005). These subunits can be sorted into four classes ($G\alpha_s$, $G\alpha_i$, $G\alpha_q$ and $G\alpha_{12}$) based on their primary sequence similarity (Simon et al., 1991). Recently, a fifth Gα class was identified, which is conserved across kingdoms including vertebrates, but is not found in the human genome (Oka et al., 2009). The classes are activated by different receptors and couple to different effectors (for some examples see fig 2). But until now it is not fully clear how specificity between receptors and G protein families is obtained, even though many contact sites are described between GPCR and G protein (Moreira, 2014). In 4.3.3 and 4.3.2 the $G\alpha_q$ and $G\alpha_{12}$ families will be described in more detail, as these two are the most important for the work presented in this thesis.

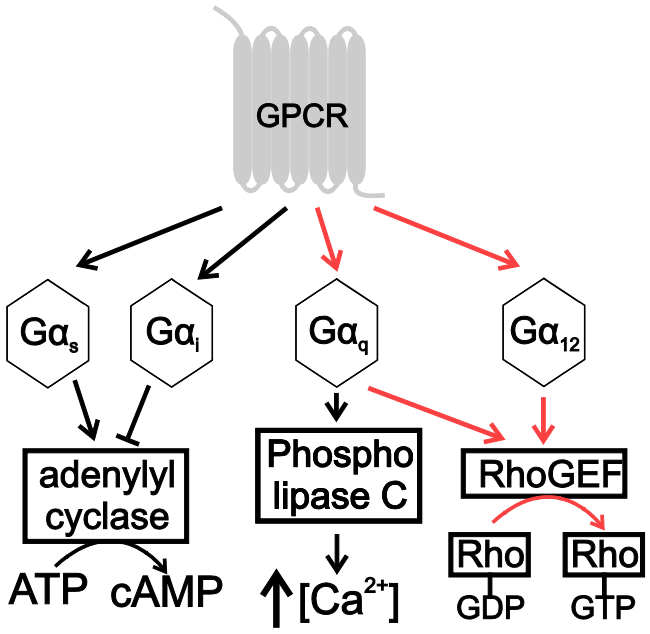

Fig. 2 The four Gα classes and their canonical effectors
Many different G protein coupled receptors (GPCRs) activate one or more classes of Ga subunits. Subsequently each class activates a distinct subset of effectors. This scheme shows the most prominent effector for each class as mentioned by McCudden et al. plus the more recently established link between $G\alpha_q$ and RhoGEFs (McCudden et al., 2005). This selection might not reflect physiological relevance. Further the activation of Gβγ and their effectors are neglected in the interest of simplicity. The red arrows indicate the two GPCR Gα RhoGEF Rho axes, which were the focus of the present study.

4.3.1.1 Structure and activation

The Gα subunit consists of a GTPase domain and a α-helical domain (see fig. 3). The GTPase domain is conserved in the entire G protein superfamily and the switch regions show significant conformational differences whether GTP or GDP is bound (Oldham and Hamm, 2008). The nucleotide binding pocket is hidden and further surrounded by the GTPase domain´s p-loop, switch I, II and III (Chung et al., 2011). Functionally, the GTPase domain is important for Gβγ binding and GTP hydrolysis. The helical domain is unique for the Gα subunits of the trimeric G proteins and consists of six α-helices, which form a lid over the nucleotide binding pocket (Oldham and Hamm, 2008). This domain increases affinity towards GTP and the GTP hydrolysis rate (Echeverría et al., 2000). All Gα subunits are lipid-modified at their N-terminus, mainly palmitylated. The lipid-modifications are crucial for structure and function of the Gα subunit and support its membrane localization (Degtyarev et al., 1994; Franco et al., 1996; Bhattacharyya and Wedegaertner, 2000; Preininger et al., 2003). The membrane localization of Gα is additionally supported by the Gβγ dimer (Sánchez-Fernández et al., 2014).

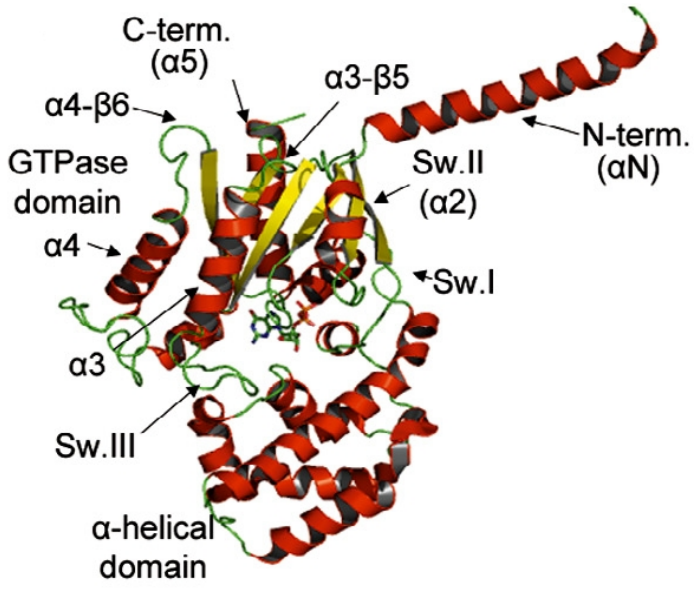

Fig. 3 Domains of the Gα subunit
Inactive Gβγ bound $G\alpha_{i1}$ structure as annotated by Baltoumas and colleagues ((Baltoumas et al., 2013), (PDB 1GP2)). The Gα subunit consists of the GTPase domain with the three switch (Sw.) regions, which bind GTP/GDP and a α-helical domain, which is unique for Gα subunits. The Gα subunits are lipid modified at their N-terminus (N-term.), which is crucial for localization at the plasma membrane.

Scientists have been investigating the binding of the Gα subunit to the GPCR and subsequent conformational changes within the G protein for a long time. Already in 1988 the Gα´s C-terminus was described as a binding site for GPCRs (Hamm et al., 1988). The crystal structure resolved the nucleotide-free $G\alpha_s$ subunit in complex with the β_2 adrenergic receptor (β_2-AR) (Rasmussen et al., 2011). In this structure the Gα´s C-terminus interacts indeed with the GPCR and additionally the Gα´s αN-β1 hinge and the α4/β6 region (Chung, 2013). However, as a basic rule dynamic movements in a protein *in vivo* should be considered, which may not be reflected in crystal structures of the protein. This is true for the Gα´s α-helical domain. Here, conformational plasticity was observed by NMR studies and electron microscopy experiments and is not represented in the crystal structure (Abdulaev et al., 2006; Rasmussen et al., 2011; Westfield et al., 2011). The helical domain of Gα has to move substantially in order to bind to the active GPCR as suggested by the crystal structure (Chung, 2013). The nucleotide binding pocket opens by this movement (Chung, 2013). No further changes are observed within Gα´s core. Nevertheless also the C-terminus and the neighboring α5 helix of the Gα subunit move upon activation (Chung, 2013). The described changes in Gα structure occur probably simultaneously with GDP release. Sequentially GTP binds and the trimeric G protein undergoes severe conformational changes. Upon hydrolysis of GTP to GDP the activation cycle terminates. Gα itself hydrolyzes GTP rather slowly, but Gα is a faster GTPase than RhoGTPases. This step can be accelerated by RGS proteins (see 4.6, (Sánchez-Fernández et al., 2014)).

Whether the rearrangement within the Gα subunit leads to dissociation of the trimeric complex or not is still under debate and may be subtype specific (Oldham and Hamm, 2008; Vilardaga et al., 2009; Bondar and Lazar, 2014): *In vitro* experiments initially introduced the idea of subunit dissociation (Hamm, 1998). But with this working model Gα subtype specific Gβγ effects could not be explained (Sadja et al., 2003). In line with this an increase in FRET for $G\alpha_i$ activation was found in living cells, which also contradicted subunit dissociation ((Bünemann et al., 2003; Frank et al., 2005), for details on FRET see 5.2.6.1, please). This finding was reproduced by bioluminescence resonance energy transfer (BRET, (Galés et al., 2006)). Additionally, Gβγ was less mobile when $G\alpha_i$ and $G\alpha_s$ were

activated than if $G\alpha_o$ was activated as measured by fluorescence recovery after photobleaching (FRAP) and also this data favor the idea of rearrangement for some Gα subtypes (Digby et al., 2006). A recent study investigated G protein dissociation by two-photon polarization microscopy and instead of fluorophore insertion this workgroup used N-terminally fluorophore-labeled Gα subunits, but to the author´s knowledge for such Gα constructs functionality in terms of inactivation kinetics has not been evaluated in detail (Bondar and Lazar, 2014). Bondar and Lazar postulated the rearrangement seen in FRET is due to the site of fluorophore insertion into the Gα subunit. Nevertheless, also this workgroup does not describe dissociation as a mandatory step for effector activation (Bondar and Lazar, 2014). All these studies were done under G protein overexpression conditions and ratio of effectors to G proteins is thus greatly reduced compared to untransfected cells. Therefore in overexpression the low affinity within the trimeric G protein might be sufficient for their further interaction after Gα activation, whereas under endogenous conditions the presence of effector with high affinity for the G protein subunits might force the trimeric G protein to dissociate (M. Bünemann, personal communication).

4.3.1.2 Effector recognition and activation, a mainly indirectly studied process

The effector recognition of active Gα is maintained by the GTPase domain, precisely switch II and α3 helix and its junction with β5 strand (fig. 3). This junction, also known as α3-β5 loop, differs both in sequence and in structure between Gα subtypes and thereby maintains effector specificity (Sprang et al., 2007; Baltoumas et al., 2013). Nevertheless, the GTPase domain structure is conserved between the four Gα families (Baltoumas et al., 2013). But structural similarity does not include electrostatic similarity and Baltoumas et al. suggest electrostatic differences as important determinate of specificity for both Gα effector and Gα RGS interactions (Baltoumas et al., 2013). In the GTPase domain a hydrophobic canyon opens upon GTP binding (Aittaleb et al., 2010). The recognized effector binds to Gα by a hydrophobic chain, which inserts into the N-terminal part of α2 helix (SwichII) and α3 helix (Sánchez-Fernández et al., 2014). For $G\alpha_q$ the same was observed in crystal structures with three different effectors, namely phospholipase C (PLC) β3, p63RhoGEF and GRK2 (Tesmer et al., 2005; Lutz et al., 2007; Waldo et al., 2010). All three effectors bind alike to $G\alpha_q$.

Binding to Gα influences effectors in many fashions: $G\alpha_i$ is an allosteric inhibitor of adenylyl cyclase, whereas $G\alpha_s$ allosterically activates and inhibits this enzyme. In case of guanosine monophosphate phosphodiesterase (PDE) $G\alpha_t$ (Transducin) sequesters an autoinhibitory subunit and thereby activates the enzyme (Sprang et al., 2007). Also the $G\alpha_q$ effectors PLCβ and p63RhoGEF are released from autoinhibition (Sánchez-Fernández et al., 2014). Further $G\alpha_q$ seems to work as a scaffold in case of extracellular signal-regulated kinase 5 (ERK5) and protein kinase C (PKC) ζ (García-Hoz et al., 2010).

The authors of this study mainly investigated effects on ERK5 phosphorylation and extrapolated from this to PKC activation. Notably, such a study design is rather common for investigations on regulation of effectors by G protein. To our knowledge in all early studies on adenylyl cyclase regulation by $G\alpha_s$ and $G\alpha_i$ and PLCβ3 regulation by $G\alpha_q$ cAMP and either PIP_2 or IP_3 levels were measured as surrogate for effector activation, respectively. Furthermore in some cases, like LARG activation by $G\alpha_q$, reporter gene activity far downstream of the effector was used as read-out (Pfreimer et al., 2011). The direct interaction between effector and G protein was shown by pull down experiments and later crystal structures were resolved for several effector G protein interactions, which gave direct but static insight into their interaction mode. Hence, the information on the kinetic of regulation was rather limited. Nevertheless already in 1989 the immediate inactivation of PDE upon $G\alpha_t$ inactivation was elucidated by measurement of free P_i due to GTP hydrolysis and pH change due to cGMP hydrolysis in the same sample (Arshavsky V. Yu. et al., 1989). Noteworthy, in earlier studies deactivation of the signaling cascade was found considerably slower than observed *in vivo* which was caused by non-physiological stoichiometry of signaling partners. In the mentioned study they increased concentrations and temperature and could than measure kinetics close to *in vivo*. This shows the limitations of biochemical approaches, since kinetics may be differ between *in vitro* and in cells due to different conditions of the interaction partners.

The first dynamic studies in living cells investigated channel opening and closing upon stimulation of GPCRs by electrophysiological methods, like for example GIRK activation by Gβγ (Dascal, 1997). The kinetics of GIRK currents upon receptor stimulation were closely resembled by activation and inactivation of $G\alpha_i$, which were determined by FRET (Bünemann et al., 2003). Also the inhibition of N-type Ca^{2+} channels by Gβγ was studied in detail by electrophysiological recordings and with regulation-block by site-specific peptides also the interaction sites were mapped (as reviewed in (Zamponi and Snutch, 1998; Zamponi and Currie, 2013)). Investigation of other effectors in living cells was hindered by the lack of electrophysiological read-outs. Hence, another method had to be applied. Therefore first FRET-based assays were developed, which monitored fluorophore labeled G protein subunits and fluorophore labeled effectors in living cells (Zhou et al., 2003). To date, such assays have been invented for effectors of different G protein families, like the interaction of adenylyl cyclase V with $G\alpha_i$, $G\alpha_s$ and Gβγ (Milde et al., 2013) or PLCβ3 and GRK2 with $G\alpha_q$ ((Pollinger, 2012) and Wolters et al., under revision). As shown in the present study and by T. Pollinger (Pollinger, 2012) the interaction of PLCβ3 with $G\alpha_q$ resembled closely $G\alpha_q$ activity, whereas Milde and coworkers found a prolonged interaction between $G\alpha_i$ and adenylyl cyclase V compared to $G\alpha_i$ activation (Milde et al., 2013). They suggested, that this prolonged interaction might explain earlier findings of higher sensitivity of cAMP production compared with activation of the Gα subunit. Nevertheless, many other important effectors of trimeric G proteins have not been studied in such depth yet, like any of the $G\alpha_{12/13}$ effectors. The present study provided the first data on dynamics of interaction of the effector LARG with $G\alpha_{13}$ and on the interaction of p63RhoGEF with $G\alpha_q$.

4.3.2 The $G\alpha_{12}$ family activates RhoGEFs and other effectors

The $G\alpha_{12}$ family consists of $G\alpha_{12}$ and $G\alpha_{13}$, which are both conserved among species and their mRNAs are shown to be expressed ubiquitously (Simon et al., 1991; Strathmann and Simon, 1991; Wilkie and Yokoyama, 1994). Both proteins are palmitylated at their N-terminus and thereby are directed to the plasma membrane (Bhattacharyya and Wedegaertner, 2000; Waheed and Jones, 2002). $G\alpha_{12}$ was found in lipid-rafts whereas $G\alpha_{13}$ did not localize to this microdomain (Waheed and Jones, 2002). The differences in localization and structure might explain functional differences between $G\alpha_{12}$ and $G\alpha_{13}$. The structural differences have been observed in chimeric crystal structures of both family members with $G\alpha_i$ (Kreutz et al., 2006). One example is the enlarged αB-αC loop in $G\alpha_{13}$, which is suggested to be responsible for different GAP activities of the same effector towards the two Gα subunits (Kreutz et al., 2006). Besides these differences $G\alpha_{12}$ and $G\alpha_{13}$ behave rather similar in regard to slow intrinsic rates of GTP hydrolysis and GDP GTP exchange (Singer et al., 1994; Kozasa and Gilman, 1995).

Many GPCRs activate $G\alpha_{12/13}$, but to find and conform GPCRs with $G\alpha_{12/13}$-selectivity is challenging (Riobo and Manning, 2005). Most GPCRs, which couple to $G\alpha_{12/13}$, couple also to other G proteins, in particular to $G\alpha_q$. In this study the thromboxane A_2 receptor was used to activate $G\alpha_{13}$, which coupled to $G\alpha_{12/13}$ and $G\alpha_q$ in platelets (Offermanns et al., 1994). Additionally, different G protein families may converge on the same downstream target.

Effectors

The best characterized downstream target of the $G\alpha_{12}$ family is RhoA (4.4.1, (Worzfeld et al., 2008)). Like for $G\alpha_q$ and its effector p63RhoGEF (4.5.2), RhoA is not activated directly by the G protein. Instead $G\alpha_{12/13}$ activates RhoGEFs, which then activate RhoA (4.5.1). Vogt et al. showed Rho activation in pertussis toxin treated, $G\alpha_{q/11}$ deficient cells as well as $G\alpha_{12/13}$ deficient cells (Vogt et al., 2003). Additionally, $G\alpha_{12}$ and $G\alpha_{13}$ interact with type I and type II classical cadherins. The cadherin´s adhesive function is blocked by $G\alpha_{12/13}$ binding and subsequently the transcriptional activator β-catenin is released. This affects cell migration independent of RhoA (Meigs et al., 2001, 2002). Interestingly, the interaction between cadherins and $G\alpha_{13}$ relies on different amino acids than RhoGEF binding (Meigs et al., 2005). Since this information was gained in the context of constitutive active Gα subunits, the physiological relevance of this signaling pathway is not yet known (Kelly et al., 2007). Furthermore interactions of $G\alpha_{13}$ with radixin have been described, which might activate the Ca^{2+}/calmodulin-dependent kinase II (CaMKII) and might have some impact on $G\alpha_{13}$-mediated Rac activation (Liu and Voyno-Yasenetskaya, 2005). Radixin might also be indirectly activated down-stream of Rho (Kelly et al., 2007).

Additional interactions have been described between the $G\alpha_{12}$ family A-kinase anchoring proteins, non-receptor tyrosine kinases and protein phosphatases, even though the physiological relevance is not yet fully understood for these interactions (Kelly et al., 2007; Worzfeld et al., 2008).

Regulation of the $G\alpha_{12/13}$ family

Regulation of $G\alpha_{12/13}$ occurs by the GAP activity of the RhoGEFs described before (see 4.5.1) and by phosphorylation (Kozasa et al., 2011). Phosphorylation of $G\alpha_{13}$ blocks its activation and is mediated by protein kinase A (PKA) (Manganello et al., 2003). Whereas $G\alpha_{12}$ is phosphorylated by PKC, which decreases the affinity of $G\alpha_{12}$ for $G\beta\gamma$ (Kozasa and Gilman, 1996).

Physiology and pathology

Knock-out studies revealed non-redundant functions for $G\alpha_{12}$ and $G\alpha_{13}$, as $G\alpha_{12}$ knock-out mice showed no apparent abnormalities and $G\alpha_{13}$ knock-out was embryonic lethal (Offermanns et al., 1997; Gu et al., 2002). In endothelial cells $G\alpha_{13}$ was found essential for proper angiogenesis and in platelets for cell shape changes upon activation and aggregation (Moers et al., 2003). These phenotypes were probably caused by loss of cell shape regulation, cell movement, cell cell or cell matrix interactions as well as cell polarization (Worzfeld et al., 2008). Many other physiological phenotypes of $G\alpha_{12/13}$ rely on these effects, as for example regulated neuronal and B-cell migration and leukocyte adhesion (Moers et al., 2003, 2008; Francis et al., 2006; Rieken et al., 2006).

In regard to cancer the $G\alpha_{12}$ family is of special interest as their wild type genes are considered oncogenes in contrast to the members of all other $G\alpha$ families due to their transforming ability (Xu et al., 1993, 1994). Furthermore, $G\alpha_{12}$ was found upregulated in human breast and prostate adenocarcinoma tissue (Kelly et al., 2006a, 2006b). Interestingly, metastatic spread was reduced in a xenograft model by blockade of $G\alpha_{12}$ and $G\alpha_{13}$ signaling in murine breast cancer cells. But this blockade did not influence either tumor growth or metastasis rate, if cells were injected into the blood stream (Kelly et al., 2006a, 2007).

$G\alpha_{13}$ is not required to maintain basal heart function, but seems to be essential for α_1 adrenergic receptor induced hypertrophic response, pressure-overload induced hypertrophy and heart failure *in vivo*, as studied in mice with a conditional, heart-specific $G\alpha_{13}$ knock-out (Maruyama et al., 2002; Takefuji et al., 2012). Further the pathological progression of pressure-overload induced hypertrophy seems to depend on LARG activation by $G\alpha_{13}$ (4.5, (Takefuji et al., 2013)). $G\alpha_{12}$ and $G\alpha_{13}$ are together with $G\alpha_q$ of crucial importance for vascular tone (4.7, (Schoner, 2008)). Several examples are described for crosstalk between $G\alpha_{12/13}$ and other G proteins, mainly $G\alpha_q$ (as reviewed by (Suzuki et al., 2009a)).

4.3.3 The $G\alpha_q$ family activates p63RhoGEF besides its canonical effector PLCβ

The $G\alpha_q$ family is composed of four members and conserved among species (Wilkie and Yokoyama, 1994): $G\alpha_q$ is ubiquitously expressed, $G\alpha_{11}$ is found everywhere except platelets, whereas $G\alpha_{14}$ is mainly found in kidney, liver and lung and $G\alpha_{16}$ in the hematopoietic system (Hubbard and Hepler, 2006). The human $G\alpha_{16}$ is considered to be an orthologue of mouse $G\alpha_{15}$ (Wilkie et al., 1992). Noteworthy, the amino acid sequence is conserved the least among this family compared to the other

Gα families and the differences occur within the nucleotide binding pocket as well as in the N- and C-terminus (Wilkie et al., 1991). Maybe, due to this $G\alpha_{15/16}$, and to a lesser extent $G\alpha_{14}$, were shown to be activated by $G\alpha_s$ and $G\alpha_{i/o}$ coupled GPCR (Hubbard and Hepler, 2006).

The $G\alpha_q$ effectors: PLCβ and p63RhoGEF

Far more research has been done on $G\alpha_q$ and $G\alpha_{11}$ than on the other two members. However in the following comparative knowledge is reviewed about effector binding by all family members:

PLCβ isoforms are the classic effectors of $G\alpha_q$ family members (Rebecchi and Pentyala, 2000; Rhee, 2001). Additionally, PLCβ 2 and 3 can be activated by Gβγ (Camps et al., 1992; Park et al., 1993). In general all active PLCβ isoforms cleave phosphatidylinositol 4,5 bisphosphate (PIP_2) into the two second messengers inositol 1,4,5 trisphosphate (IP_3) and diacylglycerol (DAG, (Rhee, 2001)). Subsequently Ca^{2+} is released from intracellular stores and PKC is activated (Sánchez-Fernández et al., 2014). Consequently, the determination of IP_3 production by cell lysates is the commonly used method to investigate PLC activity (e.g. (Camps et al., 1992; Park et al., 1993; Lyon et al., 2011)). Recently, T. Pollinger established a FRET-based assay to study PLCβ3 $G\alpha_q$ as well as PLCβ3 Gβγ interaction in single living cells (Pollinger, 2012).

Activation of all $G\alpha_q$ family members potentially leads to activation of all PLCβ isoforms by relief of PLCβ from autoinhibition (Hubbard and Hepler, 2006; Lyon et al., 2011). However, the family members differ in their activation efficacy towards PLCβ isoforms and the PLCβ isoforms show varying expression patterns. Taken together this may lead to isoform-specific PLCβ signaling under physiological conditions (Hubbard and Hepler, 2006).

p63RhoGEF is the second best described $G\alpha_q$ effector besides PLCβ, which is $G\alpha_q$ family specific (Lutz et al., 2005; Sánchez-Fernández et al., 2014). This protein activates Rho signaling by exchange of GDP for GTP on RhoA and was shown to compete with PLCβ for $G\alpha_q$ binding by biochemical assays (Lutz et al., 2005). RhoGEF activation downstream of $G\alpha_q$ seems to be a conserved mechanism like signaling from $G\alpha_q$ to PLCβ, as UNC-73 (homolog of Trio RhoGEF) was found in *C. elegans* (Williams et al., 2007). In general activation of RhoA induces stress fiber formation, is involved in cell contraction and during cell movement it is important for following of body and tail behind the leading edge (for details 4.4.1, (Etienne-Manneville and Hall, 2002)). p63RhoGEF binds also to $G\alpha_{16}$ and blocks its PLCβ activation, but surprisingly this binding does not result in Rho signaling (Yeung and Wong, 2009). This indicates yet another level of signaling differences between the $G\alpha_q$ family members, as effectors may change their function from real effectors towards a role as effector antagonist at certain $G\alpha_q$ family members. The competitive behavior of p63RhoGEF and PLCβ3 towards $G\alpha_q$ will be discussed in more detail later on (see 4.5.2.1 *PLCβ3 overlaps with p63RhoGEF and RGS2 binding to $G\alpha_q$*). Trio is another RhoGEF activated by $G\alpha_q$ and this one activates Rac in addition to Rho (see 4.5.2.1 *Trio and Kalirin, the complex siblings of p63RhoGEF*, (Vaqué et al., 2013)).

RGSs and GRKs regulate $G\alpha_q$ signaling

$G\alpha_{14}$ and $G\alpha_{15/16}$ are even less studied in terms of regulation by RGS proteins (see 4.6). Only one study focused on this topic in regard to $G\alpha_{14}$ and $G\alpha_{15/16}$ and showed blockade of $G\alpha_{16}$ signaling by RGS2 (Day et al., 2003). RGS2 is a member of the B/R4 subfamily of RGS proteins and as most of the subfamilies' members RGS2 negatively regulates $G\alpha_q$ and $G\alpha_{11}$ by its GTPase activity (Hubbard and Hepler, 2006). Additionally some RGS proteins work as effector antagonists for PLCβ by overlap of their and PLCβs binding sites (Hepler et al., 1997; Anger et al., 2004).

The previously described GRKs not only bind and phosphorylate GPCRs, but some of them bind also specifically to $G\alpha_q$ family members and block their signaling again as effector antagonists. Binding was described for active $G\alpha_q$ and $G\alpha_{11}$ with GRK2 and GRK3 (Carman et al., 1999). GRK2 blocks signaling by all $G\alpha_q$ family members besides $G\alpha_{16}$, probably by occupation of the effector binding site (Day et al., 2003). So signal attenuation is induced by GRK2 via GPCR internalization, as described earlier (see 4.2), and blockade of the effector binding site at $G\alpha_q$.

Physiology

$G\alpha_q$ mediates a wide variety of physiological and pathological functions, like hormone release, innate and adaptive immunity, hepatic glucose fluxes, long-term depression, platelet activation and induces either apoptosis or proliferation (Sánchez-Fernández et al., 2014). A somatic gain of function mutation within the $G\alpha_q$ encoding GNAQ gene results in port-wine stains and the Struge-Weber syndrome, a sporadic congenital neurocutanous disorder (Shirley et al., 2013). Similarly activating mutations were found in the $G\alpha_q$ and $G\alpha_{11}$ in approximately 80% of all uveal melanomas (van Raamsdonk et al., 2010). Also in the heart, $G\alpha_{q/11}$ signaling is crucial, as double knock-out mice died at embryonic day 11 due to heart malformation and overexpression of $G\alpha_q$ induced heart hypertrophy (Offermanns et al., 1998; Fan et al., 2005). In addition the double knock-out mice showed craniofacial defects. As described in detail later (4.7) $G\alpha_q$ together with $G\alpha_{12/13}$ plays an important role in vascular tone (Schoner, 2008).

4.3.4 The Gβγ subunits activate their own set of effectors

The second part of the trimeric G protein is the obligate heterodimer Gβγ. In human, five Gβ subunits and twelve Gγ subunits have been identified. All Gβ subunits show high sequence similarity except $G\beta_5$ and also Gγ subunits are more diverse (Khan et al., 2013). Some specificity in Gβ Gγ association is described, as for example $G\beta_2$ cannot pair with $G\gamma_1$ (Schmidt et al., 1992). The Gβ subunit forms a propeller of seven blades and an α-helical N-terminus (Oldham and Hamm, 2008). The blades are formed by seven WD40 sequence repeats, which are tryptophan-aspartic acid sequences that repeat about every 40 amino acids and form small antiparallel β strands (Neer et al., 1994). Gβ interacts by its N-terminus as well as the fifth and sixth bladder with the two α-helices, which form Gγ (Wall et al., 1995; Sondek et al., 1996). The dimer is localized at the plasma membrane due to a C-terminal

prenylation of the Gγ subunit, which is either a 15-carbon farnesyl moiety or a 20-carbon geranylgeranyl group (Wedegaertner et al., 1995).

Upon activation of the trimeric G protein, the structure of Gβγ changes only minutely but an extensive, relatively hydrophobic surface becomes accessible for effectors (Sondek et al., 1996; Aittaleb et al., 2010). This surface is a part of the effector recognition site (Davis et al., 2005). Upon GTP hydrolysis Gα reassociates with Gβγ and this terminates Gβγ´s signaling to effectors (Ford et al., 1998; Li et al., 1998).

Gβγ activates a variety of effectors

The first effector described for Gβγ was the G protein regulated inward rectifier K^+ channel (Kir, (Logothetis et al., 1987)). In the next years other effectors were found, like voltage-dependent N- and P/Q-type Ca^{2+} channels, Erk1/2 (extracellular signal-related kinase), c-Jun N-terminal kinase, mitogen-activated protein kinase, various adenylyl cyclase isoforms, PLCβ3, GRK2 and 3 and the RacGEF P-Rex1 (McCudden et al., 2005). The regulation of adenylyl cyclase is an example for regulation of a single protein by Gα subunits as well as Gβγ at the same time (Tang and Gilman, 1991). The interaction with all effectors, which have been mentioned, occurs at the plasma membrane. In addition Gβγ signaling was described also in other cellular compartments, like mitochondria, endoplasmic reticulum and nucleus (Khan et al., 2013). It´s not clear whether all of these interactions depend on activation of the trimeric G protein.

Physiology

The physiological role of Gβγ was clarified in several knock-out studies and also a polymorphism was described for $Gβ_3$. This polymorphism caused a truncated splice variant, which is unable to modulate Kir3 and calcium channels (Ruiz-Velasco and Ikeda, 2003). Additionally, the polymorphism was associated with a wide variety of pathologies, like hypertension, gastrointestinal disease, depression, obesity and therapy complications, like increased bleeding time (Khan et al., 2013).

4.4 The Rho family of small G proteins regulates mainly the cytoskeleton

The largest family within the Ras superfamily of small GTPases is the Ras homologous (Rho) family with 23 genes in human (Jaffe and Hall, 2005; Bustelo et al., 2007). The best characterized RhoGTPases RhoA, Rac and Cdc42 control the actin cytoskeleton and transcription factors, like Serum response factor (SRF) and nuclear factor κB (NFκB, (Ridley, 2006)). In addition, more than 90 other Rho effectors are described, like protein kinases, phospholipases, actin regulators and adaptor proteins (Jaffe and Hall, 2005; Ridley, 2011). It´s challenging to identify, yet unknown Rho effectors in the genome, since the RhoGTPases´ effectors lack a common well-defined RhoGTPase recognition site (Cook et al., 2014). The present study focused on regulatory processes, which tightly control RhoA activation.

RhoGTPases are regulated by RhoGEFs, GAPs and GDIs

Most small G proteins cycle between active GTP-bound and inactive GDP-bound state, alike the Gα subunits of trimeric G proteins (fig. 1C, 4.1). The intrinsic GTPase rate of RhoGTPases is rather low and can be accelerated by RhoGAPs (Ridley, 2013). Additionally, their affinity is high for GDP and GTP and this results in a dissociation half life of one or more hours (Bos et al., 2007). The exchange of the nucleotides and therefore the activation is mediated by RhoGEFs (4.5). The GTP hydrolysis is accelerated by RhoGAPs and additionally, Rho guanine nucleotide dissociation inhibitors (RhoGDIs) negatively regulate some RhoGTPases. They bind to Rho-GDP and sequester it into the cytosol (Garcia-Mata et al., 2011). In the absence of RhoGDIs most RhoGTPases are localized at the cell membrane due to post-translational modifications (Cook et al., 2014). The post-translational modifications are one or two lipid groups at their C-terminus. These lipid groups are prenyl groups, either farnesyl and geranylgeranyl, or a palmitoyl group (Wennerberg and Der, 2004). RhoGDIs can only bind the prenyl group into a hydrophobic pocket and additionally, hide the RhoGTPase´s effector binding site (Garcia-Mata et al., 2011). For some RhoGTPases, like RhoA, further post-translational modifications are described.

Physiology

Cellular processes such as cell shape, cell migration, cell cycle progression and gene transcription are regulated by RhoGTPases (Etienne-Manneville and Hall, 2002). These effects occur mainly by the Rho family´s effect on actin and microtubule dynamics (Ridley, 2011).

The three Ras proteins are commonly mutated in cancer. In contrast, until now RhoGTPases were not found mutated in cancer, with the exception of an activating Rac1 mutant in melanoma (Cook et al., 2014). But nevertheless RhoGTPases are often more active in cancer tissue than in healthy tissue. This is due to indirect activation by changes in their expression or in the activity of their regulators (Cook et al., 2014).

4.4.1 The Rho subfamily

In 1985, the members of the Rho subfamily RhoA, RhoB and RhoC were the first RhoGTPases discovered in humans (Madaule and Axel, 1985). They show a sequence homology of 88% and differ only in their C-terminal last nine to twelve amino acids and in their post-translational modification (Wheeler and Ridley, 2004; Ridley, 2013). RhoB is prenylated and palmitylated, whereas RhoA and RhoC are only prenylated (Wennerberg and Der, 2004). Further RhoA can be phosphorylated and ubiquitinated, which then leads to either its translocation into the cytosol or its degradation, respectively (Lang et al., 1996; Nethe and Hordijk, 2010). In general RhoA and RhoC localize at the plasma membrane and in the cytoplasm, whereas RhoB is mainly localized in endosomes (Adamson et al., 1992; Zalcman et al., 1995). The RhoA subfamily is activated by RhoGEFs (4.5) and also β-arrestin 1 was described to activate RhoA (Barnes et al., 2005). The activation of RhoA leads to stress fiber and focal adhesion formation as shown in early studies with murine fibroblasts, which is a

phenotype distinct from the one caused by Rac and Cdc42 activation (Ridley and Hall, 1992; Ridley et al., 1992; Nobes and Hall, 1995).

The diverse physiological functions of the RhoA subfamily

In 1993, RhoA, RhoB, RhoC were shown to be essential for cytokinesis with the help of the C3 exoenzyme (Kishi et al., 1993). In the following years the RhoA subfamily was found important in many cellular functions, like transcription, cell transformation or cell cycle progression in cell culture (Jaffe and Hall, 2005). Complete RhoA knock-out is embryonic lethal at early developmental stages (Pedersen and Brakebusch, 2012). Therefore, several conditional RhoA knock-outs were introduced in different cell types of the nervous and the hematopoetic system as well as keratinocytes, lens epithelium and cardiomyocytes (Chauhan et al., 2011; Herzog et al., 2011; Jackson et al., 2011; Katayama et al., 2011, 2012; Xiang et al., 2011; Cappello et al., 2012; Pleines et al., 2012; Zhang et al., 2012). For example RhoA knock-out in the hematopoetic system resulted in impaired platelet formation, blood clotting and inhibition of B cell development (Zhou and Zheng, 2013). The consequence of RhoA knock-out in a tissue is probably influenced by expression of RhoB and RhoC and their compensatory upregulation. Such a compensatory upregulation of RhoB and RhoC was described in RhoA knock-out fibroblasts for example (Melendez et al., 2011).

The endosome localized RhoB was shown to be involved in endocytosis and vesicle trafficking *in vitro* (Mellor et al., 1998; Sandilands et al., 2004). RhoB knock-out mice were viable, but suffered from retarded retinal vascularization, caspase-3 dependent neuronal apoptosis, thymus atrophy, impaired neuronal morphology and synaptic plasticity and were prone to develop carcinogen induced skin cancer (Liu et al., 2001; Adini et al., 2003; McNair et al., 2010; Barberan et al., 2011; Bravo-Nuevo et al., 2011). RhoA was shown to stimulate cell cycle progression and cytokinesis, regulate cell migration and to be upregulated in many different tumor types (Vega and Ridley, 2007; Ridley, 2013). Also RhoC is over expressed in a variety of cancers and additionally, the number of metastases seems to correlate positively with its expression (Karlsson et al., 2009; Thumkeo et al., 2013). In line with this RhoC knock-out mice did not show any metastasis in a lung cancer model (Hakem et al., 2005).

Amongst others, ROCK is activated by the Rho subfamily

During the mid-90s multiple Rho effectors were cloned including Rhotekin, Rhophilin, PKN, Citron, Rho-associated coiled-coil kinase (ROCK) and mDia (Leung et al., 1995; Madaule et al., 1995; Reid et al., 1996; Watanabe et al., 1996, 1997). RhoC was shown to activate the formin FMNL3, which is not activated by RhoA (Vega et al., 2011). Details on the effectors ROCK, Rhotekin and transcriptional activation downstream of the RhoA subfamily can be found below:

RhoA activates the serine/threonine kinase ROCK, which in turn phosphorylates and activates myosin light chain (MLC) and inactivates MLC phosphatase (MLCP, fig. 4 ,(Amano et al., 1996; Kimura et al., 1996)). Additionally, ROCK activates LIMK, which leads to inactivation of the actin depolymerisation factor cofilin (Maekawa et al., 1999; Ohashi et al., 2000). By these two mechanisms

ROCK regulates myosin and actin dynamics downstream of RhoA. Noteworthy, ROCK is also activated independent of RhoA for example by Caspase-3 and granzyme B (Sebbagh et al., 2005). ROCK is important in cell migration, cell cell adhesion, transcription, apoptosis, axonogenesis and T cell function (Hirose et al., 1998; Itoh et al., 1999; Sahai et al., 1999; Coleman et al., 2001; Sahai and Marshall, 2002; Heasman et al., 2010). Furthermore, as shown in rats ROCK is important in blood pressure regulation (see also 4.7) and cancer cell invasion (Uehata et al., 1997; Itoh et al., 1999). Knock-out of either one of the two ROCK isoforms resulted in intrauterine growth retardation and defects in eyelid as well as ventral body wall closure (Thumkeo et al., 2003, 2005). The double knock-out was lethal (Thumkeo et al., 2005). In Japan the ROCK inhibitor Fasudil is used in the treatment of cerebral vasospasm since many years (Morgan-Fisher et al., 2013).

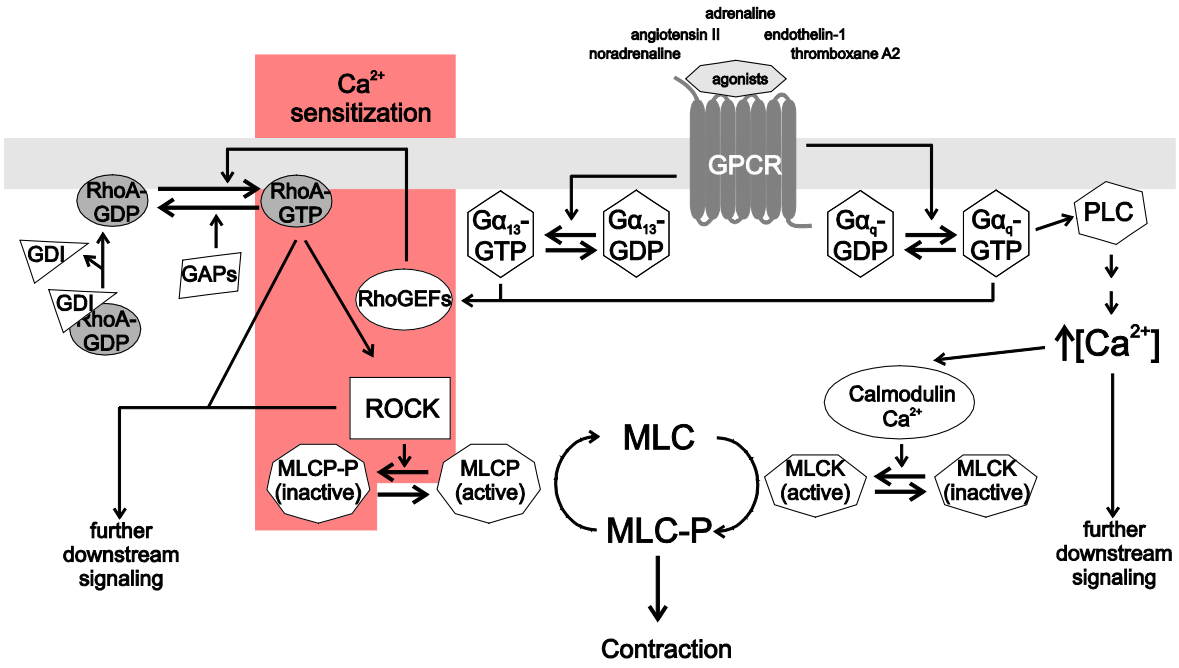

Fig. 4 The RhoA ROCK signaling in vascular smooth muscle cells
RhoA can be kept in the cytosol by RhoGDIs and GTP hydrolysis is accelerated by RhoGAPs. Therefore these two protein families inhibit RhoA signaling. In contrast RhoGEFs induce the exchange of GDP for GTP on RhoA, upon their activation by $G\alpha_q$ or $G\alpha_{12/13}$. Subsequently RhoA activates downstream effectors. One of those effectors is ROCK, which phosphorylates myosin light chain phosphatase (MLCP), beside other effectors. This process is also called Ca^{2+} sensitization in vascular smooth muscle cells. As upon inactivation of MLCP myosin light chain (MLC) is more sensitive towards phosphorylation by myosin light chain kinase (MLCK), which is a Ca^{2+} calmodulin dependent enzyme. This scheme is based on Satoh et al., but modified towards the scope of this thesis (Satoh et al., 2011). The Gβγ subunit is neglected in the interest of simplicity.

Not much is known about Rhotekin´s cellular function (Thumkeo et al., 2013). But the Rho binding domain (RBD) of Rhotekin has been of great interest for the Rho GTPase researchers in the last fifteen years. They used it to extract active RhoA from full cell lysates, which is facilitated by RBD´s high affinity for active, GTP-bound RhoA (Ren et al., 1999; Ren and Schwartz, 2000).

Downstream of RhoA c-Jun, serum response factor (SRF) and MEF2 are activated via diverse mechanisms (Marinissen and Gutkind, 2005). A SRF reporter gene assay, SRE.L, is widely used to indirectly determine Rho activity (Siehler, 2009). The serum response element (SRE) is activated by SRF together with either TCF or MRTF, which are transcriptional co-factors (Olson and Nordheim,

2010). The target genes are immediate-early as well as muscle specific genes, like β-actin and vinculin (Siehler, 2009). Selectivity between these genes is maintained by coactivation of SRF together with either TCF or MRTF (Jaffe and Hall, 2005). For the SRE.L reporter gene assay the serum response element (SRE) was mutated to exclude TCF binding (Hill et al., 1995). MRTFs are activated downstream of RhoA upon dissociation from monomeric actin (Olson and Nordheim, 2010). RhoA decreases the amount of monomeric actin in the cytosol by two mechanism and thus activates SRE.L: (A) minimized actin depolymerisation due to inactivation of cofilin by ROCK and (B) increased actin filament assembly due to mDia activation (Siehler, 2009).

4.5 Most RhoGEFs contain a DH-PH domain

The activation of RhoGTPases is the primary function of RhoGEFs, which are divided into dedicator of cytokinesis (DOCK) RhoGEFs and the B-cell lymphoma (Dbl) RhoGEFs (Cook et al., 2014). The DOCK RhoGEFs act solely on Rac and/or CDC42 and are therefore neglected in the following (Pakes et al., 2013). The Dbl RhoGEFs consists of 70 members with 28 acting on RhoA in human and are activated by integrins, receptor tyrosine kinases and heterotrimeric G proteins of the $G\alpha_{q/11}$ and $G\alpha_{12/13}$ family (Burridge et al., 2004; Cook et al., 2014). Upon the Dbl RhoGEFs all members share a catalytic Dbl homology (DH, ≈200 amino acids) domain and almost all a regulatory pleckstrin homology (PH, ≈100 amino acids) domain, which is located C-terminal of the DH domain (Rossman et al., 2005; Cook et al., 2014). Besides these domains the Dbl RhoGEFs vary in their structure. For example two RhoGEF proteins (Trio and Kalirin) possess two DH-PH domains each and in addition many other domains (4.5.2.1 *Trio and Kalirin, the complex siblings of p63RhoGEF*, (Rossman et al., 2005)).

Mechanistically the activation of RhoGTPases by RhoGEFs is a highly conserved process, even though the sequence homology is low between DH domains (Rossman et al., 2005). Upon RhoGEF binding the nucleotide binding pocket (the three switch regions and p-loop of the RhoGTPase, (2.3.1.1)) undergo conformational changes and GDP dissociates. Additionally the RhoGEF sterically displaces the cofactor Mg^{2+}, which is necessary for high affinity binding of the nucleotide (Rossman et al., 2005). Afterwards GTP and Mg^{2+} are able to bind to the GTPase, which leads again to changes in the switch region and dissociation of the complex (Rossman et al., 2005).

Significantly, the system of RhoGTPase activation by RhoGEFs was hijacked by many pathogenic bacteria, like a serovar of *Salmonella enterica* or an enteropathogenic *Escherichia coli*. The pathogenicity is mediated by the bacterial type three exotoxins, which mimic or antagonize the function of human RhoGEFs (Orchard and Alto, 2012).

DH domains have GEF activity and PH domains have more heterogeneous functions

The DH domain consists of three conserved regions (CR1 to CR3) and an only partially conserved C-terminus (helix α6), which varies in its length and orientation (Rossman et al., 2005). CR1 and CR3 interact with switch I of the GTPase and CR3 and parts of the C-terminus with switch II. Mutations in these regions interfere with GTPase binding (Aghazadeh et al., 1998; Liu et al., 1998; Rossman et al., 2005). The selectivity of Dbl RhoGEFs towards differing RhoGTPase families is maintained by the highly variable interaction site between GTPases' β2 and β3 strands and the DH's back rest (Rossman et al., 2005).

In general PH domains are found in many peripheral proteins and are known as phosphatidylinositol phosphate (PIP) binding domains and mediators of protein protein interaction (Bos et al., 2007; Shankaranarayanan et al., 2010). The PH domains of DH-PH domains are surprisingly divergent in their function (Bos et al., 2007): In some RhoGEFs the PH domain seems to increase the DH domain´s GEF activity as shown by truncation studies (Liu et al., 1998; Rossman and Campbell, 2000). For example, in leukemiaassociated RhoGEF (LARG), Dbs and PDZ-RhoGEF the PH domain builds direct contacts to RhoA and is important for full nucleotide exchange activity (Kristelly et al., 2004; Bos et al., 2007). For other RhoGEFs an inhibition of the DH domain by the PH domain is described. Examples for this are the DH domains of Son of sevenless, Trio and p63RhoGEF (Soisson et al., 1998; Bellanger et al., 2003; Lutz et al., 2007). Finally in Tiam1, intersectin and collybistin for the PH domain neither influence on *in vitro* GEF activity nor contacts to the bound GTPase were described (Worthylake et al., 2000; Snyder et al., 2002; Xiang et al., 2006).

Diverse regulatory mechanisms for Dbl RhoGEFs

Many RhoGEFs are constitutively activated by truncation of the protein N-terminal of the DH domain or by phosphorylation, which both releases the DH domain from autoinhibition (Aghazadeh et al., 2000; Schmidt and Hall, 2002). Also regulation by homo- as well as heterodimerization (4.5.1.1, *Regulation by dimerization and phosphorylation*) and subcellular sequestration was described (Rossman et al., 2005). Further and most crucial for the present thesis some RhoGEFs are activated by trimeric G proteins. Especially $G\alpha_{q/11}$ and $G\alpha_{12/13}$ activate certain RhoGEFs (4.5.1 and 4.5.2). For the RhoGEF P-Rex1 activation by Gβγ was described (Welch et al., 2002).

Pharmacologically targeting RhoGEFs

Until now, neither highly specific nor potent inhibitors were found for RhoGEFs, besides the natural product brefeldin A, which inhibits Arf activation by ArfGEF (Mossessova et al., 2003; Vigil et al., 2010). But the interaction between Arf and ArfGEF is distinct from the interaction between RhoGTPases and RhoGEFs. Recently a high throughput study was published on a direct blocker of the LARG RhoA complex, which showed an affinity of 110 µM towards RhoA *in vitro* (Gao et al., 2014). However data on the effect of this blocker in living cells or even *in vivo* are pending. Further RhoGEFs could be modulated indirectly by targeting kinases up- and downstream of RhoGEFs (Cook

et al., 2014). Like PKA upstream of LARG or Rho-associated serine/threonine kinase (ROCK) downstream of RhoA (see 4.4.1). The blocker for ROCK, Fasudil, is already in clinical use in Japan (Morgan-Fisher et al., 2013).

4.5.1 $G\alpha_{13}$-activated RhoGEFs

The $G\alpha_{12/13}$ RhoGEF Rho signaling pathway is conserved from *C. elegans* and *D. melanogaster* to mammals, with Concertina as single orthologue for $G\alpha_{12/13}$ in *D. melanogaster* (Barrett et al., 1997; Hiley et al., 2006).

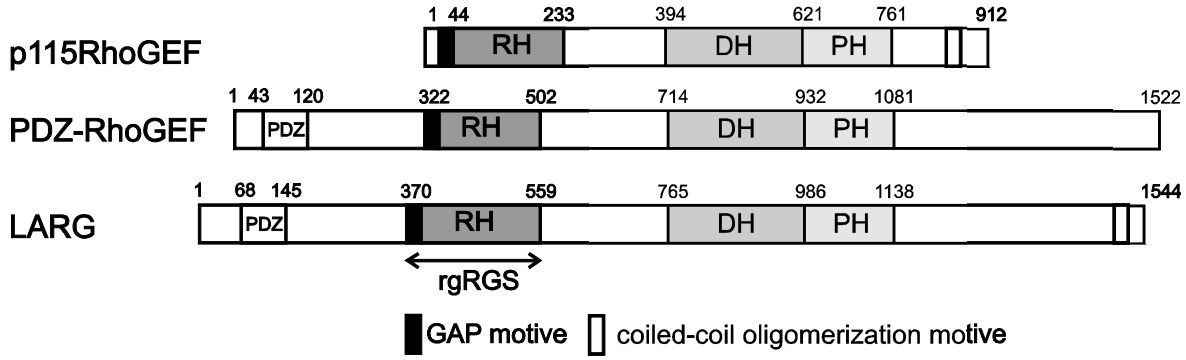

Fig. 5 Domain structure of RH-RhoGEFs
As visible all RH-RhoGEFs share the DH-PH domain and the rgRGS domain. In addition LARG shares a PDZ domain with PDZ-RhoGEF and a coiled-coil oligomerization domain with p115-RhoGEF. The scheme was adopted from Aittaleb et al. (Aittaleb et al., 2010).

In human $G\alpha_{12}$ and $G\alpha_{13}$ activate PDZ-RhoGEF[1] and leukemia-associated RhoGEF (LARG, 1544 amino acids), whereas p115RhoGEF is only activated by $G\alpha_{13}$ (Hart et al., 1998; Kozasa et al., 1998; Fukuhara et al., 1999, 2001). The activation of LARG by $G\alpha_{12}$ relies on a phosphorylation by the non-receptor tyrosine kinase Tec (Suzuki et al., 2003). Lbc RhoGEF is the fourth RhoGEF activated by this Gα subfamily and is expressed in many different splice variants (Aittaleb et al., 2010). The activation of this RhoGEF depends on $G\alpha_{12}$, but a direct interaction has not yet been shown (Aittaleb et al., 2010; Cavin et al., 2014). Due to the RH domain shared by LARG, p115RhoGEF and PDZ-RhoGEF, they are also referred to as RH-RhoGEFs (see 4.5.1.1 and fig. 4, (Aittaleb et al., 2010)). Together with Lbc RhoGEF they are additionally referred to as Lbc RhoGEFs. All of them are widely expressed in mammals, with emphasis on the hematopoetic system for p115RhoGEF and on the central nervous system for PDZ-RhoGEF (Hart et al., 1998; Fukuhara et al., 1999; Kourlas et al., 2000; Kuner et al., 2002).

4.5.1.1 RH-RhoGEFs: LARG, p115RhoGEF and PDZ-RhoGEF

LARG and p115RhoGEF have weak GAP activity

In contrast to RGS proteins (4.6) the GAP activity of p115RhoGEF is not maintained by the RH domain, but by a sequence directly N-terminal of the RH domain (Chen et al., 2003). Together the RH

[1] Most RhoGEFs have more than one name. For RhoGEFs relevant for this thesis the different names can be found in the abbreviations section as listed by Cook et al. (Cook et al., 2014).

domain and this N-terminally region build the rgRGS domain (fig. 5, (Aittaleb et al., 2010)). $G\alpha_{12/13}$ binding to the rgRGS domain of RhoGEFs and the RH domain of RGS proteins differ and this might be the reason for the rather weak GAP activity of LARG and p115RhoGEF (Aittaleb et al., 2010). Both proteins exhibit GAP activity against $G\alpha_{12}$ as well as $G\alpha_{13}$, even though p115RhoGEF was not demonstrated to be activated by $G\alpha_{12}$ (Hart et al., 1998; Kozasa et al., 1998; Chen et al., 2003; Suzuki et al., 2003). Since the trimeric G protein activates the RhoGEF and the RhoGEF accelerates the G protein's inactivation, p115RhoGEF and LARG are neither pure effectors nor pure regulators. But they are rather part of a so called "kinetic scaffolding", which transduced probably only rapid and robust activation of $G\alpha_{12/13}$ to Rho activation (Rossman et al., 2005). For PDZ-RhoGEF no GAP activity was found towards $G\alpha_{12/13}$, as Wells et al. stated referring to unpublished work by T. Kozasa and P. Steinweis (Wells et al., 2002).

RhoGEFs bind $G\alpha_{12/13}$ by their RH domain

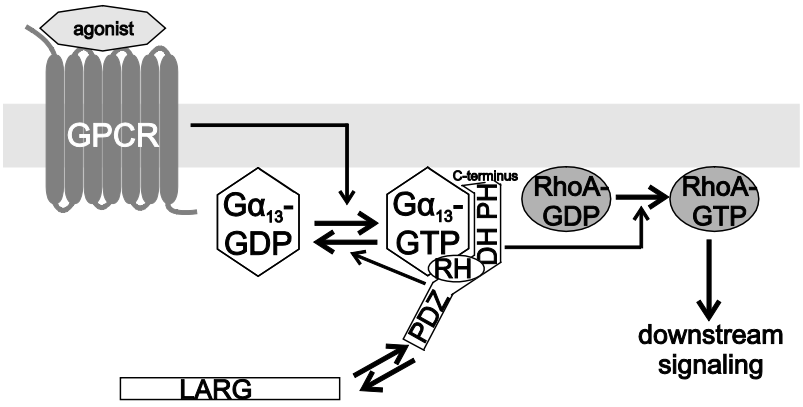

Fig. 6 Activation of LARG by $G\alpha_{13}$
Upon stimulation of a G protein coupled receptor with an agonist, $G\alpha_{13}$ becomes active. The active $G\alpha_{13}$ binds LARG by its RH domain and subsequently the C-terminus and the DH-PH domain bind. During this activation process LARG translocates from the cytosol to the plasma membrane. The scheme is based on Suzuki et al.´s hypothesis about LARG activation by $G\alpha_{13}$ (Suzuki et al., 2009b). $G\beta\gamma$ were neglected in interest of simplicity.

In a crystallography study of p115RhoGEF with a $G\alpha_{13/i}$ chimera, the RH domain was shown to bind to the canonical effector docking site of $G\alpha$ and to be important for G protein binding together with a C-terminal extension of this region (Chen et al., 2005). Three years later the structure was published of the rgRGS domain of PDZ-RhoGEF with another $G\alpha_{13}$ chimera, which was relatively similar to the one observed for p115RhoGEF (Chen et al., 2008). The structures differed in the amino acids involved in GAP activity for p115RhoGEF and this may explain PDZ-RhoGEF´s lack in GAP activity (Chen et al., 2008). In the same study a complex was found of GDP bound $G\alpha_{13}$ in close-to active conformation together with PDZ-RhoGEF, which may suggests the interaction of RH-RhoGEF with $G\alpha_{12/13}$ after GTP hydrolysis. Aittaleb and colleges suggested a competition of $G\beta\gamma$ with the RH-RhoGEF for $G\alpha_{12/13}$-GDP binding (Aittaleb et al., 2010).

In a surface plasmon resonance study $G\alpha_{13}$ interacted with the RH domain, the DH-PH domain and with C-terminal regions of LARG (fig. 6, (Suzuki et al., 2009b). The authors discuss an induced fit mechanism: First the RH domain binds the active $G\alpha_{13}$ and upon subsequent intraprotein rearrangements the DH-PH domain binds together with the C-terminal regions to $G\alpha_{13}$. This second step is probably independent of $G\alpha_{13}$´s activation state and Aittaleb et al. link it to the C-terminal region of the GTPase domain of $G\alpha_{13}$ (Aittaleb et al., 2010). The high affinity complex depends on all three interactions and a mutation was described within $G\alpha_{13}$, which abolished RH but not DH-PH domain binding (Nakamura et al., 2004; Grabocka and Wedegaertner, 2007).

Already 2007 Kreutz and colleagues showed the C-terminal 100 amino acids of $G\alpha_{13}$ to be important for activation of the GEF activity of p115RhoGEF and LARG, whereas the N-terminal α-helical domain and the switch regions are crucial for GAP activity. The Gα subunit binds the RH domain and facilitates $G\alpha_{13}$´s binding to the DH domain by this, which then leads to GEF activation (Chen et al., 2012).

For PDZ-RhoGEF a NMR study showed autoinhibition of GEF activity by the PDZ domain, the RH domain and a short acidic motive immediately N-terminal of the DH domain (Zheng et al., 2009).

Regulation by dimerization and phosphorylation

Another type of regulation was described for all three RH-RhoGEFs, which is dimerization. They can form homo- and heterodimers, which might have a negative regulatory effect. Since dimerization occurs through their C-termini and deletion of the C-terminus leads to higher SRE.L transcription (Chikumi et al., 2004). For LARG a single point mutation inhibited dimerization and led to nuclear localization of LARG (Grabocka and Wedegaertner, 2007). In this study SRE.L transcription was unchanged. Notably, GEF activity is potentiated by the binding of the Rho effector mDia1 to the C-terminus of LARG, which seems to be a positive feedback loop in the LARG Rho mDia1 axis (Kitzing et al., 2007). The LARG Rho mDia1 axis is important for microtubule organization during cell polarization (Goulimari et al., 2008).

The C-termini of PDZ-RhoGEF and LARG are phosphorylated by focal adhesion kinase (FAK), which was shown to be important for sustained Rho activation upon thrombin receptor activation (Chikumi et al., 2002a). FAK maybe initiates thereby also a positive feedback loop. LARG is additionally phosphorylated by a set of other kinases like Burtons´s tyrosine kinase, Src family kinases (SFKs) and Tec (Hamazaki et al., 1998; Mao et al., 1998; Guilluy et al., 2011). In vascular smooth muscle cells PDZ-RhoGEF is tyrosine phosphorylated by PYK2 upon stimulation with angiotensin II, which lead to enhanced GEF activity (Ying et al., 2009). Also for p115RhoGEF phosphorylation sites are described, but their phosphorylation remains to be tested in living cells (Chow et al., 2013).

RH-RhoGEFs translocate to the plasma membrane

The RH-RhoGEFs translocate to the cell membrane upon activation of $G\alpha_{12/13}$ coupled receptors or coexpression of constitutive active $G\alpha_{12/13}$ (Meyer et al., 2008). Bhattacharyya and Wedegaertner showed

the translocation of p115RhoGEF from the cytosol to the plasma membrane for the first time (Bhattacharyya and Wedegaertner, 2000). The translocation was induced by coexpression of constitutive active $G\alpha_{13}$ together with myc-tagged p115RhoGEF and depended on $G\alpha_{13}$´s localization at the plasma membrane. Further p115RhoGEF´s translocation was shown to be a reversible process upon activation and inactivation of different $G\alpha_{12/13}$ coupled receptors, with translocation within in one to two minutes and redistribution upon antagonist application within a minute (Meyer et al., 2008).
For PDZ-RhoGEF colocalization with cortical actin and microtubules was described (Togashi et al., 2000). In neurons LPA receptor activation translocates PDZ-RhoGEF to the tips of neurites and overexpressed PDZ-RhoGEF is found partially at or close to the plasma membrane (Banerjee and Wedegaertner, 2004). Recently, p115RhoGEF and PDZ-RhoGEF were artificially translocated to the plasma membrane by a rapalog system and this led to an increase in GEF activity in the absence of G protein activation (Carter et al., 2014). Thus the authors suggested GEF activity to be based on colocalization of the RhoGEF with Rho at the plasma membrane, rather than on activation of the GEF activity. Nevertheless biochemical experiments clearly show an increase in GEF activity for p115RhoGEF and LARG by $G\alpha_{13}$ in solution (Hart et al., 1998; Suzuki et al., 2003).
Endogenous and cotransfected LARG is found predominantly in the cytosol of COS7 cells (Banerjee and Wedegaertner, 2004; Grabocka and Wedegaertner, 2007). In MDCKII cells LARG is localized at the lateral cell membranes and a bit in the cytosol (Taya et al., 2001). In fibroblasts LARG is found in the microtubule organizing center and along microtubule tracks (Siehler, 2009). The translocation of LARG was monitored in living cells as part of this thesis.

Activation of PDZ containing RhoGEFs by non-GPCR receptors

PDZ containing RhoGEFs can be activated by binding of their PDZ domain to a PDZ binding motive in the C-terminus of plexin B1, a semaphorin 4D receptor and this activation mechanism is implicated in axonal growth cone collapse and angiogenesis (Swiercz et al., 2002; Basile et al., 2004). Additionally, LARG binds directly and constitutive to IGF-1 receptor and is activated by IGF-1 (Taya et al., 2001). LARG/PDZ-RhoGEF bind also to the GPCRs LPA-1 and LPA-2 via the receptor´s PDZ binding motive (Yamada et al., 2005).

RhoA binding and GEF activity

LARG has the highest catalytic activity among the RH-RhoGEFs. They are specific GEFs for RhoA, RhoB and RhoC and RhoA-GTP binds to the DH domain and forms also contacts with the PH domain (Jaiswal et al., 2011). Autoinhibition of p115RhoGEF was mapped to its RH domain (Jaiswal et al., 2011). Whereas mutations in the PH domain released LARG from autoinhibition to levels of DH domain alone, which was not the case for PDZ-RhoGEF (Kristelly et al., 2004; Oleksy et al., 2006). This difference could be due to the LARG´s relatively long linker, which allows a larger movement between DH and PH domain of LARG compared to PDZ-RhoGEF (Aittaleb et al., 2010). For all Lbc RhoGEFs a hydrophobic patch in the PH domain seemed to be important for RhoA activation in

cells (Aittaleb et al., 2009). In case of LARG its implicated in proper localization of LARG, since fusion of an unspecific plasma membrane targeting motive restored RhoA activation in the absence of this domain (Aittaleb et al., 2009).
Interestingly RhoA-GTP was described to bind to the PH domain of Lbc RhoGEFs and to induce a positive feedback loop by this (Medina et al., 2013).

Physiology and pathology

Lsc is the murine orthologue of p115RhoGEF. It was primarily characterized in hematopoetic cells and is required in normal B- and T-lymphocyte function as shown by knock-out studies (Girkontaite et al., 2001). Further knock-out mice suffered from gastrointestinal motor dysfunction (Zizer et al., 2010). p115RhoGEF is inactivated by the cytoplasmic domain of the HIV-1 transmembrane glycoprotein gp41 (Zhang et al., 1999).
In contrast PDZ-RhoGEF knock-out mice showed no obvious phenotype (Mikelis et al., 2013). LARG knock-out mice showed reduced birthrate, but no developmental defects were observed after birth (Mikelis et al., 2013). However knock-out of both PDZ-RhoGEF and LARG resulted in complex developmental defects and early embryonic lethality, probably due to major vascular defects (Mikelis et al., 2013). In LARG, PDZ-RhoGEF, p115RhoGEF triple knock-out MEFs (mouse embryonic fibroblasts) no Rho activation was found by $G\alpha_{12/13}$ coupled receptors, but stable Rho activation by $G\alpha_q$ coupled receptors (Mikelis et al., 2013).
LARG was firstly described in a fusion protein of a patient with acute myeloid leukemia (Kourlas et al., 2000; Kuner et al., 2002). This fusion protein consisted of mixed lineage leukemia (MLL) and LARG without its nuclear localization sequence (NLS) and PDZ-domain, precisely everything C-terminal of AS 308. In mice LARG mRNA was found widely expressed with higher expression in lung, liver, testis, heart and hematopoetic progenitor cells (Zinovyeva et al., 2004). Also in human LARG is ubiquitously expressed (Kourlas et al., 2000). LARG expression was found dramatically increased in bone marrow of patients with the pre-leukemic disorder Shwachman-Diamond syndrome (Rujkijyanont et al., 2007). Whereas low LARG expression levels have been found in solid tumors (Ong et al., 2009). In the heart LARG is the most abundantly expressed RhoGEF and is the central player during pressure-overload induced hypertrophy (Takefuji et al., 2013). Together with other RH-RhoGEFs and p63RhoGEF, LARG was described to be involved in vascular smooth muscle tone (4.7).

4.5.2 $G\alpha_q$-activated RhoGEFs

The hypotheses of Rho activation by $G\alpha_q$ in parallel to $G\alpha_{12/13}$ was supported by detection of Rho activation downstream of $G\alpha_q$ in $G\alpha_{12/13}$ deficient MEFs (Sah et al., 1996; Chikumi et al., 2002b; Vogt et al., 2003). Mainly three RhoGEFs were discussed to link $G\alpha_q$ activation and Rho signaling: LARG , Lbc RhoGEF and p63RhoGEF with its near relatives Trio and Kalirin (Sagi et al., 2001; Booden et al., 2002; Chikumi et al., 2002b; Pi et al., 2002; Vogt et al., 2003; Lutz et al., 2005; Rojas et al., 2007; Williams et al., 2007).

LARG was previously described in detail as $G\alpha_{12/13}$-activated RhoGEF. Whether LARG is also activated by $G\alpha_q$ is a matter of debate: LARG´s RH domain was able to coimmunoprecipitate $G\alpha_{12}$, $G\alpha_{13}$ and $G\alpha_q$ in one study (Booden et al., 2002). Two other groups were not able to coimmunoprecipitate LARG with $G\alpha_q$ (Fukuhara et al., 2000; Chikumi et al., 2002b). Further in the presence of LARG SRE.L activation was enhanced by stimulation of H_1-R or cotransfection of constitutive active $G\alpha_q$. This could be abolished by PLCβ1 coexpression, which argued in favor of LARG activation by $G\alpha_q$ (Pfreimer et al., 2011). Our laboratory could not detect interaction of $G\alpha_q$ and LARG by means of FRET, which might point against a $G\alpha_q$ LARG complex (Bodmann, diploma thesis). Additionally, the p115RhoGEF, PDZ-RhoGEF, LARG triple knock-out mice showed defects in $G\alpha_{12/13}$ mediated Rho activation, but did not show any effects on $G\alpha_q$ mediated Rho activation (Mikelis et al., 2013).

Also Lbc RhoGEF could be precipitated with $G\alpha_q$, but its activation in $G\alpha_{12/13}$ knock-out mice has not been shown (Sagi et al., 2001; Pi et al., 2002). p63RhoGEF is the most well-established link between $G\alpha_q$ activation and RhoA signaling (Lutz et al., 2005). The next section discusses p63RhoGEF in detail and gives some further information about Kalirin and Trio.

4.5.2.1 p63RhoGEF

$G\alpha_q$ binds mainly p63RhoGEF´s PH domain

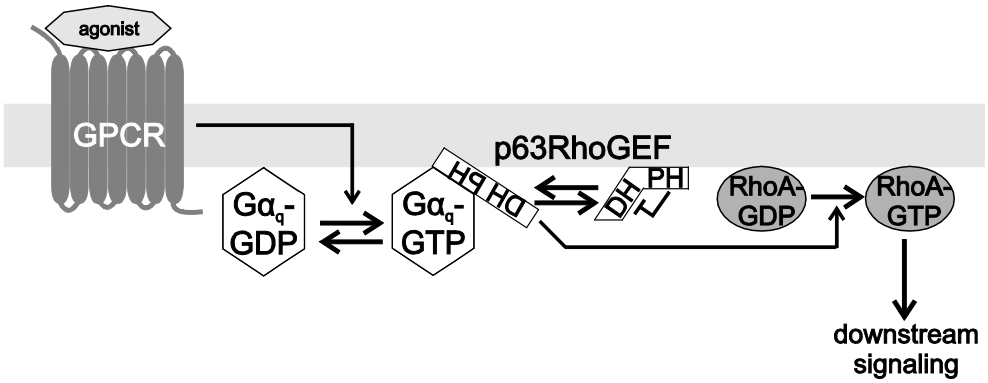

Fig. 7 Activation of p63RhoGEF by $G\alpha_q$
In inactive p63RhoGEF the PH domain folds back onto the catalytic DH domain, which leads to autoinhibition. Active $G\alpha_q$ interacts with the PH domain and this releases the DH domain from autoinhibition. In addition, $G\alpha_q$ directly contacts the DH domain. Together both mechanisms enable full RhoGEF activity towards RhoA. The scheme is based on a figure from a review by Aittaleb and colleagues (Aittaleb et al., 2010). Gβγ were neglected here in interest of simplicity.

p63RhoGEF lacks a RH domain in contrast to the previously described RH-RhoGEFs. $G\alpha_q$ binding was localized to the C-terminal helix of the PH domain by truncation studies and releases p63RhoGEF from autoinhibition (fig. 7, (Lutz et al., 2007; Rojas et al., 2007)). Active $G\alpha_q$ bound to the same region of closely related Trio and Kalirin, as shown in the same studies. In 2007 a crystal structure was published of a $G\alpha_{i/q}$ chimera in complex with p63RhoGEF´s DH-PH domain (amino acid 149 to 502) and RhoA (fig. 30 (Lutz et al., 2007)). This structure proofed the C-terminal helix of the PH domain to be unusually long and to bind directly into $G\alpha_q$´s effector docking site. Several

mutations were introduced into this region, which diminished p63RhoGEF $G\alpha_q$ interaction and two of these mutants, F471E and L475A, were used in the present work (6.2.2 and 6.2.6). Noteworthy, also contacts are formed between p63RhoGEF´s DH-domain and its DH-PH interface with the C-terminal region of $G\alpha_q$. These interactions have mainly regulatory functions, as mutation of the corresponding amino acids of p63RhoGEF or $G\alpha_q$ (Tyr356) prevented p63RhoGEF´s activation by $G\alpha_q$, but did not affect their interaction (Lutz et al., 2007; Shankaranarayanan et al., 2010). Consequently, p63RhoGEF interacts with, but is not activated by $G\alpha_{16}$, which exhibits an isoleucine in the place of $G\alpha_q$´s Tyr356 (Moepps et al., 2008; Yeung and Wong, 2009). Also active mitogen-activated kinase (MLK3) might bind to p63RhoGEF and thereby might prevent binding to and activation by $G\alpha_q$ (Swenson-Fields et al., 2008).

PLCβ3 overlaps with p63RhoGEF and RGS2 binding to $G\alpha_q$

Similarly PLCβ1/4 and p63RhoGEF are located at the plasma membrane under basal conditions and are activated by $G\alpha_q$ via relief of autoinhibition (Shankaranarayanan et al., 2010; Lyon et al., 2011; Sánchez-Fernández et al., 2014). Both proteins bind very similar to $G\alpha_q$´s effector binding site with their helix turn helix domain and thus exclude each other from $G\alpha_q$ binding (fig 8, orange area, (Lutz et al., 2005, 2007; Adjobo-Hermans et al., 2013; Lyon et al., 2013, 2014)).

Interestingly, PLCβ3 binds additionally to switch I and II of $G\alpha_q$ and exhibits GAP activity towards $G\alpha_q$ through these interactions. Hence fast activation of PLCβ3 by $G\alpha_q$ is followed by fast inactivation of $G\alpha_q$ by PLCβ, which was entitled as “kinetic scaffolding” (Berstein et al., 1992; Waldo et al., 2010).

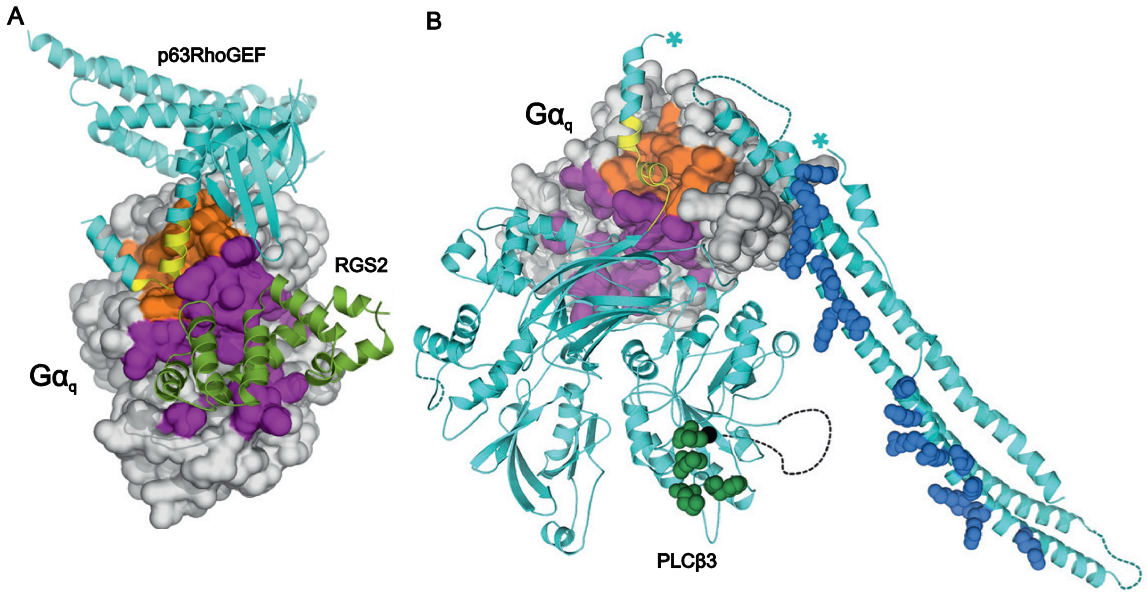

Fig. 8 Comparison of putative trimeric complex of $G\alpha_q$, RGS2 and p63RhoGEF and dimeric complex of $G\alpha_q$ and PLCβ3

On $G\alpha_q$ the canonical effector binding site is shown in orange and the RGS binding site in purple. These models were generated by Lyon and colleagues. In **A** they superimposed the structure of $G\alpha_q$ p63RhoGEF (PDB 2RGN) with the $G\alpha_q$ RGS2 (PDB 4EKC) structure (Lutz et al., 2007; Nance et al., 2013; Lyon et al., 2014). The crystal structure of PLCβ3 in complex with $G\alpha_q$ is shown in **B** (PDB 4GNK (Lyon et al., 2013)). One can recognize the overlap of PLCβ3 with RGS2 and p63RhoGEF binding to $G\alpha_q$.

This second binding site between $G\alpha_q$ and PLCβ overlapped almost completely with the classical RGS binding site at $G\alpha_q$ (fig. 8B, purple area (Waldo et al., 2010)). Hence, the $G\alpha_q$ PLCβ3 interaction blocks $G\alpha_q$´s switch I, which is freely accessible for RGS in the $G\alpha_q$ p63RhoGEF interaction (Aittaleb et al., 2010). Consequently, a trimeric complex between p63RhoGEF, $G\alpha_q$ and RGS2 was shown by biochemical assays and modulations in 2008 (see fig. 8A for a structural model, (Lutz et al., 2007; Shankaranarayanan et al., 2008; Nance et al., 2013; Lyon et al., 2014)). A part of the work presented here focused on the interaction between PLCβ3, RGS2 and p63RhoGEF with $G\alpha_q$ in living cells (6.2). Interestingly, proper signaling at the neuromuscular junction of *C. elegans* was linked to simultaneous signaling by both effectors (Williams et al., 2007).

p63RhoGEF localizes at the plasma membrane

In contrast to RH-RhoGEFs p63RhoGEF was found localized to actin-rich structures and at the plasma membrane upon overexpression (Souchet et al., 2002; Shankaranarayanan et al., 2010). The localization at the plasma membrane depends on palmitoylation of three cysteine residues in the N-terminal region of p63RhoGEF and was concluded important for p63RhoGEF`s full activity (Aittaleb et al., 2011; Goedhart et al., 2013). Consequently GEFT, which lacks the N-terminal region, appeared in the cytosol (Lutz et al., 2004; Goedhart et al., 2013). Upon $G\alpha_q$ activation GEFT translocated to the plasma membrane as shown by confocal microscopy (Goedhart et al., 2013).

RhoA is activated upon relieve of p63RhoGEF´s autoinhibition

p63RhoGEF is a GEF for RhoA, RhoB and RhoC (Rojas et al., 2007). RhoA binds to p63RhoGEF´s DH domain, which is autoinhibited by the PH domain in the absence of active $G\alpha_q$ (Lutz et al., 2007). However the interaction is regulated by the whole DH-PH domain (Lutz et al., 2004, 2007; Rojas et al., 2007; Shankaranarayanan et al., 2010): The PH domain autoinhibits the DH domain, if they are covalently linked via their α6-N6 linker and $G\alpha_q$ is not bound. Upon $G\alpha_q$ binding the affinity is enhanced between DH domain and $G\alpha_q$. This is caused by loss of autoinhibition and additional allosteric activation of the DH domain (fig. 7). The additional allosteric activation occurs through the interaction of $G\alpha_q$´s C-terminal region and the DH domain (Shankaranarayanan et al., 2010).

Trio and Kalirin, the complex siblings of p63RhoGEF

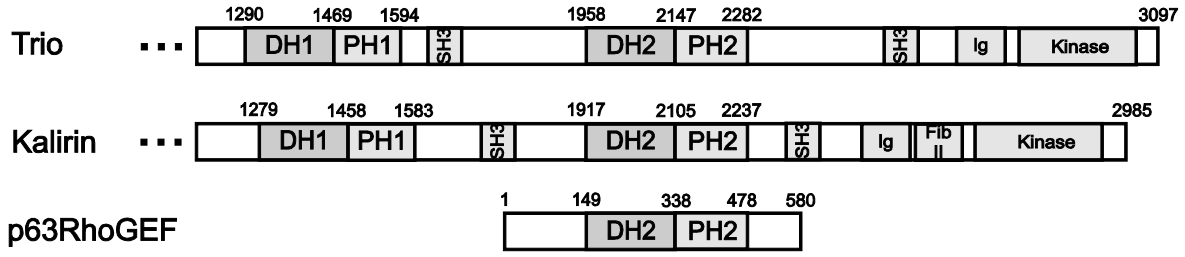

Fig. 9 Domain structure of p63RhoGEF, Trio and Kalirin
These $G\alpha_q$-activated RhoGEFs have one very similar DH-PH domain. Interestingly, Trio and Kalirin share another DH-PH domain, which activates Rac and RhoG, and they have many additional domains, for example a kinase domain in their C-terminus. For these two proteins the N-terminus is excluded from the scheme. This scheme is based on a figure from a review by Aittaleb and co-workers (Aittaleb et al., 2010).

These RhoGEFs are much more complex in structure than p63RhoGEF (fig. 9). They have two sets of DH-PH and additional domains. The first DH-PH domain activates RhoG and Rac, whereas the second one activates RhoA. The latter is closely related to p63RhoGEF and their autoinhibitory PH domains were shown 100% identical in the amino acids important for $G\alpha_q$ binding (Liu et al., 1998; Bellanger et al., 2003; Skowronek et al., 2004; Chhatriwala et al., 2007; Lutz et al., 2007; Rojas et al., 2007). However they form complex crosstalk between their other domains, heterotrimeric G proteins and their effectors (Aittaleb et al., 2010). Therefore p63RhoGEF was used as a model for RhoGEFs activated exclusively by $G\alpha_q$ in the work presented here.

Physiology and pathology

In *Cenorhabditis elegans* UNC-73E is the homologue of Trio and is for example important in egg laying and growth (Williams et al., 2007). In mammals p63RhoGEF is predominantly expressed in the brain and heart (Souchet et al., 2002; Lutz et al., 2004). Nevertheless p63RhoGEF was shown to be critically involved in angiotensin II-induced signaling in vascular smooth muscle cells and is discussed to be the main switch in $G\alpha_q$-mediated smooth muscle activation (see 2.7, (Wuertz et al., 2010; Momotani and Somlyo, 2012)). In the pathology of cancer GEFT, which is a splice variant of p63RhoGEF, was found overexpressed in rhabdomyosarcoma (Sun et al., 2014). In breast carcinoma p63RhoGEF was described to be essential for chemotactic migration and to be activated downstream of GPR116, which expression correlated with breast tumor progression, recurrence and poor prognosis (Hayashi et al., 2013; Tang et al., 2013).

Interestingly the $G\alpha_q$ p63RhoGEF RhoA axis was recently identified as target for the *Pasteurella multocida* toxin, which inhibits osteoblast genesis and causes progressive bone loss during atrophic rhinitis in various animals (Siegert et al., 2013).

4.6 RGS proteins

Function

Approximately half of all regulators of G protein signaling (RGSs) negatively regulate Gα proteins (Heximer, 2013). In order to do so RGS accelerate GTP hydrolysis at least 40-fold by stabilizing the transition state of the GTPase, which they bind with highest affinity by interaction with all three switch regions of Gα (Berman et al., 1996a, 1996b; Tesmer et al., 1997; Baltoumas et al., 2013) In human 35 RGS proteins are expressed. The RGS domain is the feature common to all of them. This domain is 120-130 amino acids long, composed of a bundle of nine α-helices and can bind directly to the activated Gα subunit (Hollinger and Hepler, 2002; Baltoumas et al., 2013). Of relevance for the present work are the B/R4 and F/RL subfamilies. The B/R4 subfamily consists of RGS1 to 5, 8, 13, 16, 18 and 21 and the F/RL subfamily, also known as RGS-like proteins, includes RhoGEFs (see 4.5), GRKs, AKAPs and sorting nexins (Ross and Wilkie, 2000). Of the F/RL family only the RhoGEFs are relevant for the present study and they were described elsewhere (see 4.5).

The B/R4 RGS proteins can exhibit GAP activity towards $G\alpha_i$ and/or $G\alpha_q$. Heximer and colleagues found the GAP activity of RGS2 towards $G\alpha_q$-stimulated IP_3 production 5-fold higher than the one of RGS4 and vice versa RGS4´s GAP activity for $G\alpha_i$-mediated signaling 8-fold higher than RGS2´s *in vitro* (Heximer et al., 1999). The $G\alpha_q$ and $G\alpha_i$ selectivity can be exchanged between RGS2 and 4 by mutation of three amino acids within the Gα binding pocket of the respective RGS protein into the corresponding amino acids of the other one (Heximer et al., 1999). Nevertheless, RGS2 wild type has GAP activity for $G\alpha_i$ in membrane-reconstituted system (Cladman and Chidiac, 2002). In 2013, the crystal structure was elucidated for RGS2´s RGS domain in complex with constitutive active $G\alpha_q$, which lacks its N-terminal helix (Nance et al., 2013). RGS2 docks to $G\alpha_q$ in an overall similar manner compared to the previously described RGS $G\alpha_{i/o}$ complexes, but is tilted by seven degrees (Nance et al., 2013). Also this interaction allows for the conserved mechanism of acceleration of GTPase activity by RGS proteins. If the three amino acids mentioned previously are mutated to the ones in RGS4, the interaction is more similar to the one observed for RGS and $G\alpha_{i/o}$. Nevertheless in ventricular myocytes RGS2, 3, 4 and 5 inhibited $G\alpha_q$ signaling equally well (Hao et al., 2006). Hence, in a signaling pathway specific GAP activity has to depend on additional aspects. One is the type of activated GPCR. Some GPCRs can be recognized by the RGS´ N-terminal region (Zeng et al., 1998; Bernstein et al., 2004; Itoh et al., 2006). As for example RGS5 inhibits $G\alpha_q$ activation by angiotensin 1 and endothelin ET_A receptor, but not by muscarinic M_3 receptor (Zhou et al., 2001). Some RGS proteins work as effector antagonists independent of the GAP activity. In order to do so, they either bind the effector or a region overlapping with the effector binding site at the Gα subunit, thus competing with the effector for binding (Cunningham et al., 2001; Salim et al., 2003; Anger et al., 2004). The latter mechanism was discovered in cells treated with GTPγS. Under this condition RGS2 could not hydrolyze $G\alpha_q$, but signaling towards PLCβ was still abolished (Cunningham et al., 2001). Other $G\alpha_q$ effectors are discussed to build high order complexes together with Gα and RGS proteins (Tesmer et al., 2005). In these complexes RGS2 and 4 would not compete for the effector

binding, but rather inhibit effector association and activation allosterically (Shankaranarayanan et al., 2008; Nance et al., 2013). A part of this study aimed to characterize the allosteric effect of RGS2 on the p63RhoGEF $G\alpha_q$ interaction and investigated downstream signaling in detail (see also 4.5.2.1 *PLCβ3 overlaps with p63RhoGEF and RGS2 binding to $G\alpha_q$*). Also Gβγ was suggested to bind RGS proteins directly, e.g. RGS3, and this interaction was discussed to directly blocked Gβγ signaling (Shi et al., 2001). Additionally direct binding was described between different RGS proteins and mediators downstream of trimeric G proteins (reviewed in (Bansal et al., 2007)).

RGS proteins are tightly regulated

RGS proteins were shown to be regulated by posttranslational modification, translocation as well as changes in expression level:

The palmitoylation at the N-terminus of RGS proteins was discussed to be involved in plasma membrane localization, whereas the lipid modification in the RGS domain are thought to either potentiate or inhibit GAP activity (Hiol et al., 2003; Osterhout et al., 2003; Jones, 2004). In addition phosphorylation can influence the GAP activity positively as well as negatively depending on the RGS protein and kinase involved (Hendriks-Balk et al., 2008).

RGS mRNA levels are regulated tissue as well as receptor specific, for example quick upregulation of RGS2 mRNA was found upon angiotensin II stimulation (Grant et al., 2000; Li et al., 2005). RGS4 mRNA was up and RGS2 mRNA downregulated in models of cardiac hypertrophy (Kach et al., 2012). The protein levels could not be examined directly due to lack of good antibodies. But RGS4 was shown to be ubiquitinated, which probably causes the described relatively short half life of less than an hour (Lee et al., 2005).

Physiology

The first RGS protein described was Sst2p, which inhibits the pheromone-induced mating response in *Saccharomyces cerevisiae* and exhibits GAP activity against the yeast Gα, Gpa1 (Dohlman et al., 1998). In mammals R4 RGS proteins are involved in a wide variety of processes as reviewed elsewhere (Hendriks-Balk et al., 2008). For example RGS2 was shown as a regulator of vascular tone (see 4.7) and was found in almost every tissue investigated in mice and humans (Kehrl and Sinnarajah, 2002). Further mice deficient in RGS2 showed defects in immune response, synapse development and increased anxiety response (Oliveira-dos-Santos et al., 2000). In the vascular pathology of atherosclerosis RGS5 was found downregulated and decreased RGS5 mRNA levels were associated with neointima formation (Geary, 2002; Li et al., 2004; Adams et al., 2006). The expression of RGS1, 13 and 16 in B cells is important for adaptive immune response (Beadling et al., 1999; Han et al., 2006). Almost every RGS protein was found expressed in the mammalian heart and cultured cardiomyocytes, however the expression levels may differ between cell types and regions of the heart (Hendriks-Balk et al., 2008; Zhang and Mende, 2011). For some the expression was really low and others, like RGS2, RGS4 or p115RhoGEF, were highly expressed (Wieland and Mittmann, 2003).

4.7 The GPCR G protein RhoGEF Rho axis in vascular tone

The arterial blood pressure is tightly regulated by many different mechanisms in order to prevent persistent, elevated levels in systolic and/or diastolic blood pressure, known as hypertension (Loirand and Pacaud, 2014). One of these mechanisms is regulation of the vascular tone, which is mainly conducted by vascular smooth muscle cells (VSMC). Their contraction depends on the phosphorylation status of 20kDa myosin light chain (MLC), which is phosphorylated by MLC kinase (MLCK) and dephosphorylated by MLC phosphatase (MLCP, fig. 4, (Puetz et al., 2009)). In the phosphorylated state the actin-activated ATPase activity is increased and crossbridge cycling occurs, which shortens/contracts the VSMC (Momotani and Somlyo, 2012). The kinase is Ca^{2+}-calmodulin dependent and activated by rise in cytosolic Ca^{2+} concentrations whereas the phosphatase is Ca^{2+} independent. Thus inactivation of MLCP results in Ca^{2+} sensitization of the system (fig. 4). The regulation of cytosolic Ca^{2+} and Ca^{2+} sensitization occurs mainly through activation of GPCRs, which are coupled to $G\alpha_q$ and $G\alpha_{12/13}$. $G\alpha_q$ activates PLC and subsequently Ca^{2+} is released from intracellular stores and flows in from the extracellular lumen (de Gasparo et al., 2000; Balakumar and Jagadeesh, 2010). In parallel RhoGEFs are activated by either $G\alpha_{q/11}$ or $G\alpha_{12/13}$, which induce Ca^{2+} sensitization via RhoA and its target ROCK. Upon activation of ROCK MLCP is phosphorylated, which reduces its catalytic activity (Uehata et al., 1997). This causes higher sensitivity of MLC for Ca^{2+} and therefore more pronounced contraction in the presence of small cytosolic Ca^{2+} concentrations (Loirand and Pacaud, 2014). In Japan a ROCK inhibitor, Fasudil, is in clinical use for treatment of cerebral vasospasm (Morgan-Fisher et al., 2013).

In interest of simplicity additional regulators like NO or RhoGAPs are neglected in the further discussion on the role of the GPCR Gα RhoGEF Rho axis in vascular tone. Until now several different RhoGEFs are shown to be involved in vascular tone regulation depending on the model of hypertension studied (Loirand and Pacaud, 2014). In arterial smooth muscle cells p63RhoGEF is the most abundant, but also p115-RhoGEF, PDZ-RhoGEF and LARG are expressed in conductance and resistance arteries (Ying et al., 2004; Jin et al., 2006; Hilgers et al., 2007; Wirth et al., 2008; Momotani et al., 2011; Cario-Toumaniantz et al., 2012). $G\alpha_q$ knock-out mice showed no aorta contraction upon Ang II stimulation, but aorta of $G\alpha_{12/13}$-deficient mice contracted almost complete (Wirth et al., 2008). This emphasizes p63RhoGEF´s role in response to Ang II, since p63RhoGEF is the only RhoGEF of the four activated by $G\alpha_q$. Additionally p63RhoGEF was found upregulated in hypertensive patients (Calò et al., 2014). Due to these and other observations p63RhoGEF was implicated as major regulator of basal blood pressure (Momotani and Somlyo, 2012). S_1P stimulation activates LARG in vascular smooth muscle cells and salt-induced hypertension was abolished by LARG knock-out mice (Wirth et al., 2008; Medlin et al., 2010). According to a recent study, LARG and PDZ-RhoGEF mediate Ca^{2+} sensitization in arterial smooth muscle cells simultaneously upon stimulation of $G\alpha_{12/13}$ coupled Txa_2-R and ET-1-R, but if one of the RhoGEFs was missing the half time until full contraction was prolonged (Artamonov et al., 2013). In our opinion this showed the importance of exact knowledge on

the kinetics of activation and inactivation of individual RH-RhoGEFs. Therefore LARG activation by $G\alpha_{12/13}$ was studied in detail in the present work (see 6.1).

An influence of RGS2 on vascular tone is most likely, since RGS2 knock-out mice have increased blood pressure and are hyperresponsive to vasoconstrictors (Heximer et al., 2003). Additionally NO induced relaxation is reduced in these mice, since no RGS2 is present, which could be activated downstream of NO production (Tang et al., 2003; Sun et al., 2005). Interestingly also in human changes in RGS2 expression influence the blood pressure as several SNPs in RGS2 were associated with hypertension in patients and decreased RGS2 levels were described for hypertensive patients (Riddle et al., 2006; Semplicini et al., 2006; Bodenstein et al., 2007; Freson et al., 2007; Gu et al., 2008; Kohara et al., 2008). This finding underlined RGS2´s function as regulator of vascular tone.

Noteworthy, in a human syndrome of normo- or hypotension in the presence of high renin and aldosterone plasma levels, the inhibitor of Ang II signaling RGS2 was found up and the signaling mediators, p115RhoGEF and p63RhoGEF, downregulated (Calò et al., 2004, 2011; Pagnin et al., 2005; Fremont and Chan, 2012). The regulation of p63RhoGEF by RGS2 in single living cells was investigated as part of the present study (see 6.2).

4.8 Aim of the study

Regulation of Rho activity by G protein coupled receptors is important for many physiological and pathophysiological conditions, including regulation of vascular tone (Wirth et al., 2008; Momotani et al., 2011; Balakumar and Jagadeesh, 2014). GPCRs regulate RhoA mainly via RhoGEFs, which are directly activated by $G\alpha_q$ and $G\alpha_{12/13}$. The best established signaling cascades link activation of $G\alpha_q$ and $G\alpha_{13}$ to p63RhoGEF and RH-RhoGEFs, respectively (fig. 10B).

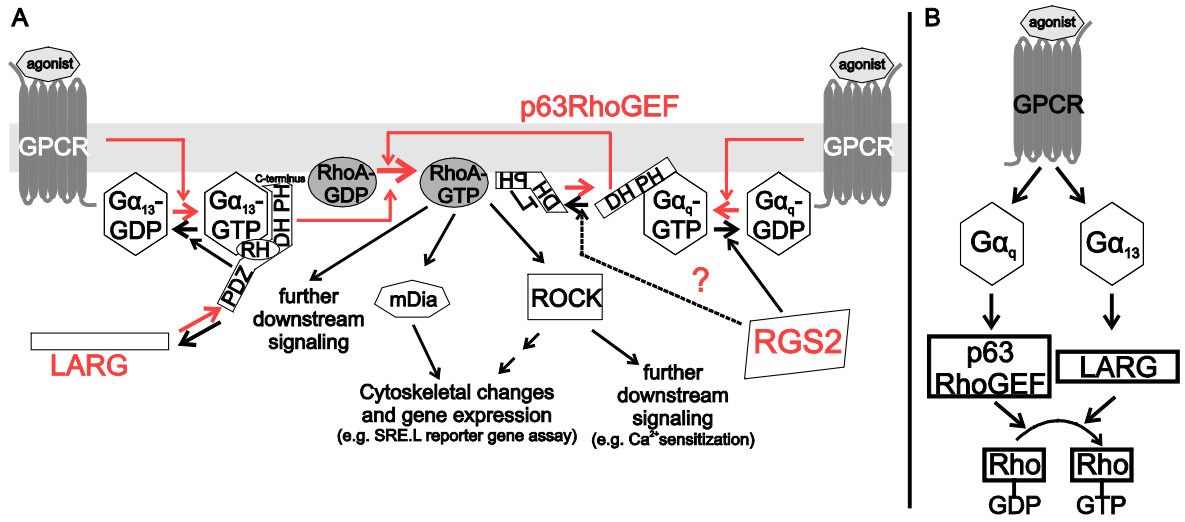

Fig. 10 GPCR signaling towards RhoGEFs
A RhoA is activated upon activation of both $G\alpha_q$ and $G\alpha_{13}$. In this study $G\alpha_q$ signaling towards RhoA via p63RhoGEF was resolved in single cells with high temporal resolution. Additionally the regulation of this interaction by the PLCβ antagonist RGS2 was studied in detail. Further activation of leukemia-associated RhoGEF (LARG) by $G\alpha_{13}$ was investigated with the same temporal and steric resolution. LARG was chosen as representative for the important family of RH-RhoGEFs. Also RhoA activation itself and gene expression was determined downstream of these pathways, in order to gain a complete picture on regulation of RhoA signaling by GPCRs. By the flow chart in **B** the parallel steps for both pathways are illustrated. The Gβγ subunit was neglected in interest of simplicity.

Until now the GPCR G protein RhoGEF Rho axis was mainly studied at endpoints, like active RhoA-GTP concentrations, SRE.L reporter gene assays or cytoskeletal changes (fig. 10A). With these methods the importance of this signaling axis was shown on the level of single cells as well as for regulation of important physiological parameters, like synaptic plasticity or blood pressure. The GPCR G protein Rho signaling pathway will interfere with other pathways to give rise to an integrated cellular response. Therefore it is important to study the temporal dynamics of the GPCR induced Rho signaling pathway. In the present study we aimed to elucidate the interaction of p63RhoGEF and the RH-RhoGEF LARG with $G\alpha_q$ and $G\alpha_{13}$, respectively, with high temporal and spatial resolution for the first time. As this information might give insight as to why RhoGEFs are activated downstream of two different Gα subfamilies and how information is integrated within one or between the two signaling pathways. Of note, this signal integration dictates the sensitivity as well as duration of the signaling upon stimulation of GPCRs by physiological agonists. Accordingly, several FRET assays were developed and the speed of RhoGEF inactivation was determined as kinetics of complex dissociation (k_{off}).

Recently adenylyl cyclase V regulation was found more sensitive towards stimulation with small agonist concentrations than the activation of its regulator $G\alpha_i$ (Milde et al., 2013). Thus we tested whether or not the concentration response relationships of the LARG $G\alpha_{13}$ and the p63RhoGEF $G\alpha_q$ interaction differed in sensitivity compared to the respective G protein activation. Such sensitivity differences between steps in the same signal transduction cascade would have to be considered for the emerging pharmacological targeting of the GPCR G protein RhoGEF Rho axis and are thus of great importance.

For sure this signaling pathway has to be tightly regulated by endogenous mechanisms besides the regulation by pharmacological tools. RGS2 was implicated as regulator for effector activation by $G\alpha_q$ for example in vascular smooth muscle cells. Therefore we wondered whether the kinetic and sensitivity of p63RhoGEF activation is regulated by RGS2, which expression is modulated by several stimuli, and used our new FRET tools in addition to well-established methods to study this in detail.

5 Material and methods

5.1 Material

5.1.1 Plasmids

DAG sensor	rat	Addgene (plasmid 14865) (Violin et al., 2003)
FLAG-LARG	human	cloned during this thesis
GIRK4-YFP	rat	L. Pott, Universität Bochum (Mintert et al., 2007)
$G\alpha_{13}$ Q226L ($G\alpha_{13}$ QL)		T. Wieland, Universität Heidelberg (personal communication)
$G\alpha_{13}$-mTur2	mouse	A.-L. Krett in the workgroup of M. Bünemann (personal communication)
$G\alpha_{13}$-wt	mouse	A.-L. Krett in the workgroup of M. Bünemann (personal communication)
$G\alpha_{13}$-YFP	mouse	A.-L. Krett in the workgroup of M. Bünemann (personal communication)
$G\alpha_{i1}$-CFP	rat	M. Bünemann, University Würzburg (Hein and Bünemann, 2009)
$G\alpha_{q}$-CFP	murine	C. Berlot, Yale University School of Medicine (Hughes et al., 2001)
$G\alpha_{q}$-wt	murine	C. Berlot, Yale University School of Medicine (Hughes et al., 2001)
$G\alpha_{q}$-YFP	murine	C. Berlot, Yale University School of Medicine (Hughes et al., 2001)
$G\beta_{1}$-Cer	human	M. Bünemann, University Würzburg (Frank et al., 2005)
$G\beta_{1}$-wt	human	M. Bünemann, University Würzburg (Bünemann et al., 2003)
$G\gamma_{2}$-wt	bovine	M. Bünemann, University Würzburg (Bünemann et al., 2003)
H_1-R	human	T. Wieland, Universität Heidelberg (Lutz et al., 2005)

LARG-insYFP	human	E.-L. Bodmann in the workgroup of M. Bünemann (Bodmann, diploma thesis)
M_3-R	human	Missouri S&T cDNA Resource Center (http://www.cdna.org; #MAR030TN00)
mCFP		M. Bünemann, University Würzburg (Hein et al., 2005)
mTur2		V. Wolters in the workgroup of M. Bünemann (Wolters et al., under revision)
p63RhoGEF	human (580aa; NP_891992)	T. Wieland, University Heidelberg (personal communication)
p63RhoGEF-CFP	human	cloned during this thesis
p63RhoGEF-CFP F471E L475A	human	cloned during this thesis
pcDNA3-mRFP		Addgene (plasmid 13032 from Doug Golenbock)
pcDNA3		Invitrogen
pcDNA3-LARG	human	cloned during this thesis
pCMV		T. Wieland, University Heidelberg (personal communication)
pGex Rho/RBD		R. Grosse, University Marburg (Brandt et al., 2002)
pHyg-LARG	human	T. Wieland, University Heidelberg (personal communication)
PLCβ3	mouse	P. Gierschick, University Ulm (Illenberger et al., 2003)
pRL-TK		Promega
pSRE.L		Provided by T. Wieland, University Heidelberg (Hill et al., 1995)
RGS2	human	Missouri S&T cDNA Resource Center (http://www.cdna.org)

RGS2-mRFP	human	cloned during this thesis
RGS2-YFP	human	S. Heximer, University of Toronto (Gu et al., 2008)
Si-eYFP-β_2AR	human	V. Wolters in the workgroup of M. Bünemann (Wolters et al., under revision)
Si-eYFP-β_2AR-mTur2	human	cloned during this thesis
Si-Venus-β_2AR-CFP	human	cloned during this thesis
Tax_2-R	human	T. Wieland, University Heidelberg (personal communication)
Venus-p63RhoGEF (V-p63RhoGEF)	human (580aa; NP_891992)	A. Rinne in the workgroup of M. Bünemann (Bodmann et al., 2014)
V-p63RhoGEF F471E	human	A. Rinne in the workgroup of M. Bünemann (Bodmann et al., 2014)
V-p63RhoGEF F471E L475A	human	A. Rinne in the workgroup of M. Bünemann (Bodmann et al., 2014)
V-p63RhoGEF L475A	human	A. Rinne in the workgroup of M. Bünemann (Bodmann et al., 2014)
YFP-LARG (LARG N-terminally tagged with eYFP)	human	E.-L. Bodmann in the workgroup of M. Bünemann (Bodmann, diploma thesis)
YFP-LARG F1098A I1100E	human	cloned during this thesis
YFP-PLCβ3	human	M. Frank in the workgroup of M. Bünemann (personal communication)
α_{2A}-AR	murine	M. Bünemann, University Würzburg (Bünemann et al., 2001)
β_2AR-CFP	human	C. Krasel, University Würzburg (Krasel et al., 2005)
β_2AR-Tur	human	C. Krasel in the workgroup of M. Bünemann (personal communication)

5.1.2 Bacteria and cell lines

Two *Escherichia coli* strands were used. The chemically competent *E. coli* strain DH5α was used for plasmid amplification and the *E. coli* strain Rosetta2 (DE3) (Novagen, Darmstadt) for protein expression. All experiments were performed in human embryonic kidney cells. In most cases HEK293TSA cells were used and for indicated experiments HEK293 cell stably transfected with murine H_1 histaminergic receptor, which were a kind gift from Roland Seifert, Medizinische Hochschule Hannover.

5.1.3 Primers

The primers were ordered from Eurofins Genomics. They synthesize the oligomers by solid phase synthesis with phosphoramidite chemistry (Caruthers et al., 1983). All primers used for QuickChange® mutagenesis or with a size longer than 29 bases were purified with a liquid chromatography based method, the High Purity Salt Free method by Eurofins Genomics. Before use all primers were dissolved to a final concentration of 100pmol/µL in ultrapure water.

5.1.3.1 Primers used for cloning

Primer name	Sequence	Cloning project	Melting temperature
5´-Flag-Larg-Bam	aaaaggatccatggattataaggatgatgatgataaaaatgagtggcacacagtctac	Flag-LARG	60°C
3´-YFP-Larg-Xho	ggtactcgagctaacttttatctgagtgcttg	Flag-LARG	60°C
5´-RGS2_Kpn1	aaaaaaggtaccatgcaaagtgctatgttcttggc	RGS2-RFP	62°C
3´-RGS2_Not1	aaaaaagcggccgcggtgtagcatgaggctctgtgg	RGS2-RFP	62°C
5´-BamHI-Si	aaaaaaggatccatgaagacgatcatcgccctgagctacatcttctgcctggtattcgccatggtgagcaagggcgag	Si-Venus-β_2AR-CFP	60°C
3´-Venus-XbaI	aaaaaatctagacttgtacagctcgtcc	Si-Venus- β_2AR-CFP	60°C

5.1.3.2 Primers used for QuickChange® site-directed mutagenesis

Primer name	Sequence	Cloning project
5´-p63RhoGEF-FELA	cgggacgaactcaacgcagcgcagtcacccattgag	p63RhoGEF-CFP F471E L475A
3´-p63RhoGEF-FELA	ctcaatgggtgactgcgctgcgttgagttcgtcccg	p63RhoGEF-CFP F471E L475A
5´-mTurq2-TTC	ctggagtacaactacttcagcgacaacgtc	Si-eYFP-beta2AR-mTur2
3´-mTurq2-TTC	gacgttgtcgctgaagtagttgtactccag	Si-eYFP-beta2AR-mTur2
5´-LARG-F1098A	caacagataacaaagctttagccgtcatttccatgtcagac	YFP-LARG F1098A I110E
5´-LARG-I1100E	gataacaaagctttagccgtcgaatccatgtcagacaatggcgc	YFP-LARG F1098A I110E

5.1.3.3 Sequencing primers

In most cases standard primers form Eurofins Genomics were used, which are listed at http://www.eurofinsgenomics.eu/media/968735/standard-vector-primer.pdf. Additional primers are listed below and were also ordered from Eurofins Genomics.

Primer name	Sequence	Binds to LARG
Seq_Larg_1	caggactgactgtagcagtg	from bp875
Seq_Larg_2	agtgaaagagcctcgaaatttg	from bp1679
Seq_Larg_3	tttggagaaagtcaaagtgagg	from bp2247
Seq_Larg_4r	tgatttcccagaggtactcag	until bp3594

5.1.4 Chemicals

1 kb ladder	New England BioLabs, Frankfurt
Acetylcholine	Sigma-Aldrich, Steinheim
Acrylamide/ Bisacrylamide	Carl Roth, Karlsruhe
Agar	Applichem, Darmstadt
Ammonium persulfate (APS)	Sigma-Aldrich, Steinheim
Ampicillin	Applichem, Darmstadt
Bovine serum albumin (BSA)	Sigma-Aldrich, Steinheim
Bovine serum albumin (BSA) (delipidized)	Sigma-Aldrich, Steinheim

Bromophenol blue	Sigma-Aldrich, Steinheim
Calcium chloride	Sigma-Aldrich, Steinheim
Cheluminate-HRP PicoDetect	Applichem, Darmstadt
cOmplete ULTRA Tablets, Mini, EDTA-free, EASYpack (protease inhibitor cocktail)	Roche, Mannheim
Desoxyribonucleotides (dNTPs)	New England BioLabs, Frankfurt
Dimethyl sulfoxide	Sigma-Aldrich, Steinheim
DMEM high glucose	Capricorn, Ebsdorfergrund
dNTP mix	New England BioLabs, Frankfurt
DTT	Sigma-Aldrich, Steinheim
EDTA	Sigma-Aldrich, Steinheim
Effectene Transfection Reagent	Qiagen, Hilden
Ethanol absolute	Roth, Karlsruhe
Ethidium bromide	Promega, Mannheim
FCS superior	Biochrom, Berlin
G-418 Sulphate	PAA, Pasching
Glycine	Carl Roth, Karlsruhe
HEPES	Sigma-Aldrich, Steinheim
Histamine	Sigma-Aldrich, Steinheim
Isopropanol	Roth, Karlsruhe
Isopropylβ-D-1-thiogalactopyranoside (IPTG)	Applichem, Darmstadt
Kanamycin sulfate	Roth, Karlsruhe
LB-medium powder according to Lennox	Applichem, Darmstadt
LE Agarose	Biozym, Hessisch Oldendorf
L-glutamine 200 mM	Biochrom, Berlin
Magnesium chloride	Sigma-Aldrich, Steinheim
Magnesium sulfate	Sigma-Aldrich, Steinheim
Methanol	Lenz-Chemie, Westerburg
Milk powder	Carl Roth, Karlsruhe
Noradrenaline bitartrate	Sigma-Aldrich, Steinheim
PBS	Biochrom, Berlin

PEG 3000	Sigma-Aldrich, Steinheim
Penicillin/Streptomycin (10.000 U/mL / 10mg/mL)	Biochrom, Berlin
peqGOLD Protein Marker IVv	PEQLAB Biotechnologie, Erlangen
Polyethylenimine (PEI, linear. 25kDa)	Polysciences, Eppelheim
PolyFect Transfection Reagent	Qiagen, Hilden
Poly-L-lysine-hydrobromide	Sigma-Aldrich, Steinheim
Potassium chloride	Sigma-Aldrich, Steinheim
Protino® Glutathione Agarose 4B (Glutathione-coated agarose beads)	Machery-Nagel, Düren
Sodium chloride	Sigma-Aldrich, Steinheim
Sodium deoxycholate	Sigma-Aldrich, Steinheim
Sodium dodecyl sulfate (SDS)	Carl Roth, Karlsruhe
TEMED	Carl Roth, Karlsruhe
Tris	Sigma-Aldrich, Steinheim
Tris-Acetat	Sigma-Aldrich, Steinheim
Trition X-100	Sigma-Aldrich, Steinheim
Trypsin/ EDTA (1:250)	Biochrom, Berlin
U46619 (Txa_2-R agonist)	Biomol, Hamburg
β-mercaptoethanol	Sigma-Aldrich, Steinheim

5.1.5 Consumables

Cell culture dish 6 cm & 10 cm (coated)	Greiner, Solingen
Cell culture plate 6-well (coated)	Greiner, Solingen
Cell culture plate 96-well (coated)	Greiner, Solingen
Cell scraper 16cm	Sarstedt, Nümbrecht
Cover slips 25 mm	VWR, Darmstadt
Cuvettes	Bio-Rad, München
Parafilm	Brand, Wertheim
Pasteur pipets	Hartenstein, Würzburg
PCR-tubes 0,2 mL	Brand, Wertheim
Petri dish (uncoated)	Hartenstein, Würzburg

Pipet tips 10 µL, 200 µL, 1000 µL	Greiner, Solingen
Polyvinylidene fluoride (PVDF) membrane	Roche, Mannheim
Reaction tubes 1,5 & 2,0 mL	Hartenstein, Würzburg
Reaction tubes 15 mL & 50 mL	Greiner, Solingen
Ritips for multipette Plus®	Kobe, Marburg
Whatman paper	VWR, Darmstadt
White 96-well plates	Perkin Elmer, Waltham, USA

5.1.6 Kits

Dual-Luciferase® Reporter Assay System	Promega, Mannheim
Plasmid Midi Kit	Qiagen, Hilden
QIAquick Gel Extraction Kit	Qiagen, Hilden

5.1.7 Enzymes

Phusion DNA polymerase	New England BioLabs, Frankfurt
Restriction endonucleases, various	New England BioLabs, Frankfurt
Ribonuclease A (RNAse A)	Roth, Karlsruhe
T4 DNA ligase	New England BioLabs, Frankfurt
T4 DNA polymerase	New England BioLabs, Frankfurt

5.1.8 Antibodies

5.1.8.1 Primary antibodies

Against	**Produced in**	**Catalog no.**	**Company**	**Dilution**
Actin	mouse	691001	MP Biomedicals, Santa Ana	1:100.000
$G\alpha_{13}$	goat	sc-26788	Santa Cruz, Heidelberg	1:200
GFP	goat	600-101-215	Rockland, Gilbertsville	1:300
LARG (H-70)	rabbit	sc-25638	Santa Cruz, Heidelberg	1:2000
Rho	rabbit	2117S	Cell Signaling, Darmstadt	1:2000

5.1.8.2 Secondary antibodies

All secondary antibodies are conjugated to horse radish peroxidase.

Against	Produced in	Catalog no.	Company	Dilution
Goat	horse	PI-9500	Vector Laboratories, Burlingame	1:3.500
Mouse	horse	7076	Cell Signaling, Darmstadt	1:3.500
Rabbit	goat	7074	Cell Signaling, Darmstadt	1:3.500

5.1.9 Equipment

300 Volt Electrophoresis Power Supply	Labnet, Ried im Innkreis
Autoclav VX-95	Systec, Bergheim
Cell chamber Attofluor	Invitrogen, Darmstadt
ChemiDoc (gel analyzer)	Bio-Rad, München
Digital Sonifier	Branson
F100 Compact Ice flaker	Icematic, Düsseldorf
Feinwaage 770 (precision balance)	KERN & Sohn, Balingen-Frommern
FLUOstar OPTIMA	BMG Labtech, Ortenberg
Freezer (-80 °C) FORMA 900 Series	Thermo Scientific, Waltham, USA
Freezer Premium NoFrost	Liebherr, Biberach an der Riss
Fridge Profiline	Liebherr, Biberach an der Riss
Hamilton pipet	Hamilton company, Reno, USA
Heraeus Fresco 17 Centrifuge	Thermo Scientific, Waltham, USA
Heraeus Megafuge 16R Centrifuge	Thermo Scientific, Waltham, USA
Horizontal shaker 3015	GFL, Burgwedel
Incubator APT.line^{TM} C150	Binder, Tuttlingen
Laminar flow NU-437-400E	INTEGRA Biosciences, Fernwald
Magnetic stirrer MR Hei-Standard	Heidolph, Schwabach
Microwave R-202	SHARP, Hamburg
Mini Trans-Blot® Cell	Bio-Rad, München

Mini-PROTEAN® Tetra Cell	Bio-Rad, München
Mini-PROTEAN® Tetra Cell Casting Module	Bio-Rad, München
Multilabel Reader EnVision	Perkin Elmer, Waltham,USA
Multipette Plus®	Eppendorf, Hamburg
Nano photometer	Implen, München
pH meter FiveEasy	Mettler Toledo, Giessen
Pipet Gilson Pipetman	Gilson, Limburg-Offheim
PipetHelp	Accumax, India
Sorvall RC5B Plus with Sorvall GSA rotor	Thermo Scientific, Waltham, USA
Spectrophotometer SmartSpec Plus	Bio-Rad, München
Thermocycler	SensoQuest, Göttingen
Thermomixer comfort	Eppendorf, Hamburg
Ultra Clear UV plus (ultrapure water device)	SG, Hamburg
UV light table	Eurofins MWG Operon, Ebersberg
Vortex – Genie2	Scientific Industries, Bohemia, USA

5.1.10 Microscopes

5.1.10.1 Microscope for most FRET measurements: Visitron set-up

The devices are labeled according to their primary function. False excitation or bleed through is neglected at this point and will be described in detail later (see 5.2.6). In figure 12 the spectra of YFP and CFP are shown together with the filters used during FRET measurements and figure 13 illustrates how the filters are principally installed into the microscopes.

All FRET measurements, except the ones mentioned in 5.1.10.2, have been conducted with this set-up.

Device	**Type**	**Supplier**
inverted microscope	Axiovert 100	Zeiss, Oberkochen
micromanipulator	MM 33	Merzhäuser, Wetzlar
perfusion system	VC3-8xP Series	ALA Scientific Instruments, Farmingdale, USA
light source CFP excitation[2]	precisExcite-100, 440nm	CoolLED, Andover, UK

[2] The intensity was set to 10%.

light source YFP excitation[3]	precisExcite-100, 500nm	CoolLED, Andover, UK
high performance CCD-camera	SPOT Pursuit	SPOT Imaging solutions, Sterling Heights, USA
objective	Plan/Apo N 60x/1.45 Oil	Nikon, Düsseldorf
air-cushioned optical table	Vision IsoStation™	Newport, Stahnsdorf
software	VisiView	Visitron Systems, Puchheim
Filters used during FRET measurement		
excitation filter CFP	436/20	Chroma Technology, Bellows Falls, USA
dichroic	458LP	Semrock, Rochester, USA
beam splitter (separates YFP emission from CFP emission)	505LP and 416;500;582;657	Chroma Technology, Bellows Falls, USA
CFP emission filter	470/24	Chroma Technology, Bellows Falls, USA
YFP emission filter	525/39	Semrock, Rochester, USA
Filters used to search for cells and during direct YFP measurement		
dualband excitation filter CFP/YFP	416;501	Semrock, Rochester, USA
dichroic	440;520	Semrock, Rochester, USA
dualband emission filter CFP/YFP	464;547	Semrock, Rochester, USA

[3] The intensity was set to 4%.

5.1.10.2 Microscope for some FRET measurements: Nikon set-up

This microscope was used for the FRET experiments shown in figures 31, 34, 35, 37. The devices are labeled according to their primary function. False excitation or bleed through is neglected at this point and will be described in detail later (see 5.2.6). The filters are installed in the set-up according to figure 13.

Device	**Type**	**Supplier**
inverted microscope	Eclipse Ti	Nikon, Düsseldorf
micromanipulator	MM 33	Merzhäuser, Wetzlar
perfusion system	VC3-8xP Series	ALA Scientific Instruments, Farmingdale, USA
light source[4]	Lambda DG4	Sutter, Novato. USA
high performance CCD-camera	Evolve512	Photometrics, Tucson, USA
objective	Plan/Apo VC 100x/1.40 Oil ∞/0.17 Dic N2	Nikon, Düsseldorf
air-cushioned optical table	Vision IsoStation™	Newport, Stahnsdorf
software	NIS Elements AR	Laboratory Imaging
Filters used during FRET measurement		
excitation filter CFP	430/24	Chroma Technology, Bellows Falls, USA
dichroic	T455LP	Chroma Technology, Bellows Falls, USA
beam splitter (separates YFP emission from CFP emission)	z488/800-1064	Chroma Technology, Bellows Falls, USA
CFP emission filter	480/40	Chroma Technology, Bellows Falls, USA
YFP emission filter	535/30	Chroma Technology, Bellows Falls, USA
Filters used to search for cells and during direct YFP measurement		
dualband excitation filter CFP/YFP	≈425; 500 (Item number F59-017)	Chroma Technology, Bellows Falls, USA

[4] The intensity was set to 30%.

dichroic	≈470;550; 690; 950 (Item number F58-017)	Chroma Technology, Bellows Falls, USA
dualband emission filter CFP/YFP	≈475;525 (Item number F57-017)	Chroma Technology, Bellows Falls, USA

5.1.10.3 Microscope for confocal and translocation studies: VisiTech Set-up

Device	**Type**	**Supplier**
inverted microscope	IX 71	Olympus, Hamburg
micromanipulator	MM 33	Merzhäuser, Wetzlar
perfusion system	VC3-8xP Series	ALA Scientific Instruments, Farmingdale, USA
light sources	405nm and 491nm lasers	VisiTech International, Sunderland, UK
high performance CCD-camera	EM-CCD Digital Camera	Hamamatsu, Herrsching am Ammersee
objective	UPlanSApo 100x/ 1.40 Oil	Olympus, Hamburg
air-cushioned optical table	Vision IsoStation™	Newport, Stahnsdorf
software	VoxCell Scan	VisiTech International
FRAP imaging system	VT-HAWK	VisiTech international
dichroic	T495lpxr	Chroma Technology, Bellows Falls, USA
beam splitter (separates YFP emission from CFP emission)	Optosplit II with FF560-FDi01, FF01-525/39 and FF01-593/46	Semrock, Rochester, USA
CFP emission filter	ET 470/40	Chroma Technology, Bellows Falls, USA
YFP emission filter	ET 535/30	Chroma Technology, Bellows Falls, USA

5.1.11 Databases, software

5.1.11.1 Databases

National Centre for Biotechnology Information	http://www.ncbi.nlm.nih.gov
Pubmed	http://www.ncbi.nlm.nih.gov/pubmed

5.1.11.2 Software

ApE – A plasmid Editor	M. Wayne Davis
BLAST	http://blast.ncbi.nlm.nih.gov/Blast.cgi
corelDRAW X4	Corel Cooperation, Ottawa, Canada
Fluorescence SpectraViewer	http://www.lifetechnologies.com/de/de/home/life-science/cell-analysis/labeling-chemistry/fluorescence-spectraviewer.html
GraphPad Prism 5 for Windows	GraphPad Software, La Jolla, USA
ImageJ	Wayne Rasband, National Institutes of Health, USA
Mendeley Desktop	Mendeley, Washington, USA
Microsoft Office 2010 (Word, Excel, PowerPoint)	Microsoft, Unterschleißheim
NSI-Elements AR 64bit	laboratory Imaging, Prag, Czech Republic
Optima	BMG Labtech, Ortenberg
Origin Pro	OriginLab Corporation, Northampton, USA
PCR Primer Design Tool	https://ecom.mwgdna.com/services/manage-primers/design-primer.tcl
PrimerX	http://www.bioinformatics.org/primerx/
QuantityOne	Bio-Rad, München
VisiView	Visitron Systems, Puchheim
VoxCell Scan	VisiTech International, Sunderland, UK

5.1.12 Buffer, media

Standard buffers and media are listed here. Buffers only are used for one method are listed with the according method.

FRET buffer

137mM NaCl
5,4mM KCl
10mM HEPES
2mM $CaCl_2$
1mM $MgCl_2$
in ultrapure water, pH = 7,3

LB medium

20g LB medium powder according to Lennox
ad 1 L Ultrapure water
autoclaved

RIPA buffer (Alcaraz et al., 1990)

50 mM Tris-Base, pH 7.5
500 mM NaCl
10 mM $MgCl_2$
1% (v/) Triton X-100
0.1% (w/v) SDS
0.5% (w/v) Sodium Deoxycholate
1 mM EDTA
Added fresh:
1pill/10mL buffer protease inhibitor
2mM DTT

5x SDS gel-loading buffer

250 mM Tris, pH 6.8
10 % (w/v) SDS
0.5 % (w/v) Bromophenol blue
20 % (w/v) Glycerol
200mM β-mercaptoethanol
in ultrapure water

TE buffer (Tris/EDTA)

10 mM Tris-HCl pH7,4
1 mM EDTA

5.2 Methods

5.2.1 Cell culture

Human embryonic kidney (HEK) cells were cultured at 37°C, 90-95% humidity and 5-10% CO_2 in an incubator. The cells were split every three to five days according to their growth rate. During the culture HEK293TSA cells were maintained in full medium, which consisted of DMEM medium (Dulbecco´s modified eagle´s medium high glucose) with 10% (v/v) fetal calf serum (FCS), 2mM L-glutamine, 100U/mL penicillin and 0.1mg/mL streptomycin. If the same medium was mixed with 0.5% (v/v) FCS instead of 10%, this is entitled as DMEM 0.5% FCS. Further DMEM without supplements (DMEM w/o) was used for two transfection methods (5.2.1.2.2 and 5.2.1.2.3).
Additionally mH_1-R-HEK293T cells were used for the experiments shown in figure 33A, B and 36. These cells stably express the murine H_1-R and a G-418 resistance. Therefore cells expressing these genes were protected against G-418 induced cytotoxicity and were selected for this property by culture in full medium additionally containing 1mg/mL G-418.

5.2.1.1 Cell splitting

Cells were detached from a cell culture dish by incubation with trypsin/EDTA for one to three minutes. Afterwards they were collected by washing of the dish with full medium and centrifugation at 1.000rpm for three minutes (Heraeus Fresco 17 centrifuge). Finally the cell pellet was resuspended with medium and seeded at a suitable density.

5.2.1.2 Transient transfection of eukaryotic cells

DNA transfer into eukaryotic cells is called transfection. Several different protocols have been invented in order to increase transfection efficiency. The method of choice depends on cell type, transfection scale and specific use of the cells after transfection. In this thesis HEK293T cells were transfected with *Effectene transfection reagent* for live cell imaging, with *PolyFect transfection reagent* for SRE.L reporter gene assays and with *polyethylenimine* (*PEI*) for affinity purification of active Rho and Western Blot.

5.2.1.2.1 Effectene transfection

Cells were plated on 6cm dishes one to three days prior to transfection. At the day of transfection the cells showed a density of 50 to 70% and in the evening they were transfected according to the manufacturer´s protocol: Briefly, the DNA mixture described for each experiment was mixed with GC buffer to a total volume of 150µL and incubated with 16µL Enhancer and 20µl Effectene. Afterwards the transfection solution was mixed with 500µl full medium and everything was added dropwise to the cells.

5.2.1.2.2 PolyFect transfection

The PolyFect transfection was used as inverse transfection method. So the DNA was added to a 96well plate first and then transfection reagent and cells were added. The DNA composition used for each condition can be found in the results part and the volume was filled up with DMEM without supplements (DMEM w/o) to 10µL. Afterwards 1.25µl PolyFect plus 8.75µL DMEM w/o were added and everything was incubated for ten minutes. Finally 100µL cell suspension (DMEM 0.5% FCS) was added. In the next hours cells were transfected while they settled down.

5.2.1.2.3 PEI transfection

Large scale transfection (one 10cm dish per condition) was done with unbranched, linear, 25kDa polyethylenimine (Polysciences) (Boussif et al., 1995). Therefore DNA was mixed with PEI in a stoichiometry of 1:3 (w/w) in a total volume of 1mL DMEM w/o and incubated in the dark at 20°C for 30min. Afterwards the mixture was added dropwise to the cells in full medium and medium was exchanged after six hours for DMEM 0.5% FCS.

5.2.1.3 Cell transfer onto coverslips

Cells were transferred onto coverslips in order to examine them by fluorescence microscopy on the following day. In advance coverslips were placed one to one into wells of a 6-well plate and pretreated. The coverslips were incubated with approximately 100µL poly-L-lysine for 30min and then washed with PBS once. The cells were split (see 5.2.1.1) onto coverslips in full medium and low density. The low density should allow for single cell measurements on the next day.

5.2.2 Molecular biology

5.2.2.1 Casting agar plates

Bacteria colonies were grown on agar plates. Therefore 1.5% (w/v) agar was solved in LB medium and autoclaved. The solution was chilled to approximately 40°C and if necessary supplemented with an antibiotic (ampicillin 100µg/ml, kanamycin 50µg/ml). Afterwards the solution was poured on Petri dishes and coagulated at room temperature. Agar plates are good for some weeks at 4°C.

5.2.2.2 Production of chemically competent E. coli

If bacteria should be transformed with DNA, they have to be made competent in advance (Chung et al., 1989).

E. coli (strain DH5α) were cultured on an antibiotic-free agar plate at 37°C overnight. From this plate one colony was picked and culture in 10mL LB medium (37°C, overnight). This preculture was filled up with LB medium to 250mL and cultured. The growth was monitored by absorptiometry (see. 5.2.2.3). At an OD_{600} of 0.5-0.7 bacteria were harvested in the logarithmic growth phase by centrifugation at 5.000rpm for ten minutes (Heraeus Fresco 17 centrifuge). The pellet was carefully resuspended in 25mL ice-cold TBS buffer and incubated on ice for one to two hours. Subsequently bacteria were aliquoted and frozen in liquid nitrogen. Competent bacteria were stored at -80°C.

TSB buffer
10 % (w/v) PEG 3000
5 % (v/v) DMSO
20 mL $MgCl_2$
in LB medium

5.2.2.3 Absorptiometry of bacteria suspensions

The concentration of bacteria within a suspension can be estimated by absorptiometry. Therefore the absorbance at 600nm was measured with a Smart Spec Plus spectrophotometer. First pure LB medium was measured as blank and afterwards the bacteria culture every 30 min.

5.2.2.4 Transformation of bacteria

Plasmid DNA can be amplified in *E. coli* (strain DH5α). These chemically competent *E. coli* (5.2.2.2) were transformed by the modified heat-shock method (Chung et al., 1989). Therefore DNA (0.2 to 5µL dependent on concentration) was incubated with 20µl KCM buffer, 100µl chemically competent *E. coli* and ad 200µL ultrapure water on ice for 20min. Afterwards the mixture was incubated at room temperature for 10min. After addition of LB medium the bacteria were grown shaking, at 37°C for 50min and then plated on an agar plate supplemented with either ampicillin or kanamycin. Overnight only bacteria, which expressed a resistance against the antibiotic on the plate, grew into colonies at 37°C.

KCM buffer (potassium calcium magnesium buffer)
500 mM KCl
150 mM $CaCl_2$
250 mM $MgCl_2$

Protein expression was done in the *E.coli* strain Rosetta2 (DH3). These bacteria have to be transformed by the heat-shock method according to the manufacturer. Therefore 0.2µg DNA was

mixed with one aliquot *E.coli* and incubated on ice for 30min. Then a heat-shock of 42°C for 30s was applied, which was followed by 5min on ice. After addition of 950µL LB medium the bacteria were grown shaking at 37°C for an hour and then plated on agar as described before.

5.2.2.5 Production of glycerol stocks of bacteria

E.coli carrying a plasmid can be stored for long term at -80°C, if they are kept in a glycerol stock. The glycerol protects the frozen bacteria from cell membrane damage. For this method fresh bacteria culture was mixed 1:1 with a glycerol solution (glycerol (65% (v/v)), 0.1M $MgSO_4$ and 25mM TrisHCl, pH8) and frozen at -80°C.

5.2.2.6 DNA preparation: Midi

Plasmid DNA was extracted from bacteria in large scale with the Qiagen Plasmid Midi Kit according to the manufacturer´s protocol. This kit makes use of the alkaline lysis method (Birnboim and Doly, 1979). In the end the dry DNA pellet was resuspended in ultrapure water.

5.2.2.7 DNA preparation: Mini

The small scale DNA extraction makes also use of the alkaline lysis. This time the DNA was not extracted with a kit, but with self-made buffers (see below) and a modified version of Birnboim and Doly´s protocol for DNA extraction (Birnboim and Doly, 1979; Sambrook and Russel, 2001) (Birnboim and Doly, 1979). Thus the DNA was not purified with a column. Consequently the DNA yield of a Mini preparation is not as pure as the one from a Midi preparation. Mini preparations were not used for sequencing, cloning, transformation or transfection, only for control of cloning by control digestion with restriction enzymes (5.2.2.8).

For a mini preparation 4ml LB medium were incubated with one *E.coli* colony at 37°C, shaking overnight. At the next day 2mL of this culture were centrifuged (2min, 13.300rpm, Heraeus Fresco 17 centrifuge[5]) and the leftover was stored for further use at 4°C. The bacteria pellet was resuspended in 100µL resuspension buffer and then the bacteria were lysed by alkaline lysis with 200µL lysis buffer. Already the first buffer contains RNAse to ensure complete digestion of RNA before the DNA precipitation step. Upon addition of 150µL neutralization buffer the pH changed quickly. Proteins and genomic DNA precipitated during 5min incubation on ice and subsequent centrifugation (10min, 13.300rpm). Then the supernatant was mixed with 450µL isopropanol. The salt in the solution neutralize the negative charges in the sugar phosphate backbone of the nucleotide chain and the isopropanol assists the interaction of the two. Since this makes the nucleotide chains more hydrophobic, a DNA pellet occurred upon 10min centrifugation with 12.000rpm. The pellet was washed with 70% (v/v) ethanol once, then air-dried and resuspended in ultrapure water.

[5] This centrifuge was used for the whole procedure.

Resuspension buffer	Lysis buffer	Neutralization buffer
50 mM Glucose	0,2M NaOH	60 mL Potassium acetate (5 M)
10 mM EDTA	1 % (w/v) SDS	11,5 mL Acetic acid (96 %)
25 mM Tris(base), pH 8.0	in ultrapure water	28,5 mL ultrapure water
in ultrapure water		
Added fresh:		
200µg/ml RNAse		

5.2.2.8 DNA digestion with a restriction enzyme

Restriction endonucleases, also known as restriction enzymes, are used by bacteria to cut DNA at specific sites. In most cases they recognize four to eight bases long, palindromic sequences and cut at these sites, which may result in an overhang depending on the enzyme used. An overhang allows for some specificity in the ligation step (see 5.2.2.12). In this step a ligase connects nucleotide chains. During this thesis restriction enzymes were used for cloning and to control plasmids by their digestions pattern. In both case the DNA fragments were separated according to their size by agarose gel electrophoresis (see 5.2.2.9).

2µg DNA were mixed with 0.5µl restriction enzyme, 2µl 10-fold buffer, if necessary 0.2µg 100-fold BSA and ad 20µl ultrapure water and digested at 37°C for one hour. The buffer version and BSA were used according to the manufacturer's protocol. Where indicated two restriction enzymes were used at the same time and their activity in the same buffer was checked with the manufacturer's protocol beforehand.

5.2.2.9 Agarose gel electrophoresis

DNA fragments can be separated according to their size by gel electrophoresis. Therefore agarose gels were cast with a density of 0.8% or 1% (w/v) agarose in TAE buffer. The density was adjusted to the expected fragment size. The cooled gel was loaded with 2µg DNA per slot, which was mixed with loading buffer (10-fold) to a final volume of 20µL. In addition a 1kb DNA ladder was loaded, which enabled evaluation of the fragment size. The separation occurred due to a voltage of 100V and the pore size of the agarose matrix. Smaller DNA fragments ran faster than larger ones. Afterwards the gel was illuminated with UV light and DNA fragments glowed due to the fluorescent ethidium bromide, which was added during gel casting. The DNA intercalating agent ethidium bromide binds specifically to DNA and is therefore enriched and glowing in DNA-rich regions of the gel. If needed DNA bands were cut out and DNA isolated (see 5.2.2.10) for ligation.

TAE buffer (Tris Acetate EDTA)
40 mM Tris-acetate pH 8,0
0.1 mM EDTA
in ultrapure water

5.2.2.10 DNA isolation from an agarose gel

DNA was isolated from an agarose gel if the DNA fragment was used further, for example for ligation (see 5.2.2.12). Therefore the QIAquick Gel Extraction Kit was used according to the manufacturer´s protocol and the DNA eluted with 30µL ultrapure water. Before the ligation, the DNA concentration had to be determined (see 5.2.2.11).

5.2.2.11 Determination of DNA concentration

The DNA concentration was determined with the Nano Photometer. The absorbance at 280nm and 320nm was measured for ultrapure water as blank and the DNA sample. From these values the concentration of the sample was calculated.

5.2.2.12 Ligation

The ends of DNA fragments can be reconnected with a phosphodiester bound by a ligation reaction. This is an enzymatic process mediated by T4 DNA ligase, for example. In the present work this process was used for cloning of small DNA fragments, also described as inserts, into vectors. A ligase works with higher efficiency if two compatible DNA ends overlap and such overlaps were produced with restriction enzymes at the insert and the vector of a cloning project (see 5.2.2.8). Nevertheless a T4 DNA ligase is also able to reconnect fragment, which do not have overhangs or which have mismatching overhangs.

In this thesis the small insert was used in a molecular excess of four to one over the large vector, in order to prevent closure of the vector without insert insertion. The reaction was mixed as follows and incubated for one to three hours at 16°C.

Volume/Amount	**Component**
0,5 µL	T4 DNA ligase
1 µL	10-fold T4 DNA ligase buffer
see above	insert
ca. 50 ng	vector
ad 10 µL	ultrapure water

5.2.2.13 DNA amplification

In 1986 Kary Mullis invented the polymerase chain reaction (PCR) as tool for DNA amplification (Mullis et al., 1986). The DNA amplification consists of several cycles of the same three steps and causes a monoexponential increase in DNA strands under perfect conditions. One cycle consists of melting of the template double strand, annealing of a small DNA sequence, also entitled as primer, onto the template and last but not least the elongation step. After such the cycle a next cycle is started.

For the PCRs performed during this thesis 30 cycles were conducted with a thermocycler (SensoQuest). In the first step the sample was heated to 98°C for 30s. This step leads to dissociation of the double-stranded template and therefore the single strands are accessible for the primers now. The primers anneal to their template with the matching nucleotides at a temperature, which depends on the sequence of the primer. The annealing temperature was calculated as follows:

Annealing temperature=2°C*number of T and A+4°C*number of C and G

For the primer annealing the thermocycler is set to the calculated annealing temperature for 30s. The primers were designed with an annealing temperature of 60°C to 62°. The primers used can be found in 5.1.3.1. In one PCR two primers are used each binding to one strand of the double-strands. Similar annealing temperatures were favored during the design of primer pairs for the same PCR and complementary sequences were avoided as far as possible, since this could induce primer dimerization.

For the next step the temperature is increased to the optimum temperature of the polymerase to ensure perfect elongation conditions. During the elongation step the polymerase binds one deoxyribonucleotide by another to the 3´-end of the primer matching with the template strand. DNA polymerases, which are used for PCR, have to be thermo-stable. The polymerase, Phusion, used here has 3´to 5´exonuclease activity, which allows for proof-reading. So mismatches, which occur during the polymerization, are promptly removed by the polymerase itself. The Phusion polymerase polymerizes 2kb per minute at 72°C. Therefore the duration of this step is adjusted to the length of the amplified fragment.

Afterwards the sample is heated to 98°C again and the next cycle starts. In the last cycle elongation is prolonged to ten minutes and then the reaction mix is stored at 4°C for further use. The reaction mix was prepared for the PCRs in this thesis on ice as follows:

Volume/ amount	**Component**
200 ng	template DNA
20 pmol	forward primer
20 pmol	reverse primer
500 pmol	dNTP mix
0,1 µL	Phusion
4 µL	5-fold polymerase buffer
ad 20 µL	ultrapure water

5.2.2.14 QuickChange® site-directed mutagenesis

By QuickChange® site-directed mutagenesis a DNA sequence can be mutated or in other words a base in the sequence can be exchanged. This method is evolved from ideas of Braman and colleagues (Braman et al., 1996) and inserts mutations by means of conventional PCR (see 5.2.2.13), but with the following differences: The elongation step is greatly extended; the primers have a mismatch to the annealing sequence and just 50ng template DNA is used.

Fig. 11 Localisation of the mismatch within a QuickChange® site-directed mutagenesis primer
This shows the alignment of 5´-LARG-F1098A primer (upper row) with wild type LARG (lower row) by "ApE". The mutation of phenylalanine to alanine in the amino acid sequence requires the exchange of two bases in the DNA sequence. In these two bases the primer and the template do not align (red asterisk).

In a conventional PCR the template portion between the two primers is elongated, whereas in a QuickChange mutagenesis the whole plasmid is amplified. Therefore the elongation time is extended.

In order to insert the mutation into the plasmid, the primer has this mutation flanked by matching sequences on both sides (fig. 11). This allows the primer to bind to the template and then the polymerase elongates the rest of the plasmid sequence to the primer. The mutagenesis primers are design with "PrimerX" and listed in 5.1.3.2.

After the PCR the mutated strands have to be separated from the wild type template. This separation is facilitated if fewer templates are added in the beginning. The template present is destroyed by DpnI digestion (see 5.2.2.8). DpnI is a restriction enzyme, which recognizes and cuts the sequence GATC but only when the A is N6-methylated. Only the template DNA is digested, since DNA is not methylated during PCR, but during amplification in *E.coli* DH5α.

The digestion efficiency was enhanced by precipitation of the DNA from the PCR mix with ethanol in advance. Then the pellet was air-dried and resuspended in ultrapure water. After the digestion 5µl of the reaction mix was directly transformed into *E.coli* (see 5.2.2.4) and after DNA preparation (see 5.2.2.6) the mutagenesis was controlled by sequencing (see 5.2.2.15).

5.2.2.15 Sequencing

The sequence of all cloned constructs was controlled by sequencing. Sequencing was done with the Sanger method by Eurofins MWG Operon (Sanger et al., 1977). The samples were prepared as follows: 0.75 to 1.5µg DNA, if necessary 15pmol primer, ad 15µl ultrapure water.

Eurofins Genomics supplies a range of standard primers, which were used if possible. Otherwise sequencing primers were designed using the "PCR Primer Design Tool" (see 5.1.3.3).

The results were aligned to reference sequences by means of "ApE" and the "Basic Local Alignment Search Tool".

5.2.3 Western Blot

5.2.3.1 Sample preparation

Cells were grown and transfected on 10cm dishes, medium was removed, cells were lysed with 600µl RIPA lysis buffer on ice and collected by scratching with cell scrapers. The cell lysate was cleared by centrifugation at 13.300rpm for four minutes (4°C, Heraeus Fresco 17 centrifuge) and removal of the cell debris. At this step further steps were added for "affinity purification of active Rho" (5.2.5). Otherwise immediately the cell lysate was boiled at 95°C for ten minutes and 5-fold SDS gel-loading buffer (5.1.12) was added. The last two steps destroy quaternary, tertiary and secondary structures of the proteins and SDS adds negative charges to the proteins according to their size. B-mercaptoethanol destroys disulfide bonds. The polyacrylamide gel was loaded with 20µl to 40µl sample per slot and 10µl peqGOLD protein marker.

5.2.3.2 Preparation and running a discontinuous SDS PAGE

Proteins can be separated by a discontinuous sodium dodecyl sulfate (SDS) polyacrylamide gel electrophoresis (PAGE) as invented by Laemmli (Laemmli, 1970). This method allows separation of the proteins into distinct bands according to their size. The PAGE is casted in two steps, which leads to a quick pH shift in the gel during the electrophoresis.

In the upper part of the PAGE, the so called stacking gel, the isotachophoresis takes place and all proteins are focused in one band. The pH 6.8 in the stacking gel is close to the isoelectric point of glycine. Therefore glycine is uncharged and migrates slowly, whereas chloride is charged and migrates fast. Between glycine and chloride an electric field occurs and all proteins stay within this field. Since proteins with high mobility explore a weak field force and proteins with low mobility explore a strong field force, all proteins are focused in one band.

The lower resolving gel has a higher pH of 8.8 and upon entering glycine gets charged immediately. Thus glycine passes the proteins and the electric field disappears. So now the speed of each protein depends only on its charge, which is proportional to its size due to SDS.

The PAGE was cast into a Mini-PROTEAN® Tetra Cell Casting Module. The polymerization is initiated by addition of a free radical source, ammonium persulfate (APS), and a catalyst, TEMED. These two substances led to the formation of acrylamide polymers. The reaction mixture contained bisacrylamide, which allowed for crosslinks between the acrylamide branches. First the resolving gel was cast and overlayed with isopropanol. After polymerization the isopropanol was removed, the stacking gel was poured on top and a comb was added.

The gel was installed into a Mini-PROTEAN® Tetra Cell and running buffer was added. After sample loading with a Hamilton pipet, the SDS PAGEs were run at 60V until the samples entered the resolving gel and then at 125V.

Resolving gel (10%)	Stacking gel (3.3%)	Running buffer
4mL Ultrapure water	6.2mL Ultrapure water	192mM Glycine
2.5mL 1.5M Tris, pH 8.8	2.5mL 0.5M Tris, pH 6.8	25mM Tris
0.1mL 10 % (w/v) SDS	0.1mL 10 % (w/v) SDS	0.1% (w/v) SDS
3.3mL 30% Acryl/Bis (37,5:1)	1.2mL 30% Acryl/Bis (37,5:1)	
0.05mL 10%(w/v) APS	0.05mL 10% (w/v) APS	
0.01mL TEMED	0.01mL TEMED	

5.2.3.3 Wet Blot

In order to detect the separated proteins with antibodies, the proteins were transferred to polyvinylidene fluoride (PVDF) membranes by electrophoresis. This can be achieved in a semi-dry fashion or as Wet Blot within a buffer-filled tank. All Western Blots shown were done by means of Wet blotting, which is a modified version of tank transfer invented by Towbin and colleagues (Towbin et al., 1992). A Mini Trans-Blot® Cell was used according to the manufacturer´s protocol. Briefly, a sandwich was made from a gel holder cassette, two sponges, two Whatman papers, the SDS PAGE and a methanol-activated PVDF membrane. The methanol activation for two minutes enhances protein binding to the membrane. The sandwich was put into the Mini Trans-Blot® Cell, which was filled with transfer buffer and the transfer was conducted with a constant current of 220mA for 2.5h.

Afterwards the membrane was cut into pieces according to the desired protein detections. Of note, for all antibodies specificity was first tested on complete membranes. The membranes were blocked with TBST containing 5% (w/v) BSA or milk powder for one hour, rotating at room temperature. The blocking with BSA was only done for the RhoA antibody. Next the membranes were incubated with primary antibodies overnight at 4°C. The antibodies were diluted in blocking solution and antibody dilutions are mentioned with the antibodies (see 5.1.8).

The next day the membranes were washed three times for five minutes with TBST and then the according horse radish peroxidase (HRP) -conjugated, secondary antibody was added for another hour at room temperature. Finally the membranes were washed three times for 15min with TBST.

The membranes were incubated with the HRP substrate and developed with ChemiDoc. Images were saved and processed with “QuantityOne” and “ImageJ”.

Transfer buffer	TBST
25mM Tris	20mM NaCl
192mM glycine	20mM Tris
20% (v/v) methanol	0.05% (v/v) Tween-20

5.2.4 SRE.L reporter gene assays

The SRE.L reporter gene assay was used to determine transcriptional activity downstream of RhoA (see 4.4.1) (Hill et al., 1995; Mao et al., 1998). The reporter gene construct pSRE.L consists of the *Photinus pyralis* luciferase gene under the control of a modified serum response element (SRE), which cannot bind the transcription factor TCF anymore (see 4.4.1 *Amongst others, ROCK is activated by the Rho subfamily* for details). Therefore luminesce at 570nm is a surrogate parameter for transcriptional activity downstream of RhoA activation. Besides the pSRE.L the constitutive active reporter gene construct pRL-TK was transfected. This plasmid encodes for *Renilla reniformi*s luciferase and transcription is regulated by the constitutive active *Herpes simplex* thymidine kinase promoter. Thus luminescence at 475nm was used to correct for transfection efficiency, cell number and cell viability. Each condition was transfected with PolyFect Transfection Reagent in triplicates in a 96well plate and further processed with the Dual-Luciferase® Reporter Assay System according to manufacturer´s protocol. Luminescence was detected for both wavelengths by the multilabel reader EnVision.

Briefly all conditions were transfected with the same DNA amount (125ng/well): pSRE.L (21.6), pRL-TK (3.4) and as indicated RhoGEF, receptor, G protein, empty vector. Agonist-stimulated assays were lysed after 48h with 20µL passive lysis buffer per well, whereas the other assays were lysed after 24h. In response to transfection efficiency 2 to 10µL lysate was transferred to a white 96-well plate. In all cases volume of at least 2µL were pipetted in order to reduce pipetting errors. To every well 25µL LARII and after the first measurement 25µL Stop´n´Glow was added with a multipette Plus®. The ratio of luminescence at 570nm and 475nm was calculated and normalized to control. These values are depicted as relative luciferase activity (mean±S.E.M.) for every condition. The data were processed by "MARS" and "Excel". As control condition three wells were transfected with both reporter gene constructs and 100ng empty vector on every plate. For each condition the leftover lysate of all three wells was collected and the complete volume was loaded on SDS PAGE as described (see 5.2.3).

5.2.5 Affinity purification of active RhoA

In 1999 Ren and colleagues developed a method to determine active RhoA in cells (Ren et al., 1999). The main principle of this method is specific binding of a Rho binding domain (RBD) to active RhoA and precipitation of this complex. Therefore RBD, which is fused to a Glutathione-S-transferase (GST) -tag, was transformed into *E.coli* Rosetta2 (DE3) (5.2.2.4) and several colonies were inoculated in at least 10mL LB overnight. At the next day the overnight culture was diluted 1:100 in 1L LB medium and grown until an OD_{600} of 0.4 was measured (5.2.2.3). Then RBD expression was induced by addition of 300µM isopropylβ-D-1-thiogalactopyranoside (IPTG). The bacteria were centrifuged (5000rpm, 15min, 4°C, Sorvall RC5B Plus) and the pellet was resuspended in 10mL bacteria lysis buffer on ice. Next the bacteria suspension was sonified for 10min (Digital Sonifier, 1s, 1s break, 10% intensity) in order to homogenize the bacteria lysate. Upon centrifugation (10.000g, 30min, 4°C, Heraeus Megafuge 16R) the cell debris was precipitated and all soluble proteins were found in the supernatant. The supernatant was incubated with glutathione-coated agarose beads

(20µl/condition) for 30min, rotating at 4°C. The beads had been washed in lysis buffer beforehand according to the manufacturer´s protocol. Afterwards the bead-bound RBD (RBD beads) was harvested by centrifugation (500g, 5min, 4°C, Heraeus Megafuge 16R) and washed three times with lysis buffer. In the meantime RIPA buffer (5.1.12) was prepared freshly. The RBD beads were distributed equally to as many reaction tubes as conditions. Per condition one 10cm dish HEK293T cells had been transfected with PEI on the previous day as described (5.2.1.2.3). The medium was removed from the cell culture dish, 600µL RIPA buffer was added and cells collected with a cell scraper. Next the HEK293T cell lysate was cleared by centrifugation (13.300rpm, 4min, 4°C, Heraeus Fresco 17) and the supernatant was transferred to the RBD beads. During rotation for 30 to 45min at 4°C, the active RhoA was bound by RBD beads. Therefore active RhoA could be harvested by centrifugation (500rpm, 5min, 4°C, Heraeus Fresco 17) next. After this step the supernatant contained inactive RhoA and all other cellular protein. 100µL of this were used as loading control and supplemented with 5x SDS gel loading buffer (5.1.12). The pellet was washed three times with RIPA buffer and finally resolved in Laemmli buffer. The loading control and precipitate were further analyzed by Western Blot (5.2.3).

Bacteria lysis buffer

50 mM	Tris-Base, pH 7.5
500 mM	NaCl
1% (w/v)	Triton X-100
2%-10% (w/v)	Glycerol
2 mM	EDTA

Added fresh:

1pill/10mL buffer protease inhibitor

4mM	DTT

Laemmli buffer

125mM	TrisHCl
4% (w/v)	SDS
20% (v/v)	Glycerol
0,004%	Bromophenol blue

pH 6.8

5.2.6 Fluorescence microscopy

For all fluorescence microscopic experiments HEK293T cells were transfected (5.2.1.2.1) two days in advance. On the day before the measurements the cells were split onto poly-l-lysine coated coverslips (5.2.1.3) and shortly before the measurement a coverslip was fixed in an Attofluor cell chamber. The chamber was filled with FRET buffer (5.1.12). During the measurement the cells were continuously superfused with FRET buffer by a perfusion system, which exchanged solutions at the cell within 10ms. Also the agonists were applied with this device at the time points indicated in the graphs as black bar. All agonists were freshly diluted in FRET buffer, except U46619. This Txa_2-R agonist was delivered in methyl acetate. Methyl acetate was evaporated and the substance was dissolved in ethanol (100%) at a final concentration of 2.5mM and stored in aliquots at -20°C. At the day of experiment U46619 was diluted in FRET buffer containing 0.1% (w/v) delipidized bovine serum albumin (BSA). In this case the corresponding amount of ethanol and delipidized BSA was added to FRET buffer and used as wash buffer. For all experiments with U46619 only one cell was measured per coverslip. In the other cases three cells were measured at most per coverslip. Further agonist solution was applied once per cell, if not mentioned otherwise.

5.2.6.1 FRET measurement

5.2.6.1.1 Theoretical background of FRET measurement

Protein protein interactions can be measured by Förster/fluorescence resonance energy transfer. Simplified FRET occurs, if two fluorophores are in close proximity and the emission spectrum of the donor fluorophore overlaps with the excitation spectrum of the acceptor fluorophore, because in this case the donor does not emit light, but rather excites the acceptor radiation free (Förster, 1948). This phenomenon is used to study protein-protein interactions (intermolecular FRET) and conformational changes of a protein (intramolecular FRET) (Vilardaga et al., 2009). The most popular fluorophore pair is YFP and CFP for studies between biomolecules (Miyawaki, 2011). These two proteins are engineered from the green fluorescence protein (GFP), which is a monomeric, fluorescent protein and was found in the jellyfish *Aequorea victoria* (Prasher et al., 1992; Heim and Tsien, 1996). Unfortunately the FRET amplitude does not allow for distance estimations, because the FRET

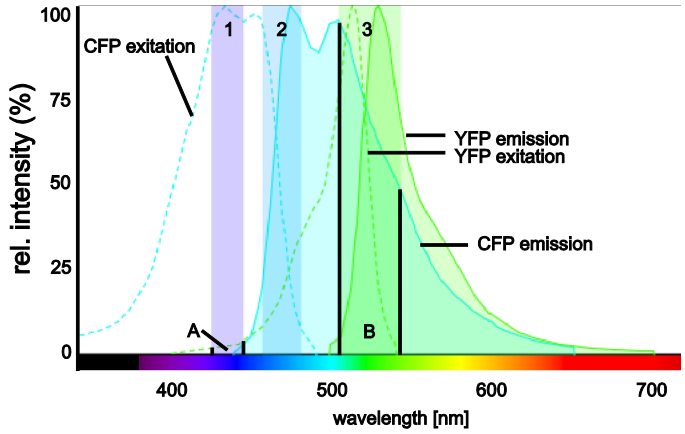

Fig. 12 Spectra of YFP and CFP
Excitation and emission spectra of YFP and CFP were overlayed with the CFP excitation filter (1), CFP emission filter (2) and YFP emission filter (3) of the Visitron set-up. Direct excitation of YFP is shown in area A and bleed through in area B. The spectra were plotted and modified using the "Fluorescence SpectraViewer" and "CorelDRAW".

amplitude depends on three factors (Jares-Erijman and Jovin, 2003): (I) the distance of the fluorophores (<10nm), which enters into FRET with the sixth power. (II) The spectral overlap of the used fluorophores is important, since the acceptor has to emit the excitation energy, which is needed by the donor. (III) The FRET amplitude is maximal with parallel dipoles. But engineering the dipole orientation is complicated by flexibility in the linker between fluorophore and protein of interest and fast rotation of the fluorophore (Lohse et al., 2012). In the FRET application of sensitized emission also the stoichiometry of fluorophores influences the FRET amplitude: if the donor is expressed in excess over the acceptor, the FRET ratio will decrease. Since the acceptor fluorescence will grow whereas the donor fluorescence will not change and thus the FRET ratio of donor over acceptor will decrease.

FRET can be measured in several ways. In this thesis donor recovery after acceptor photobleaching (5.2.6.1.10) and sensitized emission are conducted. In order to simplify nomenclature all sensitized emission measurements were termed as FRET measurements (5.2.6.1.2) and donor recovery after acceptor photobleaching experiments were termed as such. If sensitized emission is measured, several aspects have to be controlled: Two factors add unto the actual YFP emission due to FRET (Berney and Danuser, 2003): The light used to excite of the donor, CFP, excites to some extent also directly the acceptor, YFP. This is termed “direct excitation of YFP” and is illustrated as area A in figure 12. In the same figure also bleed through is visualized (area B). Bleed through describes the CFP emission, which is collect together with the YFP emission. This is again caused by spectral overlap, but this time of their emission spectra. In this thesis all FRET measurements were corrected for bleed through and direct excitation (see 5.2.6.1.2). Additionally the proteins of interest could be harmed by the fluorophore tag, since the GFP derivatives have a size of 27kDa. Previously or in this thesis the functionally was shown for all fluorophore-labeled used constructs, besides the downstream signaling of the LARG constructs (see. 7.1).

5.2.6.1.2 FRET measurements (Sensitized emission)

The FRET measurements were conducted at room temperature at one of two inverse microscopes, as specified in 5.1.10.1, 5.1.10.2 and figure 13. In dual excitation mode (fig. 13B) cells were chosen which expressed YFP and CFP in the region of the cells corresponding to the localization of the untagged version of the protein. Then the light path was changed to the FRET measurement mode (fig. 13A) and the cells were superfused as described in 5.2.6. The cells were illuminated with 2Hz or 0.5Hz for 60 or 30ms (Visitron and Nikon set-up, respectively) and the $F_{YFP(440nm,535nm)}$ and $F_{cFP(440nm,480nm)}$ fluorescence was detected separately with a CCD-camera. At the end of the measurement the light path was changed to dual excitation mode and $F_{YFP(500nm,535nm)}$ was measured upon excitation at 500nm. This information was needed for every measured cell during data processing, in order to correct for direct excitation of YFP by 440nm. In the results section the term “excitation at 500nm/440nm” described the excitation spectrum reaching the sample as filtered by the CFP excitation filter or Dualband for CFP and YFP excitation, respectively.

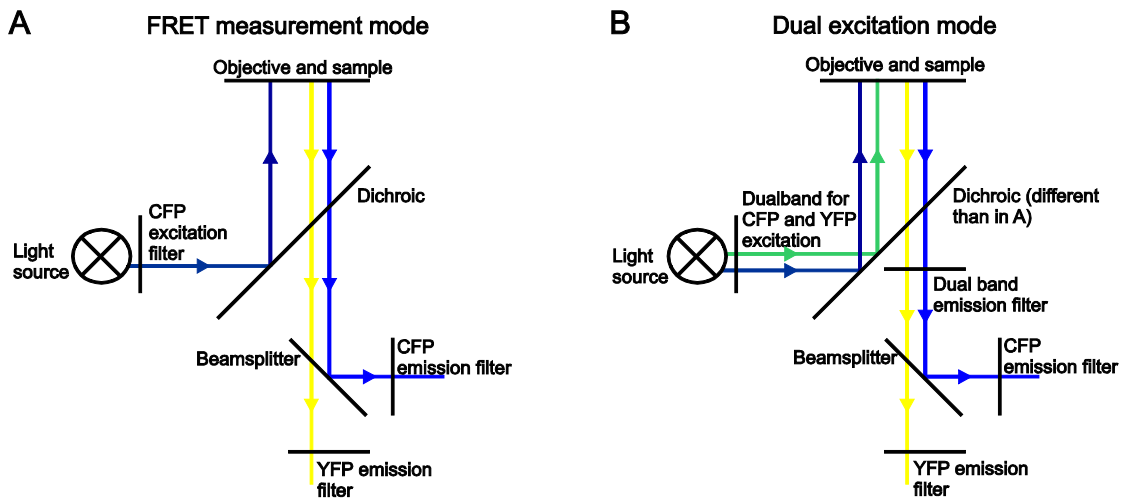

Fig. 13 Light paths for FRET measurement and dual excitation of CFP and YFP
In **A** the light path is depicted during FRET measurement and **B** shows the light path in dual excitation mode, which is used for direct excitation of YFP and bleaching experiments.

The images were displayed with VisiView or NIS Elements AR, respectively and stored. Than the data were processed using Excel and Origin as follows:
First the intensity of a background region was subtracted for both fluorescences and then F_{YFP} was corrected for direct excitation and bleed through:

$$F_{YFP(corr)} = F_{YFP(440nm,535nm)} - BT*F_{CFP(440nm,480nm)} - DE*F_{YFP(500nm,535nm)}$$

The correction constants for direct excitation (DE) and bleed through (BT) were measured for both FRET set-ups on a regular basis as described in 5.2.6.1.2.
Then the ratio was calculated of corrected F_{YFP} over F_{CFP}. Further bleach correction had to be done for all cells measured with 2Hz or faster at the Visitron set-up (5.2.6.1.4).

5.2.6.1.3 Detection of correction factors for bleed through and direct excitation

For the direct excitation correction constant (DE) cells were transfected only with YFP. Intensity was measured for the same cell in FRET measurement mode (excitation 440nm) as well as dual excitation mode (excitation 500nm) and the ratio of these intensities makes the DE. A cell transfected only with CFP was used to determine the bleed through correction constant (BT). The cell was measured in FRET measurement mode, is excited at 440nm. The intensity in YFP and CFP channel were measured and the ratio of this makes BT. For both correction factors mean of ten cells were measured and evaluated approximately every six month.

5.2.6.1.4 Correction for photo bleaching effects

All cells measured at 2Hz or faster at the Visitron set-up had to be corrected for photo bleaching, since repetitive excitation with high intensity harms the fluorophores and this leads to a decrease in fluorescence over time. The decrease in FRET ratio over time due to bleaching is best described by a

monoexponential function. Therefore a monoexponential function was fitted to the baseline of the FRET ratio trace and the fitted function was subtracted from the FRET ratio trace. In some cases also the FRET ratio before agonist application is of interest. Therefore the mean basal value before agonist application of the original trace was added to the FRET ratio trace at every time point. The whole procedure is visualized in figure 14.

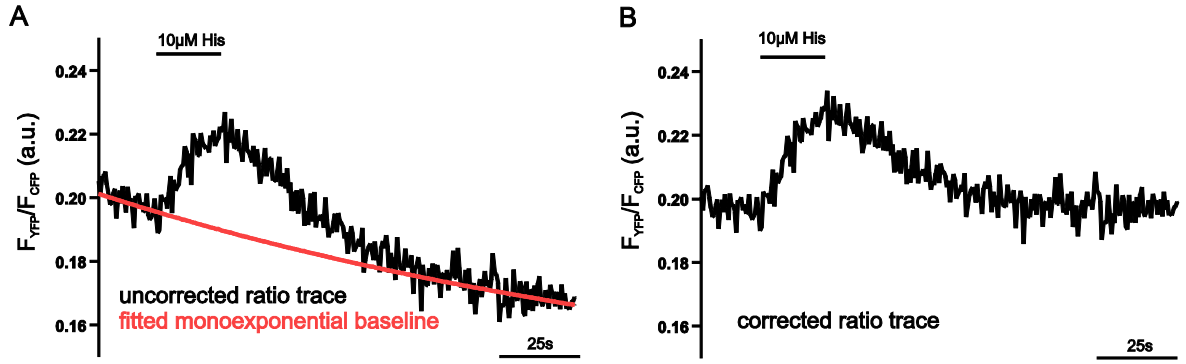

Fig. 14 Bleach correction
A shows the ratio trace of FRET between $G\alpha_q$-YFP and p63RhoGEF-CFP before correction together with the fitted monoexponential function in red. In **B** the bleach corrected traces of the same cell is shown.

5.2.6.1.5 Plotted $\Delta(F_{YFP}/F_{CFP})$ and determination of FRET response $\Delta(F_{YFP}/F_{CFP})$

For most FRET traces $\Delta(F_{YFP}/F_{CFP})$ is plotted, which depicts the FRET ratio at every given time point subtracted by the mean FRET ratio 15s before agonist application. The FRET response was evaluated as difference of mean FRET ratio 15s before agonist application and mean FRET ratio within the agonist plateau.

5.2.6.1.6 Normalization

Some traces are depicted as normalized F_{YFP}/F_{CFP}. In these cases a high and variable FRET ratio was observed before agonist application, which was caused by the transfected FRET pair. Therefore cells measured under these conditions were normalized: F_{YFP}/F_{CFP} of every given time point was divided by the mean FRET ratio before agonist application.

Also some traces were normalized to maximal response in order to emphasize the kinetic differences between conditions. Therefore the $\Delta(F_{YFP}/F_{CFP})$ at every given time was divided by the $\Delta(F_{YFP}/F_{CFP})$ in the plateau of agonist application.

5.2.6.1.7 Measurement and evaluation of concentration response curves

Concentration response curves were measured as described for regular FRET measurements. But two agonist concentrations were applied to the same cell immediately after each other. The same reference concentration was used for all cells and test concentrations of one transfection condition. For both concentrations the response amplitude was determined and the response amplitude of the test concentration was shown relative to the reference concentration. For each data point at least three cells

were measured and the data were plotted with “GraphPad Prism”. Afterwards a concentration response curve was fitted by the following “dose-response curve” with “GraphPad Prism”:

$$Y = Bottom + (Top-Bottom) / (1 + 10^{((logEC50 - X)*Hill\ Slope)})$$

During the fit only the Bottom was constrained and Top, Hill Slope as well as EC_{50} were set variable. X gives the logarithm of the test concentration and Y the relative response amplitude.

5.2.6.1.8 Evaluation of kinetics

The kinetics of wash-in or -out were evaluated with “OriginPro”. A monoexponential function $y = A_0*e^{-x/t1} + y_0$ was fitted to the graph (fig. 15). In this function y described the FRET ratio at a given time point x and t_1 shows the time constant in seconds. For all fits R^2 values were calculated and fits worse than 0.70 were excluded from further evaluation. The arithmetic mean was plotted for the inverse of t_1, which is k. For wash-in kinetics (k_{on}) the graph was fitted from the start of wash-in until the plateau was reached. Accordingly for wash-out kinetics (k_{off}) the graph was fitted from the start of wash-out until the baseline plateau was reached. For k_{on} and k_{off} cells were measured with 2Hz and stimulated with supersaturating (1µM U46619) and saturating (10nM U46619; 10µM His) agonist concentrations, respectively.

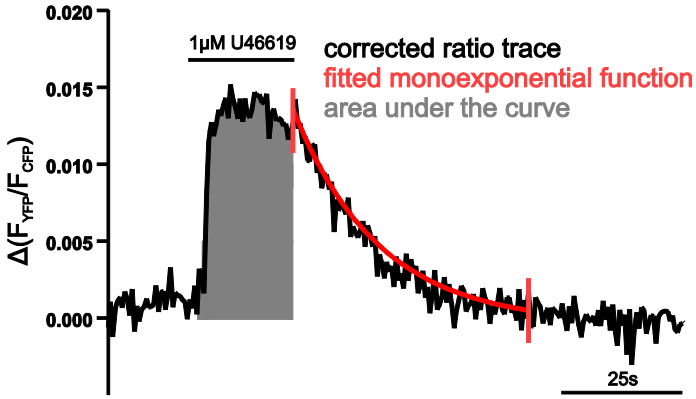

Fig. 15 Evaluation of kinetics and area under the curve
As an example the k_{off} of FRET between $G\alpha_{13}$ and Gβ was fitted with a monoexponential function (y=A1*exp(-x/t1)+y0). For this curve a t1 of 15.856s was found with an adjoint R-Square of 0.9544. The fitted monoexponential curve is shown in red. For the same cell the area under to curve was evaluated and is shown as grey area.

5.2.6.1.9 Area under the curve

The influence of RGS2 on the steady state of $G\alpha_q$ p63RhoGEF was studied by evaluation of the area under the curve (AUC) until agonist wash-out (fig. 15, grey area). In “GraphPad Prism” the AUC was evaluated for individual cells with the flowing settings: the baseline y=0, a minimum peak height of less than 10% of the distance between minimal and maximal Y, all peaks must be broader than 9 data points and go above baseline. Then the AUC was plotted as arithmetic mean.

5.2.6.1.10 Donor recovery after acceptor photobleaching

Two proteins may show FRET before agonist application. The magnitude of FRET under such steady state conditions can be estimated by bleaching of the acceptor and monitoring the increase in donor fluorescence. The measurement was done in dual excitation mode at the Visitron set-up (fig. 13B) and the intensity was increased to 70% for the 500nm light source. The cells were bleached for 100s and F_{CFP} was monitored every 1.5s. For the control condition (mCFP) F_{CFP} was detected a short period before and after the bleaching whereas for the other conditions a more complex protocol was chosen (fig. 16). This protocol allows for detection of steady state FRET (Δ_{unstim}) and absolute FRET upon agonist application (Δ_{stim}). Further the data were divided by F_{CFP} before agonist application and this normalized change in F_{CFP} was plotted as %. These calculations were conducted with "Excel".

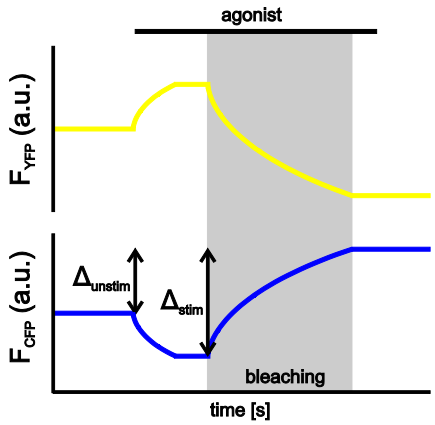

Fig. 16 Protocol for donor recovery after acceptor photobleaching
The standard protocol is shown for a condition with pronounced basal FRET and FRET increase upon stimulation with agonist. The stimulation with agonist led to an increase in F_{YFP} and decrease in F_{CFP}. If the plateau is reached, the bleaching started and took 120s. In the meantime F_{YFP} decreases due to photobleaching and F_{CFP} increases. The F_{CFP} increase is caused by the loss of FRET, due to loss of FRET acceptor YFP. After the bleaching the agonist is washed-off in order to check for residual FRET. The cells were measured in dual excitation mode.

5.2.6.1.11 Stoichiometry

The measured YFP and CFP fluorescence can be correlated to the number of fluorophores expressed in the cell. This is of special importance if the amplitude of the FRET signal is evaluated, see above (5.2.6.1.1). Control constructs were cloned, which express a yellow and a blue fluorophore at the N- and C-terminus of β_2 adrenergic receptor. So the fluorophores are located at different sites of the plasma membrane and this prevents FRET between the fluorophores (Dorsch et al., 2009). Accordingly, acceptor photobleaching experiments show little to no FRET between the two fluorophores (C. Krasel, personal communication). For every fluorophore pair tested a control construct was cloned with the exact fluorophores of this pair, e.g. Venus and CFP. Cells were transfected with 1µg of the control construct and F_{CFP} was measured in FRET mode (fig. 13A) at 440nm excitation and F_{YFP} in dual excitation mode at 500nm excitation. The background was subtracted and the mean of $F_{YFP(500nm)}$ over $F_{CFP(400nm)}$ were calculated, which gives an stoichiometry factor for a one to one expression of the fluorophores. In general for all measured cells $F_{YFP(500nm)}$ and $F_{CFP(400nm)}$ was recorded either as direct excitation for correction or during the FRET measurement. For the measured cells $F_{YFP(500nm)}$ over $F_{CFP(400nm)}$ was calculated and then this cell specific stoichiometry factor was divided by the stoichiometry factor of the control constructs. By this the fluorophore ratio was calculated for individual cells and then averaged as geometric mean for each condition. These calculations were done with "Excel".

5.2.6.1.12 Localization of fluorophore-labeled constructs

For overview images three consecutive pictures were taken from a FRET measurement at Nikon set-up and were stored with “NIS elements”. From the same cell tree, three consecutive pictures were collected in dual excitation mode with excitation only at 500nm. Further processing was done in “ImageJ”. The background was subtracted for each image and then the three images were combined with the “Z-projection by sum slices” tool of “ImageJ”.

5.2.6.2 Confocal microscopy

The measurements were done at the VisiTech set-up with VT-HAWK. This system allows for confocal imaging and was used with a 100x oil objective as specified before (5.1.10.3). The samples were excited with the 491nm laser, since only YFP-labeled proteins were monitored.
The cells were prepared as usual (3.2.6.) and superfused with FRET buffer.

5.2.6.2.1 Localization of YFP-labeled constructs

For overview confocal images three pictures were taken within 1000ms with an illumination time of 300ms and 30% laser intensity and data were stored with “VoxCell Scan”. Further processing was done in “ImageJ”. The background was subtracted for each image and then the three images were combined with the “Z-projection by sum slices” tool of “ImageJ”.

5.2.6.2.2 Translocation measurements

The cells were illuminated with 0.5Hz or 0.03Hz as indicated for 30ms and images were stored by “VoxCell Scan”. For evaluation three regions of interest (ROIs) were set, as shown in figure 17. The intensities of these regions were exported to “Excel” and further processed:

$$F_{cytosol}/F_{cell} = (F_{cytosol} - F_{background}) / (F_{cell} - F_{background})$$

The background (ROI3) was subtracted from intensities of cytosol (ROI1) and the whole cell (ROI2) for every time point. In figure 24A both intensities are plotted for a representative cell together with the ratio trace of cytosol over whole cell of the same cell. The ratio was plotted subtracted with the mean ratio before the first agonist application. Agonist applications were indicated by black bars.

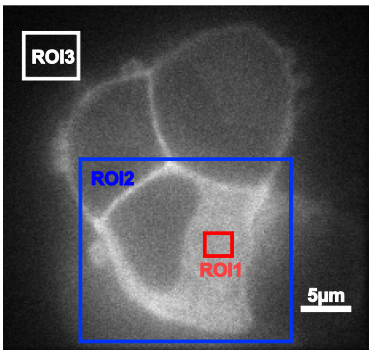

Fig. 17 Measurement of translocation
For every cell three ROIs were set: One in the cytosol, one around the whole cell and the last one into the background. In figure 24A the calculated intensities are plotted for the same cell over time.

5.2.7 Statistics

The data were statistically evaluated with “GraphPad Prism”. The following statistical tests were performed in response to the data type: one way ANOVA with Dunnet´s or Bonferroni´s multiple comparison test, Student´s t-test after Welch´s correction, extra sum-of squares F-test. Dunnet´s multiple comparison test was used if several conditions were compared to one control condition, whereas Bonferroni´s multi comparison test compares all condition with each other. The Welch´s correction was needed if the variances differed between conditions. The number of cells per condition is given in brackets in the graph or as n=x in the legend.

6 Results

Rho activation upon stimulation of GPCRs occurs mainly through two parallel pathways: $G\alpha_q$ activates p63RhoGEF and $G\alpha_{13}$ activates RH-RhoGEFs. Both pathways are implicated for example in Ca^{2+} sensitization in vascular smooth muscle cells. It had not been studied so far why two pathways evolved in parallel and how the signal is integrated within each and between both pathways. Thus in the following the temporal as well as special dynamics of the Gα RhoGEF interactions of both pathways were elucidated and correlated to effects on downstream signaling: The LARG $G\alpha_{13}$ interaction was studied as model for RH-RhoGEFs (6.1). Further the p63RhoGEF $G\alpha_q$ interaction was studied on its own and in the context of the Regulator of G protein signaling 2 (6.2).

6.1 Dynamic of the LARG $G\alpha_{13}$ interaction and its influence on agonist sensitivity

6.1.1 YFP-LARG translocated to the plasma membrane in single living cells

In order to investigate the activation of a RhoGEF of the RH-RhoGEF family by $G\alpha_{13}$ in living cells LARG was chosen as model RhoGEF. For live cell imaging two LARG constructs were used, which have been cloned during my diploma thesis (Bodmann, diploma thesis). They have a yellow fluorescent protein (YFP) either tagged to the N-terminus of LARG or inserted between the RH domain and the DH-PH domain (behind amino acid 623). YFP and the later used mTur2, Venus, CFP and Cer are derivatives of green fluorescent protein (GFP (Watkins et al., 2013)).

The RH-RhoGEFs were described to be cytosolic in their inactive state and to translocate to the plasma membrane upon activation. For all RH-RhoGEFs $G\alpha_{13}$ activation is implicated as stimulus for the translocation (Carter et al., 2014). Therefore LARG translocation is most likely a good hint for physiological $G\alpha_{13}$ LARG interaction. Nevertheless until now translocation in living cells was only investigated for p115RhoGEF (Meyer et al., 2008). We previously found YFP-LARG and LARG-insYFP in the cytosol in unstimulated cells and at the membrane upon coexpression of $G\alpha_{13}$QL (Bodmann, diploma thesis). Therefore, we hoped to establish YFP-LARG as functional effector of $G\alpha_{13}$ and to get insight into the kinetics of translocation, by investigation of the localization of LARG in response to activation of a receptor, which couples to $G\alpha_{13}$.

In order to visualize translocation and understand the kinetics of LARG translocation HEK293T cells were transfected with Txa_2-R, $G\alpha_{13}$-wt, Gβ-wt, Gγ-wt and YFP-LARG. The translocation was monitored by confocal microscopy of single living cells with a region of interest (ROI) in the cytosol and one around the whole cell (see fig. 17 and 5.2.6.2.2 for further information). The cells were excited at 500nm every 5s for 30ms and the thromboxane A_2 receptor (Txa_2-R) was stimulated with 10nm U46619. The agonist was applied in this study at indicated times (black bars) and exchanged for FRET buffer within 10ms at the cell by a pressure operated superfusion device. The fluorescence in the cytosol decreased remarkably during agonist application, which was slowly reversible upon agonist wash-out (fig. 18A red trace). The fluorescence of the whole cell permanently decreased during the measurement due to photobleaching of the fluorophore (fig. 18A blue trace). For further analysis the ratio of $F_{cytosol}$ over $F_{whole\ cell}$ was used, as this corrects for bleaching. The translocation was also detectable by naked eye in the images evaluated for the traces. For the cell evaluated in figure 18A an image at the beginning of the measurement and after the first stimulation with agonist was shown (fig. 18B).

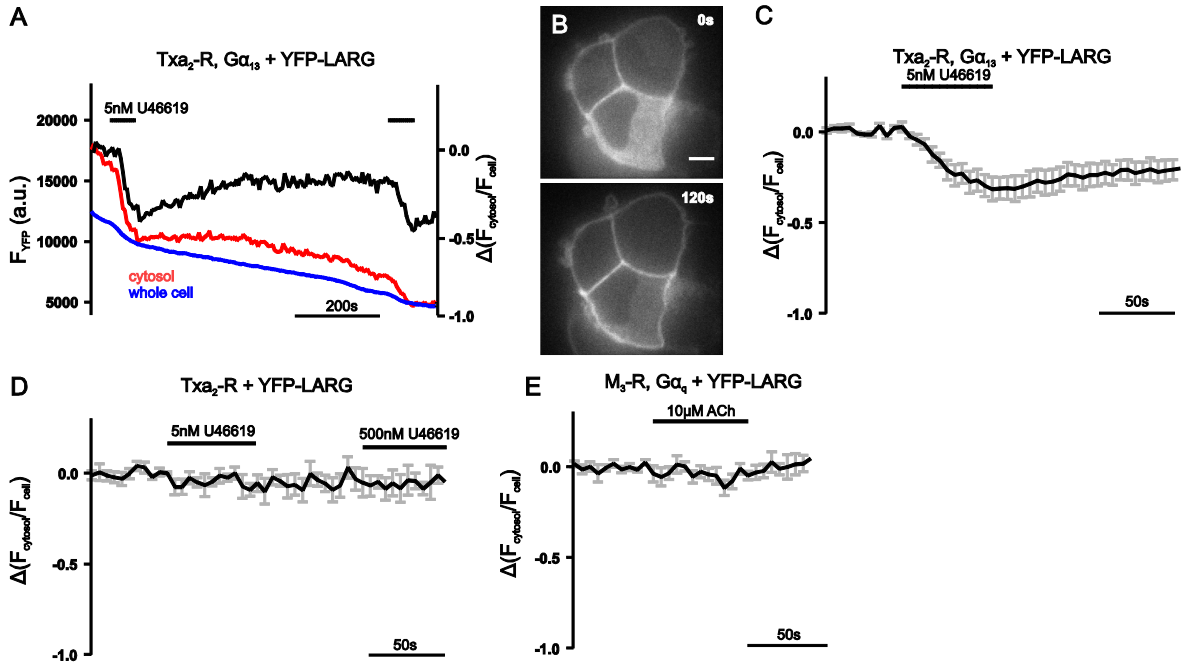

Fig. 18 YFP-LARG translocation to the plasma membrane is $G\alpha_{13}$ dependent
YFP-LARG translocated to the plasma membrane in HEK293T cells transfected with Txa_2-R, $G\alpha_{13}$-wt, Gβ-wt and Gγ-wt upon stimulation with U46619 (**A**, **B** and **C**). In **A** this is shown for the cell imaged in **B** (scale bar 5µm). The fluorescence in the cytosol (red) and of the whole cell (blue) was monitored and the ratio (black) was calculated. The loss of cytosolic fluorescence was also visible as mean±S.E.M. ratio trace of 12 individual cells. (**D)** No translocation upon stimulation with 5nM and 500nM U46619 was observed in HEK293T cells transfected with Txa_2-R and YFP-LARG, but without G protein. The same was true for cells transfected with M_3-R, $G\alpha_q$-wt, Gβ-wt, Gγ-wt, YFP-LARG and stimulated with 10µM acetylcholine (ACh) (**E**). Traces are mean±S.E.M. of eight individual cells for both conditions.

As negative control translocation was monitored in the absence of $G\alpha_{13}$ and upon stimulation of muscarinic M_3 receptor (M_3-R). When $G\alpha_{13}$ was not cotransfected, translocation of YFP-LARG did not occur even after stimulation with 500nM U46619 (fig. 18D). Also stimulation of M_3-R with 10µM acetylcholine and subsequent $G\alpha_q$ activation did not induce translocation of YFP-LARG (fig. 18E). Evaluation of downstream signaling by either wild type or YFP-tagged LARG was hindered by minor LARG expression in most experiments as discussed in detail later (6.1.7 and 6.1.8). Taken together these results suggested, that YFP-LARG reversibly translocates to the plasma membrane upon $G\alpha_{13}$, but not $G\alpha_q$ activation and this hints towards a functional interaction of $G\alpha_{13}$ and YFP-LARG.

6.1.2 FRET change between $G\alpha_{13}$-mTur2 and YFP-labeled LARG

Since translocation of LARG upon stimulation of $G\alpha_{13}$ coupled receptor did not monitor $G\alpha_{13}$ LARG interaction directly, we established a FRET-based assay to study the $G\alpha_{13}$ LARG interaction in single living cells (see 5.2.6.1 for further information on FRET). Therefore, the fluorescent protein mTurquoise2 (mTur2) was inserted into $G\alpha_{13}$ behind amino acid 127 by A.-L. Krett and the functionality was verified by her (unpublished data). In order to study the $G\alpha_{13}$ LARG interaction in HEK293T cells, cells were transfected with cyan labeled $G\alpha_{13}$ ($G\alpha_{13}$-mTur2) and YFP-LARG, whose fluorophores have overlapping excitation and emission spectra. Additionally, the $G\alpha_{12/13}$ coupled thromboxane A_2 receptor (Txa_2-R), Gβ and Gγ were cotransfected (Offermanns et al., 1994; Klages et al., 1999). Cotransfection of Gβ and Gγ was necessary to assure balanced stoichiometry of the three members of the trimeric G protein. Two days after transfection single cells were measured using an inverted microscope and a high-performance CCD camera. During the measurement cells were excited at 440nm for 60ms every 0.5s. After the measurement the cell was excited at 500nm for 60ms to excite YFP directly.
A single HEK293T cell, which was transfected with the mentioned plasmids, was stimulated with 10nM U46619 resulting in an increase in YFP fluorescence and a decrease in CFP fluorescence (fig. 19A). These changes were reflected in an increase in FRET ratio of the same cell and also in the averaged trace of 30 individual cells (fig. 19A and B). The increase occurred within a half time ($t_{1/2}$) of 3.9s as measured in nine cells upon stimulation with a super-saturating concentration of 1µM U46619 (k_{on}=0.271±0.023s^{-1}, mean±S.E.M.). Upon wash-out of the agonist the ratio decreased very slowly. The change in FRET could either reflect the change in distance between LARG and $G\alpha_{13}$ or could arise from bystander FRET, which is an unspecific change in distance between LARG or $G\alpha_{13}$ and a random fluorophore-labeled protein. To exclude this possibility, HEK293T cells were transfected with Txa_2-R, $G\alpha_{13}$-wt, Gβ-wt, Gγ-wt, membrane bound mCFP and YFP-LARG. Hence, changes in FRET upon agonist application would be due to YFP-LARG translocation to the membrane in these cells. As visible in figure 19C, no change in FRET was observable. The same is true for cells expressing $G\alpha_{13}$-mTur2 and Venus-p63RhoGEF (fig. 19D) as for Venus-p63RhoGEF the interaction with $G\alpha_q$, but not $G\alpha_{13}$ is described (see 4.5.2.1 and 6.2).

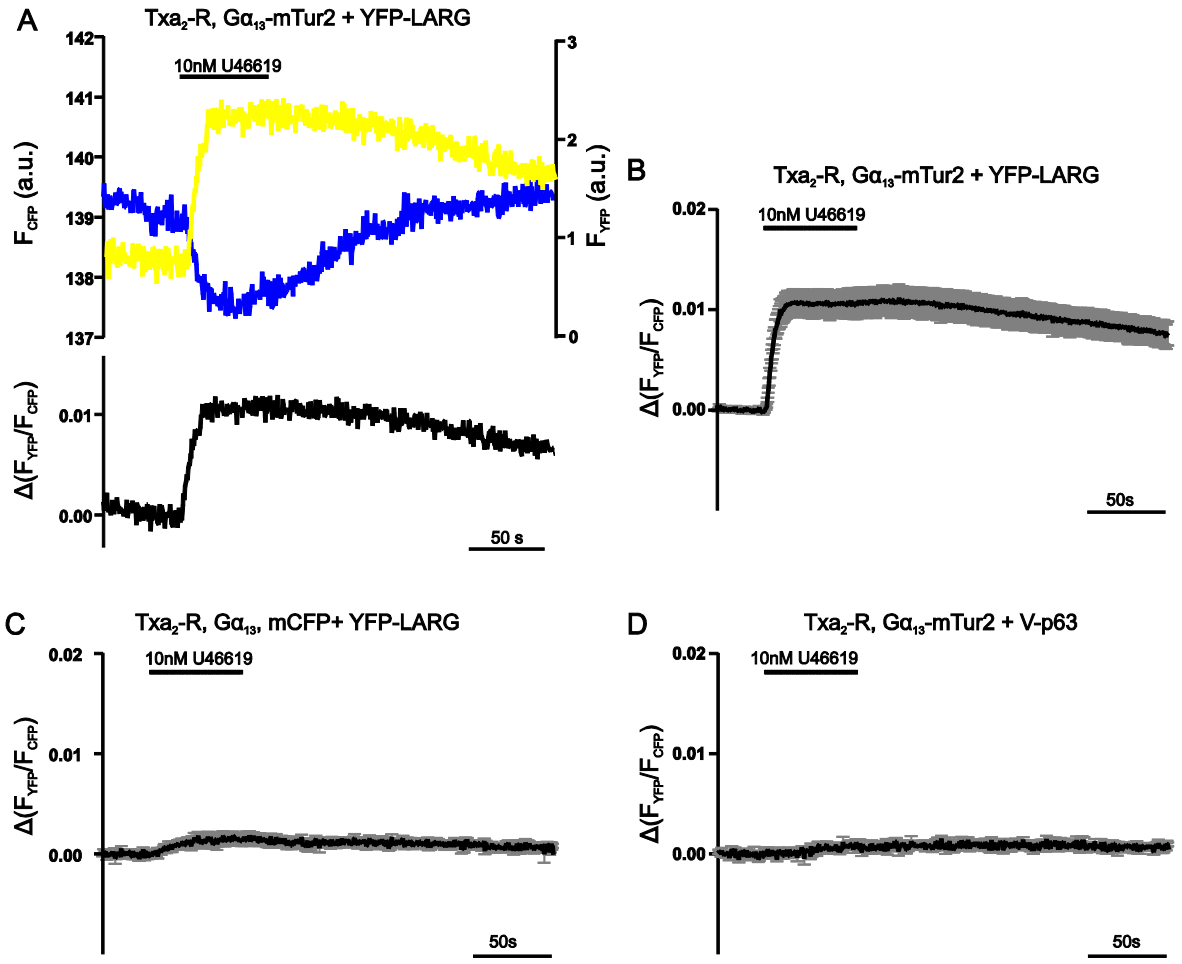

Fig. 19 Agonist-dependent FRET change between $G\alpha_{13}$-mTur2 and YFP-LARG upon activation of Txa_2-R
HEK293T cells were transfected with 0.5µg Txa_2-R, 1µg $G\alpha_{13}$-mTur2, 0.5µg Gβ-wt, 0.2µg Gγ-wt and 1µg YFP-LARG. Two days after transfection cells were measured on an inverted microscope with a high-performance CCD camera. During the measurement cells were excited for 60ms at 2Hz with 440nm. Further the cells were continuously superfused with FRET buffer and U46619 was applied using a pressure operated superfusion device were indicated by black bar. (**A** and **B**) Stimulation of Txa_2-R with 10nM U46619 led to an increase in FRET, as visible in F_{CFP} decrease (blue), F_{YFP} increase (yellow) and ratio increase (black) for a representative cell (**A**) and in a mean±S.E.M. trace of 30 individual cells (**B**). a.u., arbitrary unit(s). (**C**) Cells were transfected as before, only $G\alpha_{13}$-wt and mCFP were used instead of $G\alpha_{13}$-mTur2. These cells showed almost no increase in FRET upon agonist stimulation. (**D**) The same was true for cells transfected with Venus-p63RhoGEF (V-p63) instead of YFP-LARG. Traces are mean±S.E.M. for at least 13 individual cells.

In order to exclude artefacts in FRET between LARG and $G\alpha_{13}$ due to the N-terminal localization of YFP, the FRET experiments were repeated with LARG-insYFP (fig. 20A). The LARG-insYFP variant has YFP inserted between RH domain and DH-PH domain. Also between LARG-insYFP and $G\alpha_{13}$-mTur2 an increase in FRET could be measured upon agonist stimulation, however the FRET amplitude was approximately half the size of the FRET amplitude with YFP-LARG upon stimulation with 10nM U46619. This is not due to the lower concentration, as both concentrations are saturating (see concentration response curves in fig. 23).

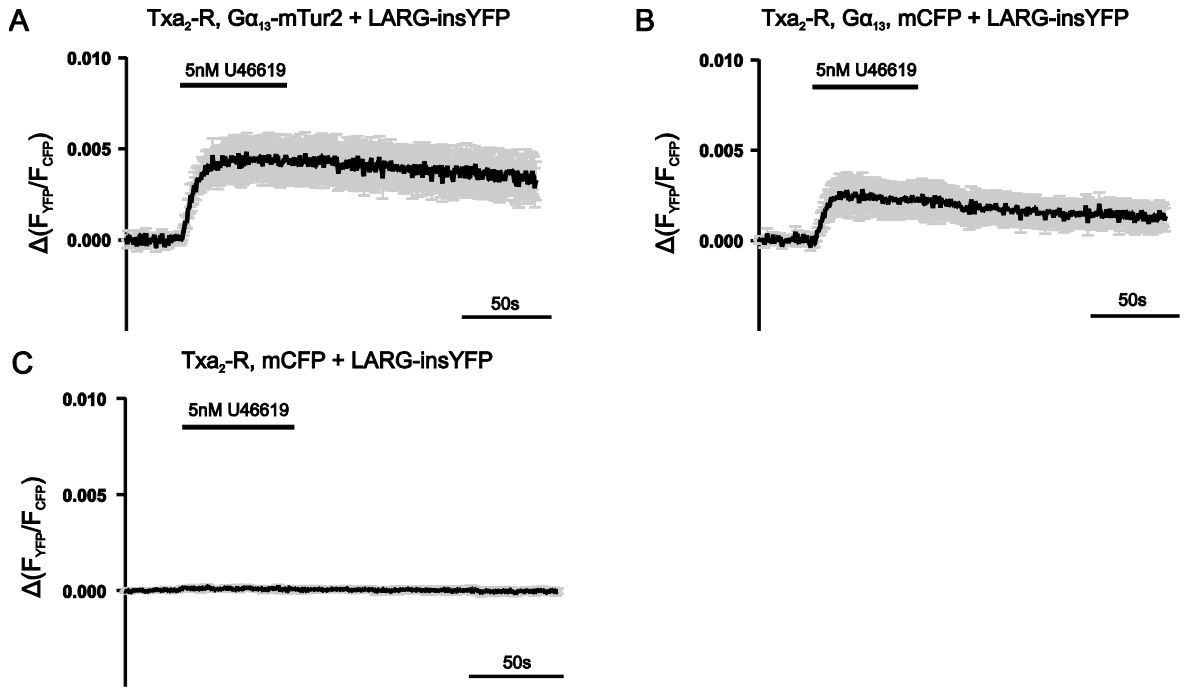

Fig. 20 Agonist-dependent change in FRET between $G\alpha_{13}$-mTur2 and LARG-insYFP
A HEK293T cells were transfected with 0.5µg Txa_2-R, 1µg $G\alpha_{13}$-wt, 0.5µg Gβ-wt, 0.2µg Gγ-wt and 1µg LARG-insYFP. The mean trace±S.E.M. of nine individual cells showed an increase upon stimulation with 5nM U46619. A smaller increase was observed for cells transfected with 1µg $G\alpha_{13}$-wt and 1µg mCFP instead of $G\alpha_{13}$-mTur2 (**B**) and no increase was found for cells transfected only with Txa_2-R and YFP-LARG (**C**). Shown are mean traces±S.E.M. of eleven cells for both conditions.

In the case of LARG-insYFP a little increase in FRET was observed if $G\alpha_{13}$ and mCFP were used instead of $G\alpha_{13}$-mTur2 (fig. 20B). This increase was most likely caused by bystander FRET between plasma membrane bound CFP and LARG-insYFP upon agonist-induced LARG translocation. Consequently, the increase in FRET was diminished if the trimeric G protein was excluded from the transfection mixture, in other words if the cells were transfected with Txa_2-R, mCFP and LARG-insYFP alone (fig. 20C).

In summary, activation of Txa_2-R lead to a fast and specific increase in FRET between $G\alpha_{13}$-mTur2 and two different YFP-labeled LARG constructs.

6.1.3 LARG dissociated slower from $G\alpha_{13}$ than $G\alpha_{13}$ reassociated with $G\beta\gamma$

The activation and deactivation of $G\alpha_{13}$ can be monitored by FRET in cells transfected with $G\alpha_{13}$-YFP and Gβ-Cer together with Txa_2-R and Gγ-wt (unpublished data by A.-L. Krett). This allowed us to compare the inactivation of the G protein with the dissociation of LARG from $G\alpha_{13}$. Upon stimulation of

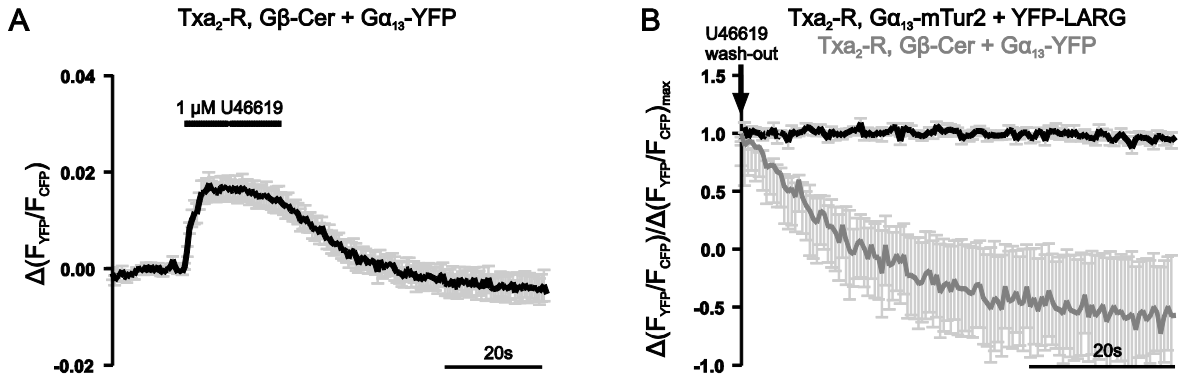

Fig. 21 Inactivation of $G\alpha_{13}$ occured faster than $G\alpha_{13}$ LARG dissociation
A HEK293T cells transfected with 0.5µg Txa_2-R, 1µg $G\alpha_{13}$-YFP, 0.5µg Gβ-Cer and 0.2µg Gγ-wt showed an increase in FRET upon stimulation with 1µM U46619. The increase was quickly reversible upon wash-out of the agonist. **B** shows the G protein inactivation (grey) and dissociation of LARG and $G\alpha_{13}$ (black) upon wash-out of the agonist. Shown are mean traces±S.E.M. of ten individual cells for **A**. **B** is an overlay of measurements of figure 21A and 19B normalized to their maximal response.

the Txa_2-R with 1µM U46619 a rearrangement of the $G\alpha_{13}$-subunits occurred as reflected by an increase in FRET (fig. 21A). Wash-out of the agonist led to a fast decrease in FRET back to control level or even below with $t_{1/2}$ of 17.50s (n=5). As visible in the overlays of the agonist wash-out of both conditions in figure 21B, the $G\alpha_{13}$ inactivation occurred faster than the dissociation of LARG and $G\alpha_{13}$.

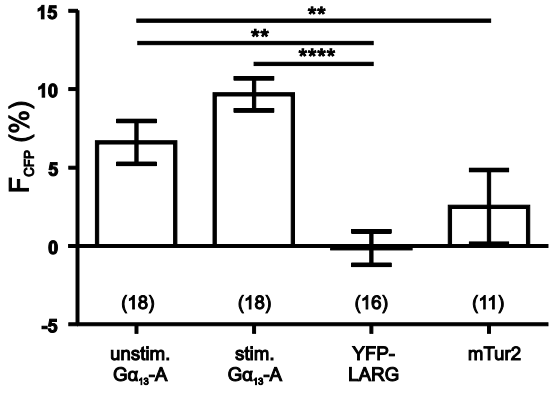

Fig. 22 Acceptor photobleaching led to an increased F_{CFP} for the $G\alpha_{13}$ Gβ FRET, but had no influence on FRET between $G\alpha_{13}$ and YFP-LARG
FRET under steady conditions would result in donor recovery upon acceptor photo bleaching. The FRET assay between $G\alpha_{13}$-YFP and Gβ-Cer was tested in the absence and presence of 1µM U46619 (unstim. and stim. $G\alpha_{13}$-A, respectively), the FRET assay between $G\alpha_{13}$-mTur2 and YFP-LARG in the presence of 10nM U46619 (YFP-LARG) and as control condition cells were transfected with 0.5µg β_2-AR-mTur2 and 0.5µg pcDNA3 (mTur2). Relative changes in F_{CFP} due to acceptor bleaching are means±S.E.M. for *n* (in parantheses) individual cells. ****P<0.0001, **P<0.01, ANOVA with Bonferroni´s multiple camparison test.

Since the $G\alpha_{13}$ and Gβγ are known to form a trimeric complex in the basal state, we wondered whether the inactive, unstimulated trimeric G protein exhibits FRET. FRET under such steady state conditions can be investigated by donor recovery after acceptor photo bleaching (5.2.6.10). This method is limited in terms of sensitivity, nevertheless it is the only way to estimate FRET under steady state condition (Hein and Bünemann, 2009). For this approach YFP was bleached by approximately 70% with high intensity at 500nm for 120s and F_{CFP} was monitored every 1.5s. If FRET was present, the cyan fluorescence would increase over time. The increase in F_{CFP} for the $G\alpha_{13}$-YFP Gβ-Cer FRET pair was

significantly higher in the absence and presence of 1µm U46619 (6.6±1.3% and 9.7±1.0%, respectively (mean±S.E.M.)) than for the YFP-LARG $G\alpha_{13}$-mTur2 FRET pair in the presence of 10nM U46619 (-0.1±1.0%, fig. 22). For YFP-LARG no significant donor recovery was observed compared to control. Hence, FRET already takes place in the inactive $G\alpha_{13}$-mTur2 Gβ-Cer Gγ complex, but does not appear between $G\alpha_{13}$-mTur2 and YFP-LARG in amounts detectable by this method.

6.1.4 Left shift in concentration response relationship of the $G\alpha_{13}$ LARG interaction compared to $G\alpha_{13}$ activation

Since the dissociation of LARG and $G\alpha_{13}$ is remarkably slower than the inactivation of the G protein, we wondered if this results in a shift in the concentration response relationship. In case of the $G\alpha_{13}$ activation 300nM U46619 were used as reference concentration, whereas 10nM U46619 were used for the $G\alpha_{13}$ LARG interaction. On each cell two agonist concentrations were applied, first the test concentration and second the reference concentration. For both stimulations the FRET amplitudes were determined and afterwards they were compared. For each FRET pair a concentration response curve was fitted by "GraphPad Prism" with constrained bottom and free hill slope (fig. 23, see 5.2.6.1.7 for details on fitting of concentration response curves). As the amplitudes of the $G\alpha_{13}$-mTur2 LARG-insYFP FRET pair are small, evaluation of small concentrations was complicated and caused probably the large variations observed for this FRET pair.

For FRET between $G\alpha_{13}$-mTur2 and LARG-insYFP or YFP-LARG EC_{50} values of 0.048nM and 0.33nM were calculated, respectively. The $G\alpha_{13}$ activation occurred with an EC_{50} value of 29.22nM. So the EC_{50} values of the $G\alpha_{13}$ LARG interaction and the $G\alpha_{13}$ activation differed almost by two

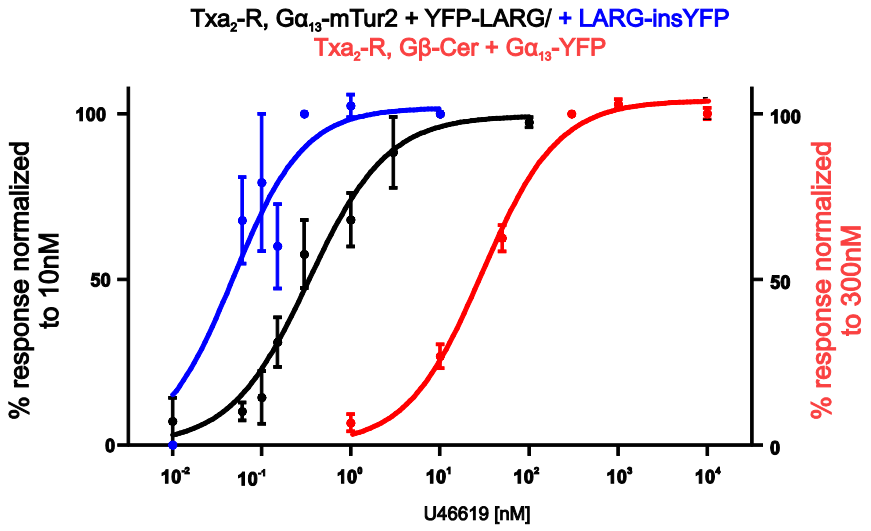

Fig. 23 Concentration response curves of $G\alpha_{13}$ activation and the $G\alpha_{13}$ LARG interaction
Cells were transfected as described for figure 20A (blue), 19A (black)and 21A (red). Each cell was first stimulated with a test concentration and afterwards with 10nM or 300nM for the $G\alpha_{13}$ LARG interaction or the $G\alpha_{13}$ activation, respectively. The concentration response curve for $G\alpha_{13}$ activation was measured by A.-L. Krett. Every concentration was tested in at least three cells, in most cases more than five cells were evaluated. For every concentration mean±S.E.M. is depicted. "Dose-response curves" were fitted to the measured values "GraphPad Prism" and are shown as continous lines.

orders of magnitude. Also the extra sum-of-squares F-test, which compared $logEC_{50}$ values, rejected the null hypothesis of equal $logEC_{50}$ values for all conditions.

As described in detail in the methods section (see 5.2.6.1.1) the amplitude of a FRET signal does not increase exponentially with decrease in fluorophore distance, but is for example influenced by the ratio of donor over acceptor fluorophores: If the donor is present in huge excess over the acceptor, the FRET amplitude will be saturated even if not all acceptors are excited. Even more, the FRET amplitude would decrease with further increase in donor fluorescence, because F_{CFP}, the donor fluorescence intensity, functions as the denominator of the FRET ratio. Due to this an excess in $G\alpha_{13}$-mTur2 would be a possible explanation for the shift in concentration response relationship, because partial interaction of LARG and $G\alpha_{13}$ would be interpreted as full interaction. Did we overestimate the $G\alpha_{13}$ LARG interaction induced by small concentrations, due to this problem? In order to investigate this possibility, we evaluated the stoichiometry of YFP-LARG and $G\alpha_{13}$-mTur2 of the cells analyzed for the concentration response curve.

For the evaluation a control construct was needed, which expresses the same fluorophores as used in the YFP-LARG $G\alpha_{13}$-mTur2 FRET pair in a one to one stoichiometry and in a distance, which abolishes FRET (see 5.2.6.1.11 for details, (Dorsch et al., 2009)). This construct was a β_2 adrenergic receptor (β_2-AR) with eYFP at its N-terminus and mTur2 at its C-terminus.

The control construct was cloned as follows: First β_2-AR-mTur (C. Krasel, personal communication) was mutated to β_2-AR-mTur2 by QuickChange® mutagenesis (see 5.1.3.2 for mutagenesis primers). Next SI-eYFP-β_2-AR from V. Wolters and β_2-AR-mTur2 were digested with HpaI and HindIII. HpaI cuts within the β_2-AR and HindIII in front of the ORF of both constructs. So the N-terminal part of β_2-AR-mTur2 was substituted by the N-terminal part of SI-eYFP-β_2-AR by ligation of the right fragments. Through this procedure SI-eYFP-β_2-AR-mTur2 was produced.

The fluorescence intensity of YFP and CFP was evaluated for cells expressing Si-eYFP-β_2-AR-mTur2, each fluorophore excited directly with 500nm and 440nm, respectively. Also the cells, which were analyzed for the YFP-LARG $G\alpha_{13}$-mTur2 concentration response curve, were evaluated the same way. Afterwards the stoichiometry of YFP-LARG and $G\alpha_{13}$-mTur2 was extrapolated from the control construct. By this method approximately two YFP-LARGs per three $G\alpha_{13}$-mTur2s were predicted for the analyzed cells (0.66±0.56 (geo. mean±S.D.)). So a pronounced excess in $G\alpha_{13}$ was probably not the reason for shift in concentration response relationship between LARG-$G\alpha_{13}$ interaction and $G\alpha_{13}$ activation.

6.1.5 LARG´s interaction with $G\alpha_{13}$ and its translocation to the plasma membrane is slowly reversible

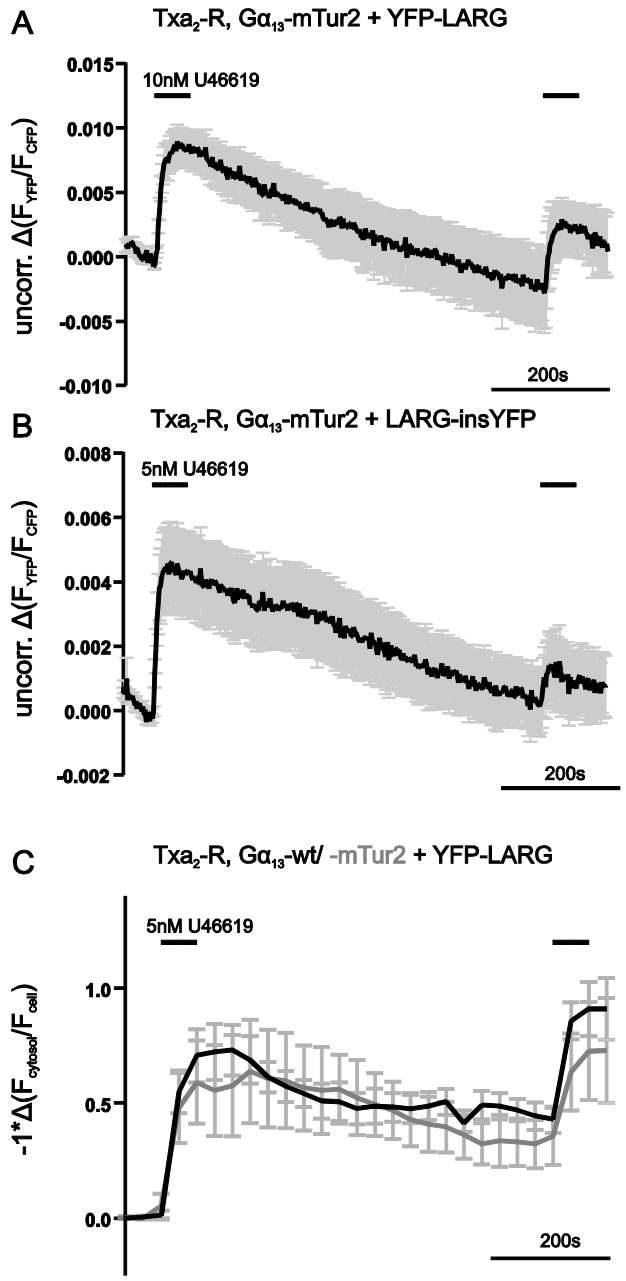

Fig. 24 LARG´s translocation and interaction with $G\alpha_{13}$ is slowly reversible
HEK293T cells were transfected as described in figure 19A, 20A and 18A for $G\alpha_{13}$ LARG interaction (**A** and **B**) and YFP-LARG translocation (**C**, black trace). Additionally, translocation of YFP-LARG was monitored in the presence of $G\alpha_{13}$-mTur2 instead of $G\alpha_{13}$-wt (**C**, grey trace). Wash-out of agonist was monitored for 10 minutes and afterwards U46619 was applied for a second time. The translocation was detected with 0.03Hz and the interaction with 0.2Hz. Mean traces±S.E.M. of at least nine individual cells. For better comparison the translocation was mirrored at the time axis.

Next we tested whether the shift in the concentration response relationship was caused by irreversible interaction of LARG and $G\alpha_{13}$. The LARG $G\alpha_{13}$ interaction and LARG translocation was monitored over ten minutes of agonist wash-out and then agonist was applied for a second time (fig. 24). The mean FRET traces in figure 24A and B are not corrected for bleaching, because correction could have led to overestimation of decrease in FRET during wash-out and thereby overestimation of the LARG $G\alpha_{13}$ dissociation. Also no comparison was done between the first and second amplitude, since loss in amplitude can be caused by photo bleaching as well. In order to facilitate comparison of kinetics the translocation trace was mirrored along the time axis (fig. 24C). Further, the sampling rate was reduced to one image every 30s to exclude underestimation of the second translocation due to bleaching. In all three assays a second increase could be observed after ten minutes. In the translocation experiment the first and second amplitude were not significantly different as evaluated by a paired t-test. From these data we assume a reversible translocation of LARG as well as interaction of the same with $G\alpha_{13}$. Noteworthy, the mean traces of YFP-LARG translocation in the presence of unlabeled and mTur2-labeled $G\alpha_{13}$ were comparable (fig 24C).

6.1.6 Does RhoA-GTP stabilize the LARG $G\alpha_{13}$ interaction?

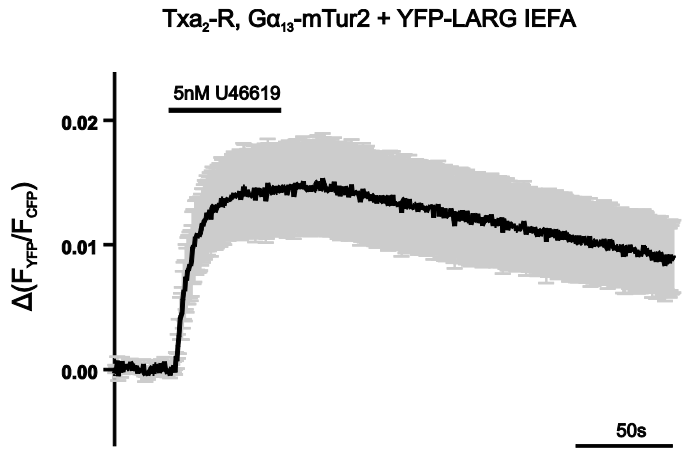

Fig. 25 Interaction of $G\alpha_{13}$ with a LARG mutant deficient in Rho-GTP binding
HEK293T cells were transfected with 0.5µg Txa_2-R, 1µg $G\alpha_{13}$-mTur2, 0.5µg Gβ-wt, 0.2µg Gγ-wt and 1µg YFP-LARG F1098A-I1000E and stimulated with agonist. The mutant is described to be deficient in RhoA-GTP binding and therefore should not participate in a putative positive feedback loop. Shown is the mean trace±S.E.M. of twelve cells.

All Lbc-RhoGEFs bind RhoA-GTP and this binding is discussed to participate in a positive feedback loop (Medina et al., 2013). Therefore we wondered whether the interaction of RhoA-GTP with LARG is the reason for the prolonged interaction of $G\alpha_{13}$ and LARG. We mutated LARG to prevent RhoA-GTP binding, as described before (F1098A and I1100E (Medina et al., 2013)). The mutations were introduced in two cycles of QuickChange® site-directed mutagenesis (see 5.1.3.2 for primer sequence) and verified by sequencing. The FRET change between $G\alpha_{13}$-mTur2 and YFP-LARG F1098A-I1100E upon stimulation with 5nM U46619 is shown in figure 25. There is no obvious difference between this trace and the mean trace for YFP-LARG wild type (fig. 19B) in terms of wash-out kinetics even though a smaller agonist concentration was applied.

6.1.7 Overexpression of LARG in HEK293T cells

For functional comparison of downstream effects of the fluorophore tagged LARG variants and wild type LARG equal expression is essential. The wild type plasmid with pHyg as backbone was a kind gift by T. Wieland, Mannheim. Full cell lysates were separated by 10% SDS PAGE and afterwards transferred to a PVDF membrane by Western Blot. The membrane was incubated with antibodies against LARG, $G\alpha_{13}$ and as loading control an antibody against RhoA was used (see 5.1.8 for a list of

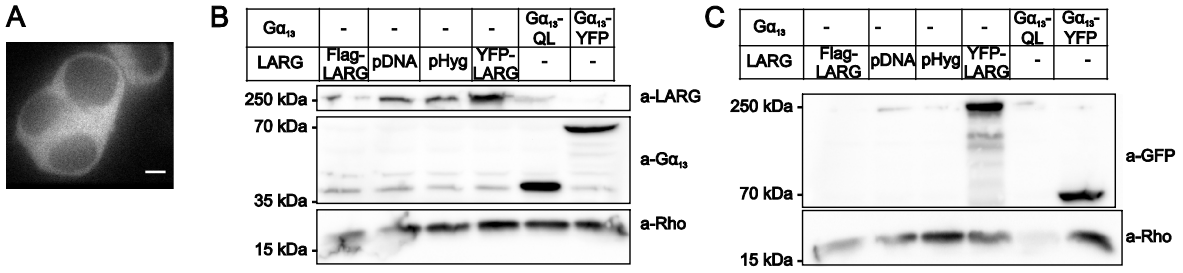

Fig. 26 Localization and overexpression of LARG constructs
A HEK293T cells were transfected with 1µg/6cm dish YFP-LARG and fluorescence was detected with a confocal FRAP imaging system (Visitech) two days after transfection. Scale bar, 5µm (**B** and **C)** Expression of differing LARG constructs (Flag-LARG, pcDNA3-LARG, pHyg-LARG and YFP-LARG) and constitutive active $G\alpha_{13}$QL as well as $G\alpha_{13}$-YFP were investigated by SDS PAGE and Western Blot. 10cm dishes of HEK293T cells were transfected with 10µg LARG constructs or 2µg $G\alpha_{13}$. After blotting PVDF membranes were incubated with a-LARG, a-$G\alpha_{13}$ and a-Rho (**B**) as well as with a-GFP and a-Rho (**C**) antibodies.

antibodies). In the two lanes on the left of figure 26B and C 2µg constitutive active $G\alpha_{13}QL$ and YFP-labeled $G\alpha_{13}$ were transfected in HEK293T cells with polyethylenimine (PEI), respectively. These constructs expressed rather equally. Whereas 10µg per 10cm dish of pHyg-LARG was far less expressed than the same amount of YFP-LARG (fig. 26B).

If LARG wild type transcription were controlled by the same promoter as YFP-LARG transcription, both constructs should be transcribed with the same rate. Therefore, LARG was cloned into pcDNA3, which is also the vector of YFP-LARG:

The plasmids YFP-LARG and empty pcDNA3 were digested with the restriction enzymes BamHI and XhoI. Thereby the LARG cDNA was separated from YFP. Afterwards LARG was ligated into pcDNA3.

But also LARG in pcDNA3 was as weakly expressed as LARG in pHyg (fig. 26B). For this reason we tried to enhance protein stability by fusion of a Flag-tag to the N-terminus of LARG. We chose this approach, because YFP-LARG is better expressed and it differs only by its N-terminal YFP from pcDNA3-LARG. But nevertheless, Flag-LARG expressed as weakly as wild type LARG (fig. 26B). The described major differences in expression, hindered comparison of LARG and YFP-LARG in respect to downstream signaling as discussed in detail in 6.1.8.

LARG cDNA was amplified from YFP-LARG with an N-terminal primer featuring the coding sequence for a Flag-tag (see 5.1.3.1 for a list of cloning primers). Afterwards the PCR product and empty pcDNA3 were digested with BamHI and XhoI, ligated and sequenced.

To estimate stoichiometry of LARG and $G\alpha_{13}$ the same cell lysates as used for figure 26B were blotted and the membrane was incubated with an antibody against GFP (fig. 26C). The GFP antibody should detect YFP equally well no matter if it´s fused to LARG or to $G\alpha_{13}$. Thus this should allow for comparison of YFP-LARG and $G\alpha_{13}$-YFP expression. Transfection of either 10µg YFP-LARG or 2µg $G\alpha_{13}$-YFP cDNA led to the same amount of YFP-labeled protein (fig. 26C). Differences in DNA amount were balanced with empty pcDNA3 and RhoA was used as loading control.

6.1.8 Determination of active RhoA and SRE.L activation by LARG

Next, we tried to monitor RhoA and SRE.L signaling downstream of LARG. Activation of RhoA can be measured by affinity purification of active GTP-bound RhoA from full cell lysates (Ren and Schwartz, 2000). In a mammalian cell the total amount of RhoA should exceed the portion of active RhoA and therefore total RhoA should not be significantly altered by precipitation of active RhoA. The RhoA binding domain (RBD) of Rhotekin has high affinity for active RhoA and can be expressed in *E. coli* as fusion protein with Glutathione-S-transferase (GST). The GST-RBD was incubated with glutathione coated agarose beads and this “predator” was used to isolate its “prey” RhoA-GTP from full cell lysates. The left over lysate was tested for expression of transfected constructs and equal amounts of total RhoA. The precipitated, active RhoA and the RhoA from the full cell lysate were detected with the same antibody, which should bind equally well to active and inactive RhoA. HEK293T cells were transfected with PEI with or without 1µg constitutively active $G\alpha_{13}QL$,

10µg YFP-LARG or pcDNA3-LARG. Differences in DNA amounts were balanced with empty pcDNA3. 24 hours after transfection cells were lysed and active RhoA was isolated.

In theory cells only transfected with empty vector should show no or only a faint RhoA band in the precipitate fraction, which represents the active RhoA fraction under basal conditions. Further expression of either $G\alpha_{13}QL$ or LARG should increase the signal of the active RhoA fraction and this should be even enhanced by coexpression of both.

In most experiments transfection of $G\alpha_{13}QL$ increased the amount of RhoA in the precipitate compared to active RhoA under basal conditions whereas the active RhoA upon LARG transfection alone or together with $G\alpha_{13}QL$ varied considerably, which paralleled the again very low LARG expression in most experiments. For the affinity purification of active RhoA experiment with the highest LARG expression the Western Blot result is shown in figure 27. In this case transfection of YFP-LARG alone led to the highest amount of RhoA in the precipitate fraction. This was even higher than if YFP-LARG was cotransfected with $G\alpha_{13}QL$. The amount of RhoA in the full cell lysate was in the same range for all conditions.

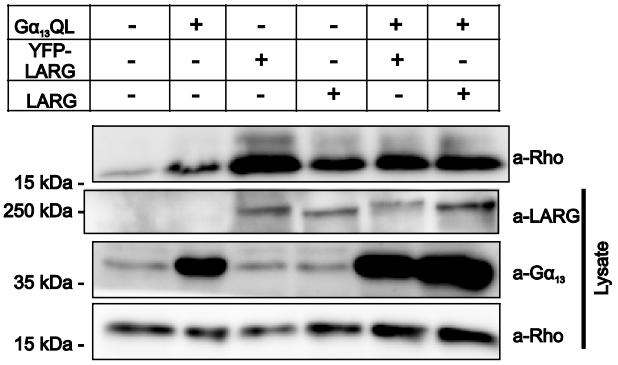

Fig. 27 RhoA activation by YFP-labeled and wild type LARG
Active Rho was determined using a GST-tagged Rho binding domain (RBD). HEK293T cells were transfected with or without 1µg $G\alpha_{13}QL$, 10µg YFP-LARG or LARG in pcDNA3. 24h after transfection cells were lysed and incubated with RBD. Active Rho was precipitated and analyzed by Western Blot (upper row, a-Rho). Full cell lysates were also investigated by Western Blot in order to check for expression of the transfected constructs (a-LARG and a-$G\alpha_{13}$) and equal loading (a-Rho).

In addition to the described transfection conditions also other G protein RhoGEF ratios were tested, but no reliable $G\alpha_{13}QL$-dependent LARG mediated Rho activation could be observed. The same problem occurred in the SRE.L reporter gene assay.

As described previously the transcription factor SRF is activated downstream of Rho activation (see 4.4.1 *Amongst others, ROCK is activated by the Rho subfamily* and 5.2.4). SRF binds together with another transcription factor, MRTF, to the serum response element (SRE) and thus the SRE.L reporter gene assay is used to determine RhoGEF activity.

In theory $G\alpha_{13}$ should activate LARG and this should lead to increased SRE.L transcription, which would be measured as increase in firefly luciferase activity. So transfection of $G\alpha_{13}$ alone and LARG alone should cause lower luciferase activities than cotransfection of both. To test this 50ng/well LARG, YFP-LARG, LARG-insYFP or empty vector were cotransfected with increasing amounts of $G\alpha_{13}QL$ (0ng (control) to 2.5ng). Luciferase activity is depicted normalized to cells transfected only with the reporter plasmids and empty pcDNA3. All conditions are measured in triplicates. This is true for all SRE.L reporter gene assays presented in this thesis.

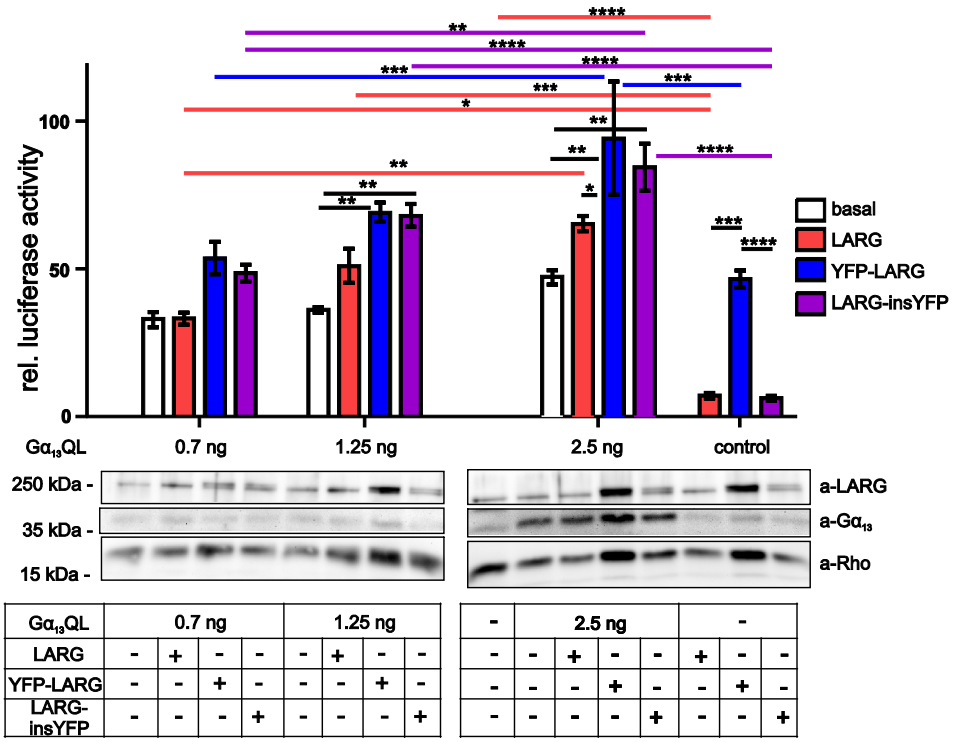

Gα13QL	0.7 ng				1.25 ng				-	2.5 ng				-			
LARG	-	+	-	-	-	+	-	-	-	-	+	-	-	+	-	-
YFP-LARG	-	-	+	-	-	-	+	-	-	-	-	+	-	-	+	-
LARG-insYFP	-	-	-	+	-	-	-	+	-	-	-	-	+	-	-	+

Fig. 28 SRE.L transcription due to activation of LARG and the two YFP-labeled LARG constructs by increasing amounts of $G\alpha_{13}QL$
In 96-well format HE293T cells were transfected as indicated with or without 50ng/well LARG (red), YFP-LARG (blue), LARG-insYFP (purple) or empty vector (basal, white), as well as differing amounts of $G\alpha_{13}QL$, if indicated, and empty pcDNA3 for equal DNA amounts. Further all conditions were transfected with the reporter gene plasmids: 21.6ng/well pSRE.L and 3.4ng/well pRL-TK, which is constitutively active. Results are relative (rel.) mean±S.E.M. luciferase activities after normalization **P<0.01, ***P<0.001, ****P<0.0001, ANOVA with Bonferroni´s multiple comparison test, comparisons between different $G\alpha_{13}QL$ concentrations of one LARG version were colored according to the LARG version. Expression of the transfected proteins was confirmed by Western Blot (lower panel, a-Rho as loading control).

$G\alpha_{13}QL$ was detectable in Western Blot (fig. 28 lower panel) only if 2.5ng/well were transfected. For the Western Blot the lysates of triplicates per condition were pooled and the complete lysates were loaded on a 10% SDS PAGE. Even though 0.7ng/well $G\alpha_{13}QL$ were not detectable in Western Blot, an increased luciferase activity was already present. For all $G\alpha_{13}QL$ concentrations no significant difference in luciferase activity between $G\alpha_{13}QL$ alone and together with LARG was measured. In line with this, LARG expression was found equal for cells transfected with and without LARG. Thus, LARG transfection did not enhance LARG expression over endogenous levels. For YFP-LARG an overexpression could be validated in the Western Blot. Also LARG-insYFP was expressed, as shown by the double band, but only in the range of endogenous LARG. For YFP-LARG and LARG-insYFP a significant effect compared to basal was found in the conditions with 1.25ng and 2.5ng $G\alpha_{13}QL$ (fig. 28 upper panel). This luciferase assay is representative for many others, with differing concentrations in $G\alpha_{13}QL$ and the LARG variants. Especially unlabeled LARG could not be reliably expressed.

In one case transfection of 50ng/well LARG and YFP-LARG led to a pronounced overexpression (fig. 29B). For this experiment 50ng/well $G\alpha_{13}QL$ was used. Later on the amount of $G\alpha_{13}QL$ was reduced stepwise to the amounts used in figure 28 in order to get an excess of the LARG variants over $G\alpha_{13}QL$. Significantly, with LARG and YFP-LARG overexpressed a significant increase in luciferase activity was observed for $G\alpha_{13}QL$ coexpression compared to the LARG variants alone (fig. 29A).
In summary, we could not reliably investigate $G\alpha_{13}$-dependent signaling downstream of LARG, due to

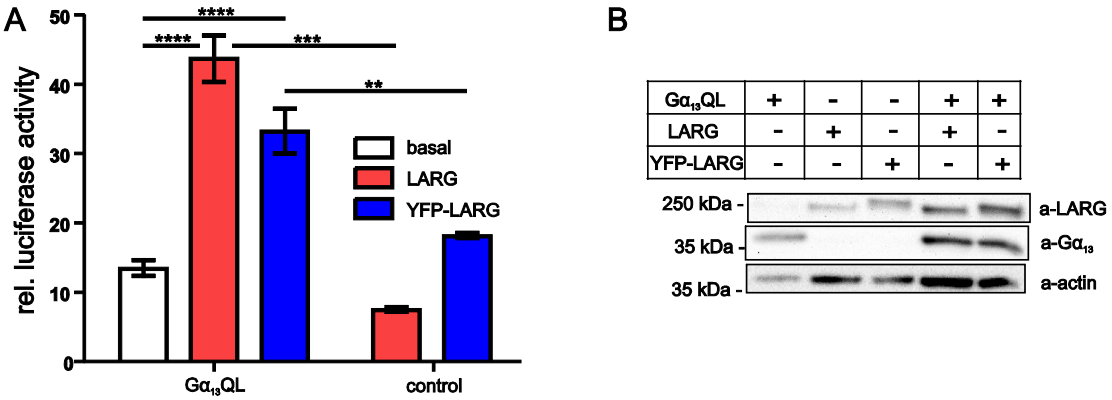

Fig. 29 SRE.L transcription due to activation of LARG and YFP-LARG by $G\alpha_{13}QL$
In 96-well format HE293T cells were transfected as indicated with 50ng/well LARG (red), YFP-LARG (blue) or empty vector (basal, white), as well as with or without 50ng/well $G\alpha_{13}QL$. All conditions were transfected with the reporter gene plasmids. (**A**) Results are relative (rel.) mean±S.E.M. luciferase activities after normalization **P<0.01, ***P<0.001, ****P<0.0001, ANOVA with Bonferroni´s multiple comparison test. Expression of the transfected proteins was confirmed by Western Blot (**B**, a-actin as loading control).

minor LARG expression in most experiments. Thus also the validation of downstream signaling by the YFP-tagged LARG was prohibited. Noteworthy, they behaved as expected for wild type in regard to interaction with $G\alpha_{13}$: YFP-LARG translocated to the plasma membrane upon activation of wild type and mTur2-tagged $G\alpha_{13}$ (fig. 24C). In addition, translocation was reflected also in terms of kinetics by an increase in FRET between $G\alpha_{13}$-mTur2 and two LARG constructs, which were tagged with YFP at different sights (fig. 24A and B).

6.2 Dynamics of the Gα$_q$ p63RhoGEF interaction and its regulation by RGS2

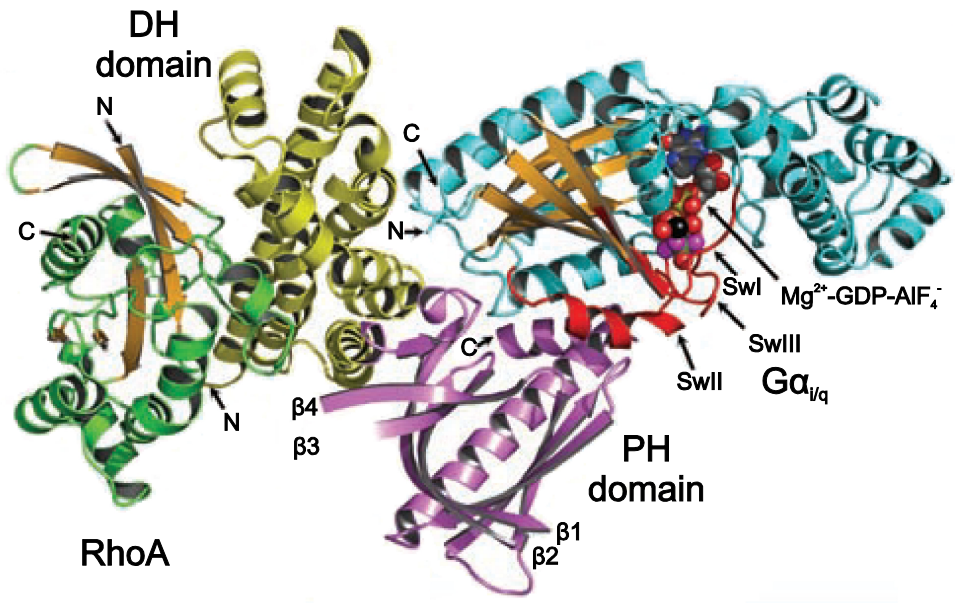

Fig. 30 Crystal structure of p63RhoGEF´s DH-PH domain in complex with RhoA and Gα$_{i/q}$
The crystal structure by Lutz and colleagues shows the interaction of RhoA (green) with p63RhoGEF´s DH domain (yellow). Gα$_q$ (blue) interacts with both DH (yellow) and PH (purple) domain. The last depicted amino acid of each domain is indicated with N and C, respectively, Gα$_{i/q}$´s three switch domains are shown in red (Lutz et al., 2007). The viewer looks from the plasma membrane towards the complex.

In order to compare the mainly Gα$_{13}$-regulated LARG with the Gα$_q$-regulated p63RhoGEF, we further studied the interaction of p63RhoGEF and Gα$_q$ in detail. p63RhoGEF´s domain structure (fig. 9) is much simpler than LARG´s structure (fig. 5) as it misses the PDZ domain and the RH domain. The interaction with Gα$_q$ occurs via its PH domain and parts of its DH domain (fig. 30, (Lutz et al., 2007)). This interaction involves only Gα$_q$´s effector binding site, but leaves its RGS binding site free for further interaction partners, which is in contrast to PLCβ´s binding to Gα$_q$ (fig. 8, (Lyon et al., 2014)). This free interaction site on Gα$_q$ can be occupied by RGS2 in a trimeric complex with p63RhoGEF, as shown in this section. Most of the results described in the following have been published (Bodmann et al., 2014).

6.2.1 The Gα$_q$ p63RhoGEF interaction can be monitored by FRET

The RhoGEF p63RhoGEF as effector of Gα$_q$ has not been studied in living cells. Therefore a FRET assay was established to study the p63RhoGEF Gα$_q$ interaction. HEK293T cells were transfected with the histaminergic H_1 receptor (H_1-R), Gα$_q$-CFP, Gβ-wt, Gγ-wt and N-terminally Venus-labeled p63RhoGEF (V-p63). Both, Venus-p63RhoGEF and Gα$_q$-CFP were found at the plasma membrane under basal conditions (fig. 31A). The H_1-R is known to couple to Gα$_q$ and was stimulated with 10µM histamine (Li et al., 1995). This led to a pronounced and fast increase in F_{YFP}, which was mirrored by decrease in F_{CFP}. After withdrawal of agonist F_{YFP} and F_{CFP} slowly recovered (fig. 31B). Accordingly, the ratio trace of the same cell and the mean trace of fifteen individual cells showed a reversible response to stimulation (fig. 31B and C). In order to verify this FRET assay with another Gα$_q$ coupled receptor, the

muscarinic M_3 receptor (M_3-R) was cotransfected with the FRET pair. Also with this receptor an increase in FRET was observed (fig. 31C). An increase in FRET was visible in approximately 75% of all cells. Absence of a FRET change was probably due to lack of receptor in these cells.

Unspecific FRET is possible as described previously for the FRET between YFP-LARG and $G\alpha_{13}$-mTur2 (see 6.1.2). Therefore Venus-p63RhoGEF was also cotransfected with $G\alpha_i$-CFP, Gβ-wt, Gγ-wt and the $G\alpha_i$ coupled α_{2A} adrenergic receptor (α_{2A}-AR). For this condition no change in FRET was observed upon stimulation with a saturating noradrenaline (NA) concentration of 100µM (fig. 31E). Also HEK293T cells, which were transfected with H_1-R, $G\alpha_q$-CFP, Gβ-wt, Gγ-wt and GIRK4-YFP instead of Venus-p63RhoGEF, did not show a change in FRET ratio (fig. 31F). So activation of $G\alpha_q$ coupled receptors and subsequent $G\alpha_q$ activation leads to a reversible and specific increase in FRET between $G\alpha_q$-mTur2 and Venus-p63RhoGEF.

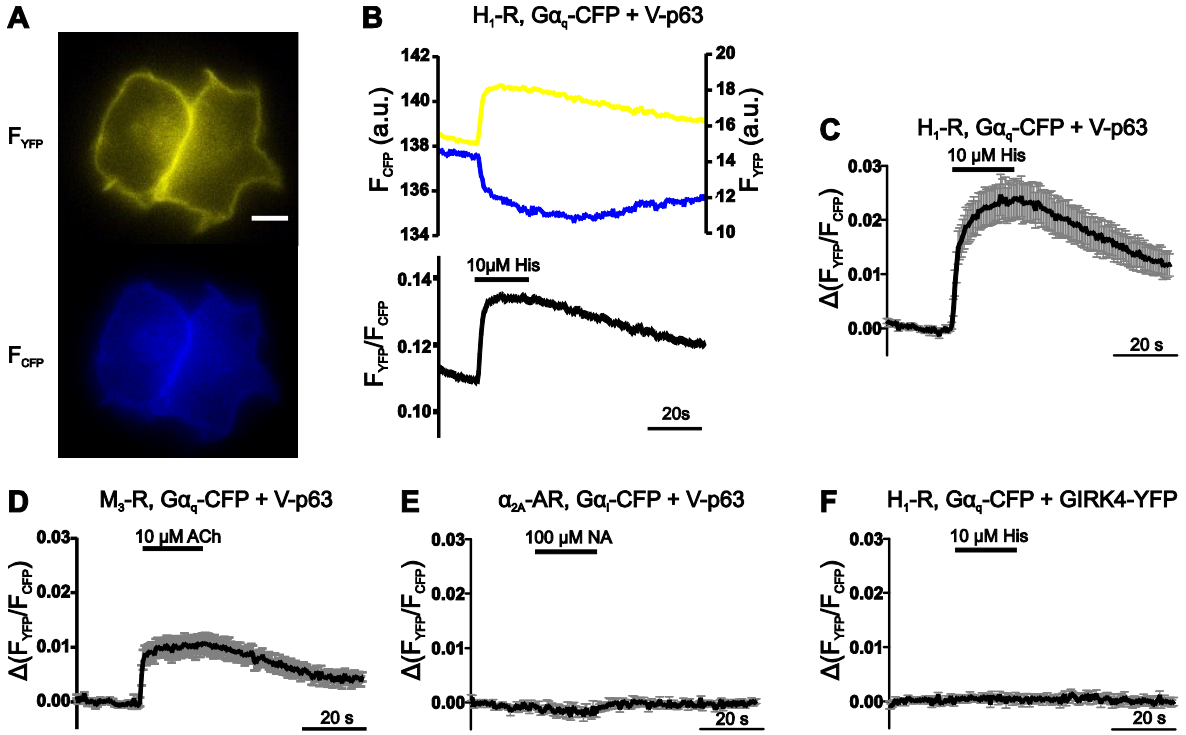

Fig. 31 FRET change between $G\alpha_q$–CFP and Venus-p63RhoGEF upon receptor stimulation
HEK293T cells were transfected with 1µg H_1-R, 1.5µg $G\alpha_q$-CFP, 0.5µg Gβ-wt, 0.2µg Gγ-wt and 0.3µg Venus-p63RhoGEF. **A** In these cells Venus-p63RhoGEF and $G\alpha_q$-CFP localized to the plasma membrane under basal conditions. Both fluorophores were excited independently. Scale bar, 5µm. **B** Upon stimulation with 10µM histamine (His) F_{YFP} (yellow) increased and F_{CFP} (blue) decreased rapidly in a representative cell. This was also reflected in an increase in ratio trace of the same cell (black) and mean±S.E.M. trace for 15 individual cells (**C**). a.u., arbitrary unit(s). **D** Activation of M_3-R instead of H_1-R with acetylcholine (ACh) had the same effect. **E** For activation of $G\alpha_i$-CFP by the α_{2A} adrenergic receptor (α_{2A}-AR) with noradrenaline (NA) no change in FRET with Venus-p63RhoGEF was observed. The same was true for FRET between $G\alpha_q$-CFP and GIRK4-YFP upon activation of H_1-R (**F**). Traces are means±S.E.M. of at least nine individual cells.

6.2.2 The interface of the $G\alpha_q$ p63RhoGEF interaction

The interaction of p63RhoGEF with $G\alpha_q$ is described to rely on p63RhoGEF´s PH domain. Therefore two mutations were inserted in this domain (F471E and L475A). Thus we wondered whether a loss in interaction abolished downstream signaling. We could show previously reduced FRET amplitude and significantly reduced fraction of responding cells upon mutation of one of the two sites (Bodmann, diploma thesis). A complete loss in FRET was observed between Venus-p63RhoGEF F471E-L475A and $G\alpha_q$-CFP.

As described previously (see 6.1.8) SRE.L reporter gene assays are widely used to determine RhoGEF activity. Since the H_1-R is known to have relatively high basal activity, the high luciferase activity by H_1-R alone was expected (Bakker et al., 2000). The single mutants as well as the double mutant showed a significant loss in luciferase activity compared to wild type p63RhoGEF upon H_1-R activation (fig. 32A). The luciferase activity of the mutants was comparable with receptor alone. The reduction in RhoGEF activity of the mutants was not caused by lower expression as determined by Western Blot (fig. 32B). We concluded that p63RhoGEF´s PH domain is crucial for $G\alpha_q$-binding and activation of downstream signaling.

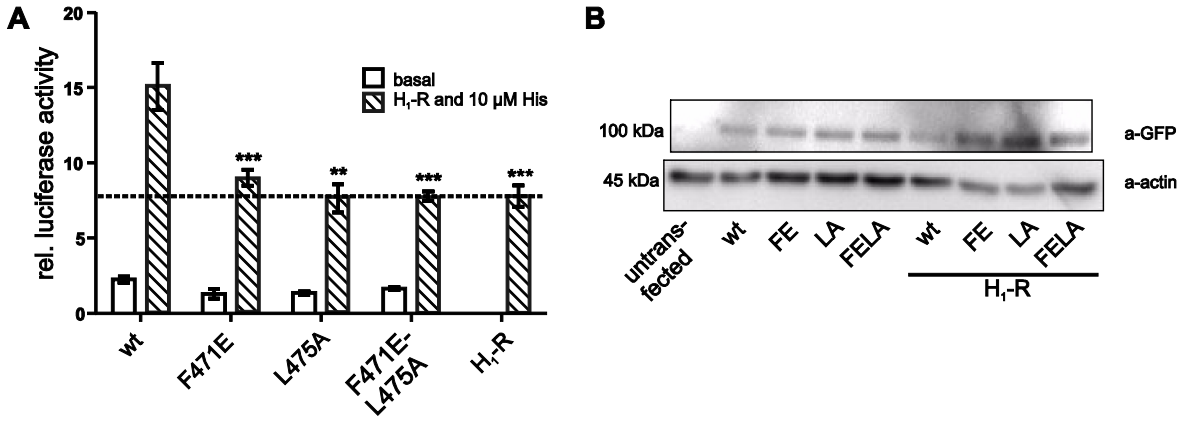

Fig. 32 Decreased SRE.L activation by $G\alpha_q$ binding deficient p63RhoGEF variants
A In 96-well format HEK293T cells were transfected with differing 10ng/well Venus-p63RhoGEF mutants alone (basal, open bars) or together with 50ng/well H_1-R and stimulated with 10µM histamine (hatched bars). Further all conditions were transfected with the reporter gene plasmids. Results are relative (rel.) mean±S.E.M. luciferase activities after normalization **P<0.01, ***P<0.001, ANOVA with Dunnett´s multiple comparison test, which compared all conditions with p63RhoGEF wild type. **B** Equal expression of Venus-p63RhoGEF was confirmed by Western Blot and actin expression was used as loading control (lower panel).

For PLCβ3 the $G\alpha_q$-binding site was described, which overlaps with the binding sites for RGS2 and p63RhoGEF (see 4.5.2.1 *PLCβ3 overlaps with p63RhoGEF and RGS2 binding to $G\alpha_q$*, (Lyon et al., 2014)). RGS2 and p63RhoGEF bind to different sites on $G\alpha_q$ (Shankaranarayanan et al., 2008). Therefore we wondered, if RGS2 would inhibit interaction of $G\alpha_q$ and PLCβ3 and thereby would inhibit production of the second messenger diacylglycerol (DAG). Further we wondered how far p63RhoGEF and PLCβ3 would interfere with each other during signaling.

The interaction of $G\alpha_q$ and PLCβ3 can be monitored by FRET between the two proteins as studied in detail by T. Pollinger (Pollinger, 2012). The interaction of $G\alpha_q$–CFP and YFP-PLCβ3 was greatly abolished by cotransfection of RGS2 in HEK293T cells, which stably express murine H_1-R (mH_1-R-HEK293T, fig. 33A). For this experiment RGS2 was tagged with a red fluorescent protein (RFP) at its C-terminus and only RGS2 expressing cells were measured.

RGS2-RFP was cloned as follows: RGS2 was PCR amplified from RGS2-YFP with the primers listed in 5.1.3.1. A KpnI and a NotI restriction site were N- and C-terminally, respectively, introduced into RGS2 with this step. Next the PCR product and pcDNA3-mRFP were digested with KpnI and NotI and the fragments were ligated.

Active PLCβ hydrolyses phosphatidylinositol 4,5-bisphosphate (PIP_2) into inositol triphosphate (IP_3) and diacylglycerol (DAG). Thus, DAG levels are an established surrogate parameter for PLCβ activity. The cellular DAG levels can be measured with a FRET-based sensor (Violin et al., 2003). An increase in FRET reflects an increase in cellular DAG concentrations. Cotransfection of RGS2-RFP with the DAG sensor reduced the agonist dependent increase in FRET in mH_1-R-HEK293T cells (fig. 33B). Hence, RGS2 cotransfection disrupts the PLCβ3 $G\alpha_q$ interaction and production of the second messenger DAG.

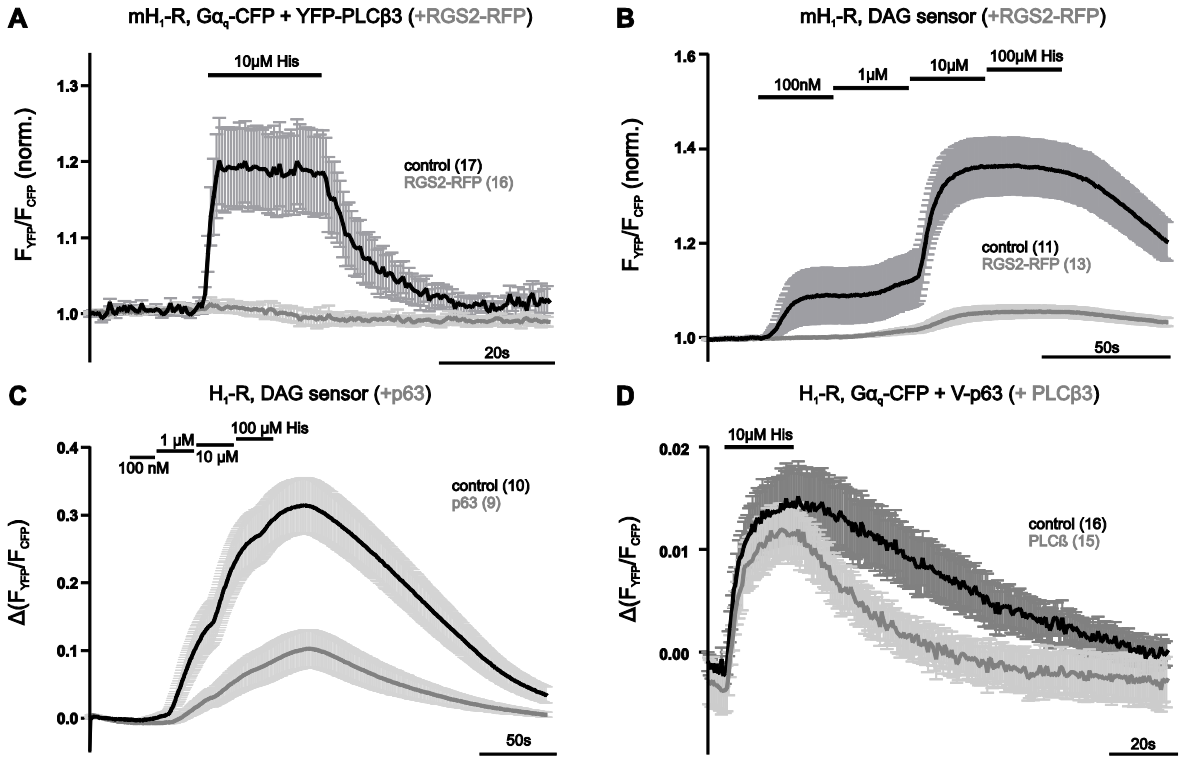

Fig. 33 Influence of RGS2 and p63RhoGEF on PLCβ3 signaling
HEK293T cells stabily expressing murine H_1-R (mH_1-R) were cotransfected with 1µg $G\alpha_q$-CFP and 1µg YFP-PLCβ3 alone (black) or together with 0.5µg RGS2-RFP (grey) and stimulated with 10µM histamine (**A**). **B** The production of diacylglycerol (DAG) was monitored in mH_1-R-HEK293T cells transfected with a FRET-based DAG sensor (0.5µg) and 0.5µg pcDNA3. An increase in FRET reflects an increase in DAG levels. DAG levels were drastically reduced in the presence of 0.5µg RGS2-RFP (grey). For **C** HEK293T cells were transfected with 1µg H_1-R and the DAG sensor (0.5µg) in the absence (black) and presence of 0.3µg p63RhoGEF (grey). **D** HEK293T were transfected like in figure 31A (black) or additionaly with 1µg PLCβ3 (grey). All traces are mean±S.E.M., *n* (in parentheses).

p63RhoGEF coexpression with the DAG sensor and H_1-R in HEK293T cells reduced also the histamine-induced increase in DAG (fig. 33C). In contrast, the amplitude in FRET between $G\alpha_q$ and p63RhoGEF was not changed by PLCβ3 coexpression (fig 33D). Since the amplitude in the plateau phase of agonist stimulation reflects the steady state of protein interaction, this result indicates no influence of PLCβ3 on the steady state of the $G\alpha_q$ p63RhoGEF interaction. This is also reflected in unchanged dissociation of $G\alpha_q$ and p63RhoGEF in the presence of PLCβ3: For all cells shown in figure 33D the dissociation kinetics were determined by fitting of a monoexponential function to the wash-out curve. The k_{off} did not significantly differ as analyzed with Student´s t-test after Welch´s correction (k_{off}=0.064±0.047 and in the presence of PLCβ3 0.040±0.006, n ≥7, mean±S.E.M.).
In summary the PH domain is crucial for p63RhoGEF´s binding to and activation by $G\alpha_q$. Furthermore p63RhoGEF and RGS2 can compete with PLCβ3 for binding to $G\alpha_q$.

6.2.3 RGS2 accelerated $G\alpha_q$ inactivation and the $G\alpha_q$ p63RhoGEF dissociation

RGS2 belongs to the GTPase activating protein family and accelerates GTP hydrolysis of active Gα subunits. Therefore we wondered how RGS2 influences the p63RhoGEF $G\alpha_q$ interaction. In HEK293T cells, which were transfected with H_1-R, $G\alpha_q$-CFP, Gβ-wt, Gγ-wt and Venus-p63RhoGEF, we studied the area under the curve (AUC) and decline upon agonist wash-out in the absence and presence of RGS2. The steady state of the $G\alpha_q$ p63RhoGEF interaction was not altered by RGS2 as

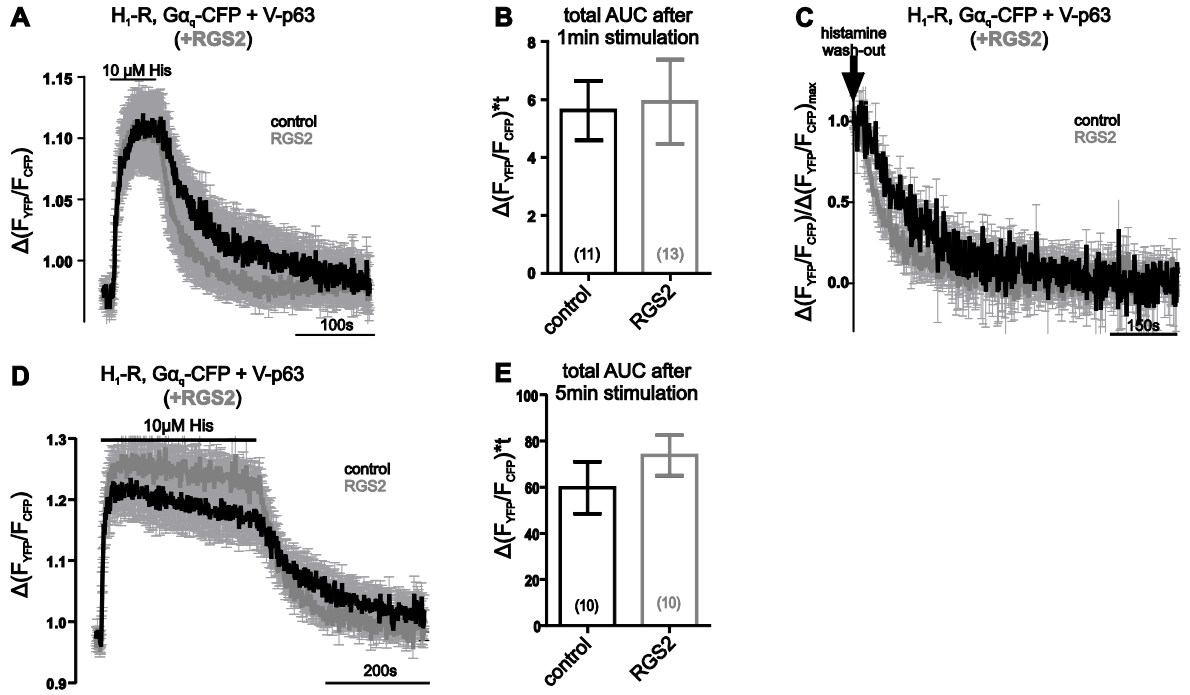

Fig. 34 RGS2 accelerates the $G\alpha_q$ p63RhoGEF dissociation without an influence on steady state
HEK293T cells were transfected with 1µg H_1-R, 1.5µg $G\alpha_q$-CFP, 0.5µg Gβ-wt, 0.2µg Gγ-wt and 0.3µg Venus-p63RhoGEF. If indicated (grey) 0.5µg RGS2 was added to the transfection. **A** Cells were stimulated with 10µM histamine for one minute and area under the curve (AUC) until agonist wash-out was evaluated (**B**). The same cells were normalized to maximal response and plotted since agonist wash-out (**C**). In cells with RGS2 p63RhoGEF and $G\alpha_q$ dissociated faster than in cells without RGS2. Also stimulation with agonist for five minutes was followed by faster dissociation in the presence of RGS2 (**D**) and unchanged area under the curve until wash-out (**E**). Traces are mean±S.E.M., *n* (in parentheses).

indicated by the unchanged area under the curve upon stimulation with 10µM histamine for either one or five minutes (fig. 34B and E). The dissociation was analyzed by fitting a mono-exponential function to the decline after agonist wash-out. For the cells summarized in the raw and normalized mean trace depicted in figure 34A and C k_{off} values were evaluated. This analysis showed that the dissociation in the presence of RGS2 was three times faster than under control conditions. The k_{off} for the two conditions differed significantly, as analyzed by an unpaired Student´s *t* test after Welch´s correction (P<0.01, (Bodmann et al., 2014)).

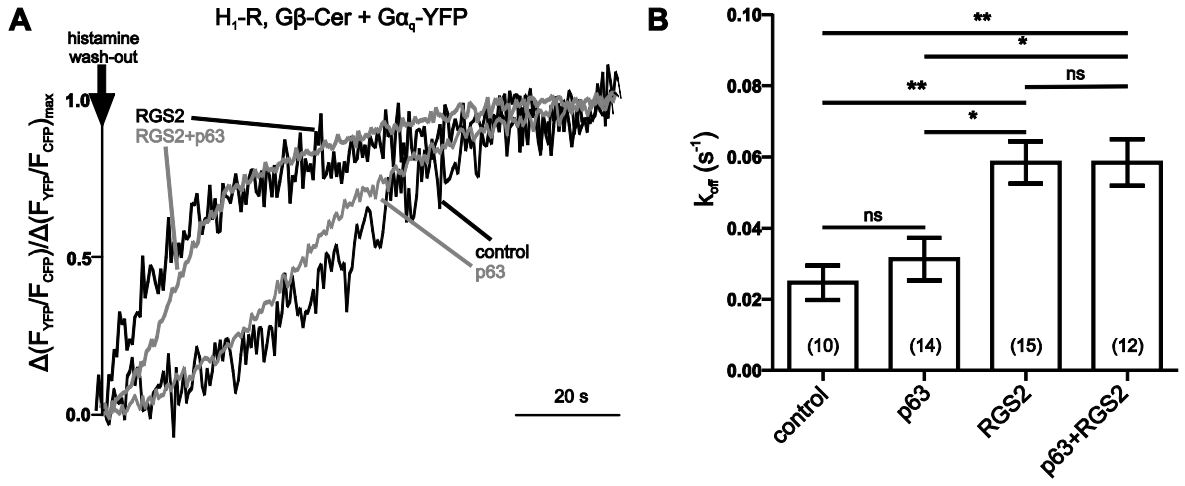

Fig. 35 Gα$_q$ reassociation is accelerated by RGS2 independent of p63RhoGEF expression
Gα$_q$ activation and inactivation was investigated in the absence or presence of either p63RhoGEF (0.3µg), RGS2 (0.5µg) or both in HEK293T cells additionally transfected with 1µg H_1-R, 1.5µg Gα$_q$-YFP, 0.5µg Gβ-Cer and 0.2µg Gγ-wt. Reassociation kinetics were estimated by fitting a deactivation mono-exponential function. **A** Normalized representative traces of the cells, which showed the k_{off} closest to the mean, for each condition. The traces are plotted since wash-out of 10µM histamine. p63RhoGEF did not affect Gα$_q$ reassociation, but RGS2 did as indicated by calculated k_{off} (**B**). Mean±S.E.M. *n* (in parentheses). *P<0.05, **P<0.01, ANOVA with Bonferroni´s multiple comparison test. ns, not significant.

The activation cycle of Gα$_q$ can be monitored by FRET. Since RGS2 accelerates Gα$_q$´s inactivation, we wondered if this is reflected in faster off-rate of FRET between Gα$_q$-YFP and Gβ-Cer. Further we wondered if p63RhoGEF exhibits GAP activity towards Gα$_q$ and/or modulates RGS2´s GAP activity.

Therefore HEK293T cells were transfected with H_1-R, Gα$_q$-YFP, Gβ-Cer, Gγ-wt and either p63RhoGEF, RGS2, none of them or both. The reassociation of Gα$_q$ and Gβγ is reflected in an increase in FRET between Gα$_q$-YFP and Gβ-Cer upon agonist wash-out. The increase can be analyzed by fitting of a mono-exponential curve, as described above. RGS2 accelerated the reassociation significantly (k_{off}=0.058s^{-1}) compared to the trimeric G protein alone (k_{off}=0.024s^{-1}), as it can be seen in the wash-out traces of representative cells (fig. 35). Whereas cotransfection of p63RhoGEF did not significantly change the reassociation of Gα$_q$ and Gβγ (k_{off}=0.031s^{-1}). In cells expressing RGS2 and p63RhoGEF the reassociation occurred with the same speed as for RGS2 alone (k_{off}=0.058s^{-1}).

6.2.4 Concentration response curves of $G\alpha_q$ activation and its interaction with p63RhoGEF superimpose independent of RGS2 expression

RGS2 accelerates $G\alpha_q$ inactivation and $G\alpha_q$ p63RhoGEF dissociation. For the LARG $G\alpha_{13}$ interaction compared to $G\alpha_{13}$ inactivation we described a prolonged interaction. This might be the reason for the left shift in concentration response relationship described in 6.1.4. Because of that we wondered if shortened $G\alpha_q$ activation or $G\alpha_q$ p63RhoGEF interaction would lead to a right shift in concentration response curve.

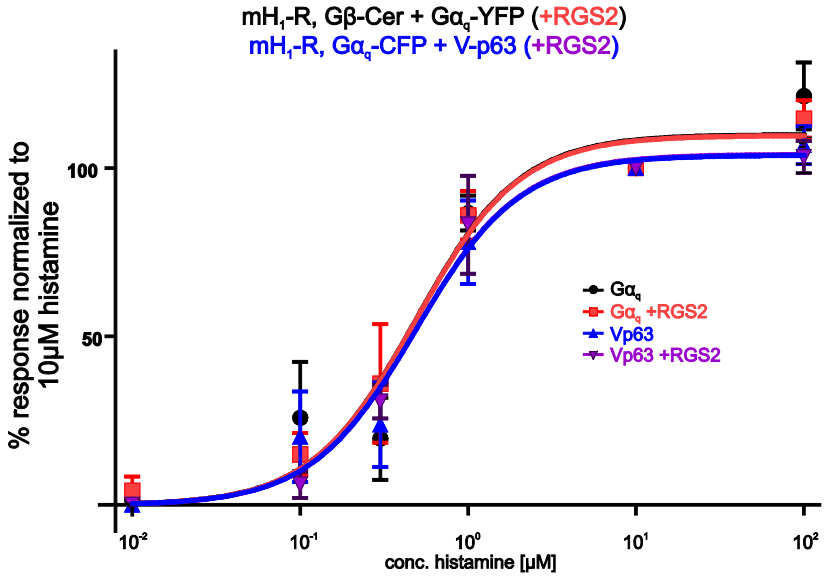

Fig. 36 Concentration response curve of $G\alpha_q$ activation and the $G\alpha_q$ p63RhoGEF interaction in the presence and absence of RGS2
For the concentration response curve HEK293T cells stabily expressing murine H_1-R were used. The single cells were transfected similarly to figure 34 and 35, respectively, but without receptor. Every cell was first stimulated with a test concentration and afterwards with 10µM histamine. Every concentration was tested in at least five individual cells. For every concentration mean±S.E.M. is depicted. To the measured values "dose-response curves" were fitted by "GraphPad Prism" and are shown as continous lines.

In order to guarantee constant receptor levels for all cells and conditions, we used again a HEK293 cell line stably expressing murine H_1-R. The cells were transfected similarly to conditions in figure 34 and 35, but without additional receptor. The measurements were evaluated as described for the concentrations response curves (6.1.4 and 5.2.6.1.7). For the $G\alpha_q$ activation and the $G\alpha_q$ p63RhoGEF interaction with and without RGS2 we found the same $logEC_{50}$ values, as analyzed by extra sum-of-squares F-test. Histamine activated all conditions with an EC_{50} of around 0.5µM. As discussed in 6.1.4 we analyzed the stoichiometry of G protein and RhoGEF in the cells used for the concentration response curve. We calculated 0.56±0.11 (geo. mean±S.D.) Venus-p63RhoGEFs per $G\alpha_q$-CFP for the analyzed cells with SI-Venus-β_2-AR-CFP as control construct. Therefore $G\alpha_q$ proteins were expressed approximately in a 2:1 stoichiometry in respect to p63RhoGEFs.
The control construct was cloned as follows: Venus was PCR amplified from Venus-p63RhoGEF with the primers listed in 5.1.3.1. By this PCR a BamHI restriction site and a SI-sequence were added at the

N-terminus of Venus and a XbaI restriction site at the C-terminus. Next the PCR product and SI-eYFP-β_2-AR were digested with BamHI and XbaI and ligated. With this step a SI-Venus-β_2-AR was created. Next this construct was digested with HpaI and HindIII in parallel with β_2-AR-CFP (Krasel et al., 2005). With these fragments SI-Venus-β_2-AR-CFP could be ligated.

6.2.5 Interaction of $G\alpha_q$ and RGS2 is not altered by p63RhoGEF

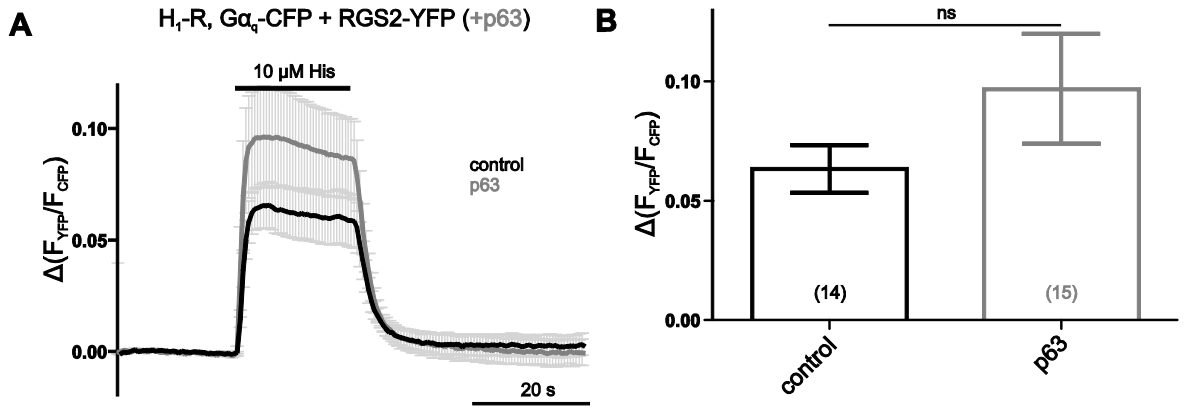

Fig. 37 p63RhoGEF did not change FRET between $G\alpha_q$-CFP and RGS2-YFP
FRET between $G\alpha_q$ and RGS2 was measured in HEK293T cells transfected with 1µg H_1-R, 1.5µg $G\alpha_q$-CFP, 0.5µg Gβ-wt, 0.2µg Gγ-wt and 0.5µg RGS2-YFP with (grey) or without (black) 0.3µg p63RhoGEF. p63RhoGEF did not change kinetics or amplitude of FRET between $G\alpha_q$ and RGS2 as visible in the mean±S.E.M. trace (**A**) and in the amplitude evaluation of the same cells (**B**). Mean±S.E.M., *n* (in parentheses).

The $G\alpha_q$ inactivation was accelerated by RGS2 in the presence of p63RhoGEF. Also the dissociation of $G\alpha_q$ and p63RhoGEF was faster in the presence of RGS2. Thus we wondered whether the $G\alpha_q$ RGS2 interaction can be monitored by FRET in cells expressing p63RhoGEF. Control HEK293T cells were transfected with H_1-R, $G\alpha_q$-CFP, Gβ-wt, Gγ-wt and RGS2-YFP and a second population was transfected additionally with p63RhoGEF. p63RhoGEF was transfected in the same amounts as used for FRET between $G\alpha_q$ and p63RhoGEF. Upon stimulation with 10µM histamine FRET increased rapidly and also declined rapidly with wash-out of the agonist (fig. 37A). The kinetics of interaction were not obviously changed by p63RhoGEF and also the FRET amplitude was not significantly different (fig. 37B, P=0.18) for the two conditions.

6.2.6 Increase in FRET between p63RhoGEF-CFP and RGS2-YFP upon agonist stimulation

The convergence of p63RhoGEF and RGS2 upon activation of $G\alpha_q$ has never been shown in living cells. In order to reveal their juxtaposition by means of FRET, we tagged p63RhoGEF C-terminally with CFP and cotransfected it together with RGS2-YFP.

p63RhoGEF-CFP was cloned as follows: β_2-AR-CFP (Dr. C. Krasel) and Venus-p63RhoGEF were digested with HindIII and XbaI and ligated in order to obtain Venus-p63RhoGEF-CFP. This construct was then digested with HindIII and BspEI, because restriction sites for this enzymes flank Venus. Next the barbed ends were blunted with a T4 DNA polymerase and the larger fragment was religated.

Functionality of p63RhoGEF-CFP was verified by SRE.L reporter gene assay (data not shown) and FRET with $G\alpha_q$-YFP (fig. 38E).

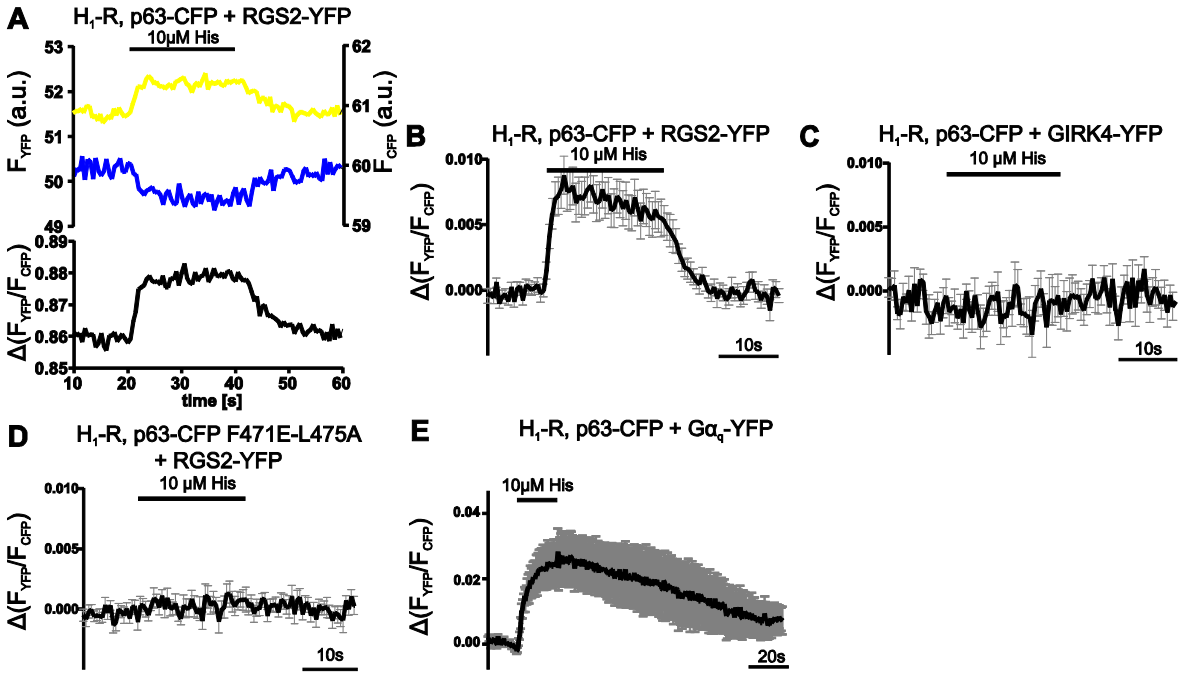

Fig. 38 Specific histamine-induced FRET change between p63RhoGEF-CFP and RGS2-YFP
Stimulation with histamine led to a fast, reversible FRET increase in HEK293T cells transfected with 0.3µg p63RhoGEF-CFP, 0.5µg RGS2-YFP, 1µg H_1-R, 1.5µg $G\alpha_q$-wt, 0.5µg Gβ-wt and 0.2µg Gγ-wt (**A** and **B**). F_{YFP} (yellow), F_{CFP} (blue) and ratio trace (black) of a representative cell and mean±S.E.M. of 16 individual cells. No change in FRET was observed in cells transfected with GIRK4-YFP (0.4µg) instead of RGS2-YFP (**C**) or $G\alpha_q$ binding deficient p63RhoGEF (p63-CFP F471E-L475A) instead of wild type p63RhoGEF (**D**). **E** Also p63RhoGEF-CFP showed agonist-dependent FRET changes with $G\alpha_q$-YFP, DNA amounts transfected as described in figure 31. (**B-E**) Shown are mean±S.E.M. traces of at least eight individual cells, a.u. arbitrary unit(s).

For the FRET measurement HEK293T cells were transfected with H_1-R, $G\alpha_q$-wt, Gβ-wt, Gγ-wt and RGS2-YFP as well as p63RhoGEF-CFP. A fast increase in FRET occurred upon stimulation with 10µM histamine and was reversible with agonist wash-out (fig. 38A and B). The change in FRET was rather small, but specific, which was indicated by three experiments: Firstly, no change in FRET was observed between p63RhoGEF-CFP and GIRK4-YFP, which localizes at the plasma membrane (fig. 38C). Secondly, no change in FRET was observed between p63RhoGEF-CFP and cytosolic Venus (data not shown). Since RGS2 translocates from the cytosol to the membrane, cytosolic and membrane bound YFP was used. Thirdly, no change in FRET occurred between RGS2-YFP and $G\alpha_q$

binding deficient p63RhoGEF (p63RhoGEF-CFP F471E-L475A, fig. 38D, see fig. 32 for characterization of the mutant). Thus the increase in FRET between RGS2 and p63RhoGEF reflects the specific convergence of the two in a trimeric complex with $G\alpha_q$.

6.2.7 Monitoring the $G\alpha_q$ p63RhoGEF RGS2 complex in living cells

In section 6.2 we examined FRET within the trimeric $G\alpha_q$ protein (fig. 35), between $G\alpha_q$ and p63RhoGEF (fig. 34), between $G\alpha_q$ and RGS2 (fig. 37) and between p63RhoGEF and RGS2 (fig. 38). In order to understand the kinetics of the trimeric complex in more detail, we compared the different assays by an overlay of the respective experiments (fig. 39). All experiments expressed $G\alpha_q$, p63RhoGEF and RGS2 either labeled or unlabeled.

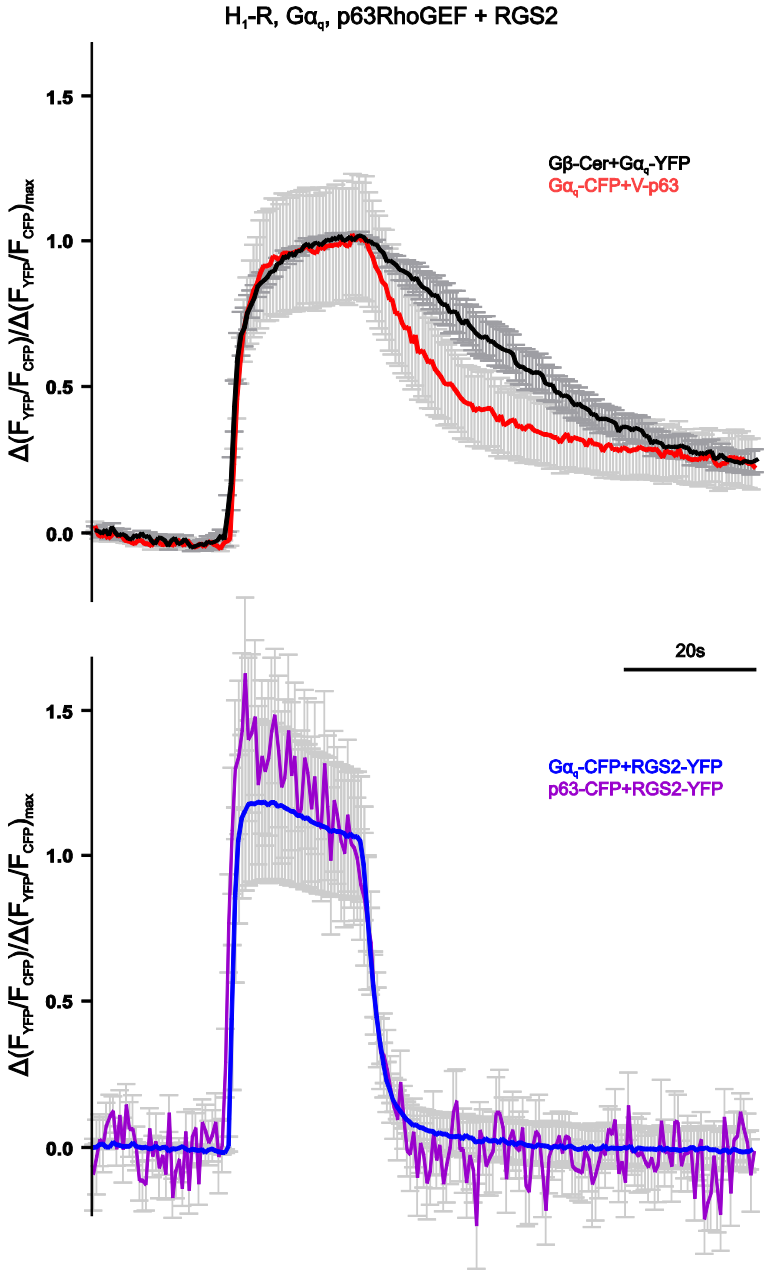

Fig. 39 Overlay of the four FRET assays monitoring the p63RhoGEF $G\alpha_q$ RGS2 complex
Traces are mean±S.E.M. of the cells shown in figure 35B (black), 34A (red), 37A (blue) and 38B (purple) in the conditions transfected with $G\alpha_q$, p63RhoGEF and RGS2, either labeled or unlabeled.

Differences in terms of kinetics were observed between the upper and the lower two sets of experiments. In the lower two sets, RGS2 is used in its fluorophore-labeled variant and functions as FRET partner. Therefore only complexes which include RGS2 are measured. The upper two sets of experiments have RGS2 cotransfected without a label. In these FRET measurements complexes with and without RGS2 are monitored, which results in a mixed phenotype for the overall FRET signal. Hence, the effect of RGS2 on $G\alpha_q$ inactivation and the $G\alpha_q$ p63RhoGEF interaction is probably underestimated in FRET assays with unlabeled RGS2 (e.g. fig 39 upper panel). With the described FRET assays

we demonstrated a dynamic complex of RGS2 and $G\alpha_q$-activated p63RhoGEF in living cells for the first time. Formation of this complex depends strictly on activation of and binding to $G\alpha_q$. In the presence of RGS2 $G\alpha_q$ inactivates faster and consequently presence of RGS2 in the trimeric complex accelerates its dissociation.

6.2.8 RGS2 negatively regulated signaling downstream of p63RhoGEF

The sensitivity towards histamine of $G\alpha_q$ activation and its interaction with p63RhoGEF is not altered by RGS2. But RGS2´s influence on signaling downstream of p63RhoGEF was not determined jet. Together with Dr. D. Brandt (AG Grosse, bpc, Marburg) we investigated Rho activation by p63RhoGEF in the presence of RGS2 (Bodmann et al., 2014): As explained in 6.1.2 activation of RhoA can be measured by affinity purification of active GTP-bound RhoA. In this assay p63RhoGEF coexpression increased Rho activity under basal conditions and after stimulation for five minutes with 10µM histamine. This p63RhoGEF-mediated response was reduced by RGS2 coexpression.

RhoGEF activity can also be estimated by SRE.L reporter gene assay (see 6.1.2). Therefore HEK293T cells were transfected in 96well format with H_1-R, with or without Venus-p63RhoGEF and/or RGS2-YFP. Fluorophore labeled constructs were used to control for equal expression by Western Blot with an antibody against GFP (fig. 40B).

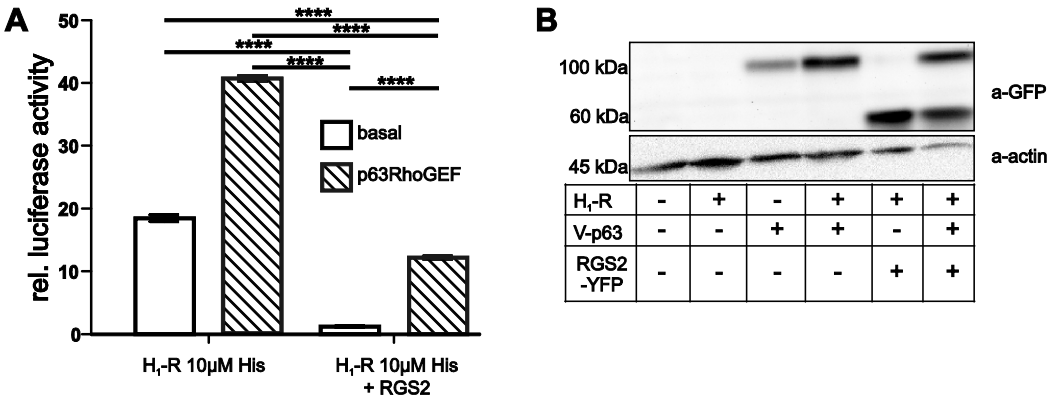

Fig. 40 SRE.L transcription upon p63RhoGEF activation is reduced by RGS2 coexpression
(**A**) In 96-well format HEK293T cells were transfected with 45ng/well H_1-R and stimulated with 10µM histamine. If so cotransfection is indicated for RGS2-YFP (45ng/well, RGS2) and/or Venus-p63RhoGEF (5ng/well, p63RhoGEF hatched bars). Further all conditions were transfected with the reporter gene plasmids. Results are relative (rel.) mean±S.E.M. luciferase activities after normalization. ****P<0.0001, ANOVA with Dunnett´s multiple comparison test. (**B**) Equal expression of Venus-p63RhoGEF (at 100kDa) and RGS2-YFP (at 60kDa) was confirmed for different conditions by Western Blot with a-GFP antibody and actin expression was used as loading control (lower panel).

RGS2 coexpression also reduced luciferase activity in cells with and without p63RhoGEF significantly (18.44 and 40.73, respectively, compared to 1.19 and 12.22, respectively, with RGS2; fig. 40A) indicating negative regulation of p63RhoGEF-mediated downstream signaling by RGS2.

7 Discussion

The activation of p63RhoGEF and RH-RhoGEFs by $G\alpha_q$ and $G\alpha_{13}$ were shown by different groups. For both pathways several physiology and pathological functions have been described, including chemotactic migration and progressive bone loss upon *Pasteurella multocida* infection for p63RhoGEFs (Hayashi et al., 2013; Siegert et al., 2013). The RH-RhoGEF LARG has been described as central player during pressure-overload induced cardiac hypertrophy and was shown to be important for synaptic plasticity for example (Takefuji et al., 2013; Kempf et al., 2014). Additionally, both pathways were shown to regulate vascular smooth muscle tone.

In contrast to this broad functional knowledge, only little was known about why RhoGEFs are activated by two different Gα subtypes and how the signal is integrated within each as well as between both pathways. Even though, this dictates the sensitivity and duration of the cellular response to GPCR activation. Such limited information on kinetics and sensitivity of the different steps in the signaling cascade is a common phenomenon in the research on G protein effector interactions (4.3.1.2). Thus we successfully established FRET assays for both interactions, $G\alpha_{13}$ with LARG and $G\alpha_q$ with p63RhoGEF, and resolved formation and dissociation of these complexes with high temporal and spatial resolution in the present work. Key findings were prolonged interaction between LARG and $G\alpha_{13}$, which was accompanied by a higher sensitivity of the LARG $G\alpha_{13}$ interaction compared to $G\alpha_{13}$ activation. Contrastingly, the p63RhoGEF $G\alpha_q$ interaction closely resembled $G\alpha_q$ activation kinetics and sensitivity. This was also true for a trimeric complex of p63RhoGEF and $G\alpha_q$ together with RGS2, which dissociated fast due to accelerated $G\alpha_q$ inactivation by RGS2.

7.1 Activation of RH-RhoGEFs by $G\alpha_{13}$

In the first part of this study we were able to elucidate the dynamics of the interaction between a RH-RhoGEF and $G\alpha_{13}$ in intact, living cells for the first time. Interestingly, upon agonist wash-out the dissociation of LARG and $G\alpha_{13}$ is more than 20-fold delayed compared to $G\alpha_{13}$ inactivation (long effector binding in fig. 41). Such a prolonged effector binding influences the equilibrium of Gα-GDP and Gα-GTP towards Gα-GTP compared to the absence or short binding of an effector. This results in a left shift of the concentration response curve (fig. 41). Thus we think the prolonged interaction is the most likely reason for the observed almost 100-fold higher sensitivity towards Txa_2-R activation of the RH-RhoGEF G protein interaction compared to the G protein activation (II). Noteworthy, this new insights on the LARG $G\alpha_{13}$ interaction were acquired with carefully validated FRET assays (I).

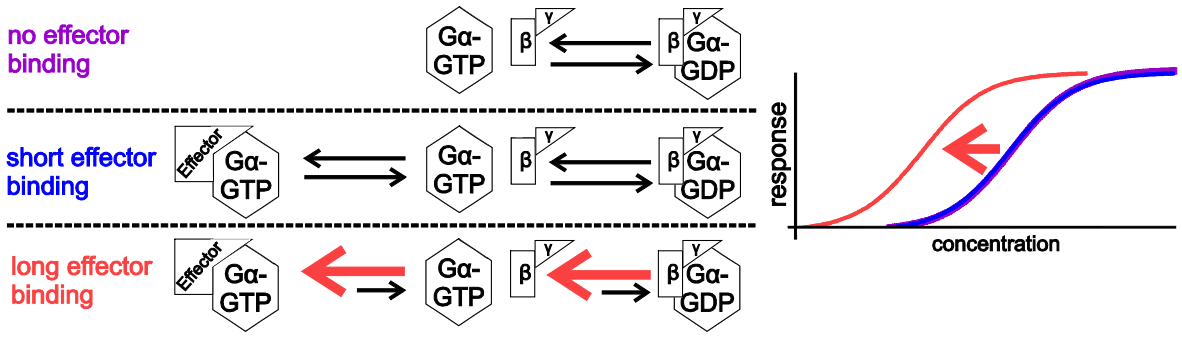

Fig. 41 Long effector binding results in left shift in concentration response curve
During activation Gα is balanced between three states (left to right): the GTP- and effector-bound, the GTP-bound and the GDP-bound state. If an effector exhibits short Gα bind (blue), the equilibrium between the GTP-bound and the GDP-bound state is not influenced and thus the concentration response curve is unchanged compared to no effector binding (purple). But if an effector exhibits prolonged Gα binding (red), the equilibrium is shifted towards the left and thus also the concentration response curve.

(I) The FRET between YFP-LARG and $G\alpha_{13}$-mTur2 increased rapidly and robust upon stimulation with small concentrations of U46619 (10nM, fig. 19A-C). This FRET increase reflects the interaction between LARG and $G\alpha_{13}$ with high temporal and spatial specificity and the used LARG constructs behave most likely like wild type in regard to $G\alpha_{13}$ interaction as shown in the following:

Upon agonist stimulation a robust increase in FRET was observed between $G\alpha_{13}$-mTur2 and YFP-LARG. Nevertheless no increase in FRET was observed between either YFP-LARG and membrane bound CFP in the presence of $G\alpha_{13}$ or between $G\alpha_{13}$-mTur2 and the $G\alpha_q$ effector Venus-p63RhoGEF (fig. 19C and D). These data point towards a FRET signal caused by interaction of $G\alpha_{13}$ and LARG rather than by close proximity at the plasma membrane, which would be described as bystander FRET.

LARG was found cytosolic in the absence of an agonist, which activates $G\alpha_{13}$ coupled receptors, and at the plasma membrane upon stimulation (Meyer et al., 2008). Also YFP-LARG as well as LARG-insYFP were found in the cytosol if transfected alone (fig. 26A, (Bodmann, diploma thesis)) or if YFP-LARG was transfected together with Txa_2-R, $G\alpha_{13}$-wt, Gβ and Gγ in the absence of agonist (fig. 18B). Thus before stimulation YFP-LARG and $G\alpha_{13}$-mTur2 are localized in two different regions

of the cell, cytosol and plasma membrane, respectively. This is of great importance as Carter and colleagues showed recently enhanced RhoGEF activity of PDZ-RhoGEF and p115-RhoGEF by their artificial translocation to the plasma membrane (Carter et al., 2014).

YFP-LARG translocated reliably to the plasma membrane upon stimulation with U46619 (fig. 18A and B). This translocation depended strictly on activation of a substantial quantity of $G\alpha_{13}$ proteins as no translocation was detected with endogenous $G\alpha_{13}$ alone (fig. 18C and D). In line with this no agonist dependent bystander FRET was observed between LARG-insYFP and membrane bound CFP in the absence of $G\alpha_{13}$ (fig. 20C). Whereas bystander FRET was shown between both proteins, if $G\alpha_{13}$ was cotransfected (fig. 20B). This is caused by LARG-insYFP translocation to the plasma membrane upon activation of cotransfected $G\alpha_{13}$ and thus LARG-insYFP and mCFP were close enough for FRET to occur. Of note, the FRET amplitude of the LARG-insYFP $G\alpha_{13}$-mTur2 FRET was larger than the one between LARG-insYFP and mCFP, suggesting a closer proximity between LARG-insYFP and $G\alpha_{13}$-mTur2 due to direct interaction. Thus we were able to monitor the LARG $G\alpha_{13}$ interaction with two LARG constructs. Since both constructs behaved similarly in terms of kinetic of the FRET signal with $G\alpha_{13}$ (fig. 24), the measured kinetics are most likely not changed by the localization of the fluorophore within LARG (see (II) for further validation of kinetics).

In order to characterize $G\alpha_{13}$-dependent signaling downstream of LARG we tried to detect RhoA activation and SRE.L transcription. In most experiments we could not reliably express wild type LARG over levels of endogenous expression, whether a Flag-tagged or one of two different wild type constructs were transfected (fig. 26). Consequently no stable $G\alpha_{13}$ dependent transcriptional activation downstream of LARG could be detected and we were not able to directly compare our fluorophore-labeled LARG versions to wild type LARG (fig. 28). Only in one SRE.L reporter gene assay wild type LARG was expressed over endogenous levels and in this assay a clear $G\alpha_{13}$ dependent transcription was induced by wild type LARG as well as YFP-LARG (fig. 29). Also the determination of active RhoA was impeded by the variable wild type LARG overexpression level (fig. 27). In addition this assay is prone to artefacts due to unequal amounts of the predator of RhoA affinity purification, RBD, between different conditions within one assay. To the author´s knowledge only a few studies were published so far using overexpressed wild type LARG, but considerably more studies on LARG knock-down (e.g. (Goulimari et al., 2008; Guilluy et al., 2010; Chiu et al., 2012; Lessey-Morillon et al., 2014)): Two studies used wild type LARG overexpression in SRE.L reporter gene assays, but they did not show overexpression by Western Blot (Aittaleb et al., 2009; Pfreimer et al., 2011). Further one study showed LARG overexpression in HEK293T cells, but in this case neither the LARG plasmid used nor the DNA amount was described (Mikelis et al., 2013). Since this low number of studies contrasts the total number of studies on LARG, overexpression of LARG might be challenging. In summary, we could characterize signaling downstream of LARG neither in general nor could compare wild type and YFP-labeled LARG in this regard. Thus it remains open whether YFP-LARG behaves exactly like wild type for the whole

signaling pathway from GPCR to RhoA and further downstream. But we are confident, that our LARG $G\alpha_{13}$ FRET assay reflects their interaction in living cells.

The activation of $G\alpha_{13}$ was elucidated and validated by A-L. Krett (unpublished data). Also we found a robust increase in FRET between $G\alpha_{13}$-YFP and Gβ-Cer (fig. 21A). Most data on trimeric G proteins suggested the dissociation of Gα and Gβγ upon stimulation, but different approaches showed a rearrangement for $G\alpha_i$ rather than dissociation (4.3.1.1, (Bünemann et al., 2003; Frank et al., 2005; Digby et al., 2006; Galés et al., 2006)). The same seem to be the case for $G\alpha_{13}$, as the FRET amplitude increased upon activation of $G\alpha_{13}$ by U46619. In line with the rearrangement of the trimeric G protein, the unstimulated G protein already showed basal FRET, as elucidated by donor recovery after acceptor photobleaching (fig. 22).

(II) Notably, the activation of $G\alpha_{13}$ was quickly and completely reversible upon agonist wash-out ($t_{1/2}$ 17.50s). This contrasted to the slow dissociation of LARG and $G\alpha_{13}$ upon agonist wash-out (fig. 22B). Nevertheless the fast inactivation measured for $G\alpha_{13}$ was in line with the inactivation kinetics measured for other G proteins ($t_{1/2}$ $G\alpha_i$: 30s (Bünemann et al., 2003), $G\alpha_q$: 48s (Wolters et al., under revision)). The slow dissociation of $G\alpha_{13}$ and LARG was validated by three approaches:

The slow dissociation between LARG and $G\alpha_{13}$ was observed in two, individual FRET assays, which used LARG constructs with YFP inserted in different sites (fig. 24A and B). Therefore if the YFP-tag would increase affinity of LARG to $G\alpha_{13}$, this effect would have to be independent of the place of insertion. This is not likely, because for example the fluorophore-tag on p63RhoGEF did not lead to a prolonged interaction with $G\alpha_q$, as discussed in 7.2.

Additionally, the slow dissociation of LARG and $G\alpha_{13}$ was mirrored by slow redistribution of LARG into the cytosol upon agonist wash-out. This was monitored by translocation experiments with wild type and mTur2-labeled $G\alpha_{13}$ (fig. 24C). This excludes an artificial change in dissociation kinetic by the mTur2 insertion into $G\alpha_{13}$. Noteworthy, p115RhoGEF redistributed more quickly into the cytosol upon inactivation of $G\alpha_{13}$ with the PAR-1 antagonist SCH 79797 (Meyer et al., 2008).

Even though the dissociation of LARG and $G\alpha_{13}$ is slow, this process is still reversible. As indicated by a second FRET increase and translocation upon stimulation with agonist after wash-out for ten minutes (fig. 24). Additionally the second translocation was not significantly different from the first one. Further the $G\alpha_{12}$ protein family is activated by a wide variety of agonists, which are for example present in cell culture medium. Therefore most likely $G\alpha_{13}$ had already been activated during cell culture in preparation of the conducted experiments. Consequently irreversible interaction of $G\alpha_{13}$ and LARG would have led to constitutive localization of LARG to the plasma membrane, which we could not detect (fig. 18A, and 24C).

Hence, $G\alpha_{13}$ and LARG dissociate, but much slower than $G\alpha_{13}$ inactivates. Such a kinetic difference in G protein inactivation compared to effector G protein dissociation was not described before, except recent findings for $G\alpha_i$ and adenylyl cyclase V (Milde et al., 2013). In this study they could show a left shift in concentration response relationship of adenylyl cyclase V-$G\alpha_i$ interaction compared to $G\alpha_i$

activation. The authors suggested the prolonged interaction as reason for the sensitization of interaction (Milde et al., 2013). Previous to these experiments cAMP-dependent signaling had been proven more sensitive to agonist stimulation than G protein mediated processes (Li et al., 1994). Also RhoA, an effector of RhoGEF activation by $G\alpha_{13}$, was completely activated by small agonist concentrations (10nM U46619) in mice platelets (Moers et al., 2003). Whereas $G\alpha_{13}$ was activated with an EC_{50} of 600nM in human platelets (Offermanns et al., 1994). So the EC_{50} values for $G\alpha_{13}$ and RhoA activation differ in platelets and we showed slow dissociation of $G\alpha_{13}$ and LARG. Consequently, the interaction of $G\alpha_{13}$ and LARG was found more sensitive to U46619 than $G\alpha_{13}$ activation in a concentration response curve (fig. 23): The EC_{50} value for $G\alpha_{13}$ activation was almost 100-fold higher than for the $G\alpha_{13}$-mTur2 YFP-LARG interaction, as measured by FRET (32.55nM and 0.30nM, respectively). FRET between $G\alpha_{13}$-mTur2 and LARG-insYFP was even more sensible to agonist application, but this was maybe overestimated. Since the maximal FRET amplitude of the LARG-insYFP $G\alpha_{13}$-mTur2 FRET was smaller than for the YFP-LARG $G\alpha_{13}$-mTur2 FRET and thus the measurement error of amplitude evaluation was larger for submaximal responses. The small amplitude could be caused either by the distance of the fluorophores during LARG $G\alpha_{13}$ interaction or by low expression of LARG-insYFP compared to $G\alpha_{13}$-mTur2. Since we could only detect LARG-insYFP in the range of wild type LARG by means of Western Blot (fig. 26B), the latter problem could well have occurred. But we could neither exclude the first because no LARG $G\alpha_{13}$ crystal structure is available, which would allow for an educated guess on the distance of the fluorophores within the complex. In future one could further validate the shift in concentration response relationship by use of the FlAsH (fluorescein arsenical hairpin binder) -tag technology (Hoffmann et al., 2005). This tag encodes for six amino acids binding specifically the small fluorescent probe FlAsH, which can be used in a FRET pair with CFP. Thus the findings with YFP-LARG/ LARG-insYFP and $G\alpha_{13}$-mTur2 could be confirmed by FRET between FlAsH-LARG and $G\alpha_{13}$-mTur2.

For the first time the interaction between $G\alpha_{13}$ and an effector was investigated in intact cells. Upon activation of Txa_2-R the RH-RhoGEF LARG translocates quickly to the plasma membrane, where it interacts with active $G\alpha_{13}$. This interaction is more sensitive to agonist stimulation than the G protein activation, which is most likely caused by the observed prolonged interaction of LARG and $G\alpha_{13}$ compared to $G\alpha_{13}$ inactivation. We were not yet able to determine whether the prolonged interaction is caused by delayed inactivation of $G\alpha_{13}$ by LARG coexpression or if LARG is still bound to $G\alpha_{13}$ after deactivation. A crystal structure and biochemical data by others may indirectly support the latter idea: $G\alpha_{13}$-GDP seems to be able to bind PDZ-RhoGEF, since a crystal structure of both in complex was resolved (Chen et al., 2008). Interestingly, $G\alpha_{13}$ adopted despite GDP binding an active-like conformation in this structure, and for PDZ-RhoGEF no GAP activity towards $G\alpha_{13}$ could be shown, which was shown for LARG (Kozasa et al., 1998; Wells et al., 2002; Suzuki et al., 2003). Thus the direct correlation of this crystal structure to the prolonged $G\alpha_{13}$ LARG interaction might be challenging. Yet the accelerated $G\alpha_{13}$ inactivation by LARG *in vitro* might support the interaction of

$G\alpha_{13}$-GDP and LARG by itself. Because if the $G\alpha_{13}$ LARG interaction is strictly limited by $G\alpha_{13}$ inactivation and LARG exhibits GAP activity towards $G\alpha_{13}$ also in living cells, we should have seen the opposite of what we saw. Precisely, the LARG $G\alpha_{13}$ dissociation should have occurred faster than the $G\alpha_{13}$ inactivation in the absence of LARG. In future the influence of LARG on $G\alpha_{13}$ activation could be tested in our $G\alpha_{13}$ $G\beta\gamma$ FRET. We were not able to reliably detect wild type LARG over endogenous levels in HEK293T cells by means of Western Blot (fig. 26 upper panel and discussed above). Thus it will be hard to control for a feasible proportion of wild type LARG transfected together with the $G\alpha_{13}$ $G\beta\gamma$ FRET pair. Therefore a LARG construct labeled with RFP might be used to control for high LARG expression in the measured cells.

Interestingly, RhoA-GTP binds directly to the PH domains of Lbc-RhoGEFs and accelerates the RhoGEF activity (Medina et al., 2013). Therefore we wondered if a LARG mutant deficient in Rho-GTP binding (F1098A and I1100E) shows an increase in FRET upon stimulation with a small agonist concentration (5nM U46619) and if the interaction with $G\alpha_{13}$ is prolonged. Since the FRET response appeared similar to wild type LARG in terms of amplitude and response, either RhoA-GTP binding is not involved in the prolonged LARG $G\alpha_{13}$ interaction or the mutant is not RhoA-GTP binding deficient in living cells (fig. 25). Also mDia1 interaction with the C-terminus of LARG was discussed as positive feedback loop (Goulimari et al., 2008). So maybe it would be worthwhile to study the influence of mDia1 on the LARG $G\alpha_{13}$ interaction. Nevertheless until now the mechanistic reason for prolonged interaction of $G\alpha_{13}$ and LARG remains elusive and should be studied in detail next, e.g. with the $G\alpha_{13}$ $G\beta\gamma$ FRET assay.

7.2 Dynamics of the $G\alpha_q$ p63RhoGEF RGS2 complex

GPCRs can activate RhoA not only through $G\alpha_{13}$ and RH-RhoGEFs, but in addition through $G\alpha_q$ and p63RhoGEF. Many GPCRs couple to both $G\alpha_q$ and $G\alpha_{13}$ at the same time and thus we were also interested in the RhoGEF activation downstream of $G\alpha_q$ (Riobo and Manning, 2005). Previous to this study, biochemical data pointed towards an influence of RGS2 on $G\alpha_q$ and p63RhoGEF, thus we investigated the putative p63RhoGEF $G\alpha_q$ RGS2 complex in detail (Shankaranarayanan et al., 2008; Bodmann et al., 2014). The work resolved (I) the dynamics of the activation dependent interaction of $G\alpha_q$ and p63RhoGEF and (II) the impact of RGS2 on this complex in single living cells. We found the interaction of a portion of $G\alpha_q$ p63RhoGEF complexes with RGS2. In these trimeric complexes RGS2 accelerates the dissociation and partially inhibits signaling downstream of p63RhoGEF.

(I) We developed a FRET assay between the plasma membrane-bound proteins $G\alpha_q$-CFP and Venus-p63RhoGEF (fig. 31A). This FRET assay monitors the activity dependent interaction between $G\alpha_q$ and p63RhoGEF (Shankaranarayanan et al., 2010). The activation of $G\alpha_q$ coupled receptors resulted in a rapid and robust increase in FRET, which was fully reversible upon agonist wash-out (fig. 31A-D). The spatial specificity of this FRET approach was verified by three means: First, upon stimulation with agonist an increase in FRET was only observed between $G\alpha_q$-CFP and V-p63RhoGEF, but neither between

Venus-p63RhoGEF and CFP-labeled $G\alpha_i$ nor between $G\alpha_q$-CFP and GIRK4-YFP (fig. 31D and F). Second, DAG activation downstream of PLCβ was abolished by p63RhoGEF cotransfection (fig. 33C). This was expected, since both proteins were described to bind to the canonical effector binding site at $G\alpha_q$ (2.3.1.1, (Lutz et al., 2007; Waldo et al., 2010)). The affinity of p63RhoGEF towards this binding site seems to be higher than PLCβ3´s affinity, as PLCβ3 cotransfection did not alter the $G\alpha_q$ p63RhoGEF interaction as investigated by FRET (fig. 33D). Third, the FRET amplitude and rate of responding cells was reduced by two mutations in p63RhoGEF (Bodmann, diploma thesis). These mutations lie within the $G\alpha_q$ binding PH domain of p63RhoGEF and mutation of either of them abolished interaction of $G\alpha_q$ and a truncated p63RhoGEF variant (amino acid 149-502) *in vitro* (Lutz et al., 2007; Rojas et al., 2007). Also downstream signaling was reduced, as we observed significantly reduced SRE.L activation in the presence of these mutations (fig. 32). These data validate the p63RhoGEF $G\alpha_q$ FRET assay as tool to detect specifically and affinity-dependent the interaction of p63RhoGEF and $G\alpha_q$ in living cells.
Additionally, the p63RhoGEF activation was closely linked to receptor activation: *In vitro* only active $G\alpha_q$ interacted with p63RhoGEF (Lutz et al., 2005, 2007). In line with this we could not detect donor recovery after acceptor photo bleaching for the $G\alpha_q$ p63RhoGEF FRET pair in the absence of agonist (Bodmann et al., 2014). Further the fast dissociation kinetic of $G\alpha_q$ and p63RhoGEF closely resembled the $G\alpha_q$ inactivation, as measured by $G\alpha_q$ Gβγ FRET (fig. 31C and 35). The same was true for the PLCβ3 $G\alpha_q$ dissociation, even though the dissociation and the $G\alpha_q$ inactivation were accelerated by PLCβ3´s intrinsic GAP activity towards $G\alpha_q$ (fig. 33A and (Pollinger, 2012)). For p63RhoGEF this shows again the low affinity towards inactive $G\alpha_q$ and fits to the observation of equal EC_{50} values of $G\alpha_q$ activation and $G\alpha_q$´s interaction with p63RhoGEF (fig. 36). Importantly, the $G\alpha_q$ activation cycle is not altered by cotransfection of p63RhoGEF (fig. 35). Thus the $G\alpha_q$ p63RhoGEF FRET assay reflects the real p63RhoGEF $G\alpha_q$ interaction in living cells, since the same amounts of p63RhoGEF were used for both assays.

(II) Previously RGS2 was shown to reduce p63RhoGEF´s affinity to $G\alpha_q$ *in vitro* and to decrease SRE.L activation downstream of p63RhoGEF activation by M_3-R (Lutz et al., 2007; Shankaranarayanan et al., 2010). Also we found reduced RhoA activation and SRE.L transcription downstream of p63RhoGEF in response to RGS2 expression(fig. 40, (Bodmann et al., 2014)). These studies were conducted with our fluorophore labeled constructs, which additionally validates their functionality in respect to up- and downstream signaling. Thus RGS2´s GTPase activity towards $G\alpha_q$ reduces p63RhoGEF signaling. Most likely RGS2 conducts its negative regulatory function in a trimeric complex of RGS2 $G\alpha_q$ p63RhoGEF, as we could show such a complex with high steric and temporal resolution: (A) $G\alpha_q$ inactivated faster in the presence of RGS2, due to RGS2´s GTPase activity (fig. 35). This was also seen if p63RhoGEF was cotransfected in addition. Consequently, RGS2 accelerated also the dissociation of p63RhoGEF and $G\alpha_q$ (fig. 34). Noteworthy, the accelerated inactivation and dissociation did not result in changes in the EC_{50} values of $G\alpha_q$ activation or its interaction with p63RhoGEF (fig. 36). (B) The interaction of RGS2 and $G\alpha_q$ occurred fast upon

stimulation with agonist and was fully reversible upon agonist wash-out (fig. 37). This interaction is not affected by p63RhoGEF, as neither the dissociation kinetic nor the amplitude was significantly changed. Therefore, we conclude that p63RhoGEF does not, or only slightly, changes orientation of RGS2 towards Gα, since this would most probably result in a change in FRET amplitude. (C) In addition to interaction of either RGS2 or p63RhoGEF with $G\alpha_q$, also the close proximity of RGS2 and p63RhoGEF could be shown by means of FRET (fig. 38). Upon stimulation of H_1-R with agonist the trimeric complex was formed, which resulted in a small, robust and rapid increase in FRET between RGS2-YFP and p63RhoGEF-CFP. This FRET change was fast reversible upon agonist wash-out and dependent on the interaction of p63RhoGEF and $G\alpha_q$. As a $G\alpha_q$ binding deficient p63RhoGEF mutant did not show FRET with RGS2 (fig. 38D). The small amplitude of the FRET change is probably caused by the big distance between the two fluorophores in the trimeric complex.

The formation of a trimeric p63RhoGEF $G\alpha_q$ RGS2 complex is in contrast to the inhibition of PLCβ3´s $G\alpha_q$ binding by RGS2: PLCβ3 and RGS2 bind to an overlapping binding site at $G\alpha_q$ as visible in crystal structures of both proteins with $G\alpha_q$ (fig. 8, (Waldo et al., 2010; Nance et al., 2013)). This overlap excludes their simultaneous binding to $G\alpha_q$. Consequently RGS2 abolished interaction of $G\alpha_q$ and PLCβ3 and DAG production as determined by FRET (fig. 33A and B).

Within a living cell probably two populations of $G\alpha_q$ p63RhoGEF complexes exist. The one includes RGS2 and the other does not. This cannot be observed by one FRET assay as FRET monitors the overall populations of complexes in one cell instead of single complexes. Nevertheless the two populations are visible if kinetics are compared for all four FRET assays, which monitor the members of the trimeric complex with all three complex members cotransfected (fig. 39): FRET assays, which use RGS2 as FRET partner, monitor exclusively RGS2 containing complexes. Whereas the other two FRET assays monitor complexes with and without RGS2. In the second condition the observed kinetics result from the mean of fast and slow $G\alpha_q$ inactivation, which are due to presence and absence of RGS2 in the individual complexes within one measured cell. Consequently the FRET assays with RGS2-YFP show faster kinetics than the other FRET assays.

For the first time we were able to analyze the p63RhoGEF $G\alpha_q$ interaction with the p63RhoGEF $G\alpha_q$ FRET assay in intact, living cells. In the meantime Goedhardt and colleagues also developed a similar FRET assay (Goedhart et al., 2013). They did not wash-out the agonist but used an inverse agonist instead. With their study they focused on the localization of p63RhoGEF due to palmitoylation. Whereas we elucidated the spatial as well as temporal behavior of this complex: The p63RhoGEF $G\alpha_q$ interaction strictly depends on $G\alpha_q$ activation and is therefore terminated by $G\alpha_q$ inactivation. If RGS2 is expressed, the signaling downstream of this complex is diminished. This negative regulation does not occur through competition of RGS2 and p63RhoGEF for the same binding site, as RGS2 and p63RhoGEF were found in close proximity during $G\alpha_q$ activation. But rather through accelerated inactivation of $G\alpha_q$ by RGS2 in a trimeric complex with p63RhoGEF.

7.3 Differences and similarities in RhoGEF activation downstream of $G\alpha_q$ and $G\alpha_{13}$ and their physiological implications

Many receptors couple to $G\alpha_{q/11}$ and $G\alpha_{12/13}$ as reviewed in detail elsewhere (Riobo and Manning, 2005). Thus p63RhoGEF downstream of $G\alpha_q$ as well as RH-RhoGEFs downstream of $G\alpha_{12/13}$ may be activated by the same GPCR. LARG and p63RhoGEF are involved in many physiological and pathophysiological pathways. LARG was found for example to repress synaptic plasticity, to be overexpressed in patients suffering from the pre-leukemic Shwachman-Diamon syndrome and seemed to be a central player during pressure-overload induced hypertrophy (Rujkijyanont et al., 2007; Takefuji et al., 2013; Kempf et al., 2014). For p63RhoGEF involvement in chemotactic migration of breast carcinoma cells was found and it was described as the target of a bacterial toxin, which can cause atrophic rhinitis (Hayashi et al., 2013; Siegert et al., 2013). Both RhoGEFs and also the other RH-RhoGEFs are involved in blood pressure regulation (see 2.7). Therefore contraction of vascular smooth muscle cells was used as a model for their cross-talk in the following. The present work found the p63RhoGEF $G\alpha_q$ interaction and therefore most likely activation of p63RhoGEF completely dependent on $G\alpha_q$ activation. This included the duration of p63RhoGEF activation as well as the EC_{50} of the $G\alpha_q$ p63RhoGEF interaction, which is similar to the EC_{50} of $G\alpha_q$ activation. In contrast to this the LARG $G\alpha_{13}$ interaction is almost 100-fold more sensitive than the $G\alpha_{13}$ activation and also the interaction of LARG and $G\alpha_{13}$ is substantially prolonged upon agonist wash-out compared to $G\alpha_{13}$ inactivation. These studies were done with two different receptors and the H_1-R is not of special importance for regulation of vascular tone. Therefore, a study on both signaling pathways downstream of a receptor coupling to both, $G\alpha_q$ and $G\alpha_{12/13}$, would be interesting, for example the angiotensin 1 receptor. This receptor was implicated in vascular tone regulation by p63RhoGEF as well as RH-RhoGEFs (Guilluy et al., 2010; Calò et al., 2014). With such a study one would get an idea about the difference in agonist sensitivity and whether LARG activation leads to prolonged signaling compared to p63RhoGEF activation. This would be of special interest, since both pathways are regulated to different degrees:

p63RhoGEF is the primarily $G\alpha_q$-activated RhoGEF in VSMCs, as such a function has not been described for Trio or Kalirin yet (Schmidt and Debant, 2014). Further the activation of p63RhoGEF is tightly, negatively regulated by RGS2, as elucidated in detail by the present study. $G\alpha_q$ and p63RhoGEF interaction leads most probably to RhoA activation only if RGS2 is not part of a trimeric complex and this is maybe dependent on RGS2 expression level (see 7.2). This would fit to the findings in hypertensive patients: RGS2 expression is downregulated in hypertensive patients and SNPs, which negatively influence RGS2 expression, are associated with hypertension (Calò et al., 2004; Riddle et al., 2006; Semplicini et al., 2006; Bodenstein et al., 2007). Thus the expression level of RGS2 seems to be of critical relevance for RhoA activation downstream of $G\alpha_q$ and p63RhoGEF.

In contrast, redundancy was shown for the RH-RhoGEFs LARG and PDZ-RhoGEF in terms of Ca^{2+} sensitization in VSMCs (Artamonov et al., 2013). Additionally, RGS2 will not affect $G\alpha_{13}$ signaling directly, as it is a GAP specific for $G\alpha_q$ and probably to a smaller extent $G\alpha_i$ (Heximer et al., 1999). For LARG and the other RH-RhoGEFs further regulatory mechanisms were described, but their impact on vascular tone has not been studied yet.

Besides their relevance towards a better understanding of signaling upstream of RhoA, this data is also important for the general understanding of G protein effector relationships. Because many G protein effectors have been described, but the kinetics of their interaction with and activation by G proteins has barely been studied. Of note, such direct correlations of G protein inactivation to G protein effector interactions were challenging in regard to study design for a long time (4.3.1.2). As determination of kinetics by biochemical assays might be distorted by experimental parameters, which can differ substantially from intracellular conditions. For example in the first *in vitro* experiments inactivation of $G\alpha_t$ and its effector PDE was considerably slow, but upon increase in protein concentration and temperature towards more physiological levels, also inactivation kinetics were determined in the physiological range (Arshavsky V. Yu. et al., 1989). In this regard G protein effectors, which are ion channels, were easier to address as their activation and inactivation can be monitored by patch-clamp in living cells. For example the activity of GIRK channels upon stimulation was measured by this method and resembled closely $G\alpha_i$ activation as determined by FRET later (Dascal, 1997; Bünemann et al., 2003). Also the kinetics of $G\alpha_q$ interaction with its effectors GRK2 and PLCβ3 resemble strictly $G\alpha_q$ activation as measured by means of FRET (Wolters et al., under revision and (Pollinger, 2012)). Further we could show the same for the p63RhoGEF $G\alpha_q$ interaction. But the G protein effector interactions do not necessarily have to resemble G protein action as prolonged interaction was shown for adenylyl cyclase V with $G\alpha_i$ before (Milde et al., 2013). Additionally, the LARG $G\alpha_{13}$ interaction seems to be an example of prolonged interaction and maybe other G protein effector pairs share this phenotype. Remarkably, in both cases of prolonged interaction, a shift in concentration response relationship was found. Hence, this new described phenotype might influence sensitivity of other G protein effector interactions as well. In the future kinetic and sensitivity of other G protein effector pairs should be studied in order to reveal the prevalence and physiological relevance of prolonged G protein effector interactions. Furthermore, data would be desirable, which clarify the mechanism of prolonged interaction.

In summary, LARG either slows down $G\alpha_{13}$ inactivation or stays in complex with inactive $G\alpha_{13}$. However, this prolonged interaction might result in higher sensitivity of the LARG $G\alpha_{13}$ interaction. Whether or not this phenotype is a common mode of G protein effector interaction has to be validated with other G protein effector pairs in the future. In vascular smooth muscle cells LARG might induce prolonged activation of downstream signaling in response to small changes in agonist due to this phenotype. Whereas p63RhoGEF may ensure constant basal tone by quick and short responses to major changes in physiological stimuli and this is further fine-tuned through the highly regulated RGS2. Of course this hypothesis has to be tested in VSMCs in the future.

References

Abdulaev, N.G., Ngo, T., Ramon, E., Brabazon, D.M., Marino, J.P., and Ridge, K.D. (2006). The receptor-bound "empty pocket" state of the heterotrimeric G-protein alpha-subunit is conformationally dynamic. Biochemistry *45*: 12986–97.

Adams, L.D., Geary, R.L., Li, J., Rossini, A., and Schwartz, S.M. (2006). Expression profiling identifies smooth muscle cell diversity within human intima and plaque fibrous cap: loss of RGS5 distinguishes the cap. Arterioscler. Thromb. Vasc. Biol. *26*: 319–25.

Adamson, P., Paterson, H.F., and Hall, A. (1992). Intracellular localization of the P21rho proteins. J. Cell Biol. *119*: 617–27.

Adini, I., Rabinovitz, I., Sun, J.F., Prendergast, G.C., and Benjamin, L.E. (2003). RhoB controls Akt trafficking and stage-specific survival of endothelial cells during vascular development. Genes Dev. *17*: 2721–32.

Adjobo-Hermans, M.J.W., Crosby, K.C., Putyrski, M., Bhageloe, A., Weeren, L. van, Schultz, C., et al. (2013). PLCβ isoforms differ in their subcellular location and their CT-domain dependent interaction with Gαq. Cell. Signal. *25*: 255–63.

Aghazadeh, B., Lowry, W.E., Huang, X.Y., and Rosen, M.K. (2000). Structural basis for relief of autoinhibition of the Dbl homology domain of proto-oncogene Vav by tyrosine phosphorylation. Cell *102*: 625–33.

Aghazadeh, B., Zhu, K., Kubiseski, T.J., Liu, G.A., Pawson, T., Zheng, Y., et al. (1998). Structure and mutagenesis of the Dbl homology domain. Nat. Struct. Biol. *5*: 1098–107.

Aittaleb, M., Boguth, C.A., and Tesmer, J.J.G. (2010). Structure and Function of Heterotrimeric G Protein-Regulated Rho Guanine Nucleotide Exchange Factors. Mol. Pharmacol. *77*: 111–25.

Aittaleb, M., Gao, G., Evelyn, C.R., Neubig, R.R., and Tesmer, J.J.G. (2009). A conserved hydrophobic surface of the LARG pleckstrin homology domain is critical for RhoA activation in cells. Cell. Signal. *21*: 1569–78.

Aittaleb, M., Nishimura, A., Linder, M.E., and Tesmer, J.J.G. (2011). Plasma membrane association of p63RhoGEF is mediated by palmitoylation and is required for basal activity in cells. J. Biol. Chem. 1–18.

Alcaraz, C., Diego, M. de, Pastor, M.J., and Escribano, J.M. (1990). Comparison of a radioimmunoprecipitation assay to immunoblotting and ELISA for detection of antibody to African swine fever virus. J. Vet. Diagn. Invest. *2*: 191–6.

Amano, M., Ito, M., Kimura, K., Fukata, Y., Chihara, K., Nakano, T., et al. (1996). Phosphorylation and activation of myosin by Rho-associated kinase (Rho-kinase). J. Biol. Chem. *271*: 20246–9.

Anger, T., Zhang, W., and Mende, U. (2004). Differential contribution of GTPase activation and effector antagonism to the inhibitory effect of RGS proteins on Gq-mediated signaling in vivo. J. Biol. Chem. *279*: 3906–15.

Arshavsky V. Yu., Antoch, M.P., Lukjanov, K.A., and Philippov, P.P. (1989). Transducin GTPase provides for rapid quenching of the cGMP cascade in rod outer segments. FEBS Lett. *250*: 353–6.

Artamonov, M. V., Momotani, K., Stevenson, A., Trentham, D.R., Derewenda, U., Derewenda, Z.S., et al. (2013). Agonist-induced Ca2+ Sensitization in Smooth Muscle: REDUNDANCY OF RHO GUANINE NUCLEOTIDE EXCHANGE FACTORS (RhoGEFs) AND RESPONSE KINETICS, A CAGED COMPOUND STUDY. J. Biol. Chem. *288*: 34030–40.

Bakker, R.A., Wieland, K., Timmerman, H., and Leurs, R. (2000). Constitutive activity of the histamine H(1) receptor reveals inverse agonism of histamine H(1) receptor antagonists. Eur. J. Pharmacol. *387*: R5–7.

Balakumar, P., and Jagadeesh, G. (2010). Multifarious molecular signaling cascades of cardiac hypertrophy: can the muddy waters be cleared? Pharmacol. Res. *62*: 365–83.

Balakumar, P., and Jagadeesh, G. (2014). A century old renin-angiotensin system still grows with endless possibilities: AT1 receptor signaling cascades in cardiovascular physiopathology. Cell. Signal. *26*: 2147–60.

Baltoumas, F.A., Theodoropoulou, M.C., and Hamodrakas, S.J. (2013). Interactions of the α-subunits of heterotrimeric G-proteins with GPCRs, effectors and RGS proteins: a critical review and analysis of interacting surfaces, conformational shifts, structural diversity and electrostatic potentials. J. Struct. Biol. *182*: 209–18.

Banerjee, J., and Wedegaertner, P.B. (2004). Identification of a novel sequence in PDZ-RhoGEF that mediates interaction with the actin cytoskeleton. Mol. Biol. Cell *15*: 1760–75.

Bansal, G., Druey, K.M., and Xie, Z. (2007). R4 RGS proteins: regulation of G-protein signaling and beyond. Pharmacol. Ther. *116*: 473–95.

Barberan, S., McNair, K., Iqbal, K., Smith, N.C., Prendergast, G.C., Stone, T.W., et al. (2011). Altered apoptotic responses in neurons lacking RhoB GTPase. Eur. J. Neurosci. *34*: 1737–46.

Barnes, W.G., Reiter, E., Violin, J.D., Ren, X.-R., Milligan, G., and Lefkowitz, R.J. (2005). beta-Arrestin 1 and Galphaq/11 coordinately activate RhoA and stress fiber formation following receptor stimulation. J. Biol. Chem. *280*: 8041–50.

Barrett, K., Leptin, M., and Settleman, J. (1997). The Rho GTPase and a putative RhoGEF mediate a signaling pathway for the cell shape changes in Drosophila gastrulation. Cell *91*: 905–15.

Basile, J.R., Barac, A., Zhu, T., Guan, K., and Gutkind, J.S. (2004). Class IV semaphorins promote angiogenesis by stimulating Rho-initiated pathways through plexin-B. Cancer Res. *64*: 5212–24.

Beadling, C., Druey, K.M., Richter, G., Kehrl, J.H., and Smith, K.A. (1999). Regulators of G protein signaling exhibit distinct patterns of gene expression and target G protein specificity in human lymphocytes. J. Immunol. *162*: 2677–82.

Bellanger, J.-M., Estrach, S., Schmidt, S., Briançon-Marjollet, A., Zugasti, O., Fromont, S., et al. (2003). Different regulation of the Trio Dbl-Homology domains by their associated PH domains. Biol. Cell *95*: 625–34.

Ben-Chaim, Y., Chanda, B., Dascal, N., Bezanilla, F., Parnas, I., and Parnas, H. (2006). Movement of "gating charge" is coupled to ligand binding in a G-protein-coupled receptor. Nature *444*: 106–9.

Berman, D.M., Kozasa, T., and Gilman, A.G. (1996a). The GTPase-activating Protein RGS4 Stabilizes the Transition State for Nucleotide Hydrolysis. J. Biol. Chem. *271*: 27209–27212.

Berman, D.M., Wilkie, T.M., and Gilman, A.G. (1996b). GAIP and RGS4 are GTPase-activating proteins for the Gi subfamily of G protein alpha subunits. Cell *86*: 445–52.

Berney, C., and Danuser, G. (2003). FRET or no FRET: a quantitative comparison. Biophys. J. *84*: 3992–4010.

Bernstein, L.S., Ramineni, S., Hague, C., Cladman, W., Chidiac, P., Levey, A.I., et al. (2004). RGS2 binds directly and selectively to the M1 muscarinic acetylcholine receptor third intracellular loop to modulate Gq/11alpha signaling. J. Biol. Chem. *279*: 21248–56.

Berstein, G., Blank, J.L., Jhon, D.Y., Exton, J.H., Rhee, S.G., and Ross, E.M. (1992). Phospholipase C-beta 1 is a GTPase-activating protein for Gq/11, its physiologic regulator. Cell *70*: 411–8.

Bhattacharya, S., and Vaidehi, N. (2010). Computational mapping of the conformational transitions in agonist selective pathways of a G-protein coupled receptor. J. Am. Chem. Soc. *132*: 5205–14.

Bhattacharyya, R., and Wedegaertner, P.B. (2000). Galpha 13 requires palmitoylation for plasma membrane localization, Rho-dependent signaling, and promotion of p115-RhoGEF membrane binding. J. Biol. Chem. *275*: 14992–9.

Bianconi, E., Piovesan, A., Facchin, F., Beraudi, A., Casadei, R., Frabetti, F., et al. (2013). An estimation of the number of cells in the human body. Ann. Hum. Biol. *40*: 463–71.

Birnboim, H.C., and Doly, J. (1979). A rapid alkaline extraction procedure for screening recombinant plasmid DNA. Nucleic Acids Res. *7*: 1513.

Bodenstein, J., Sunahara, R.K., and Neubig, R.R. (2007). N-terminal residues control proteasomal degradation of RGS2, RGS4, and RGS5 in human embryonic kidney 293 cells. Mol. Pharmacol. *71*: 1040–50.

Bodmann, E.-L., Rinne, A., Brandt, D., Lutz, S., Wieland, T., Grosse, R., et al. (2014). Dynamics of Gαq-protein-p63RhoGEF interaction and its regulation by RGS2. Biochem. J. *458*: 131–40.

Bondar, A., and Lazar, J. (2014). Dissociated GαGTP and Gβγ protein subunits are the major activated form of heterotrimeric Gi/o proteins. J. Biol. Chem. *289*: 1271–81.

Booden, M.A., Siderovski, D.P., and Der, C.J. (2002). Leukemia-associated Rho guanine nucleotide exchange factor promotes G alpha q-coupled activation of RhoA. Mol. Cell. Biol. *22*: 4053–61.

Bos, J.L., Rehmann, H., and Wittinghofer, A. (2007). GEFs and GAPs: critical elements in the control of small G proteins. Cell *129*: 865–77.

Boussif, O., Lezoualc'h, F., Zanta, M. a, Mergny, M.D., Scherman, D., Demeneix, B., et al. (1995). A versatile vector for gene and oligonucleotide transfer into cells in culture and in vivo: polyethylenimine. Proc. Natl. Acad. Sci. U. S. A. *92*: 7297–301.

Braman, J., Papworth, C., and Greener, A. (1996). Site-directed mutagenesis using double-stranded plasmid DNA templates. Methods Mol. Biol. *57*: 31–44.

Brandt, D., Gimona, M., Hillmann, M., Haller, H., and Mischak, H. (2002). Protein kinase C induces actin reorganization via a Src- and Rho-dependent pathway. J. Biol. Chem. *277*: 20903–10.

Bravo-Nuevo, A., O'Donnell, R., Rosendahl, A., Chung, J.H., Benjamin, L.E., and Odaka, C. (2011). RhoB deficiency in thymic medullary epithelium leads to early thymic atrophy. Int. Immunol. *23*: 593–600.

Bünemann, M., Bücheler, M.M., Philipp, M., Lohse, M.J., and Hein, L. (2001). Activation and deactivation kinetics of alpha 2A- and alpha 2C-adrenergic receptor-activated G protein-activated inwardly rectifying K+ channel currents. J. Biol. Chem. *276*: 47512–7.

Bünemann, M., Frank, M., and Lohse, M.J. (2003). Gi protein activation in intact cells involves subunit rearrangement rather than dissociation. Proc. Natl. Acad. Sci. U. S. A. *100*: 16077–82.

Burridge, K., Wennerberg, K., Hill, C., and Carolina, N. (2004). Rho and Rac Take Center Stage Review. *116*: 167–79.

Bustelo, X.R., Sauzeau, V., and Berenjeno, I.M. (2007). GTP-binding proteins of the Rho/Rac family: regulation, effectors and functions in vivo. Bioessays *29*: 356–70.

Calebiro, D., Nikolaev, V.O., and Lohse, M.J. (2010). Imaging of persistent cAMP signaling by internalized G protein-coupled receptors. J. Mol. Endocrinol. *45*: 1–8.

Calò, L.A., Davis, P.A., Pagnin, E., Dal Maso, L., Maiolino, G., Seccia, T.M., et al. (2014). Increased level of p63RhoGEF and RhoA/Rho kinase activity in hypertensive patients. J. Hypertens. *32*: 331–8.

Calò, L.A., Davis, P.A., and Pessina, A.C. (2011). Does p63RhoGEF, a new key mediator of angiotensin II signalling, play a role in blood pressure regulation and cardiovascular remodelling in humans? J. Renin. Angiotensin. Aldosterone. Syst. *12*: 634–6.

Calò, L.A., Pagnin, E., Davis, P.A., Sartori, M., Ceolotto, G., Pessina, A.C., et al. (2004). Increased expression of regulator of G protein signaling-2 (RGS-2) in Bartter's/Gitelman's syndrome. A role in the control of vascular tone and implication for hypertension. J. Clin. Endocrinol. Metab. *89*: 4153–7.

Camps, M., Carozzi, A., Schnabel, P., Scheer, A., Parker, P.J., and Gierschik, P. (1992). Isozyme-selective stimulation of phospholipase C-beta 2 by G protein beta gamma-subunits. Nature *360*: 684–6.

Cappello, S., Böhringer, C.R.J., Bergami, M., Conzelmann, K.-K., Ghanem, A., Tomassy, G.S., et al. (2012). A radial glia-specific role of RhoA in double cortex formation. Neuron *73*: 911–24.

Cario-Toumaniantz, C., Ferland-McCollough, D., Chadeuf, G., Toumaniantz, G., Rodriguez, M., Galizzi, J.-P., et al. (2012). RhoA guanine exchange factor expression profile in arteries: evidence for a Rho kinase-dependent negative feedback in angiotensin II-dependent hypertension. Am. J. Physiol. Cell Physiol. *302*: C1394–404.

Carman, C. V., Parent, J.L., Day, P.W., Pronin, A.N., Sternweis, P.M., Wedegaertner, P.B., et al. (1999). Selective regulation of Galpha(q/11) by an RGS domain in the G protein-coupled receptor kinase, GRK2. J. Biol. Chem. *274*: 34483–92.

Carter, A.M., Gutowski, S., and Sternweis, P.C. (2014). Regulated Localization Is Sufficient for Hormonal Control of Regulator of G Protein Signaling Homology Rho Guanine Nucleotide Exchange Factors (RH-RhoGEFs). J. Biol. Chem. *289*: 19737–46.

Caruthers, M.H., Beaucage, S.L., Becker, C., Efcavitch, J.W., Fisher, E.F., Galluppi, G., et al. (1983). Deoxyoligonucleotide synthesis via the phosphoramidite method. Gene Amplif. Anal. *3*: 1–26.

Cavin, S., Maric, D., and Diviani, D. (2014). A-kinase anchoring protein-Lbc promotes pro-fibrotic signaling in cardiac fibroblasts. Biochim. Biophys. Acta *1843*: 335–45.

Chauhan, B.K., Lou, M., Zheng, Y., and Lang, R.A. (2011). Balanced Rac1 and RhoA activities regulate cell shape and drive invagination morphogenesis in epithelia. Proc. Natl. Acad. Sci. U. S. A. *108*: 18289–94.

Chen, Z., Guo, L., Hadas, J., Gutowski, S., Sprang, S.R., and Sternweis, P.C. (2012). Activation of p115-RhoGEF requires direct association of Gα13 and the Dbl homology domain. J. Biol. Chem. *287*: 25490–500.

Chen, Z., Singer, W.D., Danesh, S.M., Sternweis, P.C., and Sprang, S.R. (2008). Recognition of the activated states of Galpha13 by the rgRGS domain of PDZRhoGEF. Structure *16*: 1532–43.

Chen, Z., Singer, W.D., Sternweis, P.C., and Sprang, S.R. (2005). Structure of the p115RhoGEF rgRGS domain-Galpha13/i1 chimera complex suggests convergent evolution of a GTPase activator. Nat. Struct. Mol. Biol. *12*: 191–7.

Chen, Z., Singer, W.D., Wells, C.D., Sprang, S.R., and Sternweis, P.C. (2003). Mapping the Galpha13 binding interface of the rgRGS domain of p115RhoGEF. J. Biol. Chem. *278*: 9912–9.

Chhatriwala, M.K., Betts, L., Worthylake, D.K., and Sondek, J. (2007). The DH and PH domains of Trio coordinately engage Rho GTPases for their efficient activation. J. Mol. Biol. *368*: 1307–20.

Chikumi, H., Barac, A., Behbahani, B., Gao, Y., Teramoto, H., Zheng, Y., et al. (2004). Homo- and hetero-oligomerization of PDZ-RhoGEF, LARG and p115RhoGEF by their C-terminal region regulates their in vivo Rho GEF activity and transforming potential. Oncogene *23*: 233–40.

Chikumi, H., Fukuhara, S., and Gutkind, J.S. (2002a). Regulation of G protein-linked guanine nucleotide exchange factors for Rho, PDZ-RhoGEF, and LARG by tyrosine phosphorylation: evidence of a role for focal adhesion kinase. J. Biol. Chem. *277*: 12463–73.

Chikumi, H., Vázquez-Prado, J., Servitja, J.-M., Miyazaki, H., and Gutkind, J.S. (2002b). Potent activation of RhoA by Galpha q and Gq-coupled receptors. J. Biol. Chem. *277*: 27130–4.

Chiu, W.-C., Juang, J.-M., Chang, S.-N., Wu, C.-K., Tsai, C.-T., Tseng, C., et al. (2012). Differential baseline expression and angiotensin II-stimulation of leukemia-associated RhoGEF in vascular smooth muscle cells of spontaneously hypertensive rats. Int. J. Nanomedicine *7*: 5929–39.

Chow, C.R., Suzuki, N., Kawamura, T., Hamakubo, T., and Kozasa, T. (2013). Modification of p115RhoGEF Ser(330) regulates its RhoGEF activity. Cell. Signal. *25*: 2085–92.

Chung, C.T., Niemela, S.L., and Miller, R.H. (1989). One-step preparation of competent Escherichia coli: transformation and storage of bacterial cells in the same solution. Proc. Natl. Acad. Sci. U. S. A. *86*: 2172–5.

Chung, K.Y. (2013). Structural Aspects of GPCR-G Protein Coupling. Toxicol. Res. *29*: 149–55.

Chung, K.Y., Rasmussen, S.G.F., Liu, T., Li, S., DeVree, B.T., Chae, P.S., et al. (2011). Conformational changes in the G protein Gs induced by the β2 adrenergic receptor. Nature *477*: 611–5.

Cladman, W., and Chidiac, P. (2002). Characterization and comparison of RGS2 and RGS4 as GTPase-activating proteins for m2 muscarinic receptor-stimulated G(i). Mol. Pharmacol. *62*: 654–9.

Coleman, M.L., Sahai, E.A., Yeo, M., Bosch, M., Dewar, A., and Olson, M.F. (2001). Membrane blebbing during apoptosis results from caspase-mediated activation of ROCK I. Nat. Cell Biol. *3*: 339–45.

Cook, D.R., Rossman, K.L., and Der, C.J. (2014). Rho guanine nucleotide exchange factors: regulators of Rho GTPase activity in development and disease. Oncogene *33*: 4021–35.

Cunningham, M.L., Waldo, G.L., Hollinger, S., Hepler, J.R., and Harden, T.K. (2001). Protein kinase C phosphorylates RGS2 and modulates its capacity for negative regulation of Galpha 11 signaling. J. Biol. Chem. *276*: 5438–44.

Dascal, N. (1997). Signalling via the G protein-activated K+ channels. Cell. Signal. *9*: 551–73.

Davis, T.L., Bonacci, T.M., Sprang, S.R., and Smrcka, A. V. (2005). Structural and molecular characterization of a preferred protein interaction surface on G protein beta gamma subunits. Biochemistry *44*: 10593–604.

Day, P.W., Carman, C. V., Sterne-Marr, R., Benovic, J.L., and Wedegaertner, P.B. (2003). Differential interaction of GRK2 with members of the G alpha q family. Biochemistry *42*: 9176–84.

Degtyarev, M.Y., Spiegel, A.M., and Jones, T.L. (1994). Palmitoylation of a G protein alpha i subunit requires membrane localization not myristoylation. J. Biol. Chem. *269*: 30898–903.

Digby, G.J., Lober, R.M., Sethi, P.R., and Lambert, N.A. (2006). Some G protein heterotrimers physically dissociate in living cells. Proc. Natl. Acad. Sci. U. S. A. *103*: 17789–94.

Dohlman, H.G., Song, J., Apanovitch, D.M., DiBello, P.R., and Gillen, K.M. (1998). Regulation of G protein signalling in yeast. Semin. Cell Dev. Biol. *9*: 135–41.

Dorsch, S., Klotz, K., Engelhardt, S., Lohse, M.J., and Bünemann, M. (2009). Analysis of receptor oligomerization by FRAP microscopy. Nat. Methods *6*: 225–30.

Dror, R.O., Arlow, D.H., Maragakis, P., Mildorf, T.J., Pan, A.C., Xu, H., et al. (2011a). Activation mechanism of the β2-adrenergic receptor. Proc. Natl. Acad. Sci. U. S. A. *108*: 18684–9.

Dror, R.O., Pan, A.C., Arlow, D.H., Borhani, D.W., Maragakis, P., Shan, Y., et al. (2011b). Pathway and mechanism of drug binding to G-protein-coupled receptors. Proc. Natl. Acad. Sci. U. S. A. *108*: 13118–23.

Echeverría, V., Hinrichs, M. V., Torrejón, M., Ropero, S., Martinez, J., Toro, M.J., et al. (2000). Mutagenesis in the switch IV of the helical domain of the human Gsalpha reduces its GDP/GTP exchange rate. J. Cell. Biochem. *76*: 368–75.

Etienne-Manneville, S., and Hall, A. (2002). Rho GTPases in cell biology. Nature *420*: 629–35.

Fan, G., Jiang, Y.-P., Lu, Z., Martin, D.W., Kelly, D.J., Zuckerman, J.M., et al. (2005). A transgenic mouse model of heart failure using inducible Galpha q. J. Biol. Chem. *280*: 40337–46.

Ford, C.E., Skiba, N.P., Bae, H., Daaka, Y., Reuveny, E., Shekter, L.R., et al. (1998). Molecular basis for interactions of G protein betagamma subunits with effectors. Science *280*: 1271–4.

Förster, T. (1948). Zwischenmolekulare Energiewanderung und Fluoreszenz. Ann. Phys. *2*: 55–75.

Francis, S.A., Shen, X., Young, J.B., Kaul, P., and Lerner, D.J. (2006). Rho GEF Lsc is required for normal polarization, migration, and adhesion of formyl-peptide-stimulated neutrophils. Blood *107*: 1627–35.

Franco, M., Chardin, P., Chabre, M., and Paris, S. (1996). Myristoylation-facilitated binding of the G protein ARF1GDP to membrane phospholipids is required for its activation by a soluble nucleotide exchange factor. J. Biol. Chem. *271*: 1573–8.

Frank, M., Thümer, L., Lohse, M.J., and Bünemann, M. (2005). G Protein activation without subunit dissociation depends on a G{alpha}(i)-specific region. J. Biol. Chem. *280*: 24584–90.

Fredriksson, R., Lagerström, M.C., Lundin, L.-G., and Schiöth, H.B. (2003). The G-protein-coupled receptors in the human genome form five main families. Phylogenetic analysis, paralogon groups, and fingerprints. Mol. Pharmacol. *63*: 1256–72.

Fremont, O.T., and Chan, J.C.M. (2012). Understanding Bartter syndrome and Gitelman syndrome. World J. Pediatr. *8*: 25–30.

Freson, K., Stolarz, K., Aerts, R., Brand, E., Brand-Herrmann, S.-M., Kawecka-Jaszcz, K., et al. (2007). -391 C to G substitution in the regulator of G-protein signalling-2 promoter increases susceptibility to the metabolic syndrome in white European men: consistency between molecular and epidemiological studies. J. Hypertens. *25*: 117–25.

Fukuhara, S., Chikumi, H., and Gutkind, J.S. (2000). Leukemia-associated Rho guanine nucleotide exchange factor (LARG) links heterotrimeric G proteins of the G(12) family to Rho. FEBS Lett. *485*: 183–8.

Fukuhara, S., Chikumi, H., and Gutkind, J.S. (2001). RGS-containing RhoGEFs: the missing link between transforming G proteins and Rho? Oncogene *20*: 1661–8.

Fukuhara, S., Murga, C., Zohar, M., Igishi, T., and Gutkind, J.S. (1999). A novel PDZ domain containing guanine nucleotide exchange factor links heterotrimeric G proteins to Rho. J. Biol. Chem. *274*: 5868–79.

Galés, C., Durm, J.J.J. van, Schaak, S., Pontier, S., Percherancier, Y., Audet, M., et al. (2006). Probing the activation-promoted structural rearrangements in preassembled receptor-G protein complexes. Nat. Struct. Mol. Biol. *13*: 778–86.

Gao, J., Ma, R., Wang, W., Wang, N., Sasaki, R., Snyderman, D., et al. (2014). Automated NMR fragment based screening identified a novel interface blocker to the LARG/RhoA complex. PLoS One *9*: e88098.

García-Hoz, C., Sánchez-Fernández, G., Díaz-Meco, M.T., Moscat, J., Mayor, F., and Ribas, C. (2010). G alpha(q) acts as an adaptor protein in protein kinase C zeta (PKCzeta)-mediated ERK5 activation by G protein-coupled receptors (GPCR). J. Biol. Chem. *285*: 13480–9.

Garcia-Mata, R., Boulter, E., and Burridge, K. (2011). The "invisible hand": regulation of RHO GTPases by RHOGDIs. Nat. Rev. Mol. Cell Biol. *12*: 493–504.

Gasparo, M. de, Catt, K.J., Inagami, T., Wright, J.W., and Unger, T. (2000). International union of pharmacology. XXIII. The angiotensin II receptors. Pharmacol. Rev. *52*: 415–72.

Geary, R.L. (2002). Expression Profiling Identifies 147 Genes Contributing to a Unique Primate Neointimal Smooth Muscle Cell Phenotype. Arterioscler. Thromb. Vasc. Biol. *22*: 2010–6.

Gilman, A.G. (1987). G proteins: transducers of receptor-generated signals. Annu. Rev. Biochem. *56*: 615–49.

Girkontaite, I., Missy, K., Sakk, V., Harenberg, A., Tedford, K., Pötzel, T., et al. (2001). Lsc is required for marginal zone B cells, regulation of lymphocyte motility and immune responses. Nat. Immunol. *2*: 855–62.

Goedhart, J., Unen, J. van, Adjobo-Hermans, M.J.W., and Gadella, T.W.J. (2013). Signaling efficiency of Gαq through its effectors p63RhoGEF and GEFT depends on their subcellular location. Sci. Rep. *3*: 2284.

Goss, D.J., Parkhurst, L.J., Mehta, H.B., Woodley, C.L., and Wahba, A.J. (1984). Studies on the role of eukaryotic nucleotide exchange factor in polypeptide chain initiation. J. Biol. Chem. *259*: 7374–7.

Goulimari, P., Knieling, H., Engel, U., and Grosse, R. (2008). LARG and mDia1 link Galpha12/13 to cell polarity and microtubule dynamics. Mol. Biol. Cell *19*: 30–40.

Grabocka, E., and Wedegaertner, P.B. (2007). Disruption of oligomerization induces nucleocytoplasmic shuttling of leukemia-associated Rho Guanine-nucleotide exchange factor. Mol. Pharmacol. *72*: 993–1002.

Grant, S.L., Lassègue, B., Griendling, K.K., Ushio-Fukai, M., Lyons, P.R., and Alexander, R.W. (2000). Specific regulation of RGS2 messenger RNA by angiotensin II in cultured vascular smooth muscle cells. Mol. Pharmacol. *57*: 460–7.

Gu, J.L., Müller, S., Mancino, V., Offermanns, S., and Simon, M.I. (2002). Interaction of G alpha(12) with G alpha(13) and G alpha(q) signaling pathways. Proc. Natl. Acad. Sci. U. S. A. *99*: 9352–7.

Gu, S., Tirgari, S., and Heximer, S.P. (2008). The RGS2 gene product from a candidate hypertension allele shows decreased plasma membrane association and inhibition of Gq. Mol. Pharmacol. *73*: 1037–43.

Guilluy, C., Brégeon, J., Toumaniantz, G., Rolli-Derkinderen, M., Retailleau, K., Loufrani, L., et al. (2010). The Rho exchange factor Arhgef1 mediates the effects of angiotensin II on vascular tone and blood pressure. Nat. Med. *16*: 183–90.

Guilluy, C., Swaminathan, V., Garcia-Mata, R., Timothy O'Brien, E., Superfine, R., and Burridge, K. (2011). The Rho GEFs LARG and GEF-H1 regulate the mechanical response to force on integrins. Nat. Cell Biol. *13*: 724–9.

Hakem, A., Sanchez-Sweatman, O., You-Ten, A., Duncan, G., Wakeham, A., Khokha, R., et al. (2005). RhoC is dispensable for embryogenesis and tumor initiation but essential for metastasis. Genes Dev. *19*: 1974–9.

Hamazaki, Y., Kojima, H., Mano, H., Nagata, Y., Todokoro, K., Abe, T., et al. (1998). Tec is involved in G protein-coupled receptor- and integrin-mediated signalings in human blood platelets. Oncogene *16*: 2773–9.

Hamm, H.E. (1998). The many faces of G protein signaling. J. Biol. Chem. *273*: 669–72.

Hamm, H.E., Deretic, D., Arendt, A., Hargrave, P.A., Koenig, B., and Hofmann, K.P. (1988). Site of G protein binding to rhodopsin mapped with synthetic peptides from the alpha subunit. Science *241*: 832–5.

Han, J., Huang, N., Kim, D., and Kehrl, J.H. (2006). RGS1 and RGS13 mRNA silencing in a human B lymphoma line enhances responsiveness to chemoattractants and impairs desensitization. J. Leukoc. Biol. *79*: 1357–68.

Hao, J., Michalek, C., Zhang, W., Zhu, M., Xu, X., and Mende, U. (2006). Regulation of cardiomyocyte signaling by RGS proteins: differential selectivity towards G proteins and susceptibility to regulation. J. Mol. Cell. Cardiol. *41*: 51–61.

Hart, M.J., Jiang, X., Kozasa, T., Roscoe, W., Singer, W.D., Gilman, A.G., et al. (1998). Direct stimulation of the guanine nucleotide exchange activity of p115 RhoGEF by Galpha13. Science *280*: 2112–4.

Hayashi, A., Hiatari, R., Tsuji, T., Ohashi, K., and Mizuno, K. (2013). p63RhoGEF-mediated formation of a single polarized lamellipodium is required for chemotactic migration in breast carcinoma cells. FEBS Lett. *587*: 698–705.

Heasman, S.J., Carlin, L.M., Cox, S., Ng, T., and Ridley, A.J. (2010). Coordinated RhoA signaling at the leading edge and uropod is required for T cell transendothelial migration. J. Cell Biol. *190*: 553–63.

Heim, R., and Tsien, R.Y. (1996). Engineering green fluorescent protein for improved brightness, longer wavelengths and fluorescence resonance energy transfer. Curr. Biol. *6*: 178–82.

Hein, P., and Bünemann, M. (2009). Coupling mode of receptors and G proteins. Naunyn. Schmiedebergs. Arch. Pharmacol. *379*: 435–43.

Hein, P., Frank, M., Hoffmann, C., Lohse, M.J., and Bünemann, M. (2005). Dynamics of receptor/G protein coupling in living cells. EMBO J. *24*: 4106–14.

Hein, P., Rochais, F., Hoffmann, C., Dorsch, S., Nikolaev, V.O., Engelhardt, S., et al. (2006). Gs activation is time-limiting in initiating receptor-mediated signaling. J. Biol. Chem. *281*: 33345–51.

Hendriks-Balk, M.C., Peters, S.L.M., Michel, M.C., and Alewijnse, A.E. (2008). Regulation of G protein-coupled receptor signalling: focus on the cardiovascular system and regulator of G protein signalling proteins. Eur. J. Pharmacol. *585*: 278–91.

Hepler, J.R., Berman, D.M., Gilman, A.G., and Kozasa, T. (1997). RGS4 and GAIP are GTPase-activating proteins for Gq alpha and block activation of phospholipase C beta by gamma-thio-GTP-Gq alpha. Proc. Natl. Acad. Sci. U. S. A. *94*: 428–32.

Herzog, D., Loetscher, P., Hengel, J. van, Knüsel, S., Brakebusch, C., Taylor, V., et al. (2011). The small GTPase RhoA is required to maintain spinal cord neuroepithelium organization and the neural stem cell pool. J. Neurosci. *31*: 5120–30.

Heximer, S.P. (2013). A "new twist" on RGS protein selectivity. Structure *21*: 319–20.

Heximer, S.P., Knutsen, R.H., Sun, X., Kaltenbronn, K.M., Rhee, M., Peng, N., et al. (2003). Hypertension and prolonged vasoconstrictor signaling in RGS2-deficient mice. J. Clin. Invest. *111*: 445–52.

Heximer, S.P., Srinivasa, S.P., Bernstein, L.S., Bernard, J.L., Linder, M.E., Hepler, J.R., et al. (1999). G protein selectivity is a determinant of RGS2 function. J. Biol. Chem. *274*: 34253–9.

Hiley, E., McMullan, R., and Nurrish, S.J. (2006). The Galpha12-RGS RhoGEF-RhoA signalling pathway regulates neurotransmitter release in C. elegans. EMBO J. *25*: 5884–95.

Hilgers, R.H.P., Todd, J., and Webb, R.C. (2007). Increased PDZ-RhoGEF/RhoA/Rho kinase signaling in small mesenteric arteries of angiotensin II-induced hypertensive rats. J. Hypertens. *25*: 1687–97.

Hill, C.S., Wynne, J., and Treisman, R. (1995). The Rho family GTPases RhoA, Rac1, and CDC42Hs regulate transcriptional activation by SRF. Cell *81*: 1159–70.

Hiol, A., Davey, P.C., Osterhout, J.L., Waheed, A.A., Fischer, E.R., Chen, C.-K., et al. (2003). Palmitoylation regulates regulators of G-protein signaling (RGS) 16 function. I. Mutation of amino-terminal cysteine residues on RGS16 prevents its targeting to lipid rafts and palmitoylation of an internal cysteine residue. J. Biol. Chem. *278*: 19301–8.

Hirose, M., Ishizaki, T., Watanabe, N., Uehata, M., Kranenburg, O., Moolenaar, W.H., et al. (1998). Molecular dissection of the Rho-associated protein kinase (p160ROCK)-regulated neurite remodeling in neuroblastoma N1E-115 cells. J. Cell Biol. *141*: 1625–36.

Hoffmann, C., Gaietta, G., Bünemann, M., Adams, S.R., Oberdorff-Maass, S., Behr, B., et al. (2005). A FlAsH-based FRET approach to determine G protein-coupled receptor activation in living cells. Nat. Methods *2*: 171–6.

Hoffmann, C., Nuber, S., Zabel, U., Ziegler, N., Winkler, C., Hein, P., et al. (2012). Comparison of the activation kinetics of the M3 acetylcholine receptor and a constitutively active mutant receptor in living cells. Mol. Pharmacol. *82*: 236–45.

Hollinger, S., and Hepler, J.R. (2002). Cellular regulation of RGS proteins: modulators and integrators of G protein signaling. Pharmacol. Rev. *54*: 527–59.

Hubbard, K.B., and Hepler, J.R. (2006). Cell signalling diversity of the Gqalpha family of heterotrimeric G proteins. Cell. Signal. *18*: 135–50.

Hughes, T.E., Zhang, H., Logothetis, D.E., and Berlot, C.H. (2001). Visualization of a functional Galpha q-green fluorescent protein fusion in living cells. Association with the plasma membrane is disrupted by mutational activation and by elimination of palmitoylation sites, but not be activation mediated by receptors or . J. Biol. Chem. *276*: 4227–35.

Illenberger, D., Walliser, C., Nurnberg, B., Diaz Lorente, M., and Gierschik, P. (2003). Specificity and structural requirements of phospholipase C-beta stimulation by Rho GTPases versus G protein beta gamma dimers. J. Biol. Chem. *278*: 3006–14.

Irannejad, R., Tomshine, J.C., Tomshine, J.R., Chevalier, M., Mahoney, J.P., Steyaert, J., et al. (2013). Conformational biosensors reveal GPCR signalling from endosomes. Nature *495*: 1–8.

Itoh, K., Yoshioka, K., Akedo, H., Uehata, M., Ishizaki, T., and Narumiya, S. (1999). An essential part for Rho-associated kinase in the transcellular invasion of tumor cells. Nat. Med. *5*: 221–5.

Itoh, M., Nagatomo, K., Kubo, Y., and Saitoh, O. (2006). Alternative splicing of RGS8 gene changes the binding property to the M1 muscarinic receptor to confer receptor type-specific Gq regulation. J. Neurochem. *99*: 1505–16.

Jackson, B., Peyrollier, K., Pedersen, E., Basse, A., Karlsson, R., Wang, Z., et al. (2011). RhoA is dispensable for skin development, but crucial for contraction and directed migration of keratinocytes. Mol. Biol. Cell *22*: 593–605.

Jaffe, A.B., and Hall, A. (2005). Rho GTPases: biochemistry and biology. Annu. Rev. Cell Dev. Biol. *21*: 247–69.

Jaiswal, M., Gremer, L., Dvorsky, R., Haeusler, L.C., Cirstea, I.C., Uhlenbrock, K., et al. (2011). Mechanistic insights into specificity, activity, and regulatory elements of the regulator of G-protein signaling (RGS)-containing Rho-specific guanine nucleotide exchange factors (GEFs) p115, PDZ-RhoGEF (PRG), and leukemia-associated RhoGEF (LARG). J. Biol. Chem. *286*: 18202–12.

Jares-Erijman, E., and Jovin, T.M. (2003). FRET imaging. Nat. Biotechnol. *21*: 1387–95.

Jin, L., Ying, Z., Hilgers, R.H.P., Yin, J., Zhao, X., Imig, J.D., et al. (2006). Increased RhoA/Rho-kinase signaling mediates spontaneous tone in aorta from angiotensin II-induced hypertensive rats. J. Pharmacol. Exp. Ther. *318*: 288–95.

Jones, T.L.Z. (2004). Role of palmitoylation in RGS protein function. Methods Enzymol. *389*: 33–55.

Kach, J., Sethakorn, N., and Dulin, N.O. (2012). A finer tuning of G-protein signaling through regulated control of RGS proteins. Am. J. Physiol. Heart Circ. Physiol. *303*: H19–35.

Kahsai, A.W., Xiao, K., Rajagopal, S., Ahn, S., Shukla, A.K., Sun, J., et al. (2011). Multiple ligand-specific conformations of the β2-adrenergic receptor. Nat. Chem. Biol. *7*: 692–700.

Karlsson, R., Pedersen, E.D., Wang, Z., and Brakebusch, C. (2009). Rho GTPase function in tumorigenesis. Biochim. Biophys. Acta *1796*: 91–8.

Katayama, K., Leslie, J.R., Lang, R.A., Zheng, Y., and Yoshida, Y. (2012). Left-right locomotor circuitry depends on RhoA-driven organization of the neuroepithelium in the developing spinal cord. J. Neurosci. *32*: 10396–407.

Katayama, K., Melendez, J., Baumann, J.M., Leslie, J.R., Chauhan, B.K., Nemkul, N., et al. (2011). Loss of RhoA in neural progenitor cells causes the disruption of adherens junctions and hyperproliferation. Proc. Natl. Acad. Sci. U. S. A. *108*: 7607–12.

Katritch, V., Fenalti, G., Abola, E.E., Roth, B.L., Cherezov, V., and Stevens, R.C. (2014). Allosteric sodium in class A GPCR signaling. Trends Biochem. Sci. *39*: 233–44.

Kaziro, Y., Itoh, H., Kozasa, T., Nakafuku, M., and Satoh, T. (1991). Structure and function of signal-transducing GTP-binding proteins. Annu. Rev. Biochem. *60*: 349–400.

Kehrl, J.H., and Sinnarajah, S. (2002). RGS2: a multifunctional regulator of G-protein signaling. Int. J. Biochem. Cell Biol. *34*: 432–8.

Kelly, P., Casey, P.J., and Meigs, T.E. (2007). Biologic functions of the G12 subfamily of heterotrimeric g proteins: growth, migration, and metastasis. Biochemistry *46*: 6677–87.

Kelly, P., Moeller, B.J., Juneja, J., Booden, M.A., Der, C.J., Daaka, Y., et al. (2006a). The G12 family of heterotrimeric G proteins promotes breast cancer invasion and metastasis. Proc. Natl. Acad. Sci. U. S. A. *103*: 8173–8.

Kelly, P., Stemmle, L.N., Madden, J.F., Fields, T.A., Daaka, Y., and Casey, P.J. (2006b). A role for the G12 family of heterotrimeric G proteins in prostate cancer invasion. J. Biol. Chem. *281*: 26483–90.

Kempf, A., Tews, B., Arzt, M.E., Weinmann, O., Obermair, F.J., Pernet, V., et al. (2014). The sphingolipid receptor S1PR2 is a receptor for Nogo-a repressing synaptic plasticity. PLoS Biol. *12*: e1001763.

Khan, S.M., Sleno, R., Gora, S., Zylbergold, P., Laverdure, J.-P., Labbé, J.-C., et al. (2013). The expanding roles of Gβγ subunits in G protein-coupled receptor signaling and drug action. Pharmacol. Rev. *65*: 545–77.

Kimura, K., Ito, M., Amano, M., Chihara, K., Fukata, Y., Nakafuku, M., et al. (1996). Regulation of myosin phosphatase by Rho and Rho-associated kinase (Rho-kinase). Science *273*: 245–8.

Kishi, K., Sasaki, T., Kuroda, S., Itoh, T., and Takai, Y. (1993). Regulation of cytoplasmic division of Xenopus embryo by rho p21 and its inhibitory GDP/GTP exchange protein (rho GDI). J. Cell Biol. *120*: 1187–95.

Kitzing, T.M., Sahadevan, A.S., Brandt, D.T., Knieling, H., Hannemann, S., Fackler, O.T., et al. (2007). Positive feedback between Dia1, LARG, and RhoA regulates cell morphology and invasion. Genes Dev. *21*: 1478–83.

Klages, B., Brandt, U., Simon, M.I., Schultz, G., and Offermanns, S. (1999). Activation of G12/G13 results in shape change and Rho/Rho-kinase-mediated myosin light chain phosphorylation in mouse platelets. J. Cell Biol. *144*: 745–54.

Kobilka, B.K. (2013). The structural basis of G-protein-coupled receptor signaling (Nobel Lecture). Angew. Chem. Int. Ed. Engl. *52*: 6380–8.

Kobilka, B.K., and Deupi, X. (2007). Conformational complexity of G-protein-coupled receptors. Trends Pharmacol. Sci. *28*: 397–406.

Kohara, K., Tabara, Y., Nakura, J., Imai, Y., Ohkubo, T., Hata, A., et al. (2008). Identification of hypertension-susceptibility genes and pathways by a systemic multiple candidate gene approach: the millennium genome project for hypertension. Hypertens. Res. *31*: 203–12.

Kourlas, P.J., Strout, M.P., Becknell, B., Veronese, M.L., Croce, C.M., Theil, K.S., et al. (2000). Identification of a gene at 11q23 encoding a guanine nucleotide exchange factor: evidence for its fusion with MLL in acute myeloid leukemia. Proc. Natl. Acad. Sci. U. S. A. *97*: 2145–50.

Kozasa, T., and Gilman, A.G. (1995). Purification of recombinant G proteins from Sf9 cells by hexahistidine tagging of associated subunits. Characterization of alpha 12 and inhibition of adenylyl cyclase by alpha z. J. Biol. Chem. *270*: 1734–41.

Kozasa, T., and Gilman, A.G. (1996). Protein kinase C phosphorylates G12 alpha and inhibits its interaction with G beta gamma. J. Biol. Chem. *271*: 12562–7.

Kozasa, T., Hajicek, N., Chow, C.R., and Suzuki, N. (2011). Signalling mechanisms of RhoGTPase regulation by the heterotrimeric G proteins G12 and G13. J. Biochem. *150*: 357–69.

Kozasa, T., Jiang, X., Hart, M.J., Sternweis, P.M., Singer, W.D., Gilman, A.G., et al. (1998). p115 RhoGEF, a GTPase activating protein for Galpha12 and Galpha13. Science *280*: 2109–11.

Krasel, C., Bünemann, M., Lorenz, K., and Lohse, M.J. (2005). Beta-arrestin binding to the beta2-adrenergic receptor requires both receptor phosphorylation and receptor activation. J. Biol. Chem. *280*: 9528–35.

Kreutz, B., Yau, D.M., Nance, M.R., Tanabe, S., Tesmer, J.J.G., and Kozasa, T. (2006). A new approach to producing functional G alpha subunits yields the activated and deactivated structures of G alpha(12/13) proteins. Biochemistry *45*: 167–74.

Kristelly, R., Gao, G., and Tesmer, J.J.G. (2004). Structural determinants of RhoA binding and nucleotide exchange in leukemia-associated Rho guanine-nucleotide exchange factor. J. Biol. Chem. *279*: 47352–62.

Kuner, R., Swiercz, J.M., Zywietz, A., Tappe, A., and Offermanns, S. (2002). Characterization of the expression of PDZ-RhoGEF, LARG and Galpha12/Galpha13 proteins in the murine nervous system. Eur. J. Neurosci. *16*: 2333–41.

Laemmli, U.K. (1970). Cleavage of structural proteins during the assembly of the head of bacteriophage T4. Nature *227*: 680–5.

Lang, P., Gesbert, F., Delespine-Carmagnat, M., Stancou, R., Pouchelet, M., and Bertoglio, J. (1996). Protein kinase A phosphorylation of RhoA mediates the morphological and functional effects of cyclic AMP in cytotoxic lymphocytes. EMBO J. *15*: 510–9.

Langmead, C.J., and Christopoulos, A. (2014). Functional and structural perspectives on allosteric modulation of GPCRs. Curr. Opin. Cell Biol. *27C*: 94–101.

Lee, M.J., Tasaki, T., Moroi, K., An, J.Y., Kimura, S., Davydov, I. V., et al. (2005). RGS4 and RGS5 are in vivo substrates of the N-end rule pathway. Proc. Natl. Acad. Sci. U. S. A. *102*: 15030–5.

Lefkowitz, R.J. (1998). G Protein-coupled Receptors: III. NEW ROLES FOR RECEPTOR KINASES AND -ARRESTINS IN RECEPTOR SIGNALING AND DESENSITIZATION. J. Biol. Chem. *273*: 18677–80.

Lessey-Morillon, E.C., Osborne, L.D., Monaghan-Benson, E., Guilluy, C., O'Brien, E.T., Superfine, R., et al. (2014). The RhoA guanine nucleotide exchange factor, LARG, mediates ICAM-1-dependent mechanotransduction in endothelial cells to stimulate transendothelial migration. J. Immunol. *192*: 3390–8.

Leung, T., Manser, E., Tan, L., and Lim, L. (1995). A novel serine/threonine kinase binding the Ras-related RhoA GTPase which translocates the kinase to peripheral membranes. J. Biol. Chem. *270*: 29051–4.

Li, H., Choe, N.H., Wright, D.T., and Adler, K.B. (1995). Histamine provokes turnover of inositol phospholipids in guinea pig and human airway epithelial cells via an H1-receptor/G protein-dependent mechanism. Am. J. Respir. Cell Mol. Biol. *12*: 416–24.

Li, J., Adams, L.D., Wang, X., Pabon, L., Schwartz, S.M., Sane, D.C., et al. (2004). Regulator of G protein signaling 5 marks peripheral arterial smooth muscle cells and is downregulated in atherosclerotic plaque. J. Vasc. Surg. *40*: 519–28.

Li, Y., Hanf, R., Otero, A.S., Fischmeister, R., and Szabo, G. (1994). Differential effects of pertussis toxin on the muscarinic regulation of Ca2+ and K+ currents in frog cardiac myocytes. J. Gen. Physiol. *104*: 941–59.

Li, Y., Hashim, S., and Anand-Srivastava, M.B. (2005). Angiotensin II-evoked enhanced expression of RGS2 attenuates Gi-mediated adenylyl cyclase signaling in A10 cells. Cardiovasc. Res. *66*: 503–11.

Li, Y., Sternweis, P.M., Charnecki, S., Smith, T.F., Gilman, A.G., Neer, E.J., et al. (1998). Sites for Galpha binding on the G protein beta subunit overlap with sites for regulation of phospholipase Cbeta and adenylyl cyclase. J. Biol. Chem. *273*: 16265–72.

Liu, A.X., Rane, N., Liu, J.P., and Prendergast, G.C. (2001). RhoB is dispensable for mouse development, but it modifies susceptibility to tumor formation as well as cell adhesion and growth factor signaling in transformed cells. Mol. Cell. Biol. *21*: 6906–12.

Liu, G., and Voyno-Yasenetskaya, T.A. (2005). Radixin stimulates Rac1 and Ca2+/calmodulin-dependent kinase, CaMKII: cross-talk with Galpha13 signaling. J. Biol. Chem. *280*: 39042–9.

Liu, X., Wang, H., Eberstadt, M., Schnuchel, A., Olejniczak, E.T., Meadows, R.P., et al. (1998). NMR structure and mutagenesis of the N-terminal Dbl homology domain of the nucleotide exchange factor Trio. Cell *95*: 269–77.

Logothetis, D.E., Kurachi, Y., Galper, J., Neer, E.J., and Clapham, D.E. (1987). The beta gamma subunits of GTP-binding proteins activate the muscarinic K+ channel in heart. Nature *325*: 321–6.

Lohse, M.J., Nuber, S., and Hoffmann, C. (2012). Fluorescence/bioluminescence resonance energy transfer techniques to study G-protein-coupled receptor activation and signaling. Pharmacol. Rev. *64*: 299–336.

Loirand, G., and Pacaud, P. (2014). Involvement of Rho GTPases and their regulators in the pathogenesis of hypertension. Small GTPases *5*: e28846.

Lutz, S., Freichel-Blomquist, A., Rümenapp, U., Schmidt, M., Jakobs, K.H., and Wieland, T. (2004). p63RhoGEF and GEFT are Rho-specific guanine nucleotide exchange factors encoded by the same gene. Naunyn. Schmiedebergs. Arch. Pharmacol. *369*: 540–6.

Lutz, S., Freichel-Blomquist, A., Yang, Y., Rümenapp, U., Jakobs, K.H., Schmidt, M., et al. (2005). The guanine nucleotide exchange factor p63RhoGEF, a specific link between Gq/11-coupled receptor signaling and RhoA. J. Biol. Chem. *280*: 11134–9.

Lutz, S., Shankaranarayanan, A., Coco, C., Ridilla, M., Nance, M.R., Vettel, C., et al. (2007). Structure of Galphaq-p63RhoGEF-RhoA complex reveals a pathway for the activation of RhoA by GPCRs. Science *318*: 1923–7.

Lyon, A.M., Dutta, S., Boguth, C.A., Skiniotis, G., and Tesmer, J.J.G. (2013). Full-length Gα(q)-phospholipase C-β3 structure reveals interfaces of the C-terminal coiled-coil domain. Nat. Struct. Mol. Biol. *20*: 355–62.

Lyon, A.M., Taylor, V.G., and Tesmer, J.J.G. (2014). Strike a pose: Gαq complexes at the membrane. Trends Pharmacol. Sci. *35*: 23–30.

Lyon, A.M., Tesmer, V.M., Dhamsania, V.D., Thal, D.M., Gutierrez, J., Chowdhury, S., et al. (2011). An autoinhibitory helix in the C-terminal region of phospholipase C-β mediates Gαq activation. Nat. Struct. Mol. Biol. *18*: 999–1005.

Ma, P., and Zemmel, R. (2002). Value of novelty? Nat. Rev. Drug Discov. *1*: 571–2.

Madaule, P., and Axel, R. (1985). A novel ras-related gene family. Cell *41*: 31–40.

Madaule, P., Furuyashiki, T., Reid, T., Ishizaki, T., Watanabe, G., Morii, N., et al. (1995). A novel partner for the GTP-bound forms of rho and rac. FEBS Lett. *377*: 243–8.

Maekawa, M., Ishizaki, T., Boku, S., Watanabe, N., Fujita, A., Iwamatsu, A., et al. (1999). Signaling from Rho to the actin cytoskeleton through protein kinases ROCK and LIM-kinase. Science *285*: 895–8.

Maier-Peuschel, M., Frölich, N., Dees, C., Hommers, L.G., Hoffmann, C., Nikolaev, V.O., et al. (2010). A fluorescence resonance energy transfer-based M2 muscarinic receptor sensor reveals rapid kinetics of allosteric modulation. J. Biol. Chem. *285*: 8793–800.

Manganello, J.M., Huang, J.-S., Kozasa, T., Voyno-Yasenetskaya, T.A., and Breton, G.C. Le (2003). Protein kinase A-mediated phosphorylation of the Galpha13 switch I region alters the Galphabetagamma13-G protein-coupled receptor complex and inhibits Rho activation. J. Biol. Chem. *278*: 124–30.

Mao, J., Yuan, H., Xie, W., Simon, M.I., and Wu, D. (1998). Specific involvement of G proteins in regulation of serum response factor-mediated gene transcription by different receptors. J. Biol. Chem. *273*: 27118–23.

Marinissen, M.J., and Gutkind, J.S. (2005). Scaffold proteins dictate Rho GTPase-signaling specificity. Trends Biochem. Sci. *30*: 423–6.

Maruyama, Y., Nishida, M., Sugimoto, Y., Tanabe, S., Turner, J.H., Kozasa, T., et al. (2002). Galpha(12/13) mediates alpha(1)-adrenergic receptor-induced cardiac hypertrophy. Circ. Res. *91*: 961–9.

McCudden, C.R., Hains, M.D., Kimple, R.J., Siderovski, D.P., and Willard, F.S. (2005). G-protein signaling: back to the future. Cell. Mol. Life Sci. *62*: 551–77.

McNair, K., Spike, R., Guilding, C., Prendergast, G.C., Stone, T.W., Cobb, S.R., et al. (2010). A role for RhoB in synaptic plasticity and the regulation of neuronal morphology. J. Neurosci. *30*: 3508–17.

Medina, F., Carter, A.M., Dada, O., Gutowski, S., Hadas, J., Chen, Z., et al. (2013). Activated RhoA is a positive feedback regulator of the Lbc family of Rho guanine nucleotide exchange factor proteins. J. Biol. Chem. *288*: 11325–33.

Medlin, M.D., Staus, D.P., Dubash, A.D., Taylor, J.M., and Mack, C.P. (2010). Sphingosine 1-phosphate receptor 2 signals through leukemia-associated RhoGEF (LARG), to promote smooth muscle cell differentiation. Arterioscler. Thromb. Vasc. Biol. *30*: 1779–86.

Meigs, T.E., Fedor-Chaiken, M., Kaplan, D.D., Brackenbury, R., and Casey, P.J. (2002). Galpha12 and Galpha13 negatively regulate the adhesive functions of cadherin. J. Biol. Chem. *277*: 24594–600.

Meigs, T.E., Fields, T.A., McKee, D.D., and Casey, P.J. (2001). Interaction of Galpha 12 and Galpha 13 with the cytoplasmic domain of cadherin provides a mechanism for beta -catenin release. Proc. Natl. Acad. Sci. U. S. A. *98*: 519–24.

Meigs, T.E., Juneja, J., DeMarco, C.T., Stemmle, L.N., Kaplan, D.D., and Casey, P.J. (2005). Selective uncoupling of G alpha 12 from Rho-mediated signaling. J. Biol. Chem. *280*: 18049–55.

Melendez, J., Stengel, K., Zhou, X., Chauhan, B.K., Debidda, M., Andreassen, P., et al. (2011). RhoA GTPase is dispensable for actomyosin regulation but is essential for mitosis in primary mouse embryonic fibroblasts. J. Biol. Chem. *286*: 15132–7.

Mellor, H., Flynn, P., Nobes, C.D., Hall, A., and Parker, P.J. (1998). PRK1 is targeted to endosomes by the small GTPase, RhoB. J. Biol. Chem. *273*: 4811–4.

Meyer, B.H., Freuler, F., Guerini, D., and Siehler, S. (2008). Reversible translocation of p115-RhoGEF by G(12/13)-coupled receptors. J. Cell. Biochem. *104*: 1660–70.

Mikelis, C.M., Palmby, T.R., Simaan, M., Li, W., Szabo, R., Lyons, R., et al. (2013). PDZ-RhoGEF and LARG are essential for embryonic development and provide a link between thrombin and LPA receptors and Rho activation. J. Biol. Chem. *288*: 12232–43.

Milde, M., Rinne, A., Wunder, F., Engelhardt, S., and Bünemann, M. (2013). Dynamics of Gαi1 interaction with type 5 adenylate cyclase reveal the molecular basis for high sensitivity of Gi-mediated inhibition of cAMP production. Biochem. J. *454*: 515–23.

Mintert, E., Bösche, L.I., Rinne, A., Timpert, M., Kienitz, M.-C., Pott, L., et al. (2007). Generation of a constitutive Na+-dependent inward-rectifier current in rat adult atrial myocytes by overexpression of Kir3.4. J. Physiol. *585*: 3–13.

Miyawaki, A. (2011). Development of probes for cellular functions using fluorescent proteins and fluorescence resonance energy transfer. Annu. Rev. Biochem. *80*: 357–73.

Moepps, B., Tulone, C., Kern, C., Minisini, R., Michels, G., Vatter, P., et al. (2008). Constitutive serum response factor activation by the viral chemokine receptor homologue pUS28 is differentially regulated by Galpha(q/11) and Galpha(16). Cell. Signal. *20*: 1528–37.

Moers, A., Nieswandt, B., Massberg, S., Wettschureck, N., Grüner, S., Konrad, I., et al. (2003). G13 is an essential mediator of platelet activation in hemostasis and thrombosis. Nat. Med. *9*: 1418–22.

Moers, A., Nürnberg, A., Goebbels, S., Wettschureck, N., and Offermanns, S. (2008). Galpha12/Galpha13 deficiency causes localized overmigration of neurons in the developing cerebral and cerebellar cortices. Mol. Cell. Biol. *28*: 1480–8.

Momotani, K., Artamonov, M. V, Utepbergenov, D., Derewenda, U., Derewenda, Z.S., and Somlyo, A. V (2011). p63RhoGEF couples Gα(q/11)-mediated signaling to Ca2+ sensitization of vascular smooth muscle contractility. Circ. Res. *109*: 993–1002.

Momotani, K., and Somlyo, A. V (2012). p63RhoGEF: a new switch for G(q)-mediated activation of smooth muscle. Trends Cardiovasc. Med. *22*: 122–7.

Moreira, I.S. (2014). Structural features of the G-protein/GPCR interactions. Biochim. Biophys. Acta *1840*: 16–33.

Morgan-Fisher, M., Wewer, U.M., and Yoneda, A. (2013). Regulation of ROCK activity in cancer. J. Histochem. Cytochem. *61*: 185–98.

Mossessova, E., Corpina, R.A., and Goldberg, J. (2003). Crystal structure of ARF1*Sec7 complexed with Brefeldin A and its implications for the guanine nucleotide exchange mechanism. Mol. Cell *12*: 1403–11.

Mullis, K., Faloona, F., Scharf, S., Saiki, R., Horn, G., and Erlich, H. (1986). Specific enzymatic amplification of DNA in vitro: the polymerase chain reaction. Cold Spring Harb. Symp. Quant. Biol. *51 Pt 1*: 263–73.

Nakamura, S., Kreutz, B., Tanabe, S., Suzuki, N., and Kozasa, T. (2004). Critical role of lysine 204 in switch I region of Galpha13 for regulation of p115RhoGEF and leukemia-associated RhoGEF. Mol. Pharmacol. *66*: 1029–34.

Nance, M.R., Kreutz, B., Tesmer, V.M., Sterne-Marr, R., Kozasa, T., and Tesmer, J.J.G. (2013). Structural and functional analysis of the regulator of G protein signaling 2-gαq complex. Structure *21*: 438–48.

Neer, E.J., Schmidt, C.J., Nambudripad, R., and Smith, T.F. (1994). The ancient regulatory-protein family of WD-repeat proteins. Nature *371*: 297–300.

Nethe, M., and Hordijk, P.L. (2010). The role of ubiquitylation and degradation in RhoGTPase signalling. J. Cell Sci. *123*: 4011–8.

Nobes, C.D., and Hall, A. (1995). Rho, rac, and cdc42 GTPases regulate the assembly of multimolecular focal complexes associated with actin stress fibers, lamellipodia, and filopodia. Cell *81*: 53–62.

Nygaard, R., Zou, Y., Dror, R.O., Mildorf, T.J., Arlow, D.H., Manglik, A., et al. (2013). The dynamic process of β(2)-adrenergic receptor activation. Cell *152*: 532–42.

Offermanns, S., Laugwitz, K.L., Spicher, K., and Schultz, G. (1994). G proteins of the G12 family are activated via thromboxane A2 and thrombin receptors in human platelets. Proc. Natl. Acad. Sci. U. S. A. *91*: 504–8.

Offermanns, S., Mancino, V., Revel, J.P., and Simon, M.I. (1997). Vascular system defects and impaired cell chemokinesis as a result of Galpha13 deficiency. Science *275*: 533–6.

Offermanns, S., Zhao, L.P., Gohla, A., Sarosi, I., Simon, M.I., and Wilkie, T.M. (1998). Embryonic cardiomyocyte hypoplasia and craniofacial defects in G alpha q/G alpha 11-mutant mice. EMBO J. *17*: 4304–12.

Ohashi, K., Nagata, K., Maekawa, M., Ishizaki, T., Narumiya, S., and Mizuno, K. (2000). Rho-associated kinase ROCK activates LIM-kinase 1 by phosphorylation at threonine 508 within the activation loop. J. Biol. Chem. *275*: 3577–82.

Oka, Y., Saraiva, L.R., Kwan, Y.Y., and Korsching, S.I. (2009). The fifth class of Galpha proteins. Proc. Natl. Acad. Sci. U. S. A. *106*: 1484–9.

Oldham, W.M., and Hamm, H.E. (2008). Heterotrimeric G protein activation by G-protein-coupled receptors. Nat. Rev. Mol. Cell Biol. *9*: 60–71.

Oleksy, A., Opalinski, Ł., Derewenda, U., Derewenda, Z.S., and Otlewski, J. (2006). The molecular basis of RhoA specificity in the guanine nucleotide exchange factor PDZ-RhoGEF. J. Biol. Chem. *281*: 32891–7.

Oliveira-dos-Santos, A.J., Matsumoto, G., Snow, B.E., Bai, D., Houston, F.P., Whishaw, I.Q., et al. (2000). Regulation of T cell activation, anxiety, and male aggression by RGS2. Proc. Natl. Acad. Sci. U. S. A. *97*: 12272–7.

Olson, E.N., and Nordheim, A. (2010). Linking actin dynamics and gene transcription to drive cellular motile functions. Nat. Rev. Mol. Cell Biol. *11*: 353–65.

Ong, D.C.T., Ho, Y.M., Rudduck, C., Chin, K., Kuo, W.-L., Lie, D.K.H., et al. (2009). LARG at chromosome 11q23 has functional characteristics of a tumor suppressor in human breast and colorectal cancer. Oncogene *28*: 4189–200.

Orchard, R.C., and Alto, N.M. (2012). Mimicking GEFs: a common theme for bacterial pathogens. Cell. Microbiol. *14*: 10–8.

Osterhout, J.L., Waheed, A.A., Hiol, A., Ward, R.J., Davey, P.C., Nini, L., et al. (2003). Palmitoylation regulates regulator of G-protein signaling (RGS) 16 function. II. Palmitoylation of a cysteine residue in the RGS box is critical for RGS16 GTPase accelerating activity and regulation of Gi-coupled signalling. J. Biol. Chem. *278*: 19309–16.

Pagnin, E., Semplicini, A., Sartori, M., Pessina, A.C., and Calò, L.A. (2005). Reduced mRNA and protein content of rho guanine nucleotide exchange factor (RhoGEF) in Bartter's and Gitelman's syndromes: relevance for the pathophysiology of hypertension. Am. J. Hypertens. *18*: 1200–5.

Pakes, N.K., Veltman, D.M., and Williams, R.S.B. (2013). Zizimin and Dock guanine nucleotide exchange factors in cell function and disease. Small GTPases *4*: 22–7.

Papoucheva, E., Dumuis, A., Sebben, M., Richter, D.W., and Ponimaskin, E.G. (2004). The 5-hydroxytryptamine(1A) receptor is stably palmitoylated, and acylation is critical for communication of receptor with Gi protein. J. Biol. Chem. *279*: 3280–91.

Park, D., Jhon, D.Y., Lee, C.W., Lee, K.H., and Rhee, S.G. (1993). Activation of phospholipase C isozymes by G protein beta gamma subunits. J. Biol. Chem. *268*: 4573–6.

Pedersen, E., and Brakebusch, C. (2012). Rho GTPase function in development: how in vivo models change our view. Exp. Cell Res. *318*: 1779–87.

Pfreimer, M., Vatter, P., Langer, T., Wieland, T., Gierschik, P., and Moepps, B. (2011). LARG links histamine-H1-receptor-activated Gq to Rho-GTPase-dependent signaling pathways. Cell. Signal. *24*: 652–63.

Pi, M., Spurney, R.F., Tu, Q., Hinson, T., and Quarles, L.D. (2002). Calcium-sensing receptor activation of rho involves filamin and rho-guanine nucleotide exchange factor. Endocrinology *143*: 3830–8.

Pleines, I., Hagedorn, I., Gupta, S., May, F., Chakarova, L., Hengel, J. van, et al. (2012). Megakaryocyte-specific RhoA deficiency causes macrothrombocytopenia and defective platelet activation in hemostasis and thrombosis. Blood *119*: 1054–63.

Pogozheva, I.D., Lomize, A.L., and Mosberg, H.I. (1997). The transmembrane 7-alpha-bundle of rhodopsin: distance geometry calculations with hydrogen bonding constraints. Biophys. J. *72*: 1963–85.

Pollinger, T. (2012). Spatiotemporale Organisation der Interaktion von G q Protein-Untereinheiten und der Phospholipase Cβ3. Universität Würzburg.

Ponimaskin, E.G., Profirovic, J., Vaiskunaite, R., Richter, D.W., and Voyno-Yasenetskaya, T.A. (2002). 5-Hydroxytryptamine 4(a) receptor is coupled to the Galpha subunit of heterotrimeric G13 protein. J. Biol. Chem. *277*: 20812–9.

Prasher, D.C., Eckenrode, V.K., Ward, W.W., Prendergast, F.G., and Cormier, M.J. (1992). Primary structure of the Aequorea victoria green-fluorescent protein. Gene *111*: 229–33.

Preininger, A.M., Eps, N. van, Yu, N.-J., Medkova, M., Hubbell, W.L., and Hamm, H.E. (2003). The myristoylated amino terminus of Galpha(i)(1) plays a critical role in the structure and function of Galpha(i)(1) subunits in solution. Biochemistry *42*: 7931–41.

Puetz, S., Lubomirov, L.T., and Pfitzer, G. (2009). Regulation of smooth muscle contraction by small GTPases. Physiology (Bethesda). *24*: 342–56.

Qin, K., Dong, C., Wu, G., and Lambert, N. a (2011). Inactive-state preassembly of G(q)-coupled receptors and G(q) heterotrimers. Nat. Chem. Biol. *7*: 740–7.

Qin, K., Sethi, P.R., and Lambert, N. a (2008). Abundance and stability of complexes containing inactive G protein-coupled receptors and G proteins. FASEB J. *22*: 2920–7.

Raamsdonk, C.D. van, Griewank, K.G., Crosby, M.B., Garrido, M.C., Vemula, S., Wiesner, T., et al. (2010). Mutations in GNA11 in uveal melanoma. N. Engl. J. Med. *363*: 2191–9.

Rask-Andersen, M., Almén, M.S., and Schiöth, H.B. (2011). Trends in the exploitation of novel drug targets. Nat. Rev. Drug Discov. *10*: 579–90.

Rasmussen, S.G.F., DeVree, B.T., Zou, Y., Kruse, A.C., Chung, K.Y., Kobilka, T.S., et al. (2011). Crystal structure of the β2 adrenergic receptor-Gs protein complex. Nature *477*: 549–55.

Rebecchi, M.J., and Pentyala, S.N. (2000). Structure, function, and control of phosphoinositide-specific phospholipase C. Physiol. Rev. *80*: 1291–335.

Reid, T., Furuyashiki, T., Ishizaki, T., Watanabe, G., Watanabe, N., Fujisawa, K., et al. (1996). Rhotekin, a new putative target for Rho bearing homology to a serine/threonine kinase, PKN, and rhophilin in the rho-binding domain. J. Biol. Chem. *271*: 13556–60.

Reiter, E., Ahn, S., Shukla, A.K., and Lefkowitz, R.J. (2012). Molecular mechanism of β-arrestin-biased agonism at seven-transmembrane receptors. Annu. Rev. Pharmacol. Toxicol. *52*: 179–97.

Ren, X.D., Kiosses, W.B., and Schwartz, M.A. (1999). Regulation of the small GTP-binding protein Rho by cell adhesion and the cytoskeleton. EMBO J. *18*: 578–85.

Ren, X.D., and Schwartz, M.A. (2000). Determination of GTP loading on Rho. Methods Enzymol. *325*: 264–72.

Rhee, S.G. (2001). Regulation of phosphoinositide-specific phospholipase C. Annu. Rev. Biochem. *70*: 281–312.

Riddle, E.L., Rana, B.K., Murthy, K.K., Rao, F., Eskin, E., O'Connor, D.T., et al. (2006). Polymorphisms and haplotypes of the regulator of G protein signaling-2 gene in normotensives and hypertensives. Hypertension *47*: 415–20.

Ridley, A.J. (2006). Rho GTPases and actin dynamics in membrane protrusions and vesicle trafficking. Trends Cell Biol. *16*: 522–9.

Ridley, A.J. (2011). Life at the leading edge. Cell *145*: 1012–22.

Ridley, A.J. (2013). RhoA, RhoB and RhoC have different roles in cancer cell migration. J. Microsc. *251*: 242–9.

Ridley, A.J., and Hall, A. (1992). The small GTP-binding protein rho regulates the assembly of focal adhesions and actin stress fibers in response to growth factors. Cell *70*: 389–99.

Ridley, A.J., Paterson, H.F., Johnston, C.L., Diekmann, D., and Hall, A. (1992). The small GTP-binding protein rac regulates growth factor-induced membrane ruffling. Cell *70*: 401–10.

Rieken, S., Sassmann, A., Herroeder, S., Wallenwein, B., Moers, A., Offermanns, S., et al. (2006). G12/G13 Family G Proteins Regulate Marginal Zone B Cell Maturation, Migration, and Polarization. J. Immunol. *177*: 2985–93.

Rinne, A., Birk, A., and Bünemann, M. (2013). Voltage regulates adrenergic receptor function. Proc. Natl. Acad. Sci. U. S. A. *110*: 1536–41.

Riobo, N.A., and Manning, D.R. (2005). Receptors coupled to heterotrimeric G proteins of the G12 family. Trends Pharmacol. Sci. *26*: 146–54.

Rojas, R.J., Yohe, M.E., Gershburg, S., Kawano, T., Kozasa, T., and Sondek, J. (2007). Galphaq directly activates p63RhoGEF and Trio via a conserved extension of the Dbl homology-associated pleckstrin homology domain. J. Biol. Chem. *282*: 29201–10.

Rosenbaum, D.M., Rasmussen, S.G.F., and Kobilka, B.K. (2009). The structure and function of G-protein-coupled receptors. Nature *459*: 356–63.

Ross, E.M., and Wilkie, T.M. (2000). GTPase-activating proteins for heterotrimeric G proteins: regulators of G protein signaling (RGS) and RGS-like proteins. Annu. Rev. Biochem. *69*: 795–827.

Rossman, K.L., and Campbell, S.L. (2000). Bacterial expressed DH and DH/PH domains. Methods Enzymol. *325*: 25–38.

Rossman, K.L., Der, C.J., and Sondek, J. (2005). GEF means go: turning on RHO GTPases with guanine nucleotide-exchange factors. Nat. Rev. Mol. Cell Biol. *6*: 167–80.

Ruiz-Velasco, V., and Ikeda, S.R. (2003). A splice variant of the G protein beta 3-subunit implicated in disease states does not modulate ion channels. Physiol. Genomics *13*: 85–95.

Rujkijyanont, P., Beyene, J., Wei, K., Khan, F., and Dror, Y. (2007). Leukaemia-related gene expression in bone marrow cells from patients with the preleukaemic disorder Shwachman-Diamond syndrome. Br. J. Haematol. *137*: 537–44.

Sadja, R., Alagem, N., and Reuveny, E. (2003). Gating of GIRK channels: details of an intricate, membrane-delimited signaling complex. Neuron *39*: 9–12.

Sagi, S.A., Seasholtz, T.M., Kobiashvili, M., Wilson, B.A., Toksoz, D., and Brown, J.H. (2001). Physical and functional interactions of Galphaq with Rho and its exchange factors. J. Biol. Chem. *276*: 15445–52.

Sah, V.P., Hoshijima, M., Chien, K.R., and Brown, J.H. (1996). Rho is required for Galphaq and alpha1-adrenergic receptor signaling in cardiomyocytes. Dissociation of Ras and Rho pathways. J. Biol. Chem. *271*: 31185–90.

Sahai, E., Ishizaki, T., Narumiya, S., and Treisman, R. (1999). Transformation mediated by RhoA requires activity of ROCK kinases. Curr. Biol. *9*: 136–45.

Sahai, E., and Marshall, C.J. (2002). ROCK and Dia have opposing effects on adherens junctions downstream of Rho. Nat. Cell Biol. *4*: 408–15.

Salim, S., Sinnarajah, S., Kehrl, J.H., and Dessauer, C.W. (2003). Identification of RGS2 and type V adenylyl cyclase interaction sites. J. Biol. Chem. *278*: 15842–9.

Sambrook, J., and Russel, D.W. (2001). Molecular Cloning (Cold Spring Harbor Laboratory Press).

Sánchez-Fernández, G., Cabezudo, S., García-Hoz, C., Benincá, C., Aragay, A.M., Mayor, F., et al. (2014). Gαq signalling: the new and the old. Cell. Signal. *26*: 833–48.

Sandilands, E., Cans, C., Fincham, V.J., Brunton, V.G., Mellor, H., Prendergast, G.C., et al. (2004). RhoB and actin polymerization coordinate Src activation with endosome-mediated delivery to the membrane. Dev. Cell *7*: 855–69.

Sanger, F., Nicklen, S., and Coulson, A.R. (1977). DNA sequencing with chain-terminating inhibitors. Proc. Natl. Acad. Sci. U. S. A. *74*: 5463–7.

Satoh, K., Fukumoto, Y., and Shimokawa, H. (2011). Rho-kinase: important new therapeutic target in cardiovascular diseases. Am. J. Physiol. Heart Circ. Physiol. *301*: H287–96.

Schmidt, A., and Hall, A. (2002). Guanine nucleotide exchange factors for Rho GTPases: turning on the switch. Genes Dev. *16*: 1587–609.

Schmidt, C.J., Thomas, T.C., Levine, M.A., and Neer, E.J. (1992). Specificity of G protein beta and gamma subunit interactions. J. Biol. Chem. *267*: 13807–10.

Schmidt, S., and Debant, A. (2014). Function and regulation of the Rho guanine nucleotide exchange factor Trio. Small GTPases *5*: e29769.

Schoner, W. (2008). Salt abuse: the path to hypertension. Nat. Med. *14*: 16–7.

Sebbagh, M., Hamelin, J., Bertoglio, J., Solary, E., and Bréard, J. (2005). Direct cleavage of ROCK II by granzyme B induces target cell membrane blebbing in a caspase-independent manner. J. Exp. Med. *201*: 465–71.

Semplicini, A., Lenzini, L., Sartori, M., Papparella, I., Calò, L.A., Pagnin, E., et al. (2006). Reduced expression of regulator of G-protein signaling 2 (RGS2) in hypertensive patients increases calcium mobilization and ERK1/2 phosphorylation induced by angiotensin II. J. Hypertens. *24*: 1115–24.

Shankaranarayanan, A., Boguth, C.A., Lutz, S., Vettel, C., Uhlemann, F., Aittaleb, M., et al. (2010). Galpha q allosterically activates and relieves autoinhibition of p63RhoGEF. Cell. Signal. *22*: 1114–23.

Shankaranarayanan, A., Thal, D.M., Tesmer, V.M., Roman, D.L., Neubig, R.R., Kozasa, T., et al. (2008). Assembly of high order G alpha q-effector complexes with RGS proteins. J. Biol. Chem. *283*: 34923–34.

Shi, C.S., Lee, S.B., Sinnarajah, S., Dessauer, C.W., Rhee, S.G., and Kehrl, J.H. (2001). Regulator of G-protein signaling 3 (RGS3) inhibits Gbeta1gamma 2-induced inositol phosphate production, mitogen-activated protein kinase activation, and Akt activation. J. Biol. Chem. *276*: 24293–300.

Shirley, M.D., Tang, H., Gallione, C.J., Baugher, J.D., Frelin, L.P., Cohen, B., et al. (2013). Sturge-Weber syndrome and port-wine stains caused by somatic mutation in GNAQ. N. Engl. J. Med. *368*: 1971–9.

Siderovski, D.P., and Willard, F.S. (2005). The GAPs, GEFs, and GDIs of heterotrimeric G-protein alpha subunits. Int. J. Biol. Sci. *1*: 51–66.

Siegert, P., Schmidt, G., Papatheodorou, P., Wieland, T., Aktories, K., and Orth, J.H.C. (2013). Pasteurella multocida toxin prevents osteoblast differentiation by transactivation of the MAP-kinase cascade via the Gα(q/11)-p63RhoGEF-RhoA axis. PLoS Pathog. *9*: e1003385.

Siehler, S. (2009). Regulation of RhoGEF proteins by G12/13-coupled receptors. Br. J. Pharmacol. *158*: 41–9.

Simon, M.I., Strathmann, M.P., and Gautam, N. (1991). Diversity of G proteins in signal transduction. Science *252*: 802–8.

Singer, W.D., Miller, R.T., and Sternweis, P.C. (1994). Purification and characterization of the alpha subunit of G13. J. Biol. Chem. *269*: 19796–802.

Skowronek, K.R., Guo, F., Zheng, Y., and Nassar, N. (2004). The C-terminal basic tail of RhoG assists the guanine nucleotide exchange factor trio in binding to phospholipids. J. Biol. Chem. *279*: 37895–907.

Snyder, J.T., Worthylake, D.K., Rossman, K.L., Betts, L., Pruitt, W.M., Siderovski, D.P., et al. (2002). Structural basis for the selective activation of Rho GTPases by Dbl exchange factors. Nat. Struct. Biol. *9*: 468–75.

Soisson, S.M., Nimnual, A.S., Uy, M., Bar-Sagi, D., and Kuriyan, J. (1998). Crystal structure of the Dbl and pleckstrin homology domains from the human Son of sevenless protein. Cell *95*: 259–68.

Sondek, J., Bohm, A., Lambright, D.G., Hamm, H.E., and Sigler, P.B. (1996). Crystal structure of a G-protein beta gamma dimer at 2.1A resolution. Nature *379*: 369–74.

Souchet, M., Portales-Casamar, E., Mazurais, D., Schmidt, S., Léger, I., Javré, J.-L., et al. (2002). Human p63RhoGEF, a novel RhoA-specific guanine nucleotide exchange factor, is localized in cardiac sarcomere. J. Cell Sci. *115*: 629–40.

Sprang, S.R., Chen, Z., and Du, X. (2007). Structural basis of effector regulation and signal termination in heterotrimeric Galpha proteins. Adv. Protein Chem. *74*: 1–65.

Strathmann, M.P., and Simon, M.I. (1991). G alpha 12 and G alpha 13 subunits define a fourth class of G protein alpha subunits. Proc. Natl. Acad. Sci. U. S. A. *88*: 5582–6.

Sun, C., Liu, C., Li, S., Li, H., Wang, Y., Xie, Y., et al. (2014). Overexpression of GEFT, a Rho family guanine nucleotide exchange factor, predicts poor prognosis in patients with rhabdomyosarcoma. Int. J. Clin. Exp. Pathol. *7*: 1606–15.

Sun, X., Kaltenbronn, K.M., Steinberg, T.H., and Blumer, K.J. (2005). RGS2 is a mediator of nitric oxide action on blood pressure and vasoconstrictor signaling. Mol. Pharmacol. *67*: 631–9.

Suzuki, N., Hajicek, N., and Kozasa, T. (2009a). Regulation and physiological functions of G12/13-mediated signaling pathways. Neurosignals. *17*: 55–70.

Suzuki, N., Nakamura, S., Mano, H., and Kozasa, T. (2003). Galpha 12 activates Rho GTPase through tyrosine-phosphorylated leukemia-associated RhoGEF. Proc. Natl. Acad. Sci. U. S. A. *100*: 733–8.

Suzuki, N., Tsumoto, K., Hajicek, N., Daigo, K., Tokita, R., Minami, S., et al. (2009b). Activation of leukemia-associated RhoGEF by Galpha13 with significant conformational rearrangements in the interface. J. Biol. Chem. *284*: 5000–9.

Swenson-Fields, K.I., Sandquist, J.C., Rossol-Allison, J., Blat, I.C., Wennerberg, K., Burridge, K., et al. (2008). MLK3 limits activated Galphaq signaling to Rho by binding to p63RhoGEF. Mol. Cell *32*: 43–56.

Swiercz, J.M., Kuner, R., Behrens, J., and Offermanns, S. (2002). Plexin-B1 directly interacts with PDZ-RhoGEF/LARG to regulate RhoA and growth cone morphology. Neuron *35*: 51–63.

Takefuji, M., Krüger, M., Sivaraj, K.K., Kaibuchi, K., Offermanns, S., and Wettschureck, N. (2013). RhoGEF12 controls cardiac remodeling by integrating G protein- and integrin-dependent signaling cascades. J. Exp. Med. *210*: 665–73.

Takefuji, M., Wirth, A., Lukasova, M., Takefuji, S., Boettger, T., Braun, T., et al. (2012). G(13)-mediated signaling pathway is required for pressure overload-induced cardiac remodeling and heart failure. Circulation *126*: 1972–82.

Tang, K.M., Wang, G., Lu, P., Karas, R.H., Aronovitz, M., Heximer, S.P., et al. (2003). Regulator of G-protein signaling-2 mediates vascular smooth muscle relaxation and blood pressure. Nat. Med. *9*: 1506–12.

Tang, W.J., and Gilman, A.G. (1991). Type-specific regulation of adenylyl cyclase by G protein beta gamma subunits. Science *254*: 1500–3.

Tang, X., Jin, R., Qu, G., Wang, X., Li, Z., Yuan, Z., et al. (2013). GPR116, an adhesion G-protein-coupled receptor, promotes breast cancer metastasis via the Gαq-p63RhoGEF-Rho GTPase pathway. Cancer Res. *73*: 6206–18.

Taya, S., Inagaki, N., Sengiku, H., Makino, H., Iwamatsu, A., Urakawa, I., et al. (2001). Direct interaction of insulin-like growth factor-1 receptor with leukemia-associated RhoGEF. J. Cell Biol. *155*: 809–20.

Terrillon, S., and Bouvier, M. (2004). Roles of G-protein-coupled receptor dimerization. EMBO Rep. *5*: 30–4.

Tesmer, J.J., Berman, D.M., Gilman, A.G., and Sprang, S.R. (1997). Structure of RGS4 bound to AlF4-activated G(i alpha1): stabilization of the transition state for GTP hydrolysis. Cell *89*: 251–61.

Tesmer, V.M., Kawano, T., Shankaranarayanan, A., Kozasa, T., and Tesmer, J.J.G. (2005). Snapshot of activated G proteins at the membrane: the Galphaq-GRK2-Gbetagamma complex. Science *310*: 1686–90.

Thumkeo, D., Keel, J., Ishizaki, T., Hirose, M., Nonomura, K., Oshima, H., et al. (2003). Targeted disruption of the mouse rho-associated kinase 2 gene results in intrauterine growth retardation and fetal death. Mol. Cell. Biol. *23*: 5043–55.

Thumkeo, D., Shimizu, Y., Sakamoto, S., Yamada, S., and Narumiya, S. (2005). ROCK-I and ROCK-II cooperatively regulate closure of eyelid and ventral body wall in mouse embryo. Genes Cells *10*: 825–34.

Thumkeo, D., Watanabe, S., and Narumiya, S. (2013). Physiological roles of Rho and Rho effectors in mammals. Eur. J. Cell Biol. *92*: 303–15.

Togashi, H., Nagata, K., Takagishi, M., Saitoh, N., and Inagaki, M. (2000). Functions of a rho-specific guanine nucleotide exchange factor in neurite retraction. Possible role of a proline-rich motif of KIAA0380 in localization. J. Biol. Chem. *275*: 29570–8.

Towbin, H., Staehelin, T., and Gordon, J. (1992). Electrophoretic transfer of proteins from polyacrylamide gels to nitrocellulose sheets: procedure and some applications. Biotechnology *24*: 145–9.

Tuteja, N. (2009). Signaling through G protein coupled receptors. Plant Signal. Behav. *4*: 942–7.

Uehata, M., Ishizaki, T., Satoh, H., Ono, T., Kawahara, T., Morishita, T., et al. (1997). Calcium sensitization of smooth muscle mediated by a Rho-associated protein kinase in hypertension. Nature *389*: 990–4.

Vaqué, J.P., Dorsam, R.T., Feng, X., Iglesias-Bartolome, R., Forsthoefel, D.J., Chen, Q., et al. (2013). A genome-wide RNAi screen reveals a Trio-regulated Rho GTPase circuitry transducing mitogenic signals initiated by G protein-coupled receptors. Mol. Cell *49*: 94–108.

Vega, F.M., Fruhwirth, G., Ng, T., and Ridley, A.J. (2011). RhoA and RhoC have distinct roles in migration and invasion by acting through different targets. J. Cell Biol. *193*: 655–65.

Vega, F.M., and Ridley, A.J. (2007). SnapShot: Rho family GTPases. Cell *129*: 1430.

Vigil, D., Cherfils, J., Rossman, K.L., and Der, C.J. (2010). Ras superfamily GEFs and GAPs: validated and tractable targets for cancer therapy? Nat. Rev. Cancer *10*: 842–57.

Vilardaga, J.-P., Bünemann, M., Feinstein, T.N., Lambert, N., Nikolaev, V.O., Engelhardt, S., et al. (2009). GPCR and G proteins: drug efficacy and activation in live cells. Mol. Endocrinol. *23*: 590–9.

Vilardaga, J.-P., Bünemann, M., Krasel, C., Castro, M., and Lohse, M.J. (2003). Measurement of the millisecond activation switch of G protein-coupled receptors in living cells. Nat. Biotechnol. *21*: 807–12.

Violin, J.D., Zhang, J., Tsien, R.Y., and Newton, A.C. (2003). A genetically encoded fluorescent reporter reveals oscillatory phosphorylation by protein kinase C. J. Cell Biol. *161*: 899–909.

Vogt, S., Grosse, R., Schultz, G., and Offermanns, S. (2003). Receptor-dependent RhoA activation in G12/G13-deficient cells: genetic evidence for an involvement of Gq/G11. J. Biol. Chem. *278*: 28743–9.

Waheed, A.A., and Jones, T.L.Z. (2002). Hsp90 interactions and acylation target the G protein Galpha 12 but not Galpha 13 to lipid rafts. J. Biol. Chem. *277*: 32409–12.

Waldo, G.L., Ricks, T.K., Hicks, S.N., Cheever, M.L., Kawano, T., Tsuboi, K., et al. (2010). Kinetic scaffolding mediated by a phospholipase C-beta and Gq signaling complex. Science *330*: 974–80.

Wall, M.A., Coleman, D.E., Lee, E., Iñiguez-Lluhi, J.A., Posner, B.A., Gilman, A.G., et al. (1995). The structure of the G protein heterotrimer Gi alpha 1 beta 1 gamma 2. Cell *83*: 1047–58.

Watanabe, G., Saito, Y., Madaule, P., Ishizaki, T., Fujisawa, K., Morii, N., et al. (1996). Protein kinase N (PKN) and PKN-related protein rhophilin as targets of small GTPase Rho. Science *271*: 645–8.

Watanabe, N., Madaule, P., Reid, T., Ishizaki, T., Watanabe, G., Kakizuka, A., et al. (1997). p140mDia, a mammalian homolog of Drosophila diaphanous, is a target protein for Rho small GTPase and is a ligand for profilin. EMBO J. *16*: 3044–56.

Watkins, J.L., Kim, H., Markwardt, M.L., Chen, L., Fromme, R., Rizzo, M.A., et al. (2013). The 1.6 Å resolution structure of a FRET-optimized Cerulean fluorescent protein. Acta Crystallogr. D. Biol. Crystallogr. *69*: 767–73.

Wedegaertner, P.B., Wilson, P.T., and Bourne, H.R. (1995). Lipid modifications of trimeric G proteins. J. Biol. Chem. *270*: 503–6.

Welch, H.C.E., Coadwell, W.J., Ellson, C.D., Ferguson, G.J., Andrews, S.R., Erdjument-Bromage, H., et al. (2002). P-Rex1, a PtdIns(3,4,5)P3- and Gbetagamma-regulated guanine-nucleotide exchange factor for Rac. Cell *108*: 809–21.

Wells, C.D., Liu, M.-Y., Jackson, M., Gutowski, S., Sternweis, P.M., Rothstein, J.D., et al. (2002). Mechanisms for reversible regulation between G13 and Rho exchange factors. J. Biol. Chem. *277*: 1174–81.

Wennerberg, K., and Der, C.J. (2004). Rho-family GTPases: it's not only Rac and Rho (and I like it). J. Cell Sci. *117*: 1301–12.

Westfield, G.H., Rasmussen, S.G.F., Su, M., Dutta, S., DeVree, B.T., Chung, K.Y., et al. (2011). Structural flexibility of the G alpha s alpha-helical domain in the beta2-adrenoceptor Gs complex. Proc. Natl. Acad. Sci. U. S. A. *108*: 16086–91.

Wheeler, A.P., and Ridley, A.J. (2004). Why three Rho proteins? RhoA, RhoB, RhoC, and cell motility. Exp. Cell Res. *301*: 43–9.

Wieland, T., and Mittmann, C. (2003). Regulators of G-protein signalling: multifunctional proteins with impact on signalling in the cardiovascular system. Pharmacol. Ther. *97*: 95–115.

Wilkie, T.M., Gilbert, D.J., Olsen, A.S., Chen, X.N., Amatruda, T.T., Korenberg, J.R., et al. (1992). Evolution of the mammalian G protein alpha subunit multigene family. Nat. Genet. *1*: 85–91.

Wilkie, T.M., Scherle, P.A., Strathmann, M.P., Slepak, V.Z., and Simon, M.I. (1991). Characterization of G-protein alpha subunits in the Gq class: expression in murine tissues and in stromal and hematopoietic cell lines. Proc. Natl. Acad. Sci. U. S. A. *88*: 10049–53.

Wilkie, T.M., and Yokoyama, S. (1994). Evolution of the G protein alpha subunit multigene family. Soc. Gen. Physiol. Ser. *49*: 249–70.

Williams, S.L., Lutz, S., Charlie, N.K., Vettel, C., Ailion, M., Coco, C., et al. (2007). Trio's Rho-specific GEF domain is the missing Galpha q effector in C. elegans. Genes Dev. *21*: 2731–46.

Wirth, A., Benyó, Z., Lukasova, M., Leutgeb, B., Wettschureck, N., Gorbey, S., et al. (2008). G12-G13-LARG-mediated signaling in vascular smooth muscle is required for salt-induced hypertension. Nat. Med. *14*: 64–8.

Worthylake, D.K., Rossman, K.L., and Sondek, J. (2000). Crystal structure of Rac1 in complex with the guanine nucleotide exchange region of Tiam1. Nature *408*: 682–8.

Worzfeld, T., Wettschureck, N., and Offermanns, S. (2008). G(12)/G(13)-mediated signalling in mammalian physiology and disease. Trends Pharmacol. Sci. *29*: 582–9.

Wuertz, C.M., Lorincz, A., Vettel, C., Thomas, M.A., Wieland, T., and Lutz, S. (2010). p63RhoGEF-a key mediator of angiotensin II-dependent signaling and processes in vascular smooth muscle cells. FASEB J. *24*: 4865–76.

Xiang, S., Kim, E.Y., Connelly, J.J., Nassar, N., Kirsch, J., Winking, J., et al. (2006). The crystal structure of Cdc42 in complex with collybistin II, a gephyrin-interacting guanine nucleotide exchange factor. J. Mol. Biol. *359*: 35–46.

Xiang, S.Y., Vanhoutte, D., Re, D.P. del, Purcell, N.H., Ling, H., Banerjee, I., et al. (2011). RhoA protects the mouse heart against ischemia/reperfusion injury. J. Clin. Invest. *121*: 3269–76.

Xu, N., Bradley, L., Ambdukar, I., and Gutkind, J.S. (1993). A mutant alpha subunit of G12 potentiates the eicosanoid pathway and is highly oncogenic in NIH 3T3 cells. Proc. Natl. Acad. Sci. U. S. A. *90*: 6741–5.

Xu, N., Voyno-Yasenetskaya, T., and Gutkind, J.S. (1994). Potent transforming activity of the G13 alpha subunit defines a novel family of oncogenes. Biochem. Biophys. Res. Commun. *201*: 603–9.

Yamada, T., Ohoka, Y., Kogo, M., and Inagaki, S. (2005). Physical and functional interactions of the lysophosphatidic acid receptors with PDZ domain-containing Rho guanine nucleotide exchange factors (RhoGEFs). J. Biol. Chem. *280*: 19358–63.

Yeung, W.W.S., and Wong, Y.H. (2009). The RhoA-specific guanine nucleotide exchange factor p63RhoGEF binds to activated Galpha(16) and inhibits the canonical phospholipase Cbeta pathway. Cell. Signal. *21*: 1317–25.

Ying, Z., Giachini, F.R.C., Tostes, R.C., and Webb, R.C. (2009). PYK2/PDZ-RhoGEF links Ca2+ signaling to RhoA. Arterioscler. Thromb. Vasc. Biol. *29*: 1657–63.

Ying, Z., Jin, L., Dorrance, A.M., and Webb, R.C. (2004). Increaseed expression of mRNA for regulator of G protein signaling domain-containing Rho guanine nucleotide exchange factors in aorta from stroke-prone spontaneously hypertensive rats. Am. J. Hypertens. *17*: 981–5.

Zalcman, G., Closson, V., Linarès-Cruz, G., Lerebours, F., Honoré, N., Tavitian, A., et al. (1995). Regulation of Ras-related RhoB protein expression during the cell cycle. Oncogene *10*: 1935–45.

Zamponi, G.W., and Currie, K.P.M. (2013). Regulation of Ca(V)2 calcium channels by G protein coupled receptors. Biochim. Biophys. Acta *1828*: 1629–43.

Zamponi, G.W., and Snutch, T.P. (1998). Modulation of voltage-dependent calcium channels by G proteins. Curr. Opin. Neurobiol. *8*: 351–6.

Zeng, W., Xu, X., Popov, S., Mukhopadhyay, S., Chidiac, P., Swistok, J., et al. (1998). The N-terminal domain of RGS4 confers receptor-selective inhibition of G protein signaling. J. Biol. Chem. *273*: 34687–90.

Zhang, H., Wang, L., Kao, S., Whitehead, I.P., Hart, M.J., Liu, B., et al. (1999). Functional interaction between the cytoplasmic leucine-zipper domain of HIV-1 gp41 and p115-RhoGEF. Curr. Biol. *9*: 1271–4.

Zhang, P., and Mende, U. (2011). Regulators of G-protein signaling in the heart and their potential as therapeutic targets. Circ. Res. *109*: 320–33.

Zhang, S., Zhou, X., Lang, R.A., and Guo, F. (2012). RhoA of the Rho family small GTPases is essential for B lymphocyte development. PLoS One *7*: e33773.

Zheng, M., Cierpicki, T., Momotani, K., Artamonov, M. V, Derewenda, U., Bushweller, J.H., et al. (2009). On the mechanism of autoinhibition of the RhoA-specific nucleotide exchange factor PDZRhoGEF. BMC Struct. Biol. *9*: 36.

Zhou, J., Moroi, K., Nishiyama, M., Usui, H., Seki, N., Ishida, J., et al. (2001). Characterization of RGS5 in regulation of G protein-coupled receptor signaling. Life Sci. *68*: 1457–69.

Zhou, J.Y., Toth, P.T., and Miller, R.J. (2003). Direct interactions between the heterotrimeric G protein subunit G beta 5 and the G protein gamma subunit-like domain-containing regulator of G protein signaling 11: gain of function of cyan fluorescent protein-tagged G gamma 3. J. Pharmacol. Exp. Ther. *305*: 460–6.

Zhou, X., and Zheng, Y. (2013). Cell type-specific signaling function of RhoA GTPase: lessons from mouse gene targeting. J. Biol. Chem. *288*: 36179–88.

Ziegler, N., Bätz, J., Zabel, U., Lohse, M.J., and Hoffmann, C. (2011). FRET-based sensors for the human M1-, M3-, and M5-acetylcholine receptors. Bioorg. Med. Chem. *19*: 1048–54.

Zinovyeva, M., Sveshnikova, E., Visser, J., and Belyavsky, A. (2004). Molecular cloning, sequence and expression pattern analysis of the mouse orthologue of the leukemia-associated guanine nucleotide exchange factor. Gene *337*: 181–8.

Zizer, E., Beilke, S., Bäuerle, T., Schilling, K., Möhnle, U., Adler, G., et al. (2010). Loss of Lsc/p115 protein leads to neuronal hypoplasia in the esophagus and an achalasia-like phenotype in mice. Gastroenterology *139*: 1344–54.

Appendix

Figure index

Curiculum vitae

This page containes personal information. It is therefore excluded from online publication.

Diese Seite enthält persönliche Daten. Sie ist daher nicht Bestandteil der Online-Veröffentlichung.

Erklärung

Ich versichere, dass ich meine Dissertation

„Regulation of Rho-activating proteins by heterotrimeric G proteins:
Sensitivity of Gα RhoGEF interaction is determined by dissociation kinetics“

selbständig, ohne unerlaubte Hilfe angefertigt und mich dabei keiner anderen als der von mir ausdrücklich bezeichneten Quellen bedient habe.

Die Dissertation wurde in der jetzigen oder einer ähnlichen Form noch bei keiner anderen Hochschule eingereicht und hat noch keinen sonstigen Prüfungszwecken gedient.

Marburg, den 2.10.2014

_____

Eva-Lisa Bodmann

Danksagung

Vielen Dank.../Many thanks to...

Moritz Bünemann für die Möglichkeit, mich in seinem Labor zu promovieren und die RhoGEFs zum Thema meiner Arbeit zu machen. Das Thema hat mich stets begeistert und ich bin sehr dankbar für seine aufmerksame und kritisch Supervision meiner Arbeit. Außerdem möchte ich Ihnen herzlich für die freundliche und produktive Atmosphäre zwischen uns und in der gesamten Arbeitsgruppe danken!

Dominique Brandt aus der Arbeitsgruppe Grosse für die gemeinsame Arbeit an der Signalweiterleitung unterhalb von RGS2 und p63RhoGEF. Außerdem danke ich dir sehr für die hilfreichen Anregungen zur Etablierung des „RhoA affinity purification assays“ in unserem Labor.

Thomas Wieland für die zur Verfügung gestellten Plasmide und für wichtige Hinweise zum Umgang mit RhoGEFs im Allgemeinen. Insbesondere möchte ich Ihnen und Ihrer gesamten Arbeitsgruppe für meine Einarbeitung in den „SRF luciferase assay“ danken.

Cornelius Krasel für viele Antworten auf Fragen zu pharmakologischen Sachverhalten und dem Laboralltag. Sein großes Wissen war für mich häufig der Schlüssel zur Antwort auf ungeklärte Fragen und seine freundliche Art erlaubte mir auch die trivialsten Fragen zu stellen. Herzlich möchte ich mich auch für deine Anregungen zum Methodenteil dieser Arbeit bedanken. Für mich bist du das Rückgrat dieser Arbeitsgruppe.

Andreas Rinne für die Vorbereitung meines Projektes und viele praktische und theoretische Hinweise. Vor allem das p63RhoGEF-Projekt hat er durch seine Ideen stark beeinflusst. Der Austausch mit dir hat meine Arbeit bereichert und meine Arbeitsweise geprägt. Herzlichen Dank!

Emma Esser for her careful reading of this thesis. Additionally, I´m very grateful for all the administrative work she does in the background. Your commitment keeps our daily work running without our notice. Many thanks for this!

Anna-Lena Krett für ihre Arbeiten am $G\alpha_{13}$-Assay. Sie ermöglichten meine Untersuchungen zur Aktivierung von LARG. Unser Austausch über Signalweiterleitung unterhalb des Thromboxan Rezeptors haben meine Arbeit sehr bereichert und deine freundliche, umsichtige Art ist mitentscheidend für die gute Atmosphäre in unserer Arbeitsgruppe.

Alexandra Birk für die gemeinsame Zeit in dieser tollen Arbeitsgruppe und unsere Freundschaft. Ich bin sehr froh, dass wir uns vor vier Jahren unabhängig von einander entschlossen haben hier zu arbeiten.

The whole AG Bünemann for critical and fruitfull discussions on the small and big problems of scientific work and the fun in the lab. If I would have colleagues like you the rest of my life, I would learn a lot as well as would be happy to come to work every day. Never give up on your projects even if it´s hard some times. The day an experiment finally works will be worth the effort.

Meinen Praktikumsbetreuern und den von mir betreuten Praktikanten. Die Praktikumsbetreuer haben mir ihre kleinen und großen Labortricks verraten und an „meinen“ Praktikanten durfte ich die Weitergabe von Wissen üben.

Meiner Mutter für den Freiraum, meine Ziele zu verfolgen. Diesen Freiraum habe ich nur, weil ich in der Gewissheit lebe bei dir immer Zuspruch und Beratung zu finden.

Meinem Vater für die Beharrlichkeit und viele gefahrene Kilometer für ein gemeinsames Abendessen. Ich bin sehr froh, dass du mein Vater bist.

Meinen Wahl- und „echten“ Verwandten in Ingelheim, auf dem Hunsrück und in Marburg. Ihr habt mich unterstützt bei all meinen Schritten und mich wesentlich geprägt. Ich bin froh um jeden von euch und möchte keinen missen. Besonders erwähnt sei meine Großmutter Mimi, welche mir mit ihrer Tapferkeit immer ein Vorbild sein wird und mit der ich die ersten Tage des Schreibens an dieser Arbeit verbringen durfte. Außerdem Andreas Rothauer, welcher in mir die Begeisterung für die Laborarbeit weckte.

Meinen Freunden für viele schöne Erlebnisse und Gespräche, welche mich auch längere Durststrecken im Labor für ein paar Stunden vergessen ließen. Ihr alle prägt mein Leben jeden Tag und macht es besonders. Vielen Dank!

Moritz Thiele danke ich für viele kleine Wichtigkeiten und große Unwichtigkeiten und vor allem dafür, dass er ist wie er ist.